

NUREG/CR-4830  
SAND86-2689  
R3  
Printed March 1987

-8232-2/65511

C.1

8024



8232-2/065511



00000001 -

# MELCOR Validation and Verification 1986 Papers

Christi D. Leigh, Editor

Prepared by  
Sandia National Laboratories  
Albuquerque, New Mexico 87185 and Livermore, California 94550  
for the United States Department of Energy  
under Contract DE-AC04-76DP00789

Prepared for  
U. S. NUCLEAR REGULATORY COMMISSION

SF2900018-01

1062446

#### **NOTICE**

This report was prepared as an account of work sponsored by an agency of the United States Government. Neither the United States Government nor any agency thereof, or any of their employees, makes any warranty, expressed or implied, or assumes any legal liability or responsibility for any third party's use, or the results of such use, of any information, apparatus product or process disclosed in this report, or represents that its use by such third party would not infringe privately owned rights.

Available from  
Superintendent of Documents  
U.S. Government Printing Office  
Post Office Box 37082  
Washington, D.C. 20013-7082  
and  
National Technical Information Service  
Springfield, VA 22161

NUREG/CR-4830  
SAND86-2689  
R3

MELCOR Validation and Verification  
1986 Papers

Christi D. Leigh, Editor

March 1987

Sandia National Laboratories  
Albuquerque, New Mexico 87185  
Operated by  
Sandia Corporation  
for the  
U.S. Department of Energy

Prepared for  
Division of Reactor System Safety  
Office of Nuclear Regulatory Research  
U.S. Nuclear Regulatory Commission  
Washington, D.C. 20555  
Under Memorandum of Understanding DOE 40-550-75  
NRC Fin No. A1369



## Abstract

This report is a compilation of papers that documents the MELCOR validation and verification results obtained during 1986. It is intended that a report of this nature be published annually. The format used for this report follows that of a conference proceeding in that individual papers from various authors are combined into one report. This format was selected in part to encourage participation from MELCOR users outside Sandia. The format also has other advantages. One is that authors of individual papers can be properly credited. Another is that different reviewers can be selected for each test according to their expertise, and the review load can be distributed. Finally, each test report can be prepared, reviewed, and distributed individually before the composite report is published.



## Contents

Preface .....	vii
MELCOR 1.6 Calculations for Adiabatic Expansion of Hydrogen, Two-cell Flow C. D. Leigh and S. E. Dingman .....	1-1
MELCOR 1.6 Calculations for a Saturated Liquid Depressurization Test C. J. Shaffer .....	2-1
MELCOR 1.6 Calculations for the HDR Containment Experiment V44 C. J. Shaffer .....	3-1
MELCOR 1.0 Calculations for the Battelle-Frankfurt Gas Mixing Tests R. K. Byers .....	4-1
MELCOR 1.0 and HECTR 1.5 Calculations for Browns Ferry Reactor Building Burns S. E. Dingman and F. E. Haskin .....	5-1
MELCOR 1.0 Calculations for Cooling of a Structure in a Fluid P. N. Demmie .....	6-1
MELCOR 1.0 Calculations for Radial Conduction in Annular Structures S. E. Dingman .....	7-1
MELCOR 1.1 Calculations for a Semi-infinite Solid Heat Structure Test C. J. Shaffer .....	8-1
MELCOR 1.5 Calculations for ABCOVE Aerosol Experiments AB5, AB6, and AB7 C. D. Leigh .....	9-1
Appendix A: MELCOR Standard Test Problems from 1986 .....	A-1
Appendix B: Input Decks for MELCOR Standard Test Problems .....	B-1
ST001: Adiabatic Expansion of Hydrogen .....	B-1
MELGEN Input .....	B-1
MELCOR Input .....	B-2
MELPLT Input .....	B-2
Analytical Data .....	B-3
ST002: Radial Conduction in Annular Structures .....	B-4
MELGEN Input .....	B-4
MELCOR Input .....	B-5
MELPLT Input .....	B-5
ST003: Cooling of a Structure in a Fluid .....	B-6
MELGEN Input .....	B-6
MELCOR Input .....	B-7
MELPLT Input .....	B-8
Analytical Data .....	B-8
ST004: Semi-infinite Heat Structure Test .....	B-10
MELGEN Input .....	B-10

MELCOR Input .....	B-13
MELPLT Input .....	B-13
ST005: Saturated Liquid Depressurization Test .....	B-20
MELGEN Input .....	B-20
MELCOR Input .....	B-22
MELPLT Input .....	B-22
ST006: Browns Ferry Reactor Building Burns .....	B-24
MELGEN Input .....	B-24
MELCOR Input .....	B-49
MELPLT Input .....	B-50
ST007: HDR Steam Blowdown Test .....	B-51
MELGEN Input .....	B-51
MELCOR Input .....	B-79
MELPLT Input .....	B-79
ST008: ABCOVE Aerosol Experiments Test AB6 .....	B-86
MELGEN Input .....	B-86
MELCOR Input .....	B-88
MELPLT Input .....	B-89
NaOH Data .....	B-90
NaI Data .....	B-91
ST009: Battelle-Frankfurt Test .....	B-91
MELGEN Input .....	B-91
MELCOR Input.....	B-106
MELPLT Input .....	B-106
Experimental Data .....	B-111
HECTR Data .....	B-113
RALOC Data .....	B-111
Appendix C: Comparison Plots for MELCOR Standard Test Problems .....	C-1
Distributon .....	Dist-1



## Preface

MELCOR is a fully integrated, relatively fast running code that models the progression of severe accidents in light water nuclear power plants (LWRs). An entire spectrum of severe accident phenomena is modeled in MELCOR. Characteristics of severe accident progression that can be modeled in MELCOR include the thermal hydraulic response in the reactor coolant system, reactor cavity, containment, and confinement buildings; core heatup and degradation; hydrogen production, transport and combustion; core-concrete attack; heat structure response; radionuclide release and transport; and the impact of engineered safety features on thermal hydraulic and radionuclide behavior. MELCOR is being developed at Sandia National Laboratories for the United States Nuclear Regulatory Commission (NRC) to succeed the Source Term Code Package. MELCOR has been designed to facilitate sensitivity and uncertainty analyses and is currently being used to analyze severe-accident progression, source terms and associated sensitivities and uncertainties in several NRC-sponsored research programs.

The NRC in its report "Validation and Verification" [1], has established a multilevel approach to code validation. On the first level, past and near-term future experimental results that are suitable for code validation are identified. On the second level, specific comparisons to relevant experimental data with each of the detailed mechanistic codes are performed. On the third level, the SCTP and MELCOR calculations are compared to the detailed mechanistic code calculations. The cases for comparison, when possible, will be a subset of the same cases selected for data comparisons with the detailed mechanistic codes. This selection process will produce code-to-code as well as code-to-data comparisons for the integrated codes.

This report is a compilation of papers that documents the MELCOR validation and verification results obtained during 1986. It is intended that a report of this nature be published annually. The format used for this report follows that of a conference proceeding in that individual papers from various authors are combined into one report. This format was selected in part to encourage participation from MELCOR users outside Sandia. The format also has other advantages. One is that authors of individual papers can be properly credited. Another is that different reviewers can be selected for each test according to their expertise, and the review load can be distributed. Finally, each test report can be prepared, reviewed, and distributed individually before the composite report is published.

Validation and verification loosely refer to the processes undertaken to achieve confidence in computer codes. Fairley [2] indicates that validation addresses the question, "Are we building the right product?" It is the "process that defines the domains wherein solutions generated by the software are acceptable representatives of physical processes." As a practical matter, we principally use the term validation to refer to the comparison of code predictions with experimental results. The experiments selected for comparison may examine separate effects or be integral in nature (i.e., several code modules must be exercised simultaneously in order to simulate integral experiments).

According to Fairley, verification involves answering the question, "Are we building the product right?" He calls it the "process which demonstrates that the software correctly performs its stated capabilities." Verification is achieved via detailed inspections of coding and by performing tests specifically designed to identify defects that may exist in the various code modules. In this report, verification tests are frequently comparisons of MELCOR predictions to analytic solutions or to results obtained using other well-established codes.

The terms test and testing are used herein to refer to comparisons of MELCOR predictions to results obtained from any other source--experimental, analytic, or other codes. The process of comparing one code's predictions to those obtained using other codes is referred to as benchmarking. Figure 1 depicts the conceptual overlap of the commonly used terms validation, verification, testing, inspection, and benchmarking.

```

<-----Validation----->X<-----Verification----->
<-----Testing----->X<--Inspections-->
<--Comparisons with Experiments-->X<--Other Comparisons-->
      <---Benchmarking Against Other Codes--->

```

Figure 1. Definition of Terms Related to Validation

All of the tests that are included in this report were conducted at Sandia National Laboratories. We believe that on-site testing (testing at Sandia) is essential to the development of the code. Also, on-site testing is needed in order to establish a set of standard test problems that can be used to check revised versions of the code. However, for formal tests such as those documented in this report, we agree with G. J. Myers of IBM that, "It is impossible to test your own program." [3] Therefore, in no case is the developer of a module assigned the task of formally testing that module. In fact, it is expected that tests of MELCOR conducted outside of Sandia will be included as part of future MELCOR validation and verification reports.

Another important part of validation and verification philosophy is also taken from Myers [3], "Never alter the program to make testing easier." MELCOR has evolved substantially since our validation and verification efforts began. Although guided in part by the results of early validation and verification tests, the revisions that have been made to MELCOR over the last year were not done with any specific test in mind. All of the tests were run on established versions of the code. The version of the code that was used to perform the test is given in the title of each paper.

MELCOR test problems are chosen on the basis of current technical and programmatic considerations. Such considerations include:

1. MELCOR status and suitability of the current version for the test being considered
2. Availability of information required for preparation of the MELCOR input deck
3. Availability of results from other codes which would provide bases for comparison
4. Availability of resources required to perform the test
5. MELCOR models which would be invoked and their degree of testing to date
6. Usefulness of the input deck for future tests or applications
7. The risk significance of the phenomena or accident sequence modeled for the test

The structure that has been outlined for this program is designed to minimize duplication of effort, to select tests on the basis of well-defined priorities, and to document test results. At the same time, it is recognized that too much rigidity can be inhibitive, and excessive documentation requirements can be counterproductive. It is believed that with the current structure a balance is gained which maximizes the effectiveness of the overall validation and verification effort subject to resource constraints.

The tests that have been selected to date involve phenomena that take place in the containment of a light water reactor facility. This includes testing of the Burn Package, the Containment Spray Package, the Control Volume Hydrodynamics Package, the Heat Structure Package, and the Radionuclide Package. The focus has been primarily on containment phenomena because of the data available in that area and because the CONTAIN code developed at Sandia National Laboratories was available for comparison.

Some of the input decks used to develop the results presented in this report have been selected as standard test problems and run on the latest released version, MELCOR 1.6.0. A list of these standard test problems is given in Appendix A.

#### References

1. J. T. Larkins and M. A. Cunningham, Nuclear Power Plant Research Severe Accident Research Plan, U.S. Nuclear Regulatory Commission, Office of Regulatory Research, NUREG-0900, Revision 1.
2. R. E. Fairley, Software Engineering Concepts, McGraw-Hill, New York, 1979.
3. G. J. Myers, Software Reliability, Wiley Interscience, NY, 1976.



MELCOR 1.6 Calculations for  
Adiabatic Expansion of Hydrogen, Two-cell Flow

C. D. Leigh and S. E. Dingman  
Sandia National Laboratories  
Albuquerque, New Mexico 87185  
United States of America

Abstract

MELCOR calculations for the adiabatic flow of hydrogen between two control volumes have been performed and compared to the closed form analytical solution. The MELCOR results differ only slightly from the analytical solution. The differences are caused by the use of a temperature dependent heat capacity in MELCOR, which introduces some deviation from the ideal gas assumptions.

1. Introduction

This paper compares MELCOR predictions of the adiabatic flow of hydrogen between two control volumes to results obtained from an exact analytic solution for an ideal gas.

2. Test Description

Given two control volumes which are pressurized with hydrogen and the pressure in Control Volume 1 is greater than that in Control Volume 2, a flow path is opened between the two control volumes at time zero; hydrogen from the higher pressure control volume expands into the lower pressure control volume until the two pressures equilibrate. Assuming adiabatic flow and treating hydrogen as an ideal gas, analytic expressions for the control-volume temperatures and pressures as functions of the mass transferred are:

$$T_1 = T_{1o} \left( \frac{m_1}{m_{1o}} \right)^{\gamma - 1} \quad (1)$$

$$P_1 = P_{1o} \left( \frac{m_1}{m_{1o}} \right)^{\gamma} \quad (2)$$

$$T_2 = \frac{m_{2o} T_{2o}}{m_2} + \frac{m_{1o} T_{1o}}{m_2} \left[ 1 - \left( \frac{m_1}{m_{1o}} \right)^{\gamma} \right] \quad (3)$$

$$P_2 = P_{2o} + \left( \frac{V_1}{V_2} \right) P_{1o} \left[ 1 - \left( \frac{m_1}{m_{1o}} \right)^\gamma \right] \quad (4)$$

where  $T_1$ ,  $T_{1o}$ ,  $P_1$ ,  $P_{1o}$ ,  $m_1$ , and  $m_{1o}$  are the temperature, initial temperature, pressure, initial pressure, mass, and initial mass of the hydrogen in cell 1 and  $T_2$ ,  $T_{2o}$ ,  $P_2$ ,  $P_{2o}$ ,  $m_2$ , and  $m_{2o}$  are the temperature, initial temperature, pressure, initial pressure, mass, and initial mass of the hydrogen in cell 2.  $\gamma$  is the ratio of specific heats.

In this comparison, MELCOR is used to model the two-volume pressure equilibration. MELCOR results for the temperature and pressure in both control volumes (as a function of the mass remaining in the donor cell) are compared to values calculated with the closed form analytic solution.

### 3. Model and Case Descriptions

MELCOR was used to model the adiabatic flow of hydrogen between two control volumes as described in Section 2. The initial conditions, control volume sizes, and flow path parameters were varied over a wide range to provide a thorough test of the MELCOR packages. Six cases were run according to the specifications given in Table 1.

Table 1. Specifications for MELCOR Runs

Case No.	Vol(1) (m <sup>3</sup> )	Vol(2) (m <sup>3</sup> )	Initial Conditions			Flow Area (m <sup>2</sup> )	Loss Coeff. (-)
			T(1-2) (K)	P(1) (Pa)	P(2) (Pa)		
1	1000.	1000.	300.	2.E5	1.E5	.05	2.
2	1000.	1000.	300.	5.E5	1.E5	.05	2.
3	100.	1000.	300.	2.E5	1.E5	.05	2.
4	10000.	1000.	300.	2.E5	1.E5	.05	2.
5	1000.	1000.	300.	2.E5	1.E5	50.	2.
6	1000.	1000.	300.	2.E5	1.E5	.05	.1

### 4. Results

The analytic and MELCOR results for the six cases are compared in Figures 1 through 12. These figures show the temperatures and pressures for both cells as a function of the mass in Cell 1. In all cases, the agreement is excellent. The slight differences are due in part to using a temperature-dependent heat capacity in MELCOR which introduces some deviation from the gas assumption and in part to the time-step selection.

## 5. Defects Identified

In previous analyses of this test, oscillatory pressures and temperatures that diverged during the transient were calculated by MELCOR. The testers eliminated the oscillations in those calculations by forcing MELCOR to use a smaller time step (the maximum time step size was reduced from 10 s to 1 s). The test has been repeated on a more recent version of MELCOR to determine whether or not this defect has been corrected and to examine a wider variation in parameters.

The oscillatory behavior that occurred when using an earlier version of MELCOR was not present in any of the cases examined here. As an example, plots of the transient temperatures, pressures, control volume masses, and system time step for Case 1 are included in Figure 13.

## 6. Summary and Conclusions

The previous MELCOR defect that produced oscillatory behavior for this test has been corrected. The current version of MELCOR (1.6) produces results that agree very well with the analytic solution.

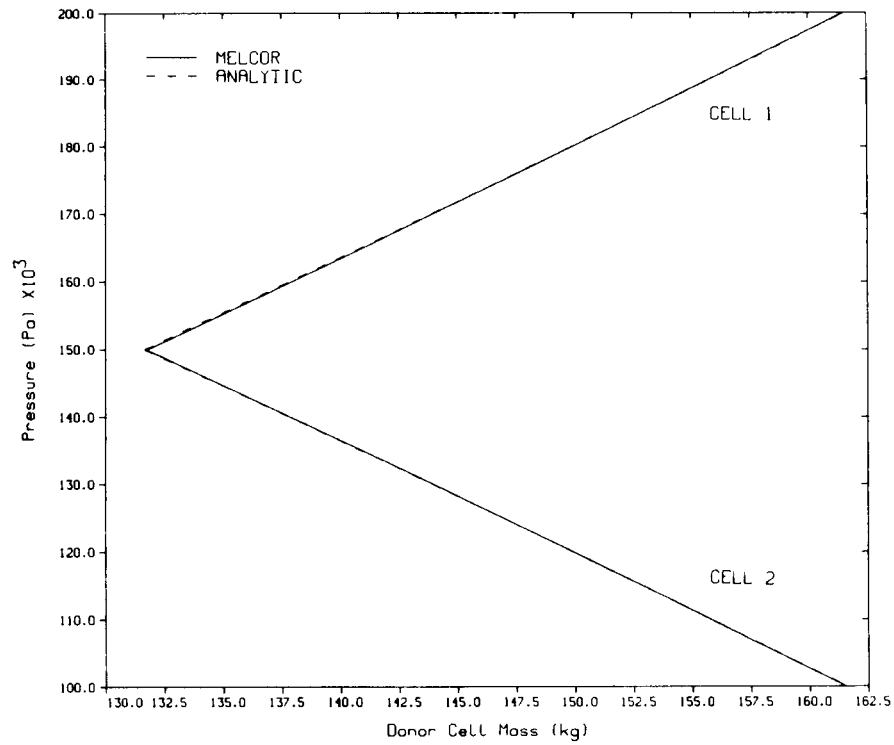


Figure 1. Pressure in Both Cells as a Function of Cell 1 Mass for Case 1.

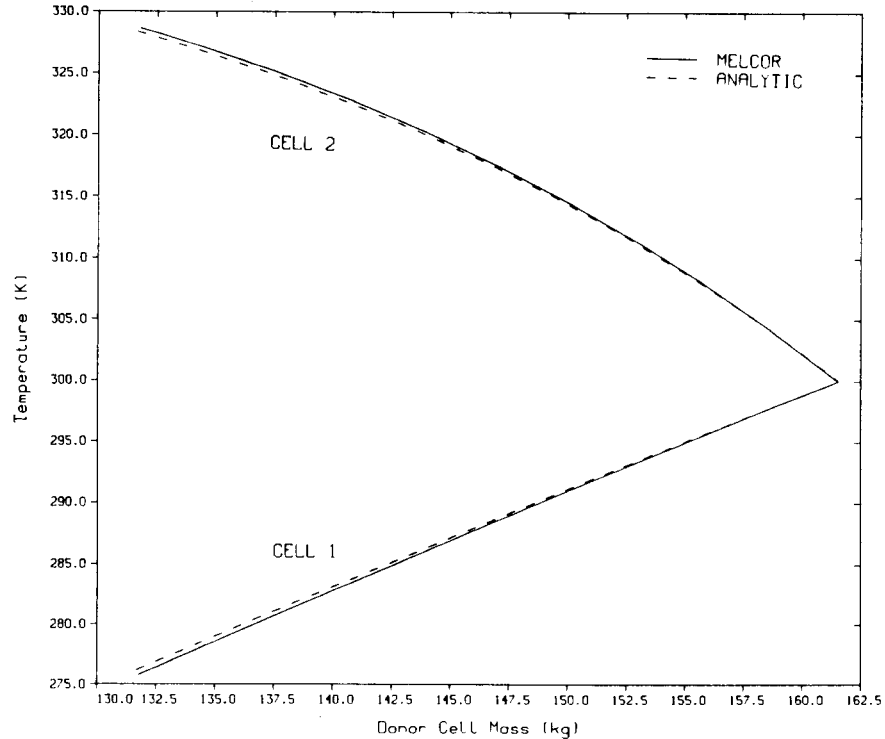


Figure 2. Temperature in Both Cells as a Function of Cell 1 Mass for Case 1.



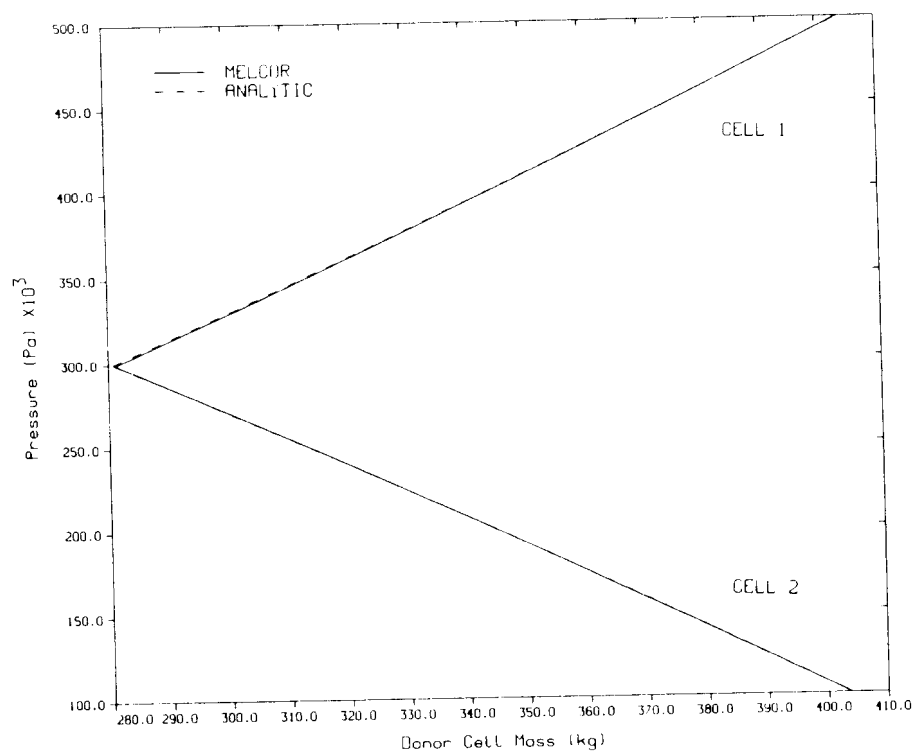


Figure 3. Pressure in Both Cells as a Function of Cell 1 Mass for Case 2.

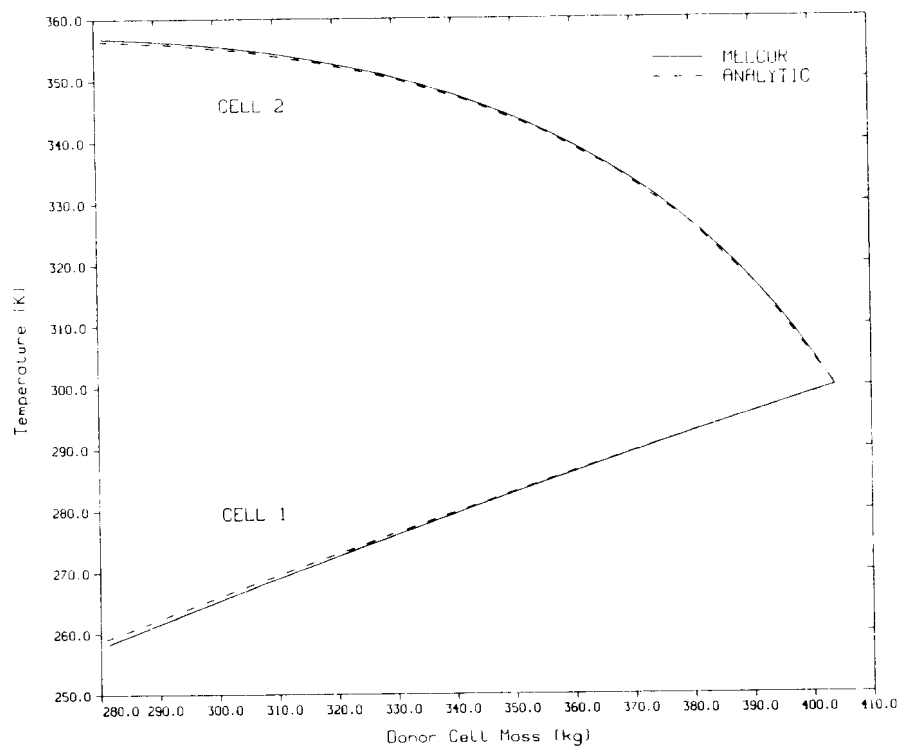


Figure 4. Temperature in Both Cells as a Function of Cell 1 Mass for Case 2.

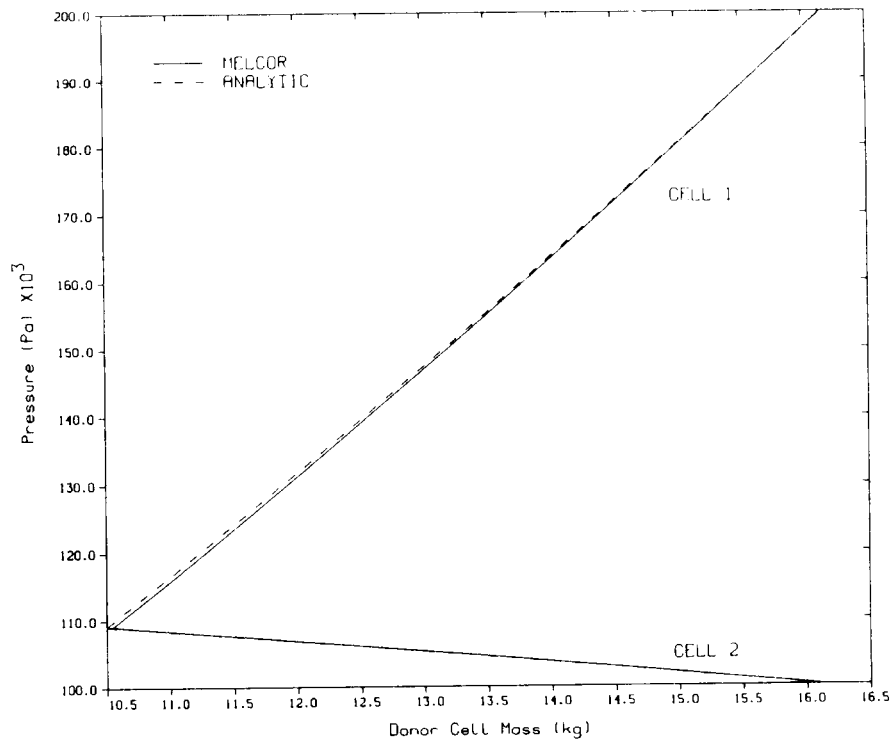


Figure 5. Pressure in Both Cells as a Function of Cell 1 Mass for Case 3.

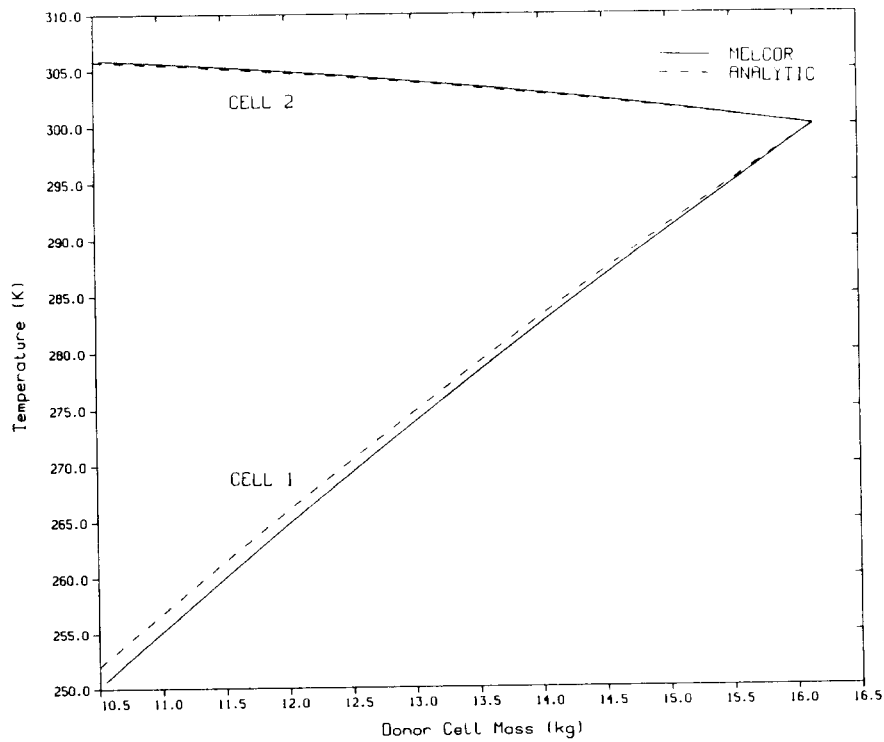


Figure 6. Temperature in Both Cells as a Function of Cell 1 Mass for Case 3.

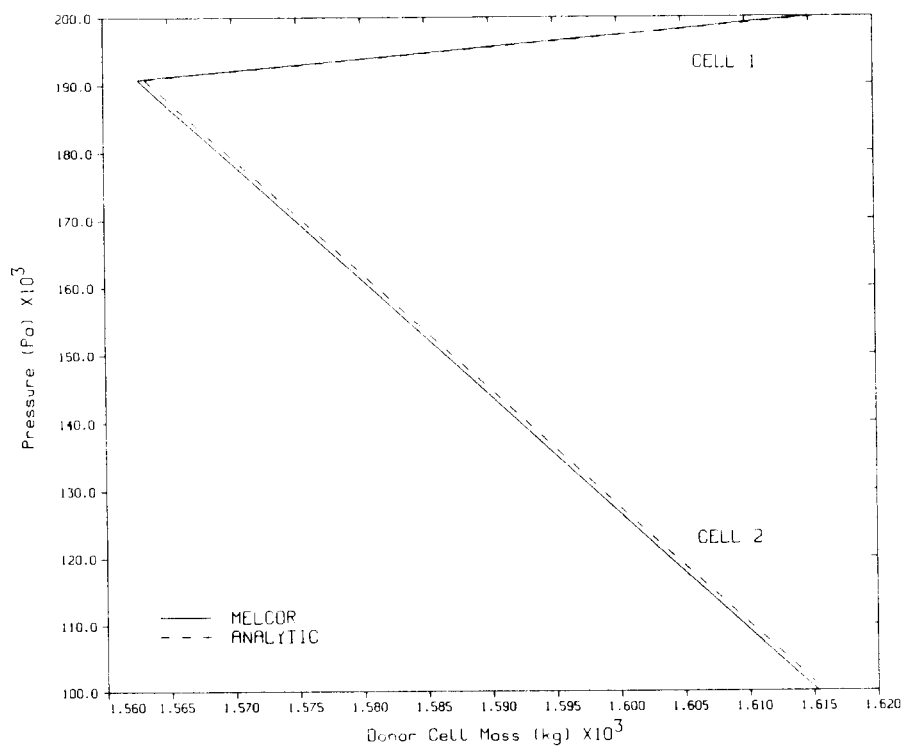


Figure 7. Pressure in Both Cells as a Function of Cell 1 Mass for Case 4.

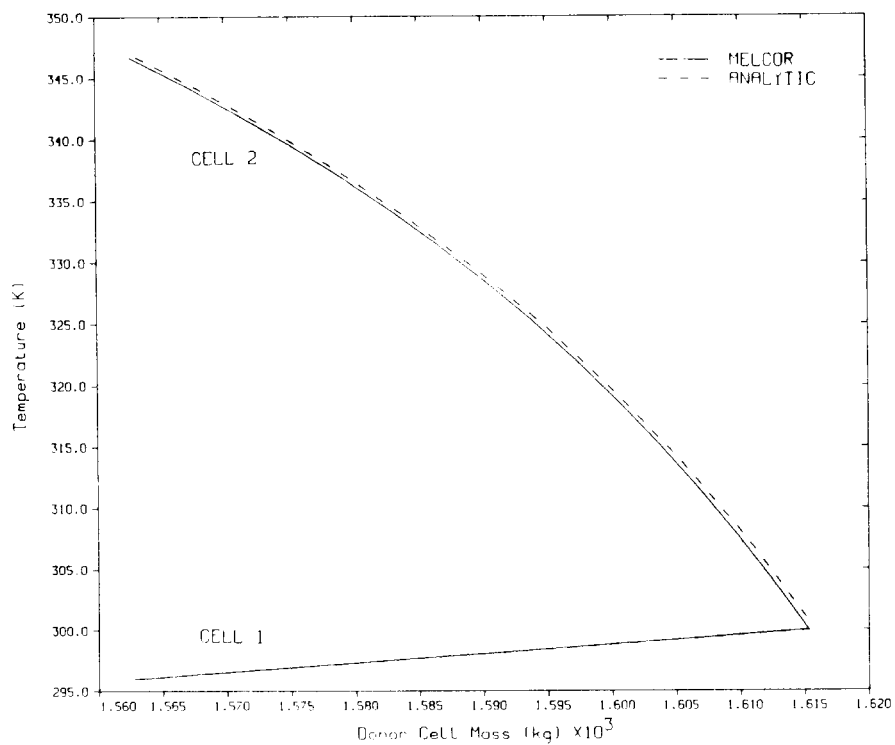


Figure 8. Temperature in Both Cells as a Function of Cell 1 Mass Case 4.

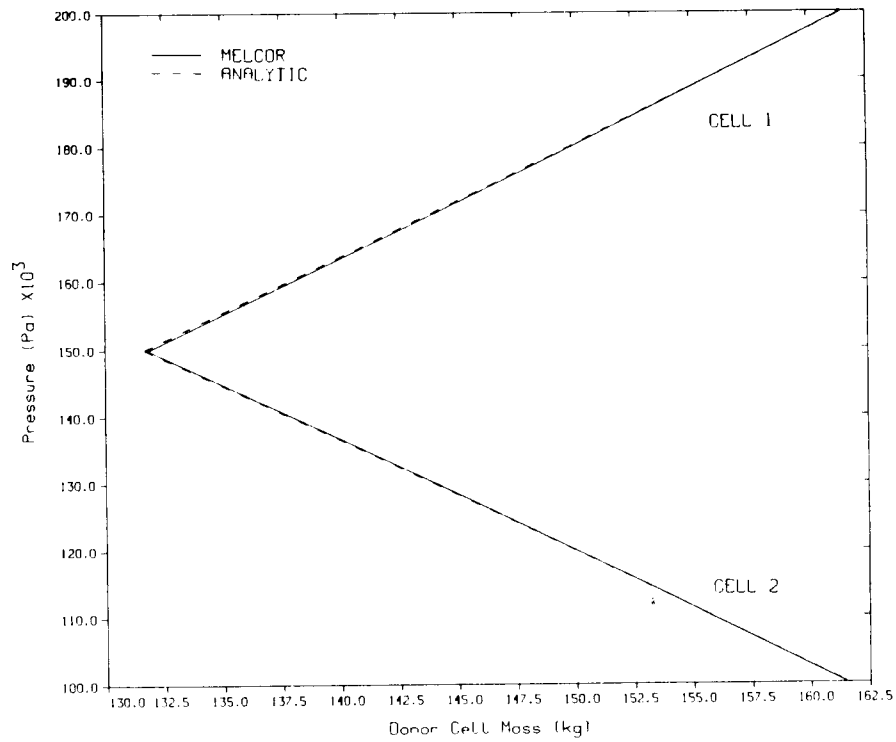


Figure 9. Pressure in Both Cells as a Function of Cell 1 Mass for Case 5.

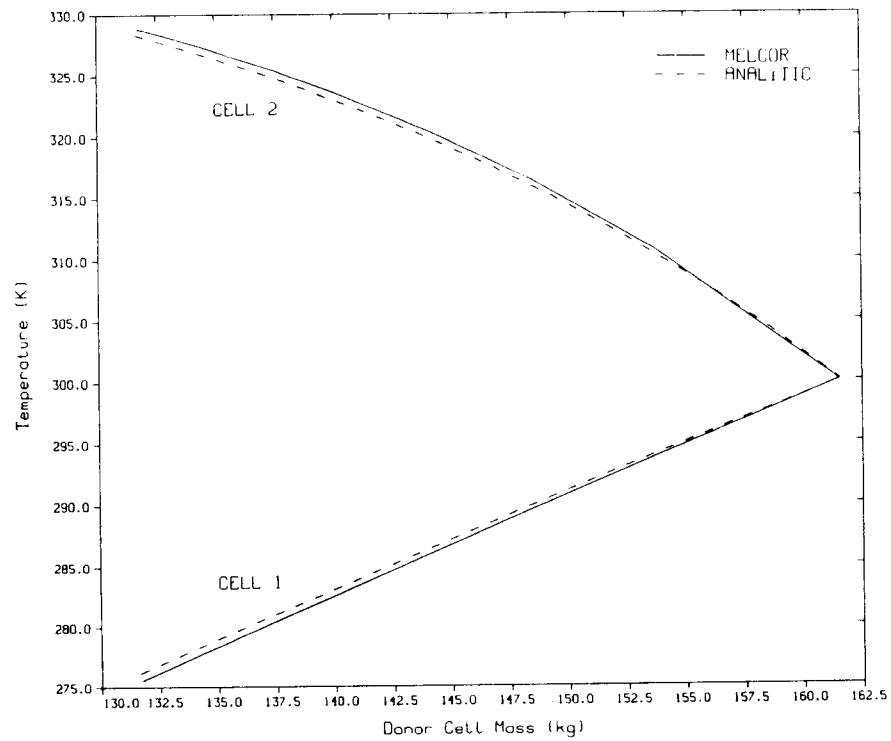


Figure 10. Temperature in Both Cells as a Function of Cell 1 Mass Case 5.

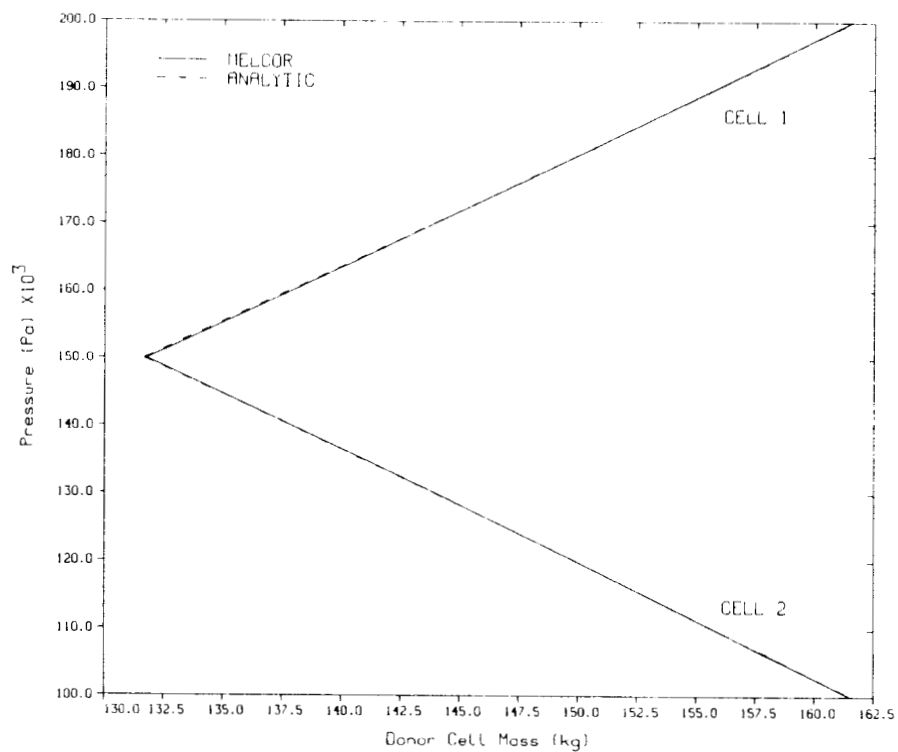


Figure 11. Pressure in Both Cells as a Function of Cell 1 Mass for Case 6.

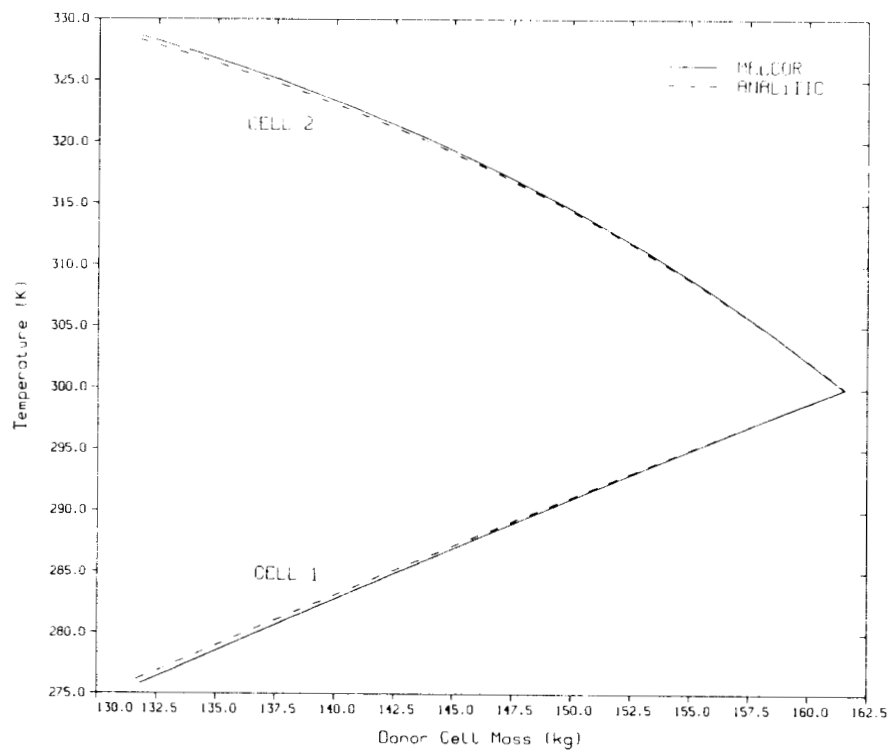


Figure 12. Temperature in Both Cells as a Function of Cell 1 Mass Case 6.

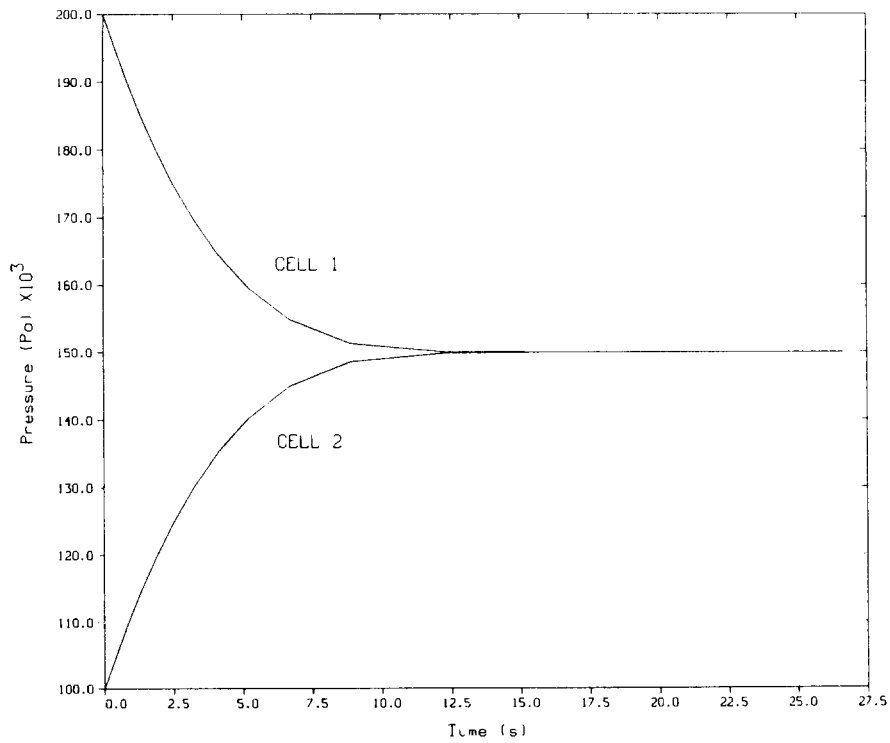
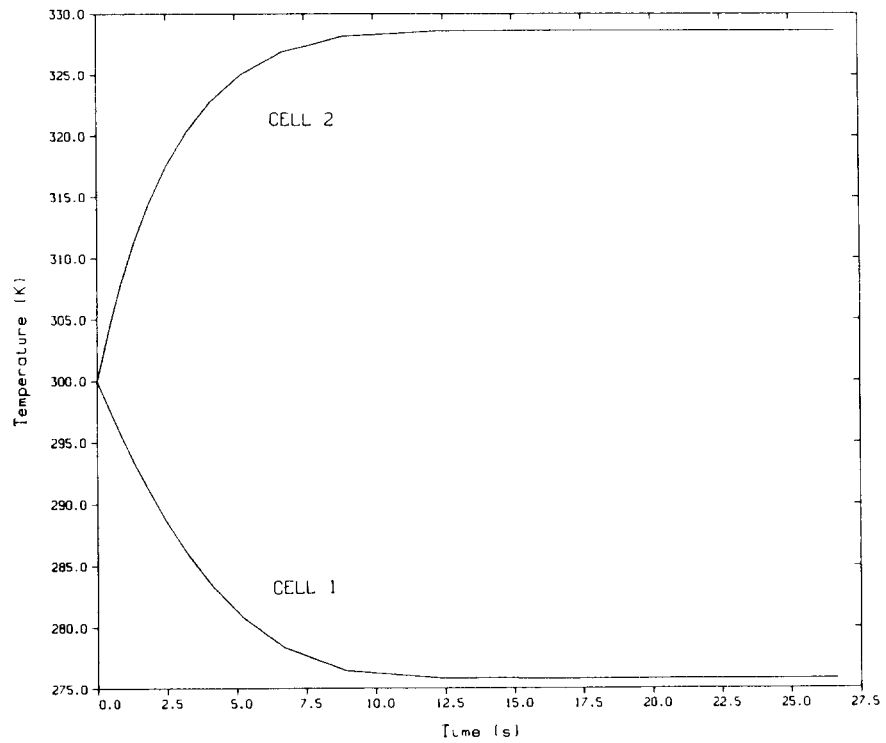


Figure 13. Time dependent Behavior for Case 1.

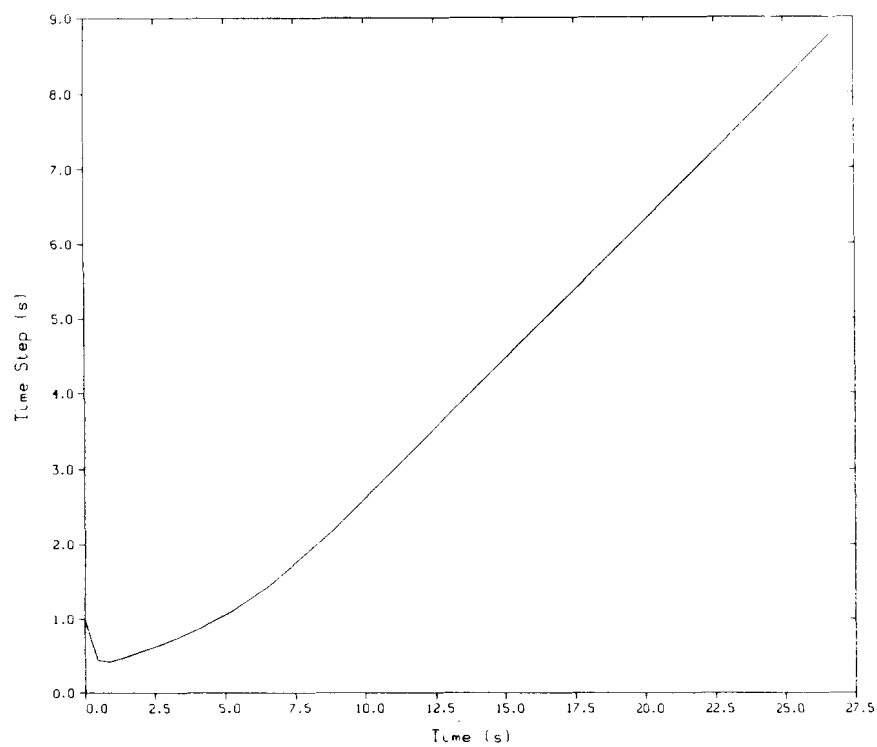
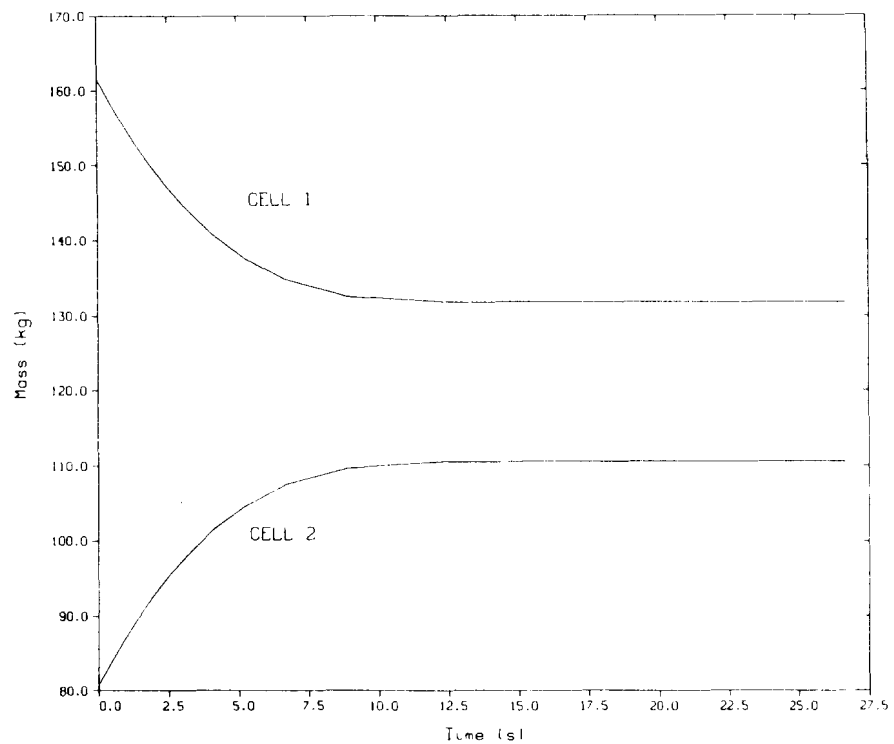


Figure 13 (cont.). Time dependent Behavior for Case 1.





MELCOR 1.6 Calculations for a  
Saturated Liquid Depressurization Test

C. J. Shaffer  
Science and Engineering Associates  
Albuquerque, New Mexico 87110  
United States of America

Abstract

A simple test involving a volume containing saturated water at high pressure depressurizing into a second larger volume tests MELCOR's ability to predict the depressurization of a reactor vessel into its containment. The results show good agreement between the MELCOR and analytical solutions.

1. Introduction

The analysis of severe accidents involves predicting the depressurization of the reactor vessel into its containment. For some accident sequences, the reactor vessel contains significant quantities of high pressure, high temperature water which will undergo rapid flashing during depressurization. MELCOR's ability to predict this depressurization is tested using a simple model with an analytical solution.

2. Test Description

A volume containing saturated water at high pressure is connected to another volume containing only a low pressure steam atmosphere by a flow path and a heat structure. The flow path is opened at time zero and the system is allowed to come into pressure and thermal equilibrium. The heat structure which thermally equilibrates the two volumes is thin enough to be unimportant in the energy balances. The initial conditions are listed in Table 1 and the system is shown schematically in Figure 1.

Table 1. Initial Conditions for the Depressurization Test

Initial Conditions	Volume 1	Volume 2
Pressure (MPa)	7.999	0.01
Temperature (K)	568.23	568.23
Water Mass (kg)	72240	0.0
Steam Mass (kg)	0.0	152.57
Void Fraction	0.0	1.0

```

*****
*                                     *
*                                     *
*   Volume 2                         *
*   4000 m3                         *
*                                     *
*                                     *
*                                     *
*                                     *
*                                     *
*                                     *
*****
*                                     *
*   0.02 m2                         *
*   Volume 1                         *
*   100 m3   ***                     *
*                                     *
*   ***                     *
*   ***HS                   *
*   ***                     *
*****

```

Figure 1: Model Description

### 3. Analytical Solution

The analytical solution is obtained from mass and energy balances.

$$u_f + xu_{fg} = (U_o + E_s) / M_t \quad (1)$$

$$v_f + xv_{fg} = V / M_t \quad (2)$$

$$U_o = M_{1o}u_{1o} + M_{2o}u_{2o} \quad (3)$$

$$E_s = M_s C_p (T_i - T_f) \quad (4)$$

where

$u_f$  = specific internal energy of liquid  
 $u_{fg}$  = specific internal energy of evaporation  
 $v_f$  = specific volume of liquid  
 $v_{fg}$  = specific volume of evaporation  
 $x$  = steam quality at equilibrium  
 $M_t$  = total H2O mass  
 $V$  = total volume  
 $M_{1o}$  = initial volume 1 mass  
 $M_{2o}$  = initial volume 2 mass  
 $u_{1o}$  = initial specific internal energy of volume 1  
 $u_{2o}$  = initial specific internal energy of volume 2  
 $M_s$  = mass of structure

$C_p$  = structure specific heat  
 $T_i$  = initial structure temperature  
 $T_f$  = final structure temperature

This test was designed with  $E_s$  about six orders of magnitude smaller than  $U_0$  so the structure can be removed from the energy balance.

Using the Keenan and Keyes[1] steam tables and the initial conditions of Table 1, the above equations reduce to the following.

$$u_f + xu_{fg} = 1.30886E6 \quad (\text{J/kg}) \quad (5)$$

$$v_f + xv_{fg} = 0.0566356 \quad (\text{m}^3/\text{kg}) \quad (6)$$

Equations 5 and 6 are solved for the steam quality by iterating on pressure. The final values are 1.037 MPa with a saturation temperature of 454.7 K and a quality of 0.297.

#### 4. Results

The MELCOR results are compared to the analytical solution in Table 2. The MELCOR calculation was run using MELCOR 1.6 on a VAX and the results taken from the largest volume (volume 2). At the end of the calculation (3000 seconds), the pressures and temperatures of the two volumes differed by only 0.0003 MPa and 0.28 K.

Table 2. Comparison of Results

		Analytical	MELCOR	Difference
Pressure	MPa	1.037	1.034	0.003 (0.3%)
	Psia	150.6	150.0	0.6
Temperature	K	454.7	454.8	0.1
	F	358.8	359.0	0.2
Quality	-	0.297	0.2964	0.0006 (0.2%)

#### 5. Conclusions

These results show good agreement between MELCOR predictions and the analytical solution. They demonstrate MELCOR's ability to predict the depressurization of a reactor vessel into its containment with the involvement of very rapid flashing of saturated water within the vessel. Even the small differences noted in Table 2 could be due to the slight non-equilibrium that exists at the end of the calculation.

## 6. References

1. J.H. Keenan, F.G. Keyes, P.G. Hill, and J.G. Moore, Steam Tables: Thermodynamic Properties of Water Including Vapor, Liquid, and Solid Phases (International System of Units-S.I.), John Wiley and Sons, 1969.

MELCOR 1.6 Calculations for the  
HDR Containment Experiment V44

C. J. Shaffer  
Science and Engineering Associates  
Albuquerque, New Mexico 87110  
United States of America

Abstract

The MELCOR code has been used to simulate the HDR experiment V44. The HDR-V44 experiment is a reactor-scale steam blowdown experiment conducted in 1982 by Kernforschungszentrum Karlsruhe (KfK) at the decommissioned HDR reactor facility near Frankfurt, West Germany. The MELCOR predicted peak containment pressure is about 24% higher than measured but the longer term pressures are in good agreement. The MELCOR predicted main compartment temperature peaks about 20 K higher than measured with good long term agreement. Agreement between MELCOR predictions and the experimental results is similar to that obtained using the CONTAIN code.

1. Introduction

The containment of a nuclear power plant constitutes the final barrier against the accidental release of radioactive fission products to the environment. The reactor-scale steam blowdown experiments conducted at the HDR facility near Frankfurt, West Germany by Kernforschungszentrum Karlsruhe (KfK) in 1982 [1] contribute to the understanding of the physical processes taking place within the containment after a loss-of-coolant accident and expand the data base of energy and mass transfer within a large and complex containment building. The HDR containment is enclosed by a cylindrical steel shell with an overall height of 60 meters, a diameter of 20 meters, and a total volume of 11,300 cubic meters. The primary containment is subdivided by concrete walls into 62 subcompartments containing a large amount of internal metallic structures.

Experiment V44 is one of a series of six water and steam blowdown experiments conducted to simulate full-scale loss-of-coolant accidents. Experiment V44 was initiated from saturated steam conditions, and had the highest reactor pressure vessel liquid level with the vessel nearly full. A MELCOR 1.6 calculation has been performed for the HDR-V44 experiment, and the results have been compared to the experimental data[2] and the CONTAIN calculation for HDR-V44[3].

## 2. Test Description

The HDR containment is enclosed by a cylindrical steel shell with an overall height of 60 m, a diameter of 20 m, and a total volume of 11,300 m<sup>3</sup> as shown in Figures 1 and 2. An outer concrete containment surrounds the steel shell leaving an annular space between the primary and secondary containments. The primary containment is subdivided by concrete walls into 62 subcompartments with widely differing and complex shapes containing a large amount of internal metallic structure. The HDR containment in general has a high ratio of surface area to volume, a high steel to concrete surface area ratio, and complex interior geometries. The reactor pressure vessel which has a central stand pipe mounted inside for bottom discharge, blows down into the break subcompartment (room 1603) onto a jet impingement plate just downstream of the discharge pipe. The location of the break is a radius of 6.5 m, an angle of 206 degrees, and an elevation of 14.5 m (bottom of the steel containment shell is at an elevation of -10.0 m). The experimental blowdown mass and energy flow rates are shown in Figures 3 and 4. The test instrumentation includes about 230 pressure and temperature sensors. The sensors selected for comparison with MELCOR results are listed in Table 1.

Table 1: Sensors Selected for Comparison

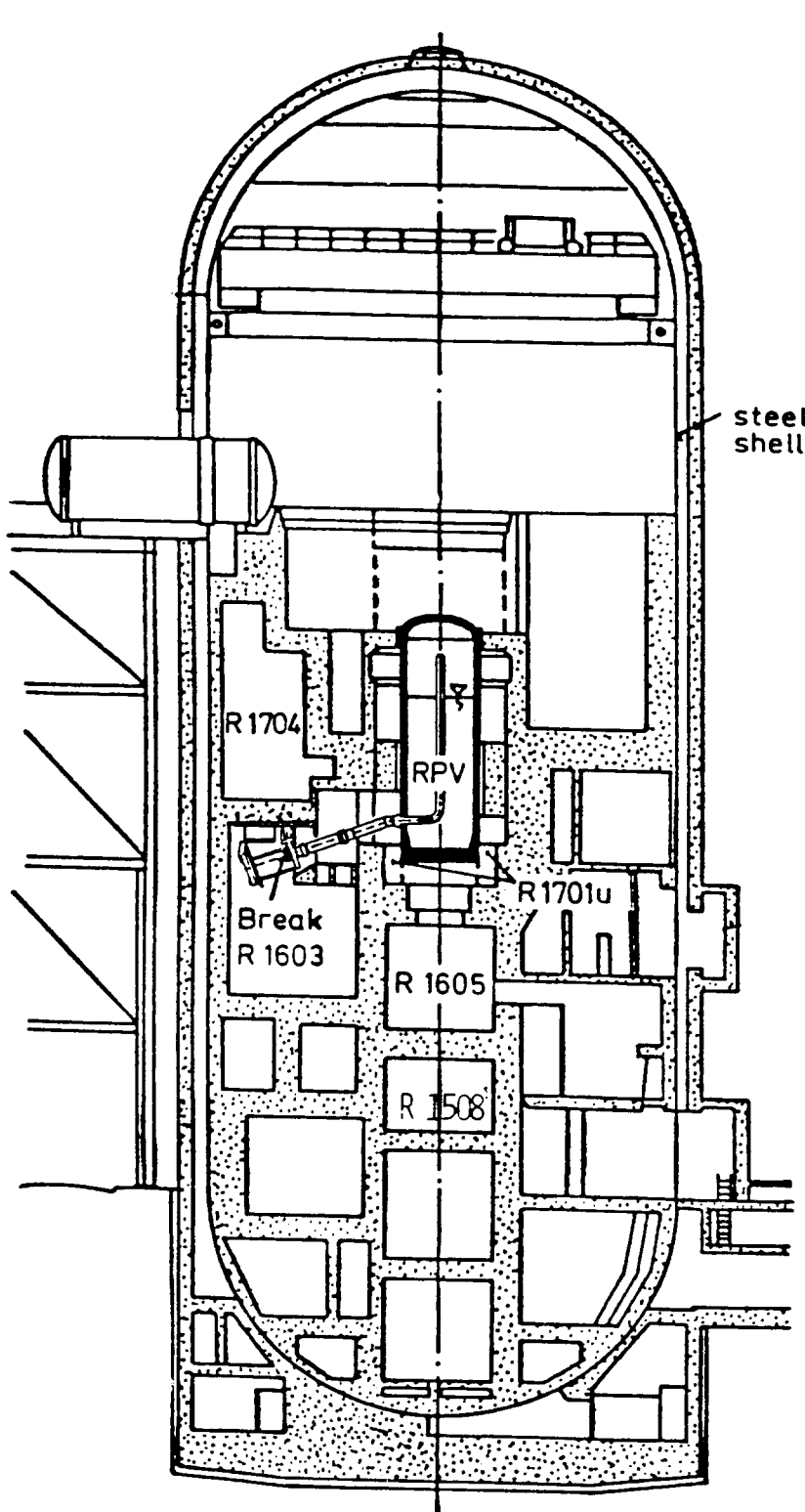
Sensor	Type	Location		
		Radius (m)	Angle (deg.)	Elevation (m)
CP6202	Pressure	10.05	0	11.0
CP6311	Pressure	4.96	245	10.5
CT403	Temperature	0.00	0	50.0
CT404	Temperature	1.95	50	40.0
CT406	Temperature	1.10	50	45.0
CT410	Temperature	3.10	50	34.0
CT6303	Temperature	8.65	220	10.7
CT6605	Temperature	5.00	280	10.7

## 3. Computer Model

The MELCOR calculation for HDR-V44 is patterned after a simulation that was performed with CONTAIN[3]. The MELCOR computer model consists of 5 volumes, 9 flow paths, and 41 heat structures. The heat structures are either steel, concrete, or steel lined concrete.

The experimentally measured blowdown flow shown in Figures 3 and 4 is input as a fog source into volume 1 (break room) with tabular input. The reactor vessel is not modeled.

Volume descriptions are shown in Table 2. Volume 1 consists only of containment room 1603 where the vessel break occurs. Volumes 2 and 3 are relatively small



### HDR containment data

Diameter: 20 m  
 Height: 60 m  
 Volume: 11.300 m<sup>3</sup>  
 Internal surface area: 30.000 m<sup>2</sup>  
 Number of compartments: 62

Figure 1. The HDR Containment

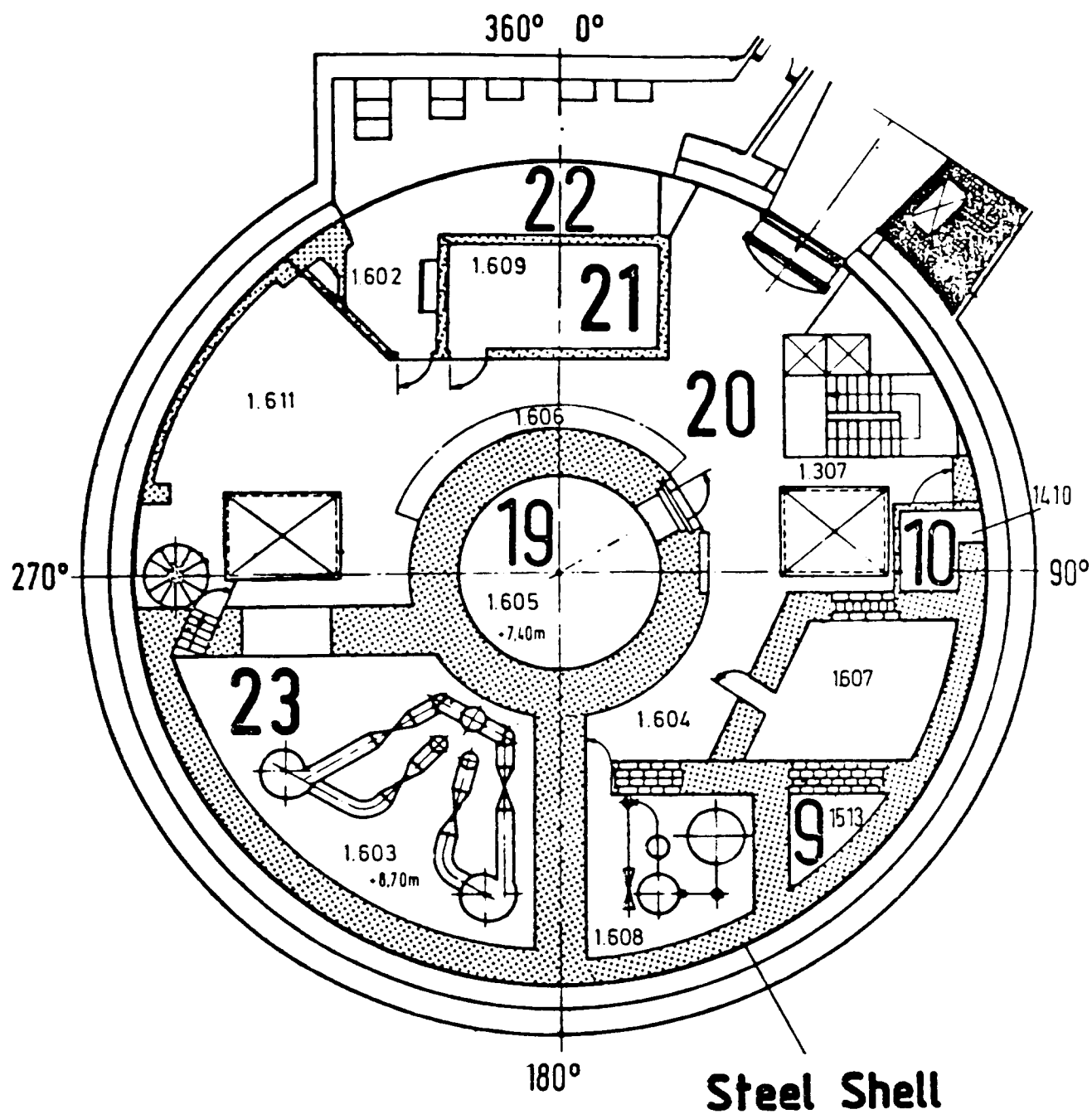


Figure 2. Plan View of the HDR Containment at the Break Room Level



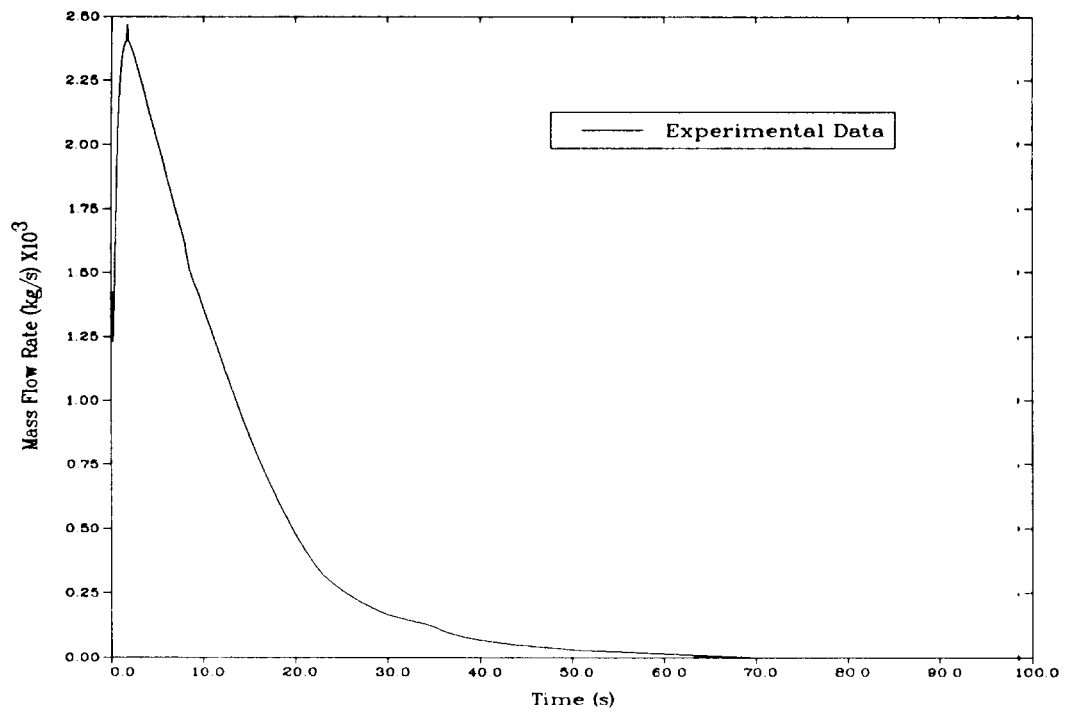


Figure 3. Blowdown Mass Flow Rate

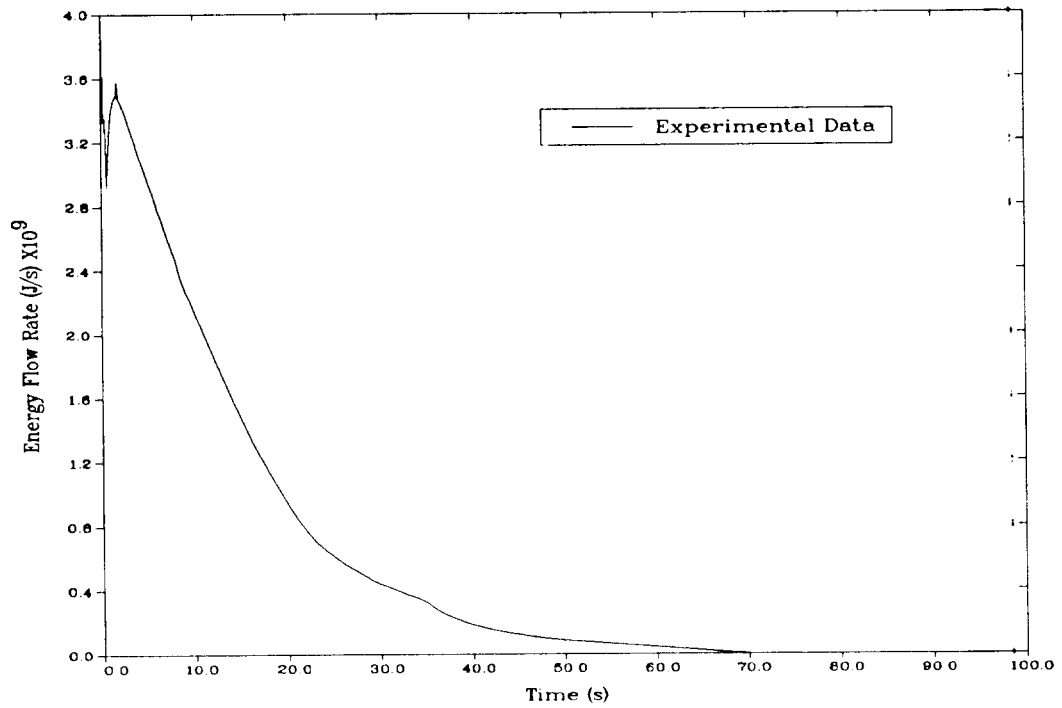


Figure 4. Blowdown Energy Flow Rate

Table 2: Volume Descriptions

No.	Description	Volume m <sup>3</sup>	Lower Elevation m	Upper Elevation m	Height m	Floor Area m <sup>2</sup>
1	R1603	280	18.8	26.3	7.5	37.3
2	R1701u	44	24.0	34.4	10.4	4.2
3	R1701o,1704	912	27.6	35.9	8.3	109.9
4	R1201-1514	3003	4.0	18.0	14.0	214.5
5	R1602-11004	7102	35.4	63.5	28.1	252.7

Table 3: Flow Path Descriptions

No.	From Vol.	To Vol.	From Alt. m	To Alt. m	Flow Area m <sup>2</sup>	Flow Diameter m	Flow Length m	Loss Coefficient
1	1	2	24	25	3.196	2.017	2.0	1.028
2	1	3	26	28	2.593	1.817	3.0	0.866
3	1	4	19	17	0.283	0.600	3.0	1.636
4	1	5	26	36	2.128	1.646	11.0	1.116
5	2	3	28	29	1.700	1.471	2.0	1.020
6	2	5	34	36	1.374	1.323	3.0	1.389
7	3	4	28	17	1.500	1.382	12.0	1.389
8	3	5	35	36	15.014	4.372	12.0	0.782
9	4	5	17	36	14.049	4.229	20.0	0.803

volumes located next to the break room. Volume 4 consists of rooms numbered 1201 through 1514 which comprise the lower portion of the containment. Volume 5 consists of rooms numbered 1602 through 11004 which comprise the upper or dome portion of the containment. The sensors chosen for comparison with MELCOR are located in volumes 1 and 5. All volumes were initialized at atmospheric pressure, a temperature of 300 K (80 F), 100% relative humidity, and with dry floors. Flow path descriptions are shown in Table 3. All volumes are directly interconnected except volumes 2 and 4.

Heat structure descriptions are shown in Table 4. Logarithmic spaced nodes were used for all structures. Three structures were steel lined concrete. Left surfaces are in the indicated volumes and right surfaces are adiabatic. Only MELCOR calculated heat transfer coefficients are used. The calculation was started at the initiation of reactor vessel blowdown and continued to 3600 seconds.

Table 4: Heat Structure Descriptions

No.	Volume Left Right		Type	Material	Area m <sup>2</sup>	Thickness m	No. Nodes
1	1	1	wall	steel	196.8	0.001351	7
2	1	1	wall	steel	287.0	0.006118	9
3	1	1	wall	steel	144.2	0.02218	11
4	1	1	wall	steel	1.5	0.02029	11
5	1	AD*	wall	concrete	240.0	0.3048	16
6	1	AD	roof	concrete	45.2	0.3048	16
7	1	AD	floor	concrete	45.2	0.3048	16
8	2	2	wall	steel	93.0	0.001461	7
9	2	2	wall	steel	63.8	0.006746	9
10	2	2	wall	steel	20.9	0.02078	11
11	2	2	wall	steel	28.3	0.1196	13
12	2	AD	wall	st/conc	46.1	0.3302	22
13	2	AD	wall	concrete	28.7	0.3048	16
14	2	AD	roof	concrete	35.9	0.3048	16
15	2	AD	floor	concrete	35.9	0.3048	16
16	3	3	wall	steel	1028.0	0.001169	7
17	3	3	wall	steel	87.5	0.005772	9
18	3	3	wall	steel	28.4	0.01998	11
19	3	3	wall	steel	12.4	0.04977	15
20	3	AD	wall	concrete	730.5	0.3048	16
21	3	AD	wall	steel	6.2	0.060	8
22	3	AD	wall	st/conc	30.2	0.3302	22
23	3	AD	roof	concrete	106.3	0.3048	16
24	3	AD	floor	concrete	106.3	0.3048	16
25	4	4	wall	steel	3253.0	0.0009542	7
26	4	4	wall	steel	1967.0	0.006276	9
27	4	4	wall	steel	40.6	0.022295	11
28	4	4	wall	steel	11.3	0.03628	11
29	4	AD	wall	concrete	3370.4	0.3048	16
30	4	AD	wall	steel	199.6	0.030	7
31	4	AD	roof	concrete	624.8	0.3048	16
32	4	AD	floor	concrete	624.8	0.3048	16
33	5	5	wall	steel	3197.0	0.0009908	7
34	5	5	wall	steel	3667.0	0.0059235	9
35	5	5	wall	steel	404.6	0.01402	11
36	5	5	wall	steel	190.3	0.05196	13
37	5	AD	wall	concrete	1896.5	0.3048	16
38	5	AD	wall	steel	1605.3	0.027	7
39	5	AD	wall	st/conc	599.9	0.3302	22
40	5	AD	roof	concrete	595.9	0.3048	16
41	5	AD	floor	concrete	595.9	0.3048	16

\* AD indicates an adiabatic boundary is assumed.

#### 4. Results

The MELCOR results for the containment dome (volume 5) and the break room (volume 1) are compared to experimental data in Figures 5 through 8. Figures 9 and 10 compare the MELCOR results to the corresponding CONTAIN results.

The containment dome pressure calculated by MELCOR is compared in Figure 5 to the data from pressure sensor CP6202 located near the bottom of control volume 5. MELCOR over predicts the peak pressure by about 24% but is in good agreement after about 1000 seconds.

The MELCOR calculated containment dome temperature is compared in Figure 6 to the data from sensors CT403, CT406, CT404, CT410, and CT6605 located at elevations 50.0, 45.0, 40.0, 34.0, and 10.7 m, respectively, within control volume 5. The 50 m elevation is at the top of the dome. These sensors show a pronounced temperature gradient with the elevation within volume 5. For example, the gradient at 2000 seconds is about 0.6 K/m. An experimental volume average temperature would probably be between the 34 and 40 m elevation temperatures. Therefore, MELCOR over predicts the peak temperature by about 20 K but again is in good agreement after about 1000 seconds.

The MELCOR break room results are compared in Figures 7 and 8 with pressure sensor CP6311 and temperature sensor CT6303 for the first 200 seconds. The break room with a volume of only 280 m<sup>3</sup>, experiences extremely dynamic fluid flow and heat transfer processes during the reactor vessel blowdown. MELCOR over predicts the peak break room pressure by about 22% and the peak temperature by only 6 K.

The MELCOR and CONTAIN results are compared in Figures 9 and 10. CONTAIN results[3] are available for the containment dome pressure and temperature to 1500 seconds. These figures show that MELCOR and CONTAIN results are similar and in quite good agreement. The MELCOR predicted pressure is slightly lower and closer to the experimental data than CONTAIN. The MELCOR predicted temperature is slightly higher than CONTAIN and both are within the 34 and 40 m elevation experimental temperatures after about 900 seconds.

#### 5. Code Limitations Identified

This investigation suggests that the MELCOR heat transfer coefficient correlations may not be adequate for dynamic heat transfer during blowdown. The MELCOR calculated heat transfer coefficients during the blowdown are generally less than 20 W/m<sup>2</sup>/K but as high as 200 W/m<sup>2</sup>/K. The experimental data [1], [2], [4] shows heat transfer coefficients in room 1606 near the break room that range from about 6000 to 28000 W/m<sup>2</sup>/K during blowdown. This same MELCOR calculation was run with a fixed heat transfer coefficient of 400 W/m<sup>2</sup>/K for all heat structures. The result of this run was that the MELCOR calculated peak pressures and temperatures were reduced to the same general magnitude as the experimental data. In summary, MELCOR's heat transfer coefficient correlations, which are in keeping with currently accepted containment blowdown coefficient correlations, calculate coefficients too small to predict accurately the very dynamic containment heat transfer during blowdown.

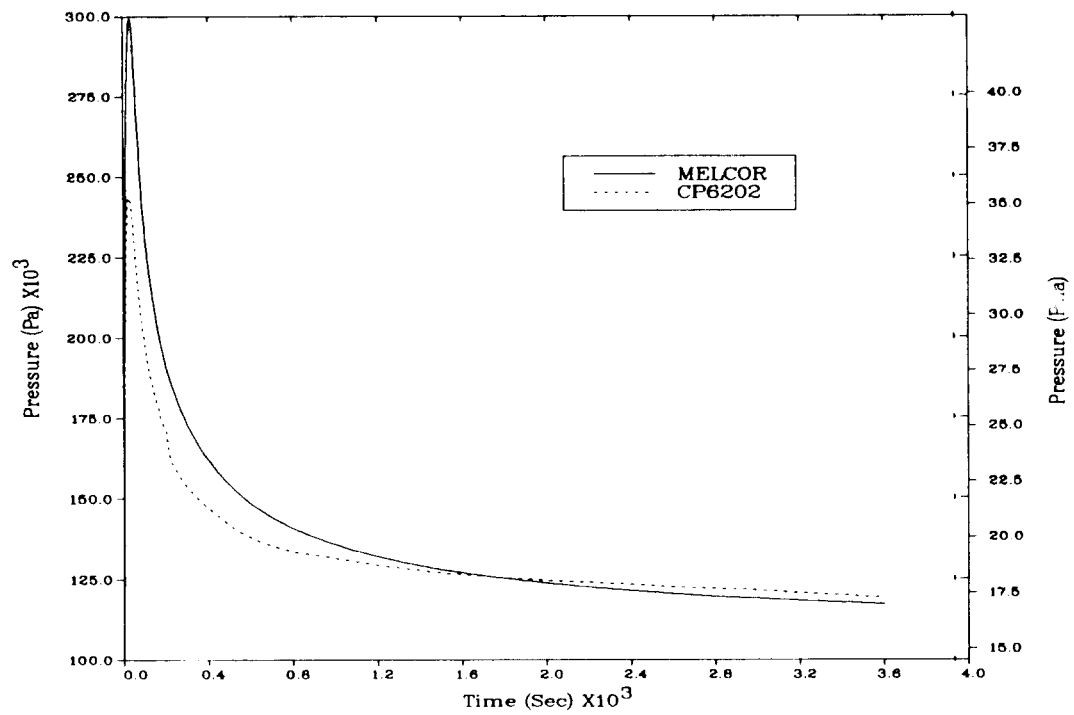


Figure 5. Containment Dome Pressure

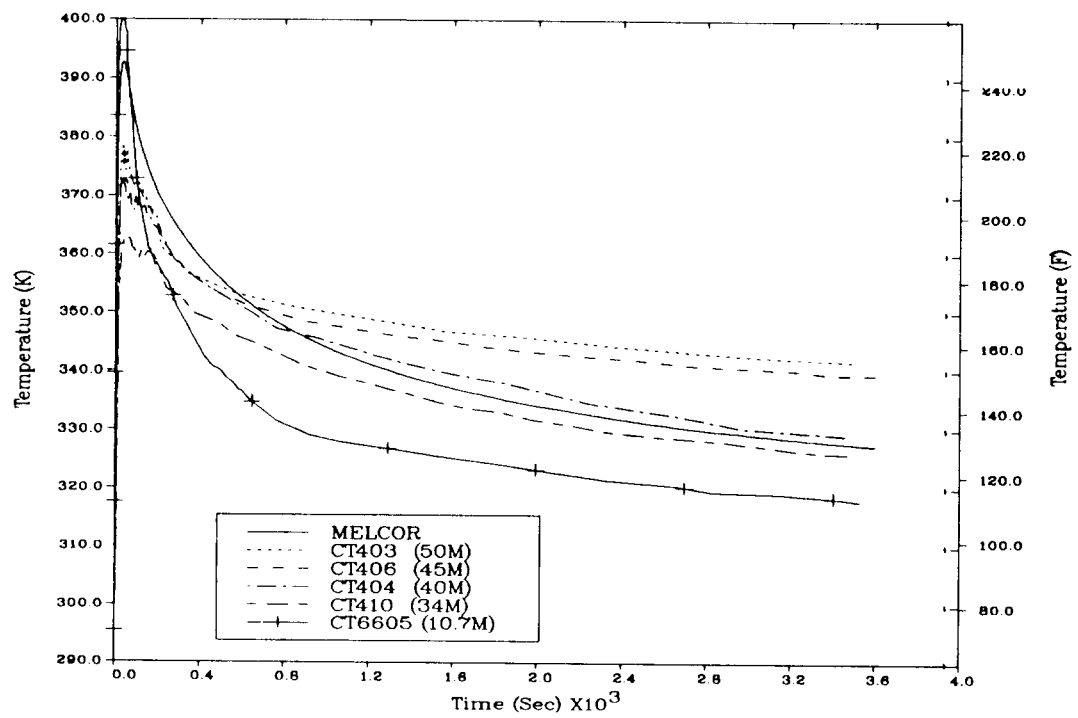


Figure 6. Containment Dome Temperature

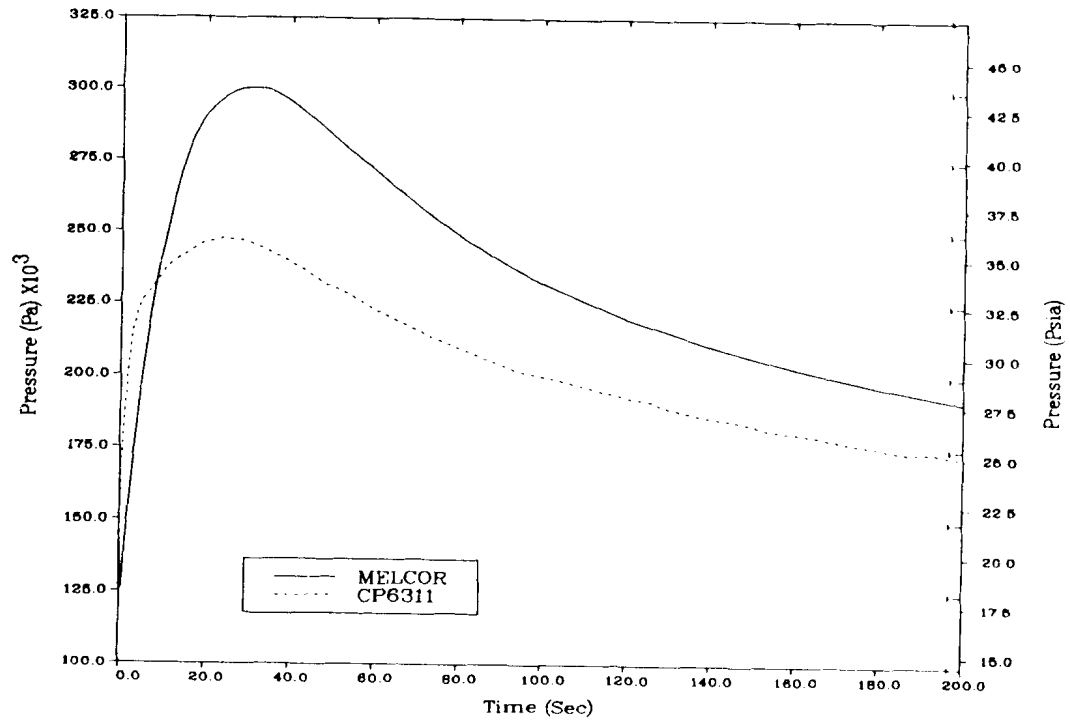


Figure 7. Break Room Pressure

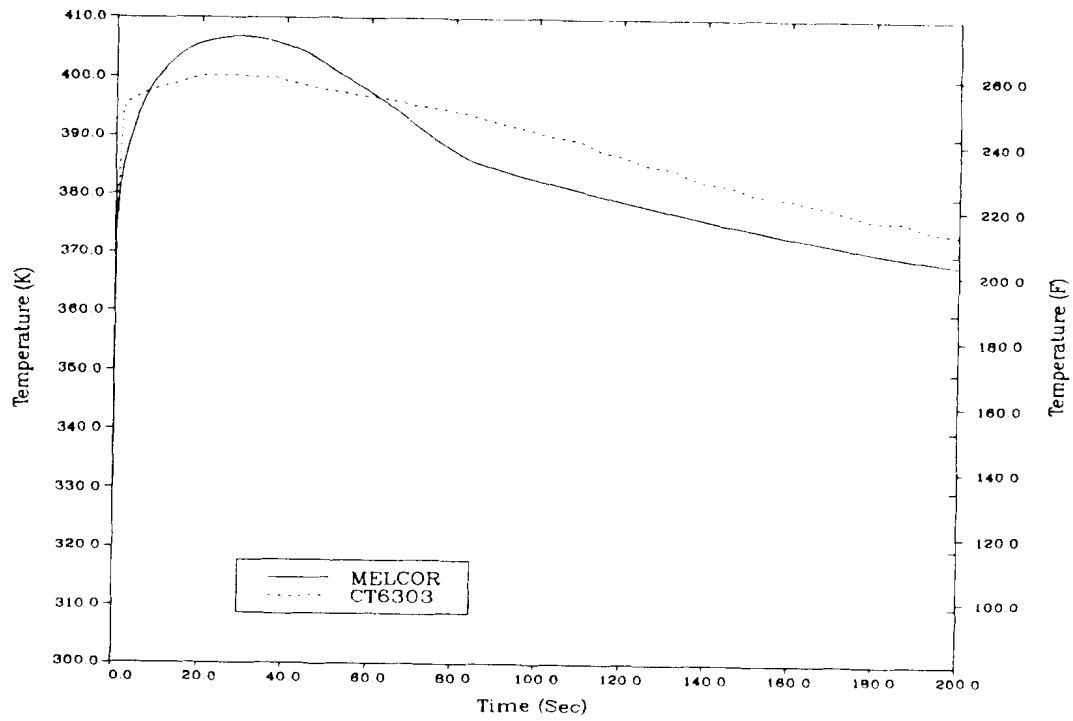


Figure 8. Break Room Temperature

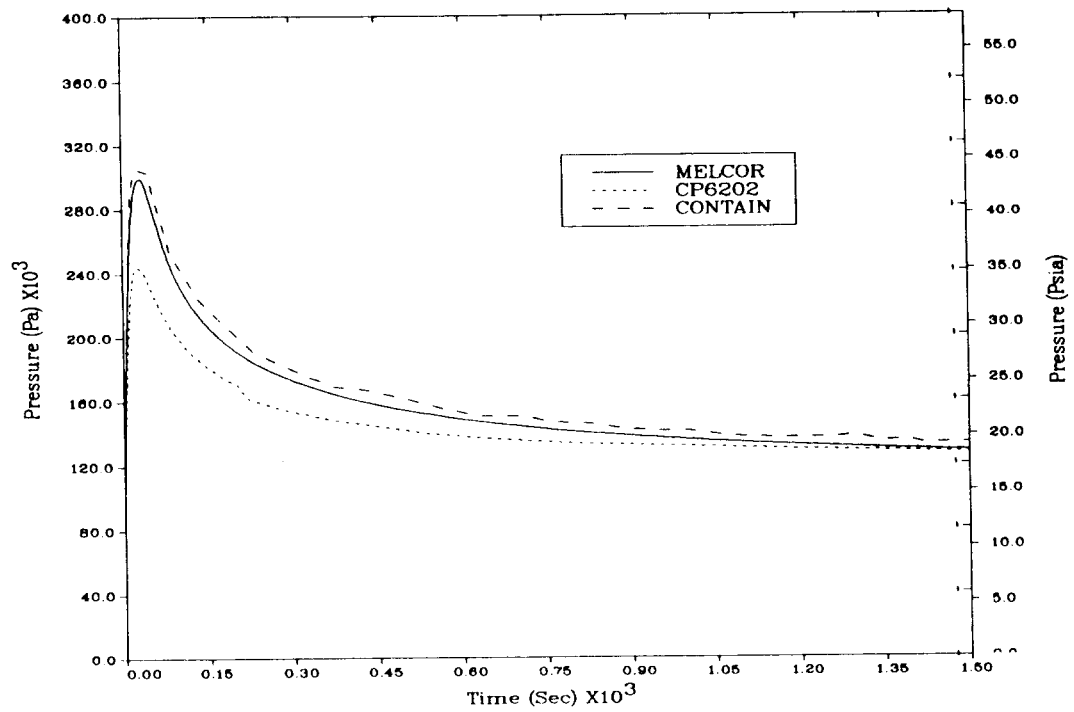


Figure 9. Containment Dome Pressure

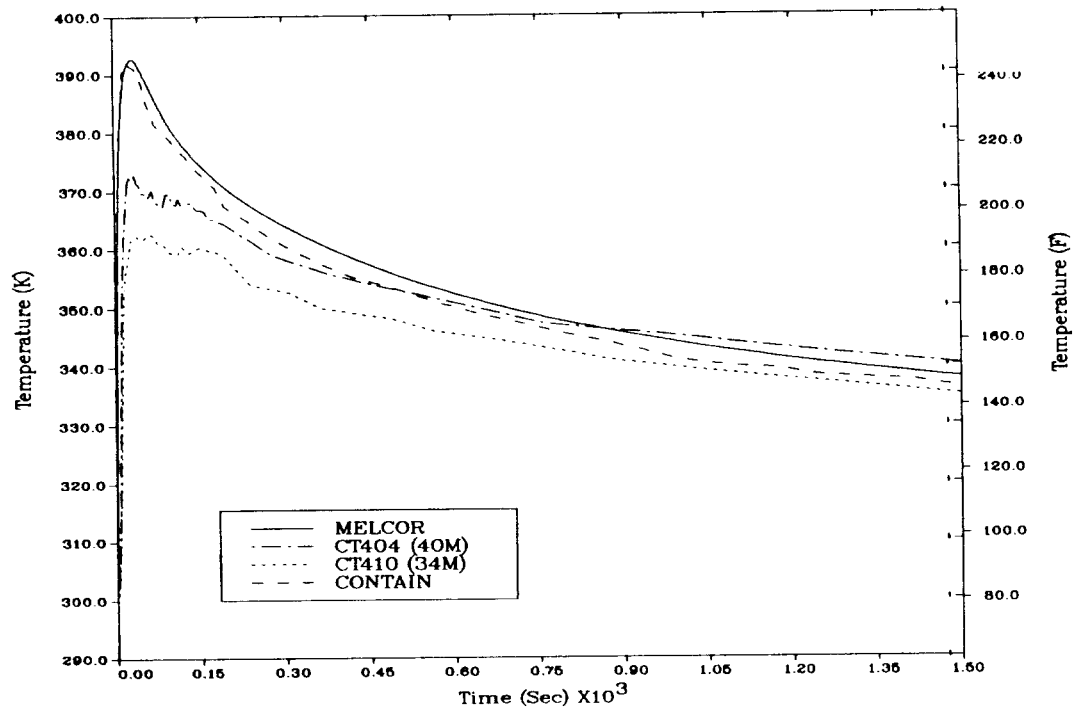


Figure 10. Containment Dome Temperature





# MELCOR 1.0 Calculations for the Battelle-Frankfurt Gas Mixing Tests

R.K. Byers  
Sandia National Laboratories  
Albuquerque, New Mexico 87185  
United States of America

## Abstract

Recent comparisons of MELCOR predictions to the Battelle-Frankfurt Gas Mixing Experiments are presented. These predictions are for a hydrogen-nitrogen gas mixture that is injected into a model containment. The MELCOR results are compared to the experimental data, the results obtained using the HECTR code, and the results obtained using the RALOC code. This comparison provides critical testing of the MELCOR control volume hydrodynamics package and the flow path package.

## 1. Introduction

The Battelle-Frankfurt Mixing Tests were comprised of a series of experiments in which hydrogen-nitrogen mixtures were injected into a model containment at the Battelle Institut e.V. Frankfurt [1],[2]. The containment model was a concrete structure with cylindrical central regions which could be isolated from the upper and asymmetric outer compartments.

## 2. Test Description

In the experiments considered here, the injected gas was two parts hydrogen by volume, introduced at nominally constant rates of  $1 - 2 \text{ m}^3/\text{hr}$  ( $0.15 - 0.3 \text{ g/s}$ ) until the hydrogen amounted to about four percent of the total containment volume. Pressures and temperatures of the mixture were very close to those in the injection region, so the distribution of the injected mixture was governed principally by buoyancy forces. The reported experimental data included variations in the hydrogen concentrations with time and location.

## 3. Model Description

MELCOR calculations were performed for tests BF-2 and BF-6, where only the inner regions of the containment were used (the first sixteen cells in Figure 1a) and for tests BF-10 and BF-19, in which the inner regions could communicate with the outer compartments (using all twenty-eight cells in Figure 1a). The gas injection was modeled as a source in Cell 15 for all four tests. In Tests

2 and 10 uniform initial temperatures in all cells were imposed, while in Tests 6 and 19, the initial temperatures in the upper portion of the containment were approximately 20 and 30 K higher than at the bottom, respectively. These four tests had also been simulated with the RALOC[3] and HECTR[4] codes. The nodalizations used in the MELCOR calculations were, with a few exceptions, the same as those used with RALOC and HECTR and are shown in Figure 1b. The HECTR nodalization for BF-10 and BF-19 involved twenty-two compartments and is shown in Figure 1b. Using a similar twenty-two compartment nodalization with MELCOR proved inadequate, however. In a calculation performed on a VAX computer with no injection, uniform temperature, and an initial pressure distribution corresponding to zero flow in a gravity field, mass flows were observed which were more than three orders of magnitude larger than the specified injection rate for the transient analysis. There are two reasons for these flows of that order of magnitude. First, in the twenty-two volume model shown in Figure 1b there are discontinuities in the bottom elevations of the volumes. When a cell is connected to adjacent cells with differing bottom elevations, there will be a flow generated due to the acceleration of gravity. In addition, when there is no liquid present (as in these calculations), the pressure gradients driving the flow should be very small. The second reason for the magnitude of the flows seen in the steady-state problem has to do with the repeated application of the numerical methods used in MELCOR. In particular, the 32-bit word length used on the VAX might produce unacceptable round-off in long calculations.

Therefore, the twenty-eight volume MELCOR model was developed. This model has fewer discontinuities in cell bottom elevations. In a short calculation with the CRAY version of MELCOR, the initial temperature for Test 10 was specified, and injection was started after 400 seconds of "steady state". The same boundary and initial conditions were used for a calculation on a VAX with the 22-volume model. The 64-bit word length and more uniform elevations in the CRAY calculation combined to produce much smaller mass flows during the steady-state period. In addition, the CRAY and VAX calculations produced significantly different results for the mass distribution of hydrogen (percentage differences were between thirty and forty percent for most locations). For this reason, all subsequent calculations were performed with the CRAY version, and the 28-volume nodalization was used for Tests 10 and 19.

#### 4. Results

Calculated results for Tests 2 and 10 (the tests with uniform initial temperatures) showed good agreement with both experimental data and with the available output from RALOC and HECTR analyses. The calculations with the three codes all used slightly different nodalizations and injection rates, but the calculated results for all three codes were similar as may be seen in Figures 2 and 3. Local hydrogen concentrations increased at almost constant rates until the end of the injection period, and rapidly achieved values corresponding to uniform distribution of the injected hydrogen. RALOC results could only be obtained for about the first 10,000 seconds of Test 10; however, the three codes are so similar in the context of these analyses that no significantly different predictions should be obtained.

In Tests 6 and 19, the initial temperatures in the upper portion of the containment were approximately 20 and 30 K higher than at the bottom,

28-VOLUME MELCOR MODEL for B-F TESTS 10 and 19

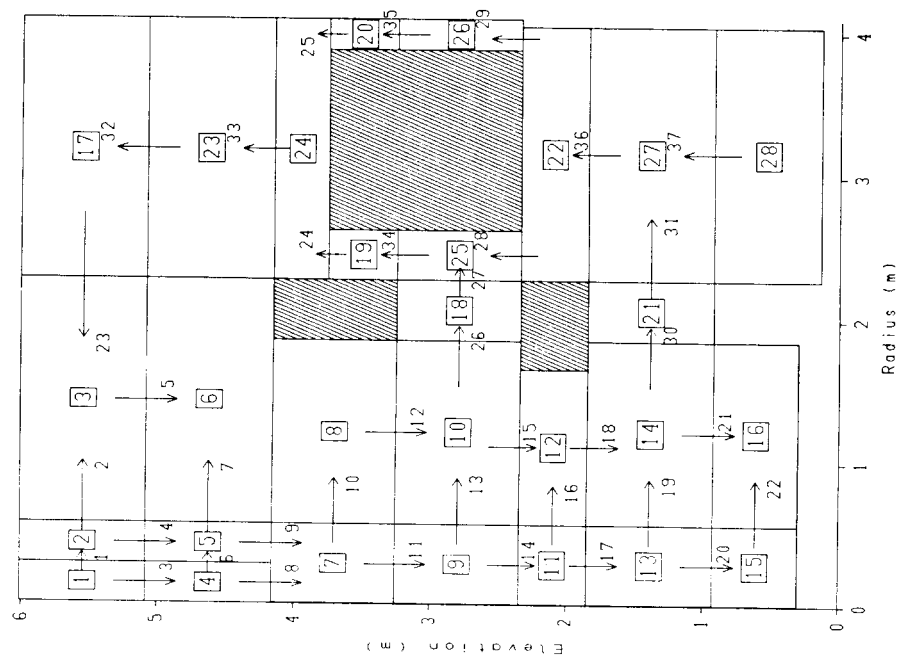


Figure 1a  
28-Volume MELCOR Model for  
Battelle Frankfurt Tests  
10 and 19.

22-VOLUME MELCOR MODEL for B-F TESTS 10 and 19

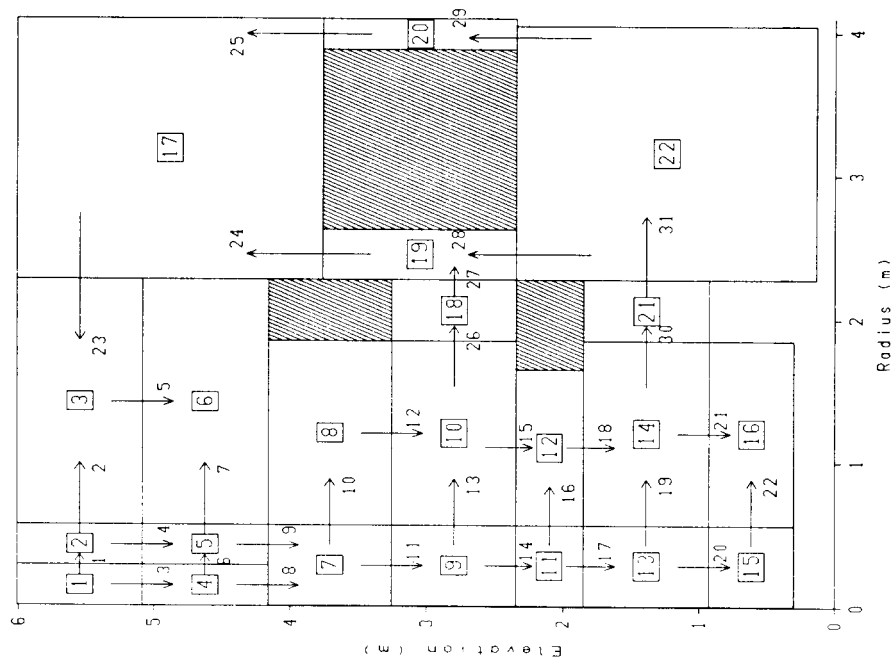


Figure 1b.  
22-Volume MELCOR Model for  
Battelle Frankfurt Tests  
10 and 19.

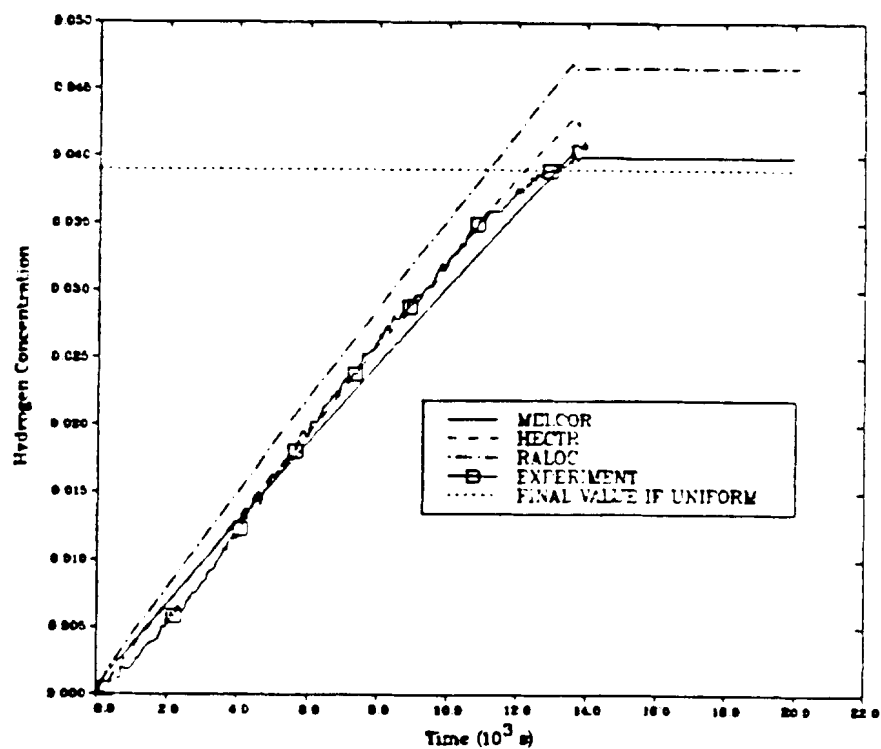


Figure 2. Hydrogen Concentration in Cell 1 for Battelle-Frankfurt Test 2

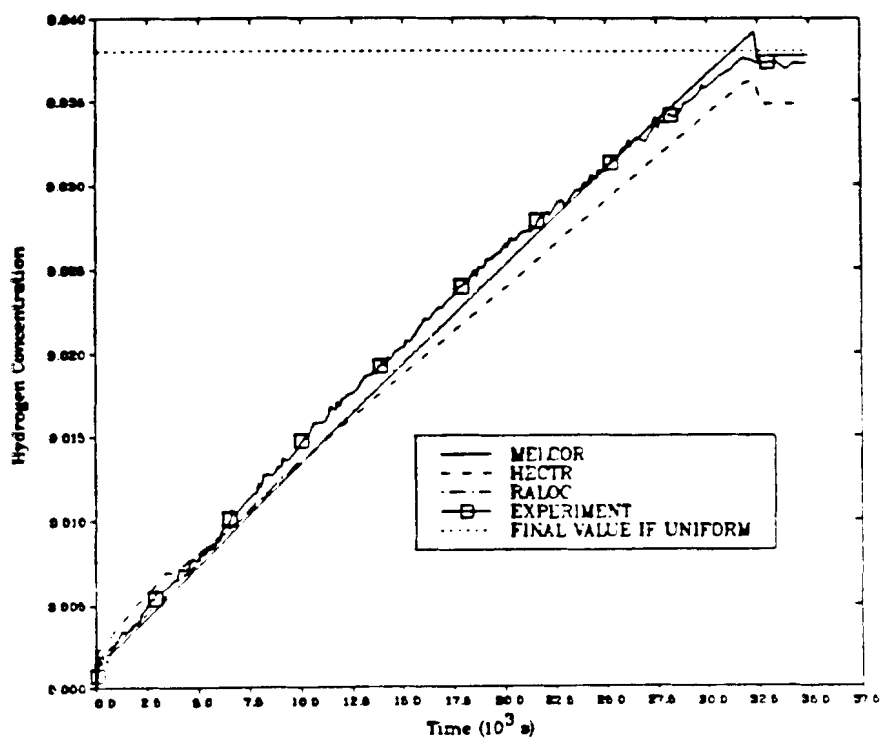


Figure 3. Hydrogen Concentration in Cell 13 for Battelle-Frankfurt Test 10

respectively. The choice of initial temperatures for each cell in the model was a matter of some ambiguity, and a number of such choices were made in attempting to obtain good agreement between HECTR and experimental results. [5] In those calculations, both the initial temperature distribution and heat transfer between the containment walls and the atmosphere were shown to have profound effects on the computed hydrogen distributions. A limited number of similar variations were carried out with MELCOR, but none of the results compared very well with the experimental data at all locations.

Calculated and experimental hydrogen concentrations near the injection point for Test 6 are shown in Figure 4. Until slightly before the end of injection at 8000 seconds, both MELCOR and HECTR agree reasonably well with data, although the HECTR result is somewhat smoother than MELCOR's. A decrease in the concentration in both calculations occurs at about the same time as in the measured data, and all three curves reach maxima well above the value at which the total injected hydrogen would be uniformly distributed. Figure 5 presents results at the top center of the containment (Cell 1), and only the HECTR prediction seems to capture at least the character of the data over its available duration. Because the initial temperatures in the upper region are higher, upward flow is delayed until the buoyancy of the lower density of the injected gas can overcome the initial density gradient. The rapid increase in the HECTR result at about 8500 seconds clearly shows this phenomenon. Earlier behavior in the RALOC and MELCOR curves might also be partly attributable to this effect. Unfortunately, the data do not extend to a late enough time that this "thermal breakthrough" could be experimentally confirmed or denied.

In Test 19, MELCOR seemed to agree best with data for the lower of the outer compartments (Cell 27), as shown in Figure 6, while the HECTR results were closest to the somewhat questionable measurement in the upper, outer region (Cell 23), as shown in Figure 7. For concentrations just above the injection source (Cell 13), neither RALOC, HECTR, nor MELCOR could be said to agree well with the data, as shown in Figure 8. That none of the codes was obviously superior in comparing with data at all locations was also true of the other nonisothermal test, Test 6.

## 6. Summary and Conclusions

In summary, we found MELCOR to be capable of producing very good agreement with Battelle-Frankfurt hydrogen mixing tests, when initial temperatures were assumed to be uniform and very nearly equal to the temperature of the injected gas. We also found that relatively large flows could be calculated for what should be a zero-flow steady state, and that these flows can be substantially reduced by careful selection of initial pressures, by eliminating elevation discontinuities where possible, and by taking advantage of a large computer-word length. Finally, it appears that a fairly large number of sensitivity studies would be required to obtain good agreement between MELCOR and experiment when the initial temperatures are not uniform; this is also true of at least two other codes, HECTR and RALOC, which are suitable for modeling this type of mixing test.

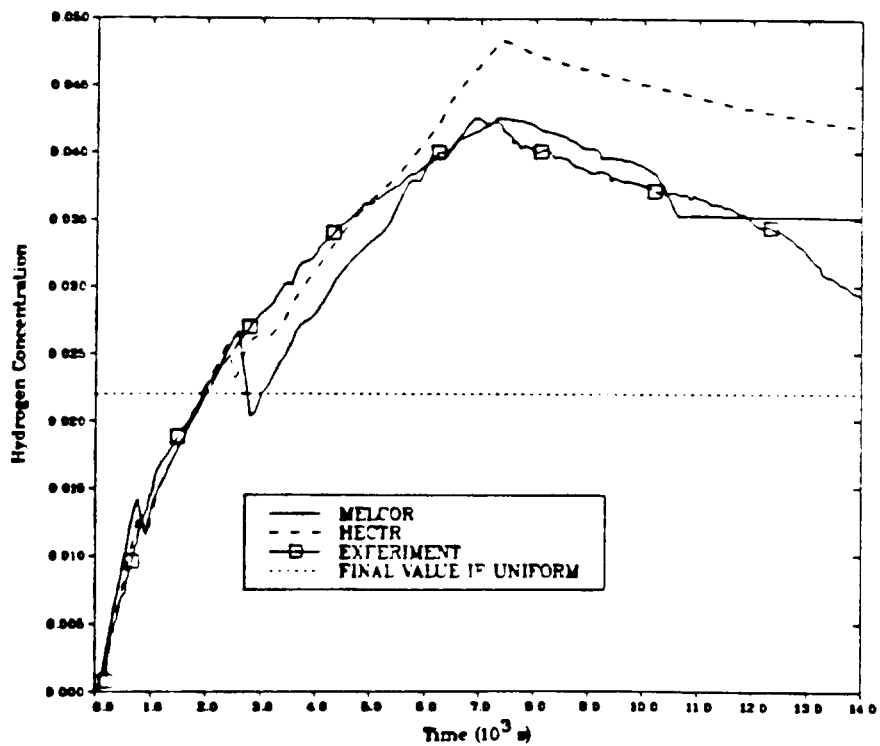


Figure 4. Hydrogen Concentration in Cell 13 for Battelle-Frankfurt Test 6

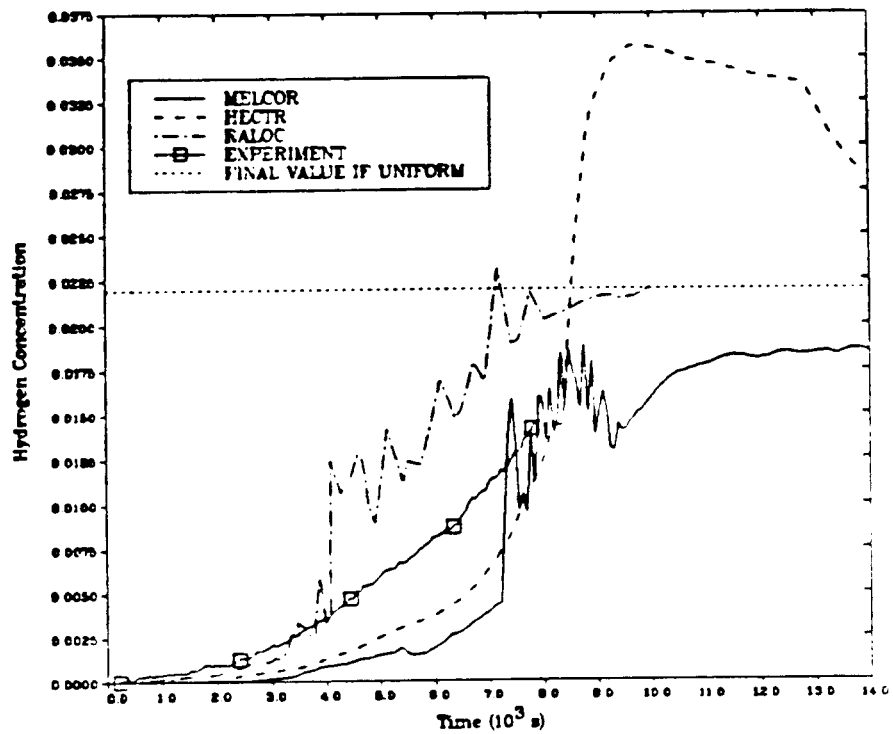


Figure 5. Hydrogen Concentration in Cell 1 for Battelle-Frankfurt Test 6

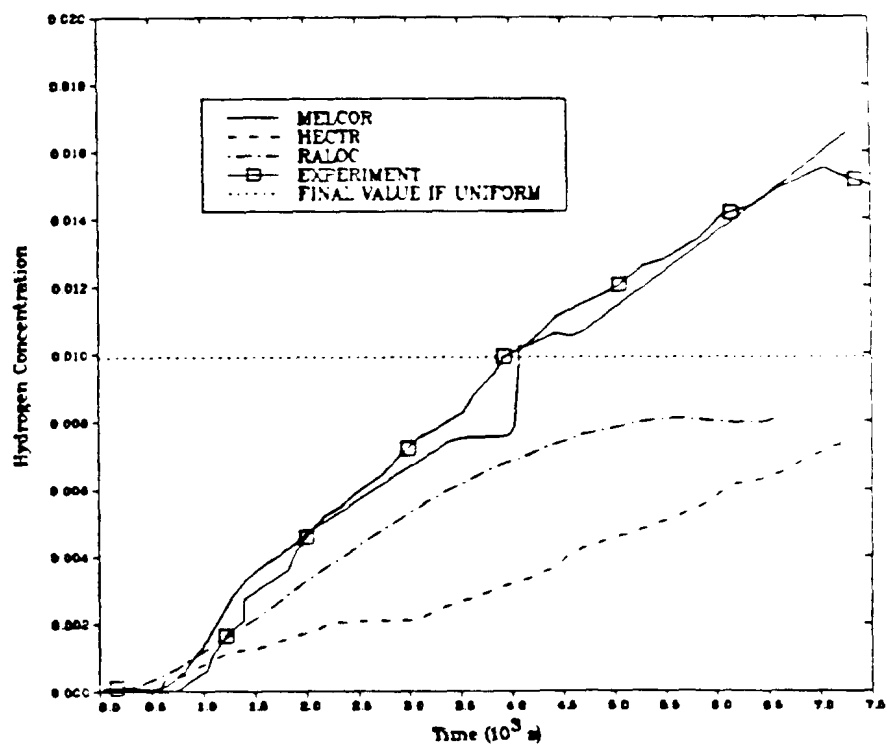


Figure 6. Hydrogen Concentration in Cell 27 for Battelle-Frankfurt Test 19

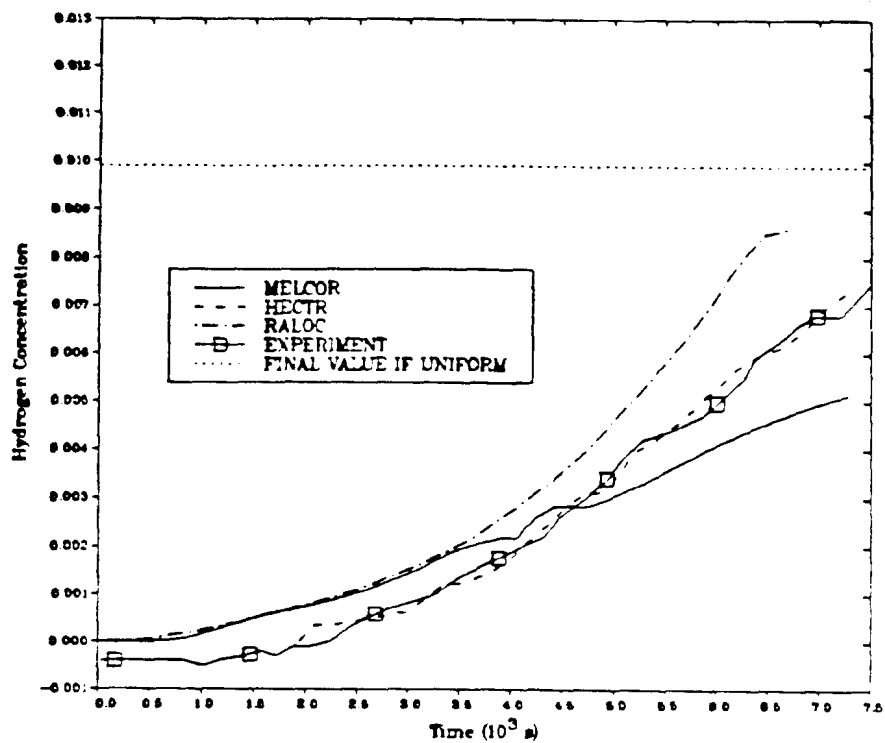


Figure 7. Hydrogen Concentration in Cell 23 for Battelle-Frankfurt Test 19

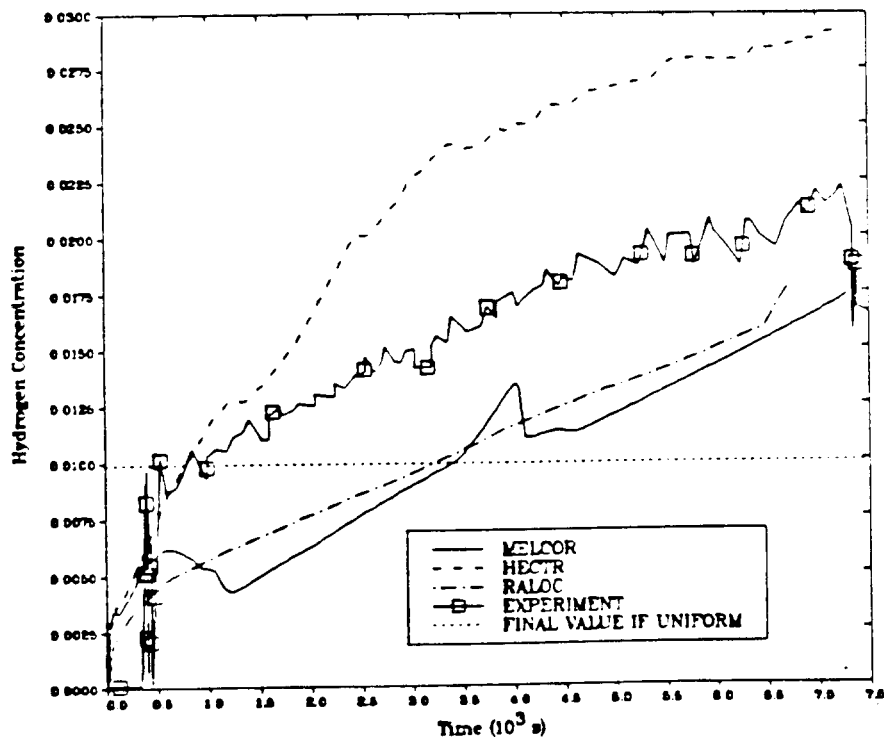


Figure 8. Hydrogen Concentration in Cell 13 for Battelle-Frankfurt Test 19

## 7. References

1. G. Langer, R. Jenior, and H. G. Wentlandt, Experimental Investigation of the Hydrogen Distribution in the Containment of a Light Water Reactor Following a Coolant Loss Accident, NRC Translation 801, BF-F-63.363-3, Battelle Institut e.V. Frankfurt, Federal Republic of Germany, October 1980.
2. Research Project 150.375, Experimental Investigation of the Hydrogen Distribution in a Model Containment (Preliminary Experiments II), NRC Translation 1065, BF-R-64.036-1, Battelle Institut e.V. Frankfurt, Federal Republic of Germany, May 1982.
3. L. D. Buxton, D. Tomasko, and G. C. Padilla, An Evaluation of the RALOC Computer Code, NUREG/CR-2764, SAND82-1054, Sandia National Laboratories, Albuquerque, New Mexico, August 1982.
4. M. J. Wester and A. L. Camp, An Evaluation of HECTR Predictions of Hydrogen Transport, NUREG/CR-3463, SAND83-1814, Sandia National Laboratories, Albuquerque, New Mexico, September 1983.
5. A. L. Camp, Private Communication, Sandia National Laboratories.



# MELCOR 1.0 and HECTR 1.5 Calculations for Browns Ferry Reactor Building Burns

S.E. Dingman and F.E. Haskin  
Sandia National Laboratories  
Albuquerque, New Mexico 87185  
United States of America

## Abstract

Following drywell failure in postulated severe accidents at Browns Ferry, hydrogen burns could occur in the reactor building. MELCOR and HECTR calculations for such burns have been performed. When using the same flame speed, the two codes predict similar pressure responses. However, the magnitude of the pressure rises differs somewhat because the preburn conditions are slightly different. These differences are due to different treatments of the control volume gravity head and heat transfer/condensation in the two codes. Some MELCOR improvements are suggested.

## 1. Introduction

This paper compares MELCOR and HECTR [1] calculations of the Brown's Ferry secondary containment response to hydrogen burns that occur when hydrogen is released to the reactor building following drywell failure. Results from both codes are discussed, including calculations using HECTR models that are not currently available in MELCOR. These additional HECTR calculations are discussed in this report because they show how the models affect the calculated results, indicating a need for new MELCOR models. The input decks for these calculations were based on a CONTAIN [2] input deck provided by S. R. Greene of ORNL. Gas source rates were also provided by S. R. Greene.

## 2. Test Description

This test examines the response of the Browns Ferry reactor building, shown in Figure 1, following failure of the drywell steel shell. Initially, the reactor building is at atmospheric conditions. Following drywell failure, hydrogen from the drywell is pushed into the reactor building, such that a hydrogen burn (or series of hydrogen burns) is possible. The pressure rises during these burns will affect the release to the environment. There is also the potential for equipment failure due to temperature rises during the burns. Since there are no igniters in the reactor building, the threshold for burning cannot be reliably predicted. For the calculations presented herein, it is postulated that ignition occurs whenever the hydrogen mole fraction exceeds 8%. The corresponding pressure and temperature rises for the burns for various flame

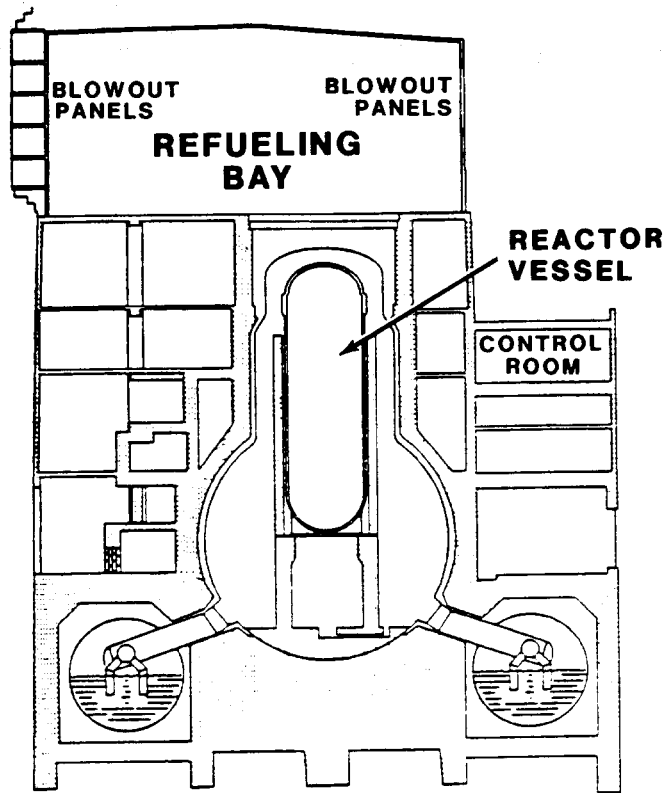


Figure 1. Browns Ferry Reactor Building

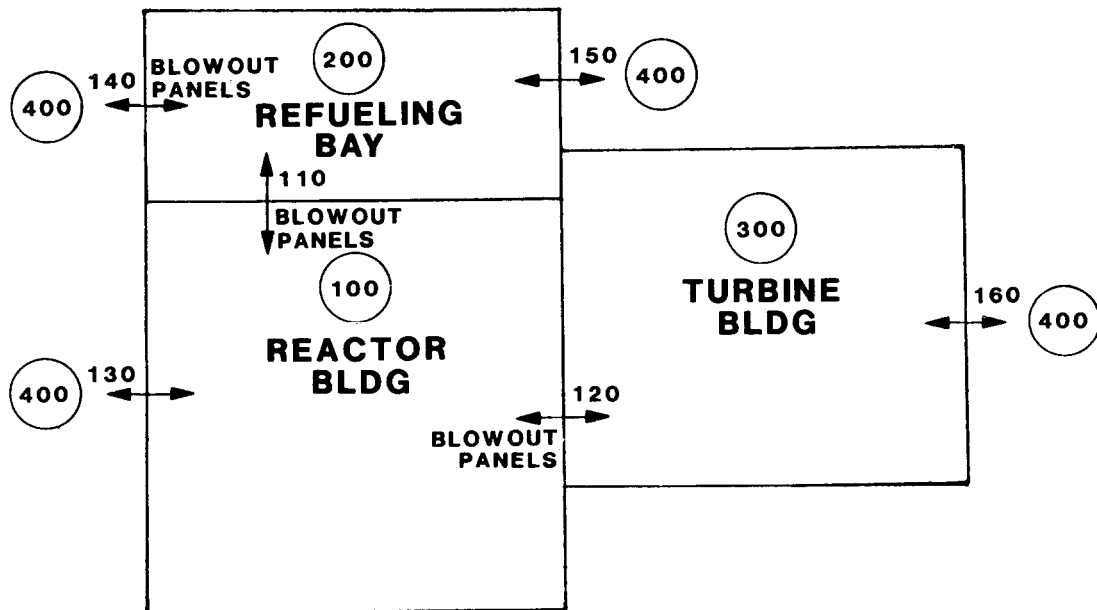


Figure 2. MELCOR Nodalization for the Browns Ferry Secondary Containment

speeds are examined. The effects of radiative heat transfer and fire sprays, which are not currently available in MELCOR 1.0 are examined.

### 3. Model and Case Descriptions

Both MELCOR and HECTR were used to model the thermal-hydraulic response of the Brown's Ferry secondary containment as described in Section 2. The nodalization used for MELCOR is shown in Figure 2. The MELCOR input model consists of four compartments, six flow junctions, and 29 heat structures. The compartments represent the reactor building, refueling bay, turbine building, and the environment. Three flow junctions are included to model blowout panels and the remaining three junctions are included to model leakage to (or infiltration from) the environment. The heat structures are used to model the floors, walls, and ceilings of the reactor building, refueling bay, and turbine building. The HECTR nodalization was as similar as possible to the MELCOR nodalization.

Preliminary calculations showed that the MELCOR and HECTR default flame speed correlations gave sufficiently different values when significant quantities of steam were present that direct comparison of the calculated results were not meaningful. The variation in the flame speeds in high steam environments is so large that neither of the default correlations can be strongly supported. Therefore, rather than using the default correlations, the flame speed was varied from 1 to 10 m/s in both the MELCOR and HECTR calculations. This also allowed us to examine the sensitivity of the results to the flame speed. Two additional sets of HECTR calculations were run that included effects of reactor building sprays and radiative heat transfer from the gases to passive heat sinks. The cases considered are listed in Tables 1 and 2.

### 4. Results

The pressures calculated by MELCOR and HECTR during the first burn for Case 2 (5 m/s, no radiation, no sprays) are compared in Figure 3. Although the burns begin at slightly different times in the transient, the codes calculate similar pressure responses after the burns begin. The difference in burn timing will be discussed below.

The peak pressures as a function of the flame speed for the remaining MELCOR and HECTR calculations are shown in Figure 4. For both codes, the peak pressure increases as the flame speed increases, as expected. Differences in the magnitudes of the increases are due to different treatments of the control volume gravity head and heat transfer/condensation in the two codes. These contributors are discussed in the following paragraphs.

#### Gravity Head Treatment

MELCOR defines the control volume pressure at the pool/atmosphere interface (which is basically the bottom of the control volume for these calculations) whereas HECTR defines the control volume pressure at its vertical midpoint. When performing flow calculations, both codes account for the pressure

Table 1. MELCOR Cases

Case	Flame Speed (m/s)	Radiation	Sprays
1	10.	No	No
2	5.	No	No
3	1.	No	No

Table 2. HECTR Cases

Case	Flame Speed (m/s)	Radiation	Sprays
1	10.	No	No
2	5.	No	No
3	1.	No	No
4	10.	Yes	No
5	5.	Yes	No
6	1.	Yes	No
7	10.	Yes	Yes
8	5.	Yes	Yes
9	1.	Yes	Yes

variation due to differences in the control volume and flow junction elevations that result from the gravity head. Thus, the initial pressures specified for the two codes can be adjusted such that flow rate calculations are not affected by this modeling difference. However, since the number of moles in a control volume is defined by its pressure and temperature, adjusting the pressure to match the gravity head, will yield a different initial mole content in the two codes. We chose to match the gravity head rather than mole content.

When these calculations were performed, it was not possible in either MELCOR or HECTR to account for the gravity head between the control volume and junction elevations when calculating pressure differences for blowout panels. Since MELCOR and HECTR use different references for the control volume elevations, it was not possible to match the blowout panel performance. In MELCOR, the blowout panels between the reactor building and turbine building were blown out before the first burn, but in HECTR they did not blow out until the burn started. As a result, the preburn temperature in the reactor building was lower in MELCOR than in HECTR. With a lower temperature, more moles of hydrogen were required to accumulate in the reactor building to yield the 8% ignition limit. Thus, the first burn occurred later in MELCOR and it resulted in a larger pressure rise.

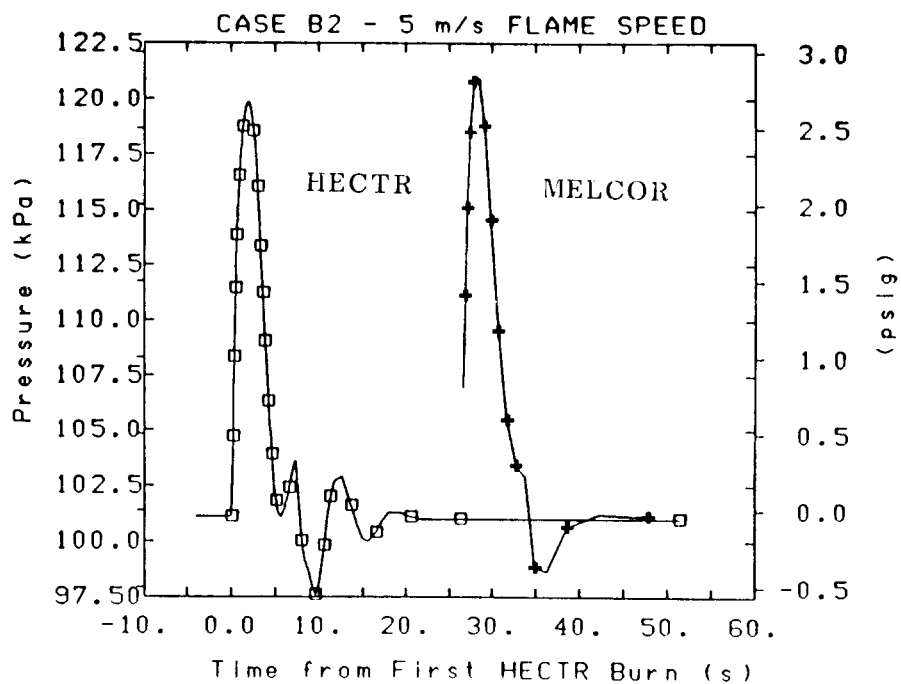


Figure 3. Pressure Comparison for the First Burn in Case 2.

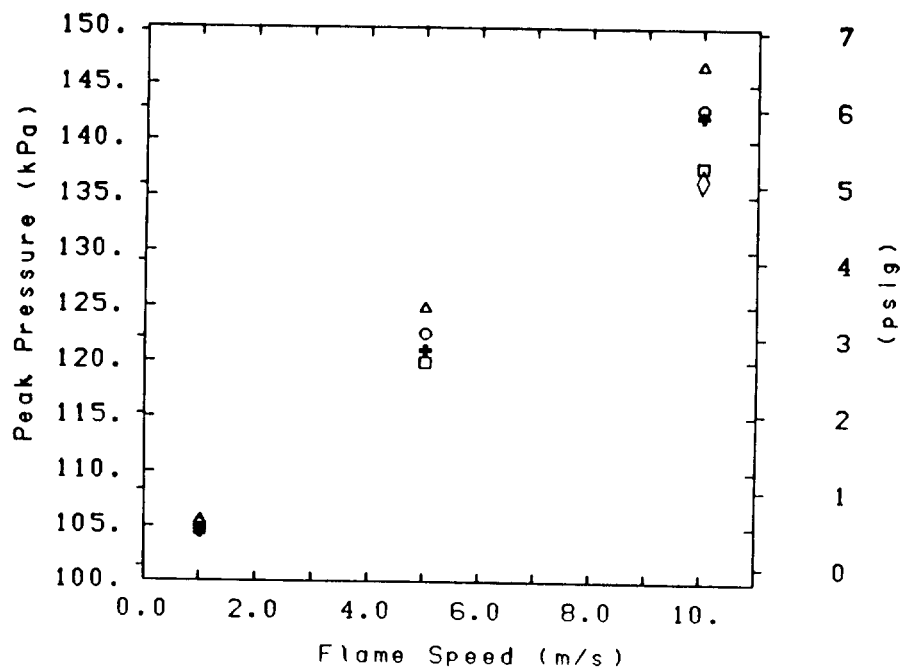


Figure 4. Peak Pressure Versus Flame Speed.  $\Delta$  HECTR with radiation and sprays;  $\circ$  HECTR with radiation and no sprays; + MELCOR without radiation and sprays;  $\square$  HECTR without radiation and sprays;  $\diamond$  MELCOR 1.6.

## Heat Transfer / Condensation

The heat flux to surfaces in the reactor building was generally lower in MELCOR than in HECTR. This is mainly due to differences in heat transfer correlations; an internal flow type of convective heat transfer correlation (Dittus-Boelter) is used in MELCOR, whereas an external flow correlation [1] is used in HECTR. The MELCOR correlation is appropriate for control volumes such as the reactor vessel, but an external flow correlation should be added for containment surfaces.

MELCOR and HECTR also use different methods to determine the convective velocity for heat transfer calculations. In MELCOR, the user inputs a control volume area which is used in conjunction with an average control volume flow rate to define a velocity. In HECTR, the user specifies a constant velocity, which is used during portions of the calculation in which burns are not occurring. During burns, HECTR uses the flame speed as the convective velocity. There are problems with both approaches. Using a constant velocity does not allow for variations during the transient, but using average inflows and outflows from a control volume to determine the velocity may not give an accurate representation of conditions within the control volume. For this test problem, we specified the MELCOR area and HECTR velocity such that the velocities used were approximately the same.

Although the condensation/evaporation rates were much smaller than the convective heat transfer rates for these calculations, modeling differences between HECTR and MELCOR could affect results in other comparisons, so they will be briefly discussed here.

The condensation rates in MELCOR are calculated using

$$Sh = Nu (Sc/Pr)^{1/3} \quad (1)$$

whereas at the time these calculations were performed HECTR used

$$Sh = Nu (Pr/Sc)^{2/3}. \quad (2)$$

To resolve this discrepancy, several different heat transfer texts were reviewed, and it was concluded that the MELCOR treatment is correct. The error in HECTR has been reported and is being corrected.

The heat flux to surfaces in the reactor building was generally lower in MELCOR than in HECTR, but the surface temperature increases during the burns were higher in MELCOR. There are too many differences in this calculation to determine the exact cause of this discrepancy. Possible causes include differences in nodalization of the structures and different treatments of liquid films in the two codes.

## Effect of Radiation and Sprays

The HECTR calculations that included radiative heat transfer and sprays were significantly different from the calculations discussed above (See Figure 4).

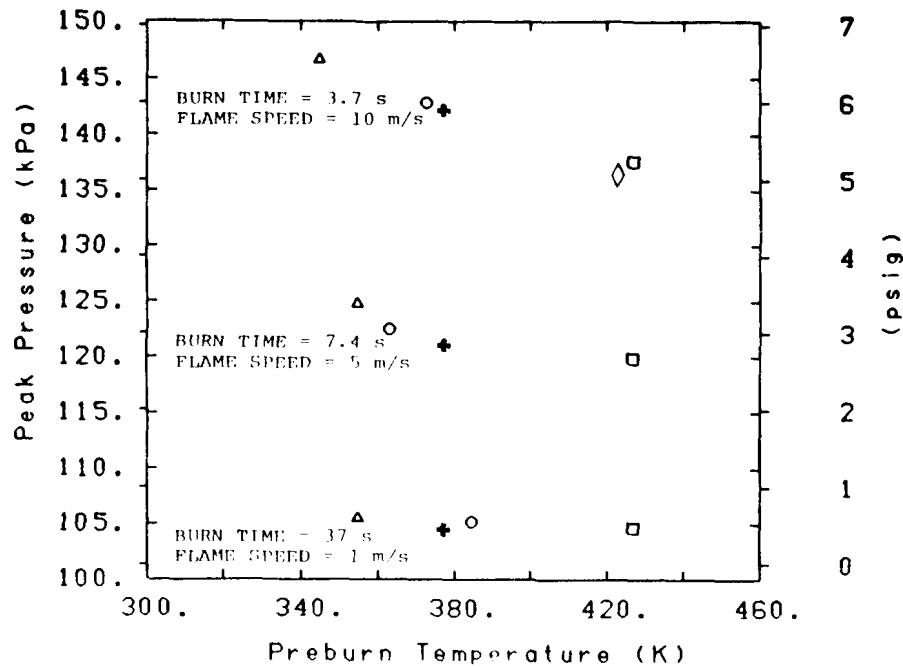


Figure 5. Peak Pressure as a Function of the Preburn Temperature.  
 △ HECTR with radiation and sprays; ○ HECTR with radiation and no sprays; + MELCOR without radiation and sprays; □ HECTR without radiation and sprays; ◇ MELCOR 1.6.

Including radiative heat transfer resulted in lower temperatures at the initiation of the burn. Thus, there were more moles of hydrogen in the reactor building prior to the first burn than in the cases without radiation, giving larger pressure rises. The peak pressure is plotted as a function of the preburn temperature in Figure 5 to illustrate this effect. When spray injection was included, the reactor building was cooled even further prior to the first burn, giving a still larger pressure rise.

#### MELCOR 1.6 Calculations

A calculation for case 3 was performed using MELCOR 1.6. The heat structure package was revised substantially for MELCOR 1.6. The MELCOR 1.6 results indicate that the preburn temperature in MELCOR was closer to that of HECTR without radiation and sprays, and therefore, the peak pressure is closer to the HECTR calculation. These results are shown on Figure 4 and Figure 5.

#### 5. Summary and Conclusions

The calculations showed good agreement between HECTR and MELCOR results. However, the need for additional test problems that compare results from MELCOR and HECTR has been identified. Suggested problems are listed below:

- (1) Comparison of pressure and temperature rises during burns starting at the same initial conditions, including propagation into adjoining compartments. The ignition limit and flame speed should be varied over a reasonable range.
- (2) Comparison of heat transfer rates (with and without condensation) for a wide range of temperatures, convective velocities, and steam concentrations. The same nodalization should be used for the structures in both codes. Structure surface temperatures should also be compared.

The HECTR calculations that included radiative heat transfer and sprays showed that these effects can be important. Radiative heat transfer from gas to surfaces should be included in MELCOR. A spray model is currently available in MELCOR, but the capability to turn on the sprays based on pressure and/or temperature is not currently available. This should be added such that spray actuation can be correctly modeled.

## 6. References

1. S.E. Dingman, et al., HECTR Version 1.5 User's Manual, NUREG/CR-4507, SAND86-0101, Sandia National Laboratories, April 1986.
2. K.D. Bergeron, et al., User's Manual for CONTAIN 1.0, NUREG/CR-4085, SAND84-1204, Sandia National Laboratories, May 1985.



MELCOR 1.0 Calculations  
for Cooling of Structures in a Fluid

P. N. Demmie  
Sandia National Laboratories  
Albuquerque, New Mexico 87185  
United States of America

Abstract

MELCOR calculations were performed for the cooling of two uniform structures (rectangular and cylindrical) with constant thermal properties and heat transfer coefficients. The temperatures as a function of time for the structures are compared in this paper to the exact analytical solution and to SCDAP results. The good agreement between the MELCOR results, the SCDAP results, and the exact analytical solution show that the finite-difference methods used in the MELCOR Heat Structure Package produce accurate results.

1. Introduction

This paper presents a MELCOR calculation for the cooling of two structures in a fluid and compares the results of this calculation to both an analytic solution and the results of the calculation of the same transient using the SCDAP Code[1]. The purpose of this calculation is to test the implementation of the internal heat conduction methodology of the MELCOR Heat Structure Package (HSP) without internal or surface power sources.

2. Test Description

MELCOR calculations were performed for two uniform solid structures (rectangular and cylindrical) with constant thermal properties and constant surface heat transfer coefficients. These structures, which were initially at 1000 K, were immersed in a fluid at 500 K. Table 1 contains the values of the thermal properties of the material in these structures as well as the other parameters that were used for the calculation. The material in these structures does not correspond to any known material but was chosen to permit comparison of the results of a MELCOR calculation with an analytic solution and the results of a SCDAP calculation [1] of the same transient.

It is well documented in heat transfer texts that lumped-heat-capacity (LHC) methods are adequate for transient heat conduction calculations for a structure if its Biot Number is less than 0.1 [2]. The Biot Number for a structure is

$$Bi = h (V/A) / k \quad (1)$$

where

Bi = Biot Number,  
h = heat transfer coefficient,  
V = volume of structure,  
A = surface area of structure, and  
k = thermal conductivity of material in structure.

A low Biot Number implies that the transfer of energy within the structure is rapid relative to the transfer of energy from the structure to the fluid. Thus, the temperature within a structure with a low Biot Number can be assumed to be uniform.

The analytic solution for the temperature of a LHC structure which is immersed in a fluid is [2]:

$$T = T_f + (T_i - T_f) \exp (-hAt/\alpha V) \quad (2)$$

where

T = uniform temperature of structure,  
T<sub>f</sub> = temperature of fluid,  
T<sub>i</sub> = initial temperature of structure,  
h = heat transfer coefficient,  
α = volumetric heat capacity (product of heat capacity and density),  
V = volume of the structure,  
A = the surface area of the structure,  
t = time.

This solution is obtained by solving the first order linear differential equation that follows from the global energy balance between the structure and the fluid under the assumption of a uniform temperature throughout the solid (i.e., the LHC method).

The Biot Number is 0.05 for both rectangular and cylindrical structures with parameters from Table 1. Hence, the temperatures that are calculated by MELCOR should be close to the analytic solution which is given by Equation 2.

### 3. Model and Calculation Description

The MELCOR code was run for a rectangular and cylindrical heat structure each with a Biot Number of 0.05 and a control volume boundary which models a temperature reservoir at 500.0 K. All parameters were chosen to permit an exact comparison of the MELCOR results with the SCDAP results. Since the SCDAP calculation used a constant time step of 0.0029 s, the MELCOR calculation also used this value.

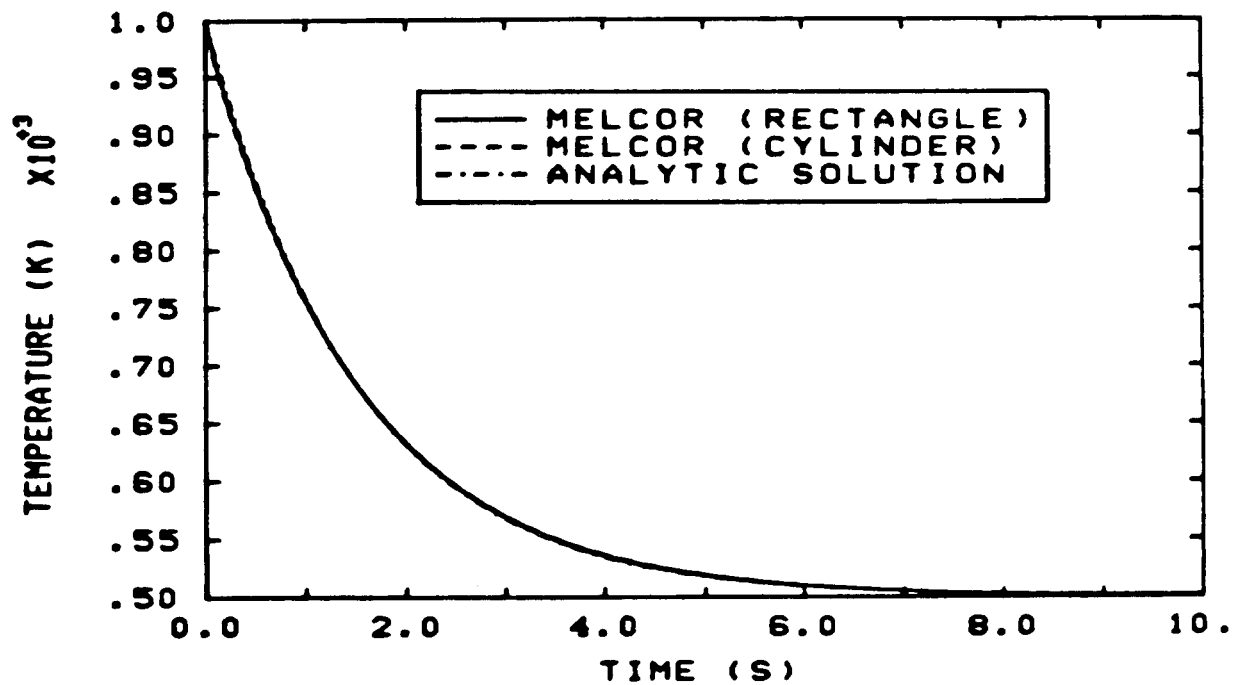


Figure 1. MELCOR Calculated Temperatures and Analytic solution.

Table 1. Parameter Values For Calculation

Parameter	Value
Thermal Conductivity of Material in Structures	50.0 W/m <sup>2</sup> /K
Density of Material in Structures	1.0 kg/m <sup>3</sup>
Heat Capacity of Material in Structures	1500.0 J/kg/K
Heat Transfer Coefficient at Surfaces	50.0 W/m <sup>2</sup> /K
Initial Temperature of Structures	1000.0 K
Fluid Temperature	500.0 K
Thickness of Rectangular Structure	0.1 m
Area of Each Surface of Rectangular Structure	1.0 m <sup>2</sup>
Radius of Cylindrical Structure	0.1 m
Height of Cylindrical Structure	1.0 m

Table 2. Surface Temperature Versus Time

Time (s)	Temperature (K)			Analytic
	MELCOR (rectangle)	MELCOR (cylinder)	SCDAP (cylinder)	
0.0	1000.00	1000.00	1000.00	1000.00
1.0	755.196	754.410	754.642	756.692
2.0	632.419	632.725	632.978	631.782
3.0	568.715	569.243	569.443	567.655
4.0	535.661	536.125	536.264	534.733
5.0	518.510	518.848	518.938	517.831
6.0	509.630	509.853	509.890	509.154
7.0	505.003	505.142	505.164	504.700
8.0	502.603	502.685	502.697	502.413
9.0	501.358	501.402	501.408	501.239
10.0	500.711	500.734	500.735	500.636

#### 4. Discussion of Results

The results of the MELCOR calculation are compared to the SCDAP results and the analytic solution. The comparison with the SCDAP results shows the similarity between results which are obtained using the finite-difference methodology of the MELCOR HSP and the finite-element heat conduction methodology in SCDAP; the comparison with the analytic solution shows the accuracy of the MELCOR heat conduction methodology.

Figure 1 shows the temperatures for a rectangular and cylindrical structure which were calculated by MELCOR and the analytic solution which is given by Equation 2. This figure shows excellent agreement between the MELCOR results and the analytic solution. All structures are cooled as expected and have surface temperatures at the end of this 10-second calculation that are nearly equal to the fluid temperature of 500.0 K.

A comparison of the MELCOR results to the SCDAP results is given in Table 2. Results are given at 1-second intervals in the table. Excellent agreement is shown between the MELCOR results, the SCDAP results, and the analytic solution.

#### 5. References

1. G. A. Berna, "Finite Element Method for SCDAP", EGG-CDD-5697, December 1981.
2. J. P. Holman, Heat Transfer, 4th Edition, McGraw-Hill Book Company, 1976.

MELCOR 1.0 Calculations for  
Radial Conduction in Annular Structures

S. E. Dingman  
Sandia National Laboratories  
Albuquerque, New Mexico 87185  
United States of America

Abstract

MELCOR predictions of the steady state temperature distributions resulting from radial heat conduction in annular structures have been compared to the exact analytical solutions for two sets of boundary conditions and two cylinder sizes. The agreement between MELCOR results and the analytic solution is excellent in all cases.

1. Introduction

This paper compares MELCOR predictions of the steady state temperature distributions resulting from radial heat conduction in annular structures to results obtained from exact analytic solutions. Two sets of boundary conditions and two cylinder sizes are considered. In addition, a transient calculation is performed for a structure with an initially uniform temperature profile to test whether MELCOR achieves the correct steady-state temperature profile.

2. Test Description

The analytic solution for the temperature profile resulting from radial, steady state heat conduction in an annular structure given the inner and outer surface temperatures is:[1]

$$T = T_i - \ln(r/r_i) \left[ \frac{(T_i - T_o)}{\ln(r_o/r_i)} \right] \quad (1)$$

where

T = The temperature at radius r (K)  
T<sub>i</sub> = Inner surface tube temperature (K)  
T<sub>o</sub> = Outer surface tube temperature (K)  
r<sub>i</sub> = Inner tube radius (m)  
r<sub>o</sub> = Outer tube radius (m)

Given specified heat transfer coefficients and control volume temperatures at the inner and outer surfaces, the analytic solution is[1]:

$$T = T_{env,i} - \left( \frac{\ln(r/r_i)}{k} + \frac{1}{h_i r_i} \right) \left( \frac{(T_{env,i} - T_{env,o})}{\frac{\ln(r_o/r_i)}{k} + \frac{1}{h_i r_i} + \frac{1}{h_o r_o}} \right) \quad (2)$$

where

- $k$  = The thermal conductivity of the structure (W/m/K)
- $T_{env,i}$  = The temperature of the control volume adjacent to the inner surface
- $T_{env,o}$  = The temperature of the control volume adjacent to the outer surface

In this paper comparisons of the results obtained using the MELCOR Heat Structure Package to these two analytic solutions are presented.

### 3. Model and Case Descriptions

Four cases are considered according to the following specifications:

Table 1. Specifications for MELCOR Calculations

Case No.	Transient or SS	Boundary Conditions (K or W/m <sup>2</sup> /K)		Radius (m)	
		Left	Right	Inner	Outer
1	Steady	T=600	T=550	3.1856	3.3412
2	Steady	T=600,h=1000	T=550,h=5	3.1856	3.3412
3	Steady	T=600,h=1000	T=550,h=500	.00843	.00953
4	Transient	T=600	T=550	3.1856	3.3412

Two cylinder sizes are considered. One (Cases 1, 2, and 4) is typical of a BWR reactor vessel. The second (Case 3) is typical of a PWR steam generator tube. Case 4 is a transient calculation (starting with a uniform temperature across the cylinder) which tests for the correct approach to the steady state temperature profile.

#### 4. Results

The analytic and MELCOR results for the four cases are compared in Figures 1 through 4. The steady state temperature profile calculated by MELGEN is plotted for the first three cases, and the temperature profile after reaching a steady state condition in MELCOR is plotted for case 4. The agreement between the MELCOR results and the analytic results is excellent in all cases.

#### 5. References

1. J. P. Holman, Heat Transfer, pp. 25 - 30, McGraw-Hill Book Company, 1976.

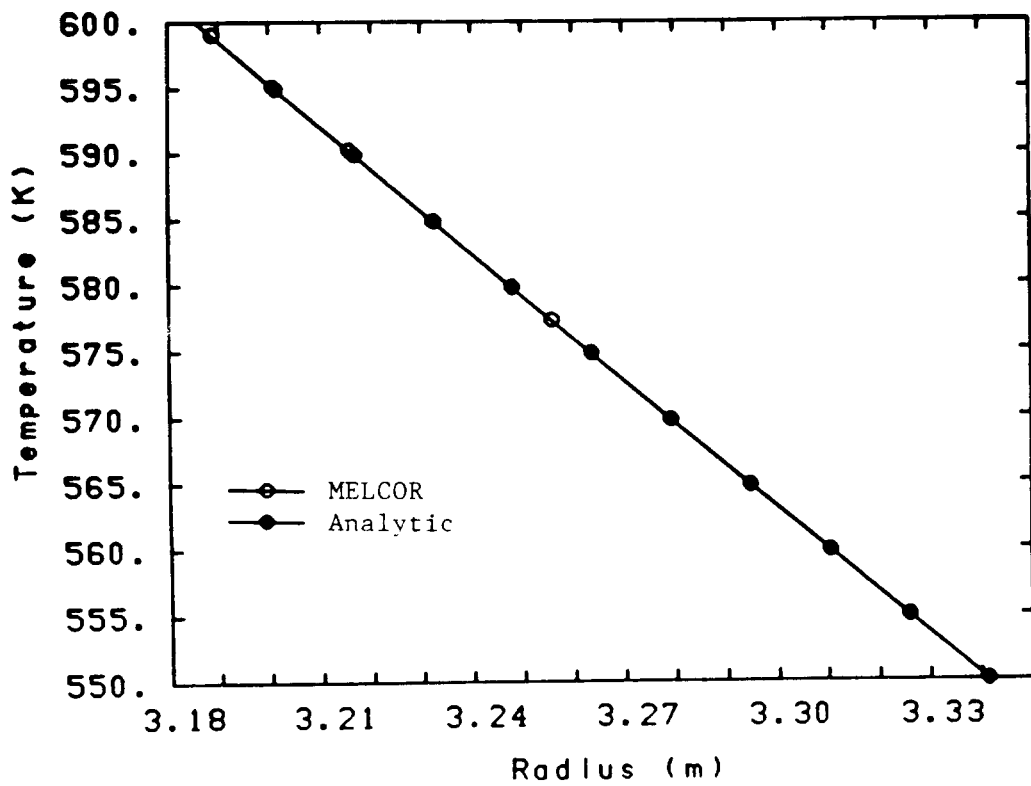


Figure 1. Temperature in the Cylinder as a Function of Radius for Case 1

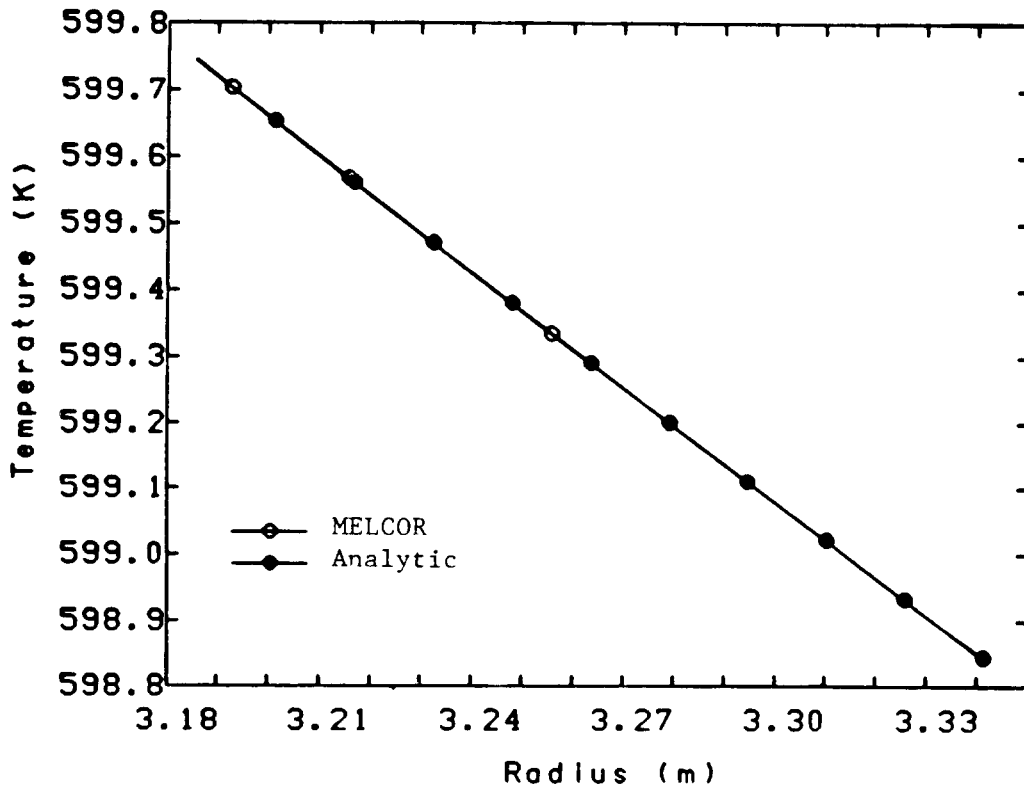


Figure 2. Temperature in the Cylinder as a Function of Radius for Case 2



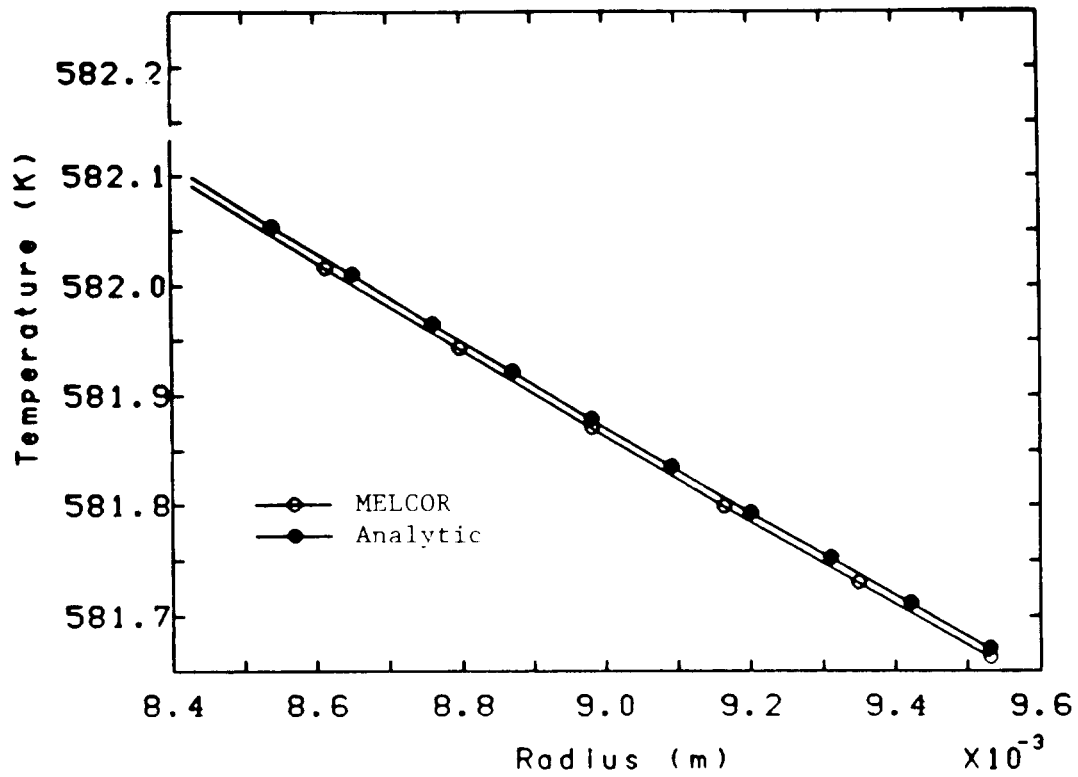


Figure 3. Temperature in the Cylinder as a Function of Radius for Case 3

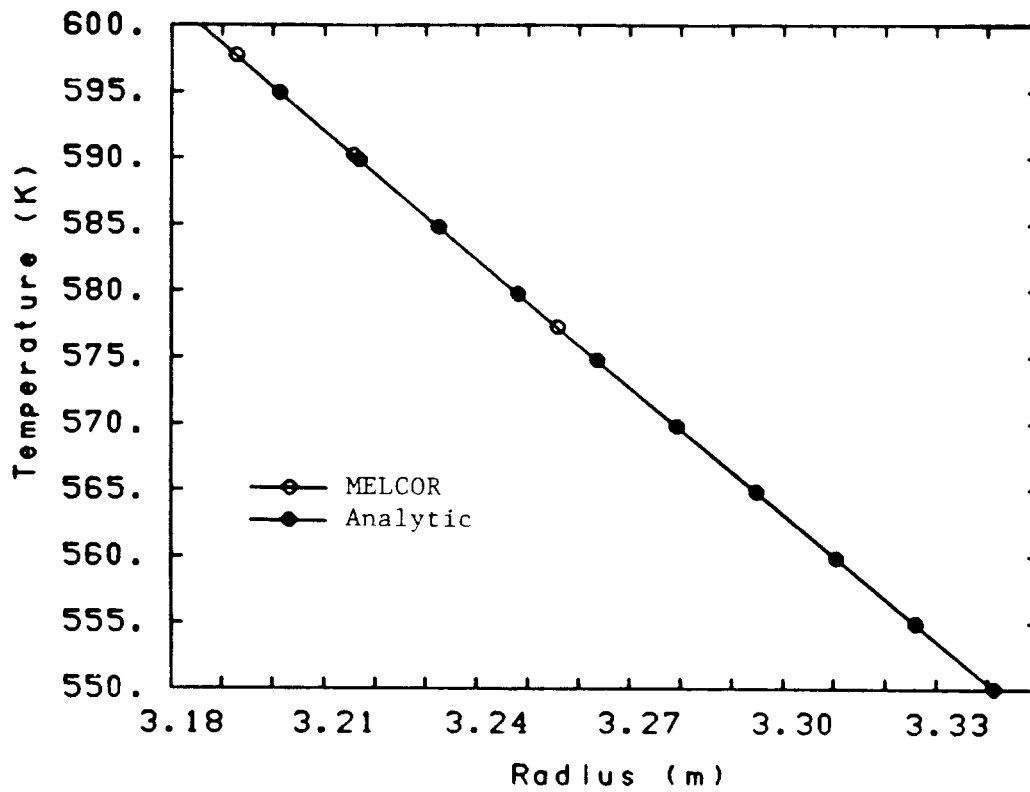


Figure 4. Temperature in the Cylinder as a Function of Radius for Case 4



# MELCOR 1.1 Calculations for a Semi-infinite Solid Heat Structure Test

C. J. Shaffer  
Science and Engineering Associates  
Albuquerque, New Mexico 87110  
United States of America

## Abstract

Predictions of the MELCOR heat structure package have been compared to the exact analytical solution for transient heat flow in a semi-infinite solid with convective boundary conditions. Comparisons have been made for steel and concrete, various thermal conductivities, atmospheric temperatures, node structures and time steps. MELCOR results appear to be more accurate for cases involving materials with low thermal conductivities like concrete rather than high thermal conductivities like steel, although in either case the accuracy of the MELCOR results is quite good (.3% error in the integrated heat flux for concrete and .6% error in the integrated heat flux for steel). Guidelines regarding node spacings in typical concrete containment walls have been developed.

## 1. Introduction

In order to test the MELCOR heat conduction models, MELCOR predictions for heat conduction in a solid are compared to the exact analytical solution for transient heat flow in a semi-infinite solid with convective boundary conditions. This test best simulates the conduction heat transfer in thick walls, in particular, the concrete containment walls of a nuclear power plant during a severe accident. This test demonstrates the accuracy of the MELCOR heat conduction models and provides guidelines for node spacing and time step sizes for concrete containment walls.

## 2. The Analytical Solution

Transient heat flow in a semi-infinite solid with convective boundary conditions is modeled in MELCOR using a finite slab heat structure of sufficient thickness to approximate a semi-infinite solid. The analytical solution for transient heat flow in a semi-infinite slab is given in Holman[1] as a function of the time and the position from the surface given the initial slab temperature, the fluid temperature, the convective heat transfer coefficient, and the thermal properties of the solid (thermal conductivity, specific heat, and density) which are all assumed constant. The solution is given by the following equation.

$$\frac{T - T_i}{T_o - T_i} = 1 - \operatorname{erf}\left[\frac{x}{2\sqrt{\alpha t}}\right] - \exp\left[\frac{hx}{k} + \frac{h^2 \alpha t}{k^2}\right] \left[1 - \operatorname{erf}\left\{\frac{x}{2\sqrt{\alpha t}} + \frac{h\sqrt{\alpha t}}{k}\right\}\right] \quad (1)$$

where  $T$  = temperature at time  $t$  and position  $x$  (K)  
 $T_i$  = initial temperature of solid (K)  
 $T_o$  = fluid temperature (K)  
 $h$  = convective heat transfer coefficient ( $\text{W/m}^2 \text{ K}$ )  
 $k$  = thermal conductivity ( $\text{W/m K}$ )  
 $\alpha$  = thermal diffusivity ( $\text{m}^2/\text{s}$ )

The time integrated surface heat flux was obtained from solving Equation 1 for the surface temperature and numerically integrating Equation 2.

$$Q = \int_0^{100,000} h (T_o - T_s) dt \quad (2)$$

where  $T_s$  is the temperature of the surface.

### 3. Test Descriptions

In the MELCOR calculations for this test, a 10 meter thick heat structure with logarithmic node spacing is assumed. The smallest node spacing is on the left side of the heat slab which is adjacent to a very large control volume. On the left side of the heat slab, a convective heat transfer boundary condition is specified with a heat transfer coefficient of  $10 \text{ W/m}^2 \text{ K}$ . An adiabatic boundary condition is specified for the right side of the heat slab.

MELCOR calculations were performed for two different materials (steel and concrete) and two different fluid temperatures to test MELCOR's ability to predict the analytical solution. Table 1 summarizes the specifications for the first three tests. These cases were run with 69 nodes within the first meter of thickness and with 10 second time steps. Case 1 is considered the base case for this report. The parameters for this case simulate the concrete wall of a containment building during a severe accident. Then, the number of nodes used and the time step sizes were varied to examine the effect on the accuracy of the results and to recommend node spacing and time step sizes for severe accident analyses.

Six different node structures were tested to survey the effect of the node spacing on calculation results. These node structures were designed to include 69 (base case), 35, 18, 11, 8, and 5 nodes in the first meter. Nodes between 0.0 and .001 meters were equally spaced while the nodes between 0.001 and 10.0 meters were logarithmically spaced according to Equation 3.

Table 1. MELCOR Specifications Cases 1, 2 and 3

Case No.	Initial Temp. (K)	Fluid Temp. (K)	Material	Density (kg/m <sup>3</sup> )	Specific Heat (J/kg K)	Thermal Conduc. (W/m K)	Thermal Diff. (m <sup>2</sup> /s)
1	300.0	450.0	Concrete	2300.0	650.0	1.6	1.07E-6
2	300.0	450.0	Steel	7850.0	500.0	47.0	1.20E-5
3	300.0	600.0	Concrete	2300.0	650.0	1.6	1.07E-6

$$\frac{X_i}{X_{i-1}} = \frac{1}{N} \quad (10) \quad (3)$$

where  $X_i/X_{i-1}$  is the ratio of adjacent node positions and  $N$  is the number of nodes desired per order of magnitude (i.e. between 1 mm and 1 cm). A graphical representation of the node locations for the six cases is given in Table 2.

Nine different time step sizes (10, 20, 30, 60, 120, 250, 500, 1000, 2000, and 5000 seconds) were run for both the 69 and 18 node structures. The 10 second and 69 node base case does the most detailed calculation and the 30 second and 18 node calculation represents more realistic parameters for a severe accident calculation.

#### 4. Results

The MELCOR results are compared to the exact solution as plots of temperatures versus time and as time integrated surface heat fluxes. All analytical results from Equations 1 and 2 were calculated with double precision on the CRAY computer. The solutions were not calculated beyond 100,000 seconds to avoid round-off errors involving the use of the error function (erf) in Equation 1. All MELCOR test cases were run out to 100,000 seconds and all surface heat fluxes were numerically integrated to 100,000 seconds. A summary of the results for the integrated heat fluxes for all the test cases is given in Table 3.

##### 4.1 The Base Case

Temperature comparison plots for 6 nodes are shown in Figure 1 for the base case (Case 1 in Table 1). The integrated surface heat flux error is 0.30%. The error is defined as the integrated flux calculated by MELCOR minus the flux from the analytical solution divided by the analytical flux. From the results shown in Figure 1, it is difficult to distinguish the differences between the

Table 2. Node Locations for MELCOR Calculations

Node Number	Location (meters)	Number of Nodes in First Meter					
		69	35	18	11	8	5
Equally Spaced Surface Nodes							
1	0.0	*	*	*	*	*	*
2	0.000125	*					
3	0.000250	*	*				
4	0.000375	*					
5	0.000500	*	*	*			
6	0.000625	*					
7	0.000750	*	*				
8	0.000875	*					
9	0.001000	*	*	*	*	*	*
Logarithmic Spaced Interior Nodes							
10	0.001122	*					
11	0.001259	*	*				
12	0.001413	*					
13	0.001585	*	*	*			
14	0.001778	*					
15	0.001995	*	*				
16	0.002239	*					
17	0.002519	*	*	*	*	*	
18	0.002818	*					
19	0.003162	*	*				
20	0.003548	*					
21	0.003981	*	*	*			
22	0.004467	*					
23	0.005012	*	*				
24	0.005623	*					
25	0.006310	*	*	*	*		
26	0.007079	*					
27	0.007943	*	*				
28	0.008913	*					
29	0.010000	*	*	*	*	*	*
..	....						
..	....						
49	0.10000	*	*	*	*	*	*
..	....						
..	....						
69	1.00	*	*	*	*	*	*
..	....						
..	....						
89	10.0	*	*	*	*	*	*

MELCOR and analytical solutions, so blowup plots are provided in Figures 2 and 3. Figure 2 shows the MELCOR predicted surface temperature lagging behind the analytical temperature by about 0.2 K. This temperature difference is relatively constant throughout the calculation and is the right order of magnitude to cause the error in the integrated heat flux. Figure 3 shows the temperature at 1 meter into the slab. Other than the 0.2 K surface temperature difference, the MELCOR and analytical results compare extremely well.

#### 4.2 Steel Thermal Properties

The steel thermal properties test case (Case 2 in Table 1) is the same as the base case except that the thermal properties represent steel instead of concrete. The results of this test case are shown in Figure 4. The integrated surface heat flux error is 0.64%. The MELCOR surface temperature lags the analytical temperature by about 0.5 to 1.0 K, and the temperature at 1 meter lags by about 0.5 K. MELCOR results for this case are not as accurate as for the base case involving concrete thermal properties. Perhaps a finer node spacing further in for steel due to the higher thermal diffusivity might produce better accuracy.

#### 4.3 High Temperature Test Case

The high temperature case (Case 3 in Table 1) is the same as the base case except that the fluid temperature was 600 K instead of 450 K. The results of this case are shown in Figure 5. The integrated surface heat flux error is 0.21%. The MELCOR surface temperature lags the analytical temperature by about 0.2 to 0.3 K. MELCOR results for this case are slightly more accurate than for the base case.

#### 4.4 Node Spacing Cases

The results obtained using different nodalizations (69, 35, 18, 11, and 8 nodes) are shown in Figures 6 through 9. The 69 node case is the base case and all of the cases were run with 10 second time steps. The node locations are shown in Table 2. The 5 node case yielded large errors (about 25%) and was not included in the figures.

The integrated surface heat flux errors for these tests are shown in Figure 6 as a function of the number of nodes in the first meter of the slab. The errors are large for the cases with few nodes and become more or less asymptotic for the finer node spacings. Actually the 35 node case has a slightly smaller error than the 69 node base case. Cases with less than about 18 nodes give errors in excess of 1%.

The surface temperatures are shown in Figures 7 and 8. The surface temperatures for the 35 and 69 node cases are practically identical. It appears that a higher degree of accuracy cannot be obtained by adding more than about 35 nodes. The 18 node case calculates reasonable results (0.88% error). The 8 node case and the 11 node case have 7.2% and 3.3% errors in the surface temperature, respectively.

Table 3. Summary of MELCOR Results for Integrated Heat Flux

Case Number	Time Step (seconds)	Number of Nodes in 1st Meter	Integrated Surface Heat Flux Error * (percent)
** Standard Test Cases			
1 (Base)	10	69	0.30
2 (Steel)	10	69	0.64
3 (High Temp.)	10	69	0.21
Other Nodalizations			
4	10	35	0.28
5	10	18	0.88
8	10	11	3.
10	10	8	7.2
12	10	5	24.6
Other Time Step Sizes			
6	20	69	0.38
7	30	69	0.31
9	60	69	0.46
11	120	69	0.56
13	250	69	0.90
15	500	69	1.2
16	1000	69	1.7
17	2000	69	3.4
18	5000	69	7.7
22	20	18	0.91
14	30	18	0.92
19	60	18	0.96
20	120	18	1.0
21	250	18	1.2
23	500	18	1.6
24	1000	18	2.4
25	2000	18	3.8
26	5000	18	8.4

\* (MELCOR-Analytical)/Analytical X 100

\*\* Analytical Time Integrated Surface Heat Flux = 5.5896E7 (Case 1),  
= 1.2729E8 (Case 2), -1.1179E8 (Case 3), [J/m\*\*2]



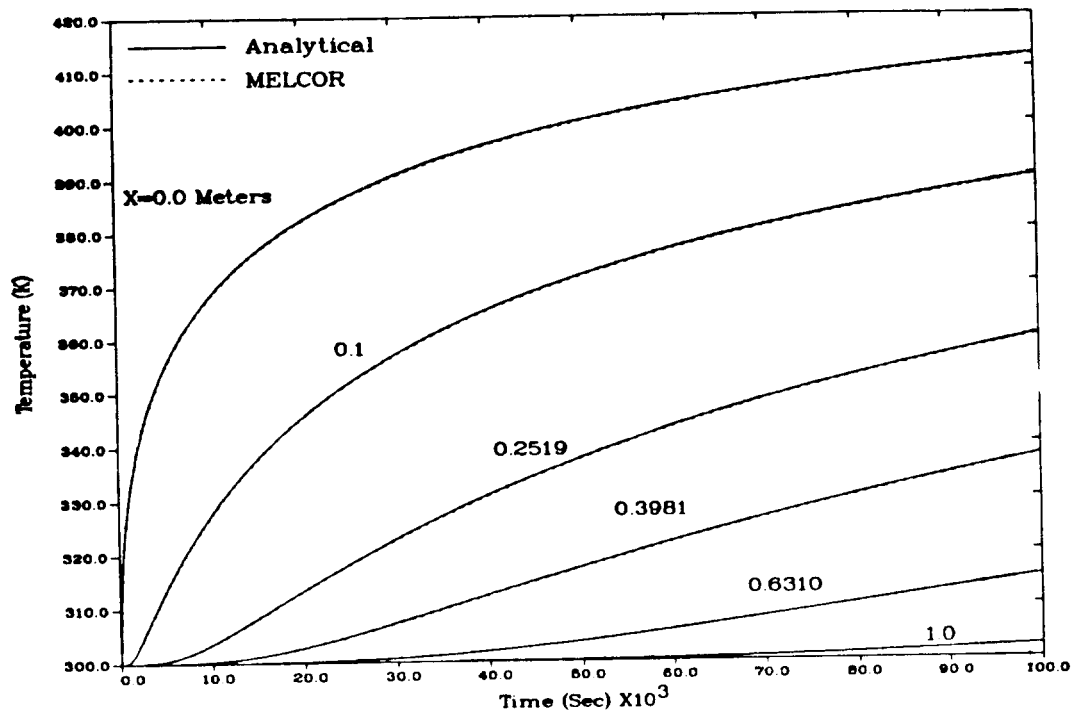


Figure 1. Time Temperature Results at Six Positions Within the Slab for the Base Case (Case 1 Table 1).

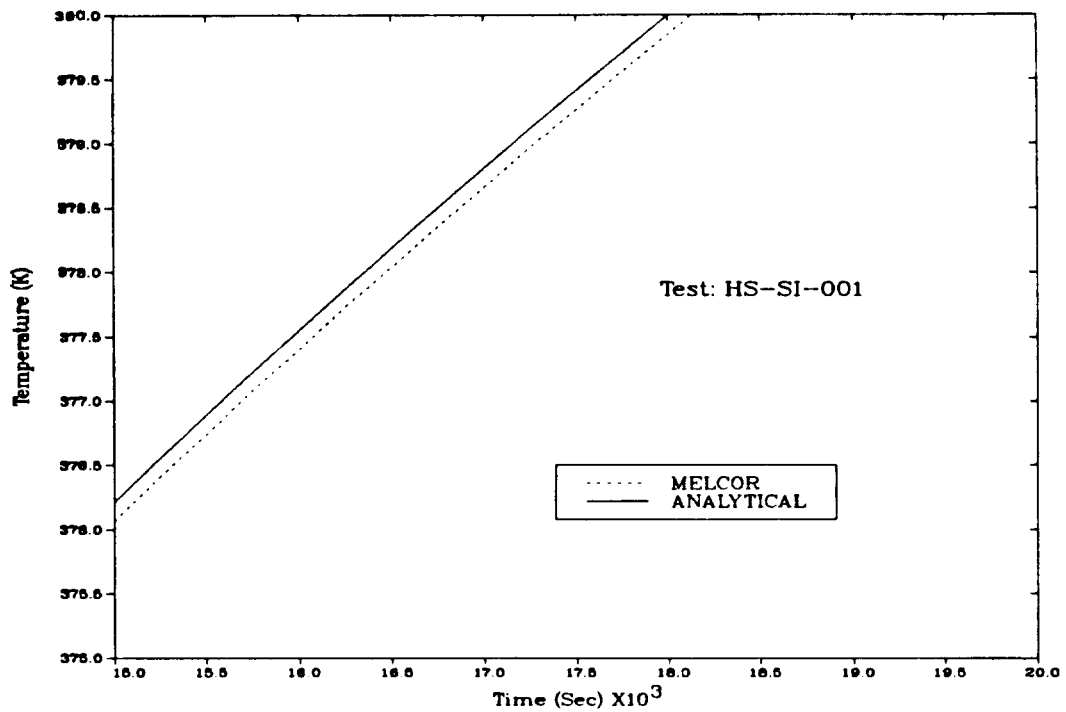


Figure 2. Surface Temperature Versus Time on an Expanded Scale for the Base Case (Case 1 from Table 1).

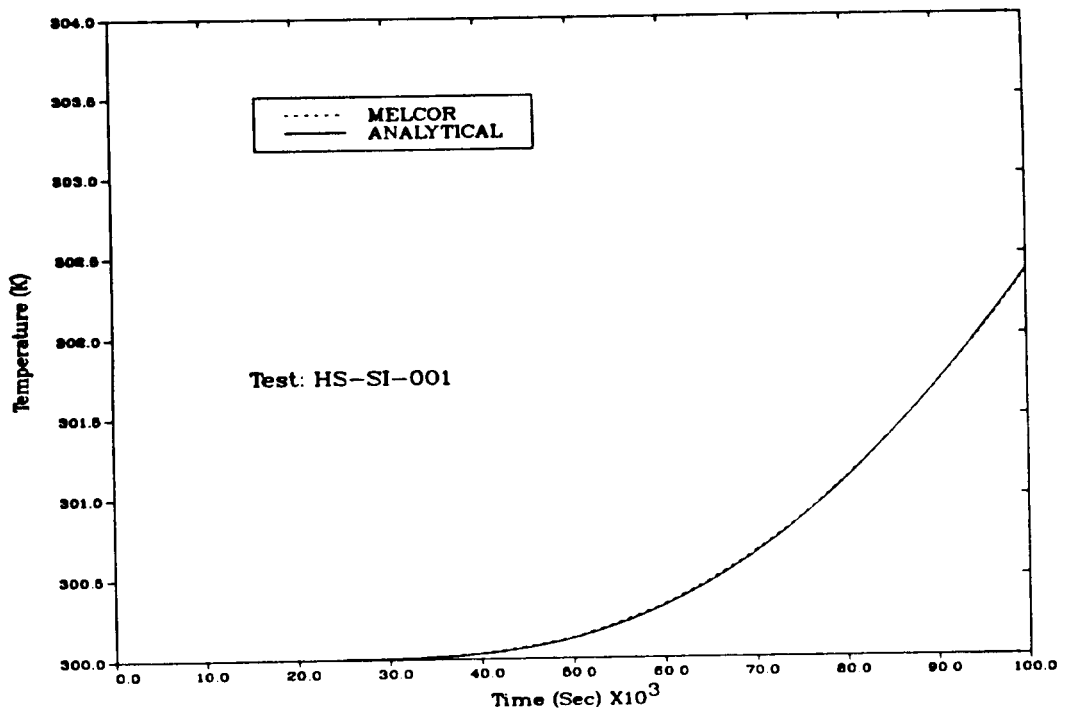


Figure 3. Slab Temperature at 1 Meter Versus Time on an Expanded Scale for the Base Case (Case 1 Table 1).

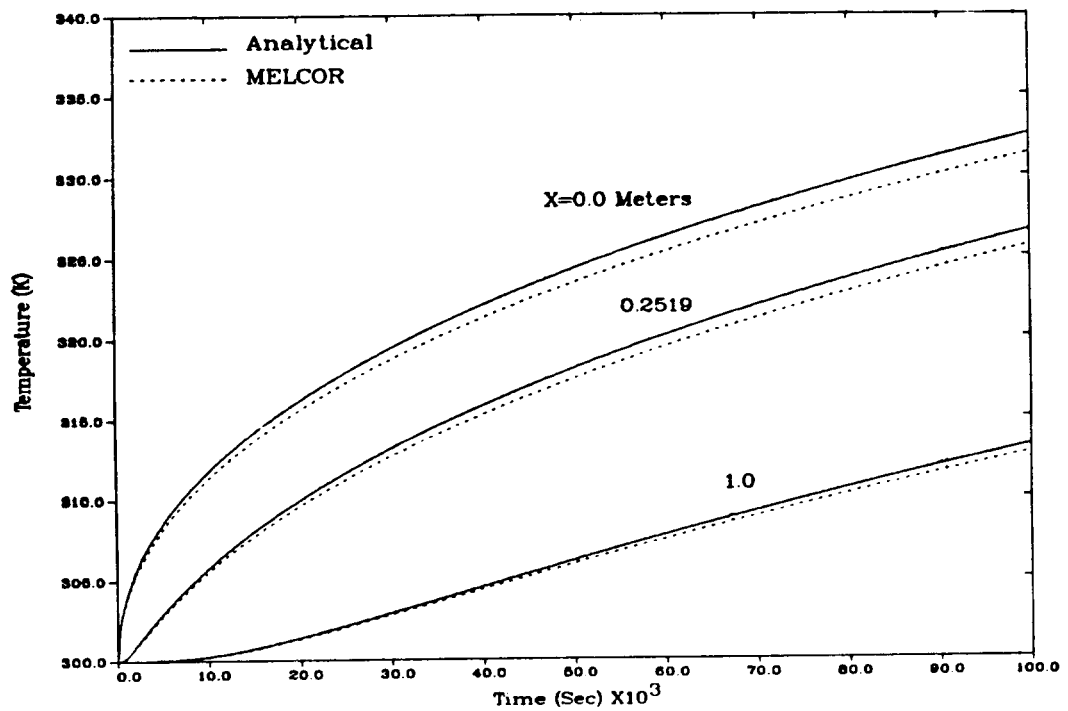


Figure 4. Time Temperature Results at Three Positions within the Slab for the Steel Properties Case (Case 2 from Table 1).

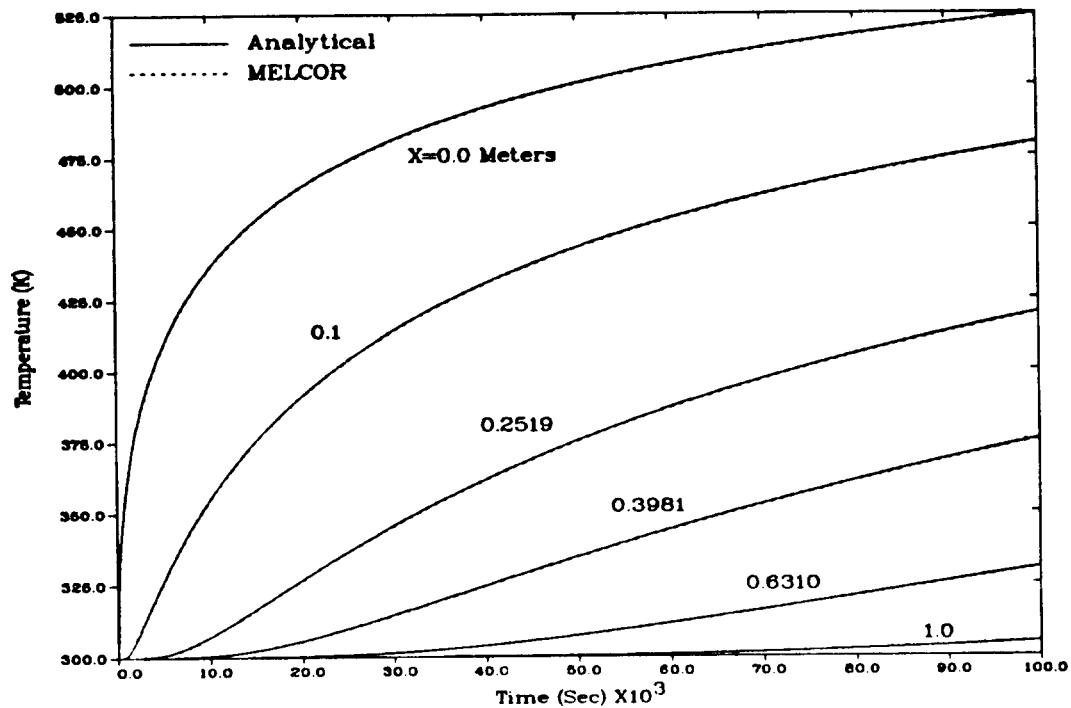


Figure 5. Time Temperature Results at Six Positions within the Slab for the High Temperature Case (Case 3 Table 1).

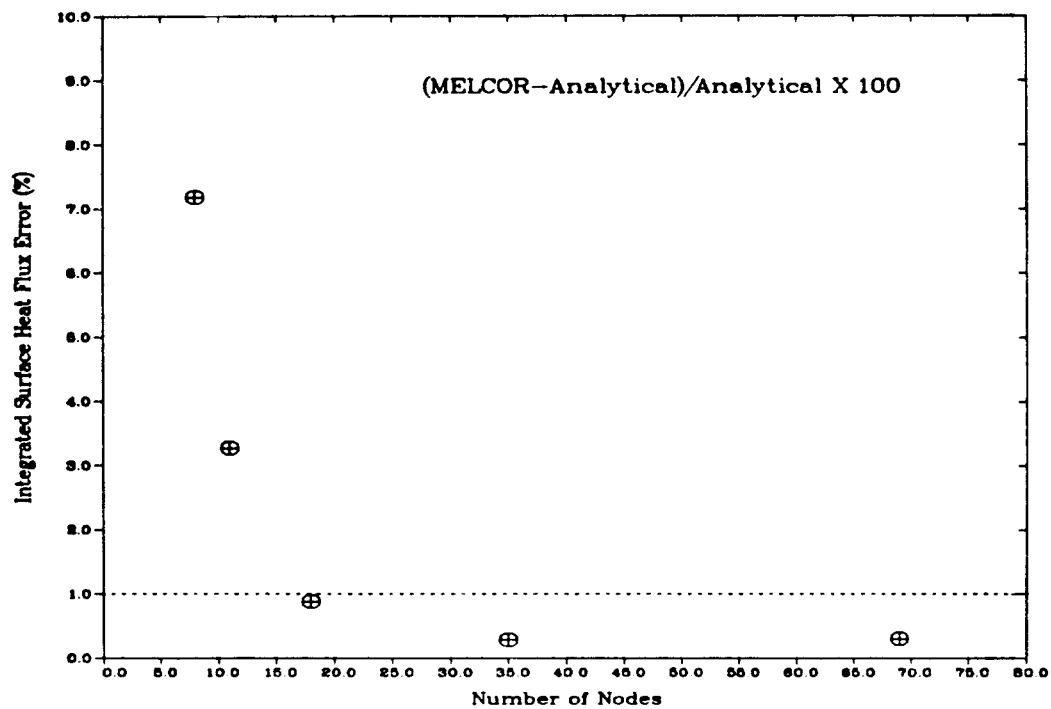


Figure 6. Node Spacing Test Errors

The temperatures at 1 meter are shown in Figure 9. The temperature is very accurately predicted for the 69 node case, but the other cases deviate somewhat from the exact solution.

#### 4.5 Time Step Size Test Cases

Test cases were run for time step sizes of 10, 20, 30, 60, 120, 250, 500, 1000, 2000, and 5000 seconds for both the 18 and 69 node structures. The results are shown in Figures 10 through 13.

The integrated surface heat flux errors for these 18 test cases are shown in Figure 10 as a function of time step size. The errors for both node structures remain within 1% for time steps less than about 100 seconds. Severe accident calculations usually use time steps of less than 60 seconds.

The surface temperature results for the 69 node cases using 10, 20, 30, 60, and 120 second time steps are shown in Figures 11 and 12. In Figure 11, the curves cannot be distinguished from one another, but Figure 12 shows an expanded section. The expanded plot shows "oscillations" in the surface temperatures which increase in amplitude with increasing time step size. These oscillations are somewhat smaller for the 18 node cases than for the the 69 node cases. For the 69 node cases, only the 10 second time step case is without observable oscillations whereas for the 18 node cases, the 10, 20, and 30 second time step cases are without oscillations. These oscillations do not seem to have much effect upon the integrated surface heat fluxes for the time step sizes of practical interest but could become important in calculations with convective heat transfer correlations that are sensitive to the surface temperature.

Figure 13 shows the temperatures at 1 meter into the slab. These temperatures are predicted reasonably well with time step sizes up to 120 seconds. The 69 node cases show better agreement with the analytical results than the 18 node cases.

#### 4.6 Practical Parameters

The base case calculation with 69 nodes and a 10 second time step size was chosen to give a very accurate prediction of the exact solution. In the interest of keeping computer run times reasonable (around 200 CPU), realistic severe accident analysis calculations are more likely to use something like the 18 nodes and 30 second time step size case for predicting the heat transfer into the containment walls. Figure 14 compares both of these cases with the analytical solution for an expanded section of the surface temperature. The integrated surface heat flux errors for these two cases are 0.30% and 0.92% for the 69 and 18 node cases, respectively. The surface temperatures of both of these calculations are apparently free of the oscillations shown in the previous section.

User judgement must be exercised in selecting the node spacing and time step sizes for a particular calculation. The need for accuracy must be balanced against the cost of the run. Consideration must be given to the accuracy of the overall heat transfer and the sensitivity of the convective heat transfer

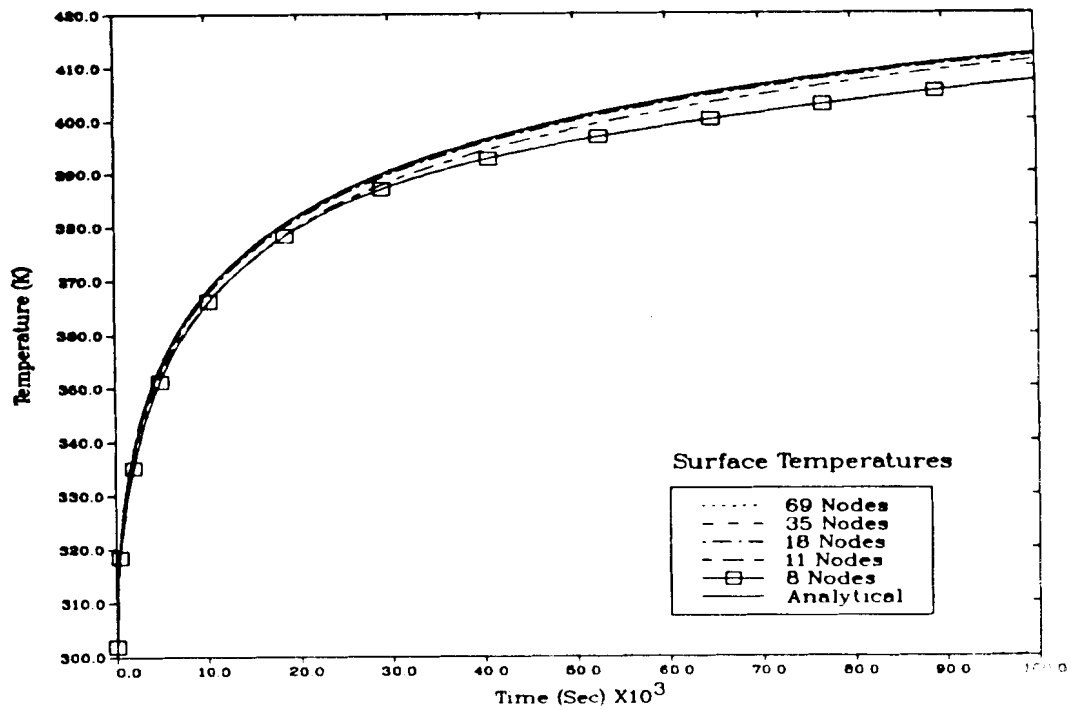


Figure 7. Surface Temperature Versus Time For Six Different Node Spacings

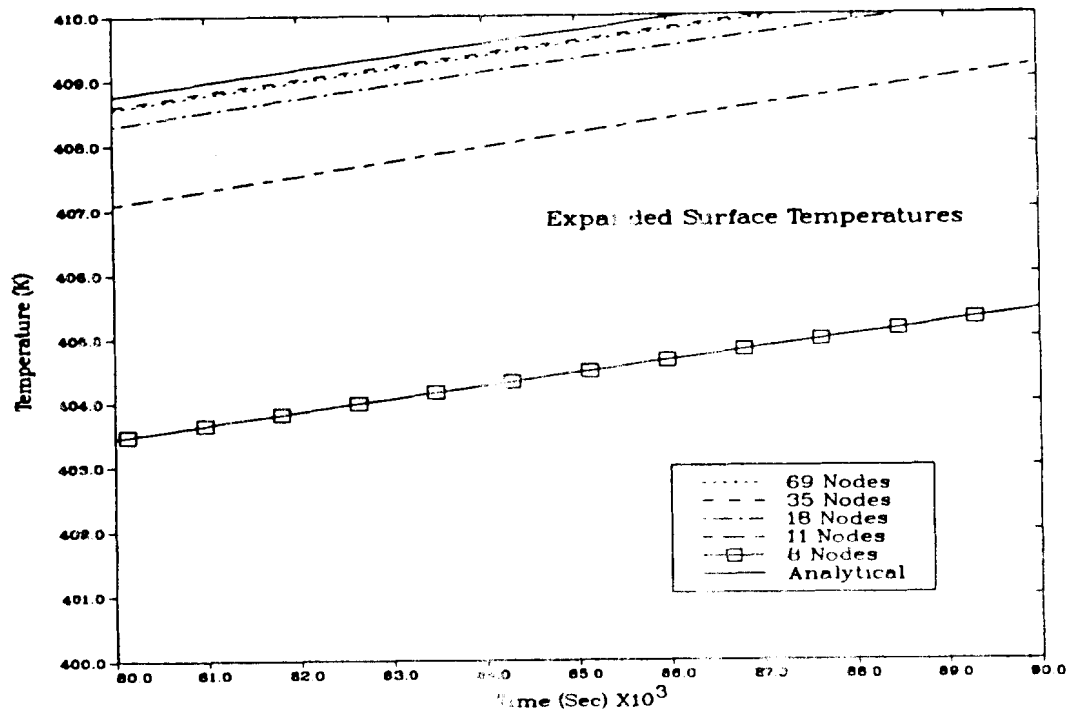


Figure 8. Surface Temperature Versus Time on an Expanded Scale for Six Different Node Spacings

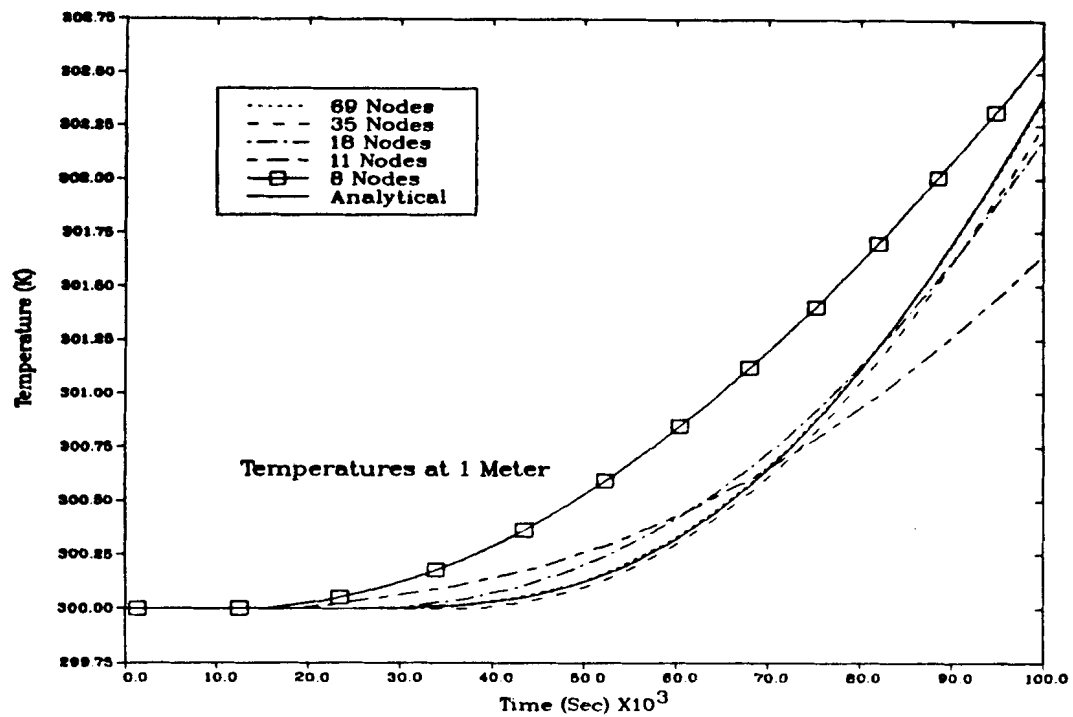


Figure 9. Temperature at 1 Meter Versus Time For Six Different Node Spacings

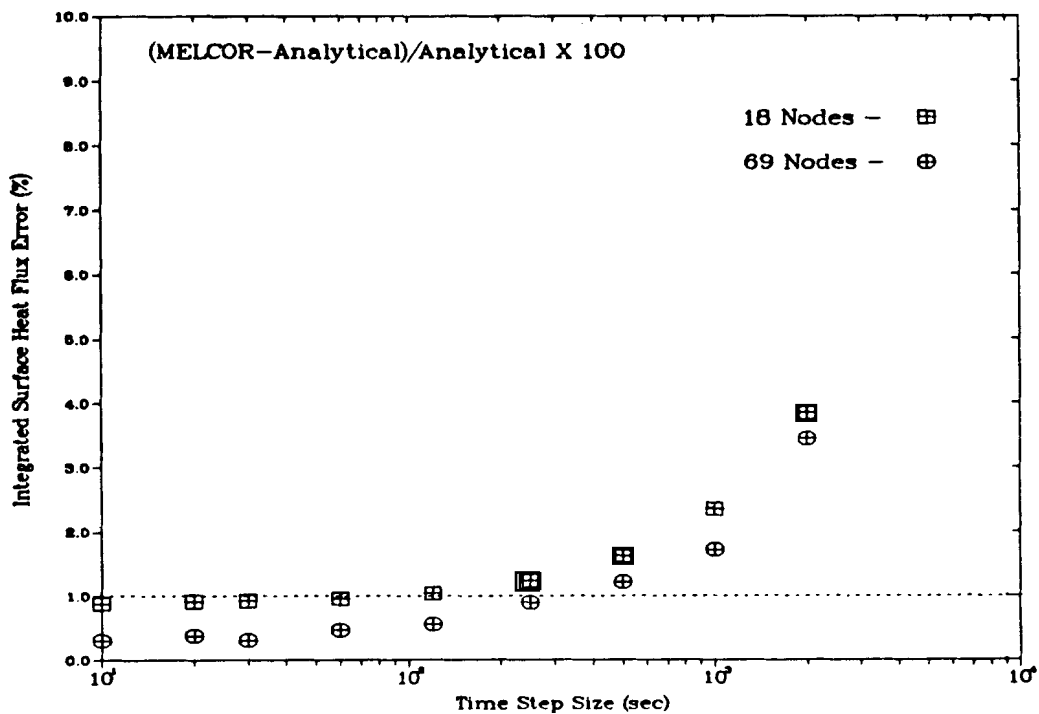


Figure 10. Variation in Integrated Surface Heat Flux with Time Step Size

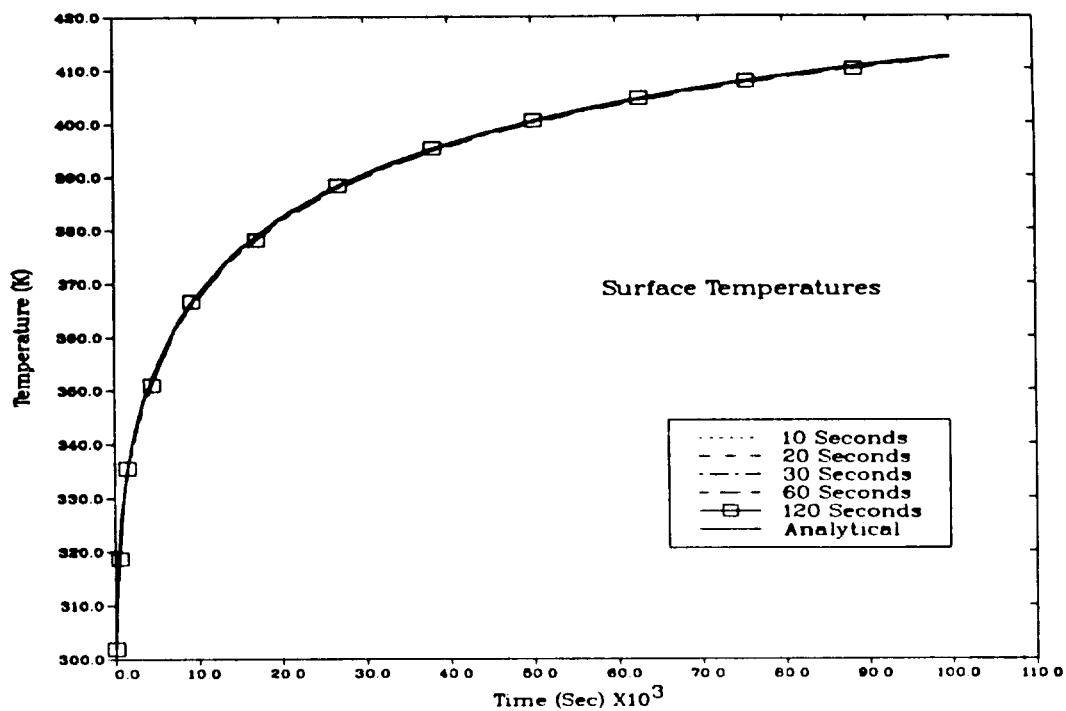


Figure 11. Surface Temperature Versus Time For Different Time Steps

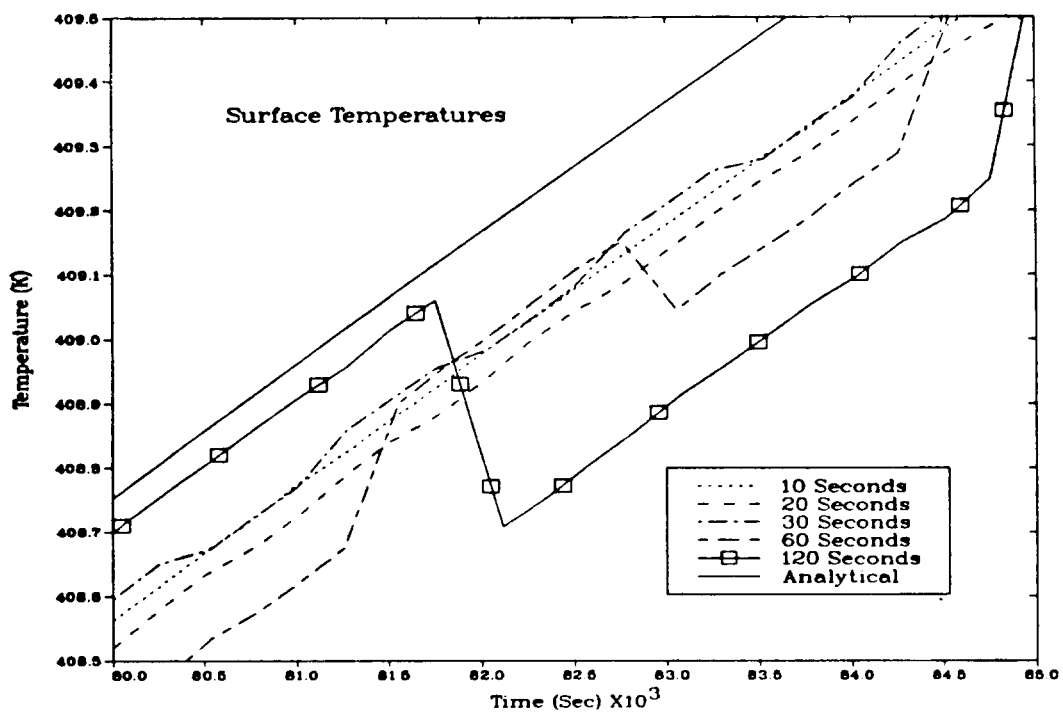


Figure 12. Surface Temperature Versus Time on an Expanded Scale for Different Time Steps

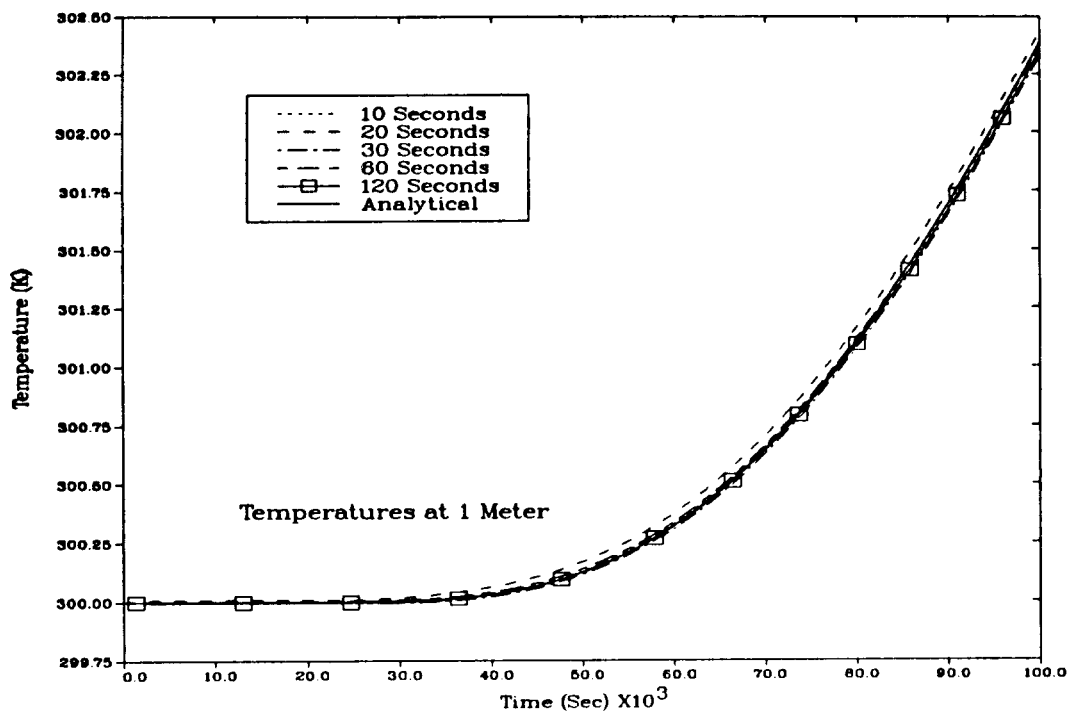


Figure 13. Temperature at 1 Meter Versus Time For Different Time Steps

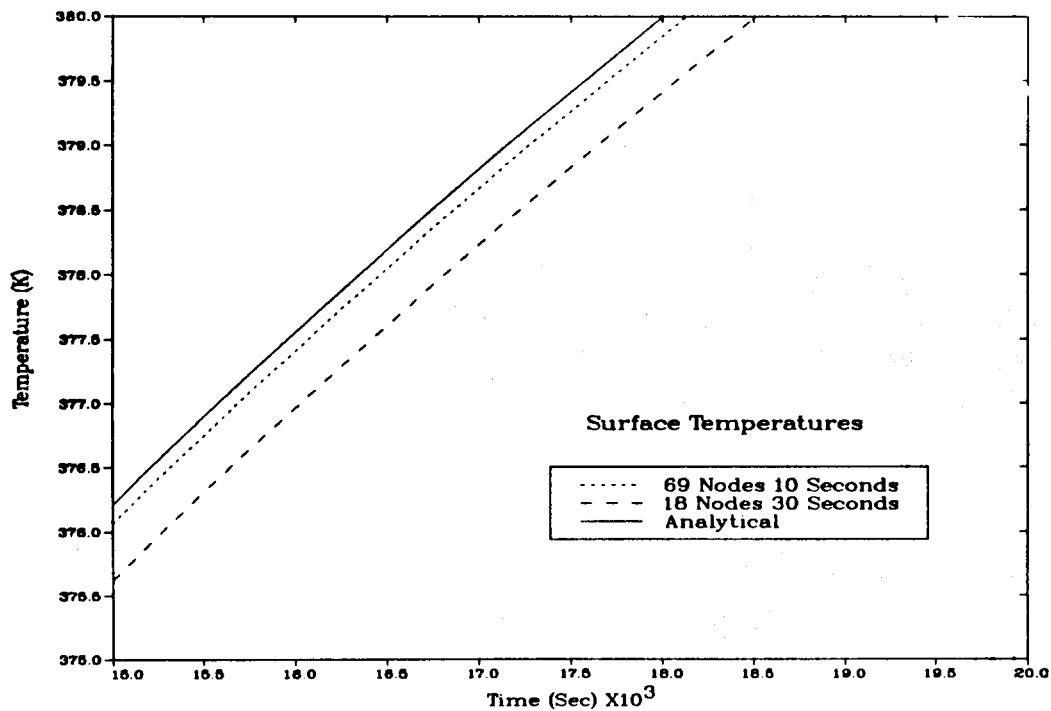


Figure 14. Surface Temperature Versus Time on an Expanded Scale for the 69 node:10 second Case and the 18 node:30 second Case



coefficient to the surface temperature. For instance, if the convective heat transfer coefficient is a function of a small temperature differential between the fluid and the wall temperatures then a relatively small error in the surface temperature might yield a much larger error in the resulting coefficient and heat flux.

## 5. Summary

Predictions of the MELCOR heat structures package heat conduction models are compared to the exact analytical solution for transient heat flow in a semi-infinite solid with convective boundary conditions. The semi-infinite solid is modeled in MELCOR as a 10 meter thick heat slab with logarithmic node spacing. The accuracy of the heat conduction models is demonstrated and node spacing and time step sizes are recommended for the modeling of the concrete containment walls in a severe accident analysis calculation of a nuclear power plant.

The results of three standard test cases compared relatively well with the analytical solution. Cases modeling concrete compared more closely than the case modeling steel. The best MELCOR predicted surface temperature for concrete lags the exact solution by about 0.2 K resulting in an error of about 0.3% in the time integrated surface heat flux. The temperature lag for steel was about 0.5 to 1.0 K resulting in an error of about 0.6%.

Node structures ranging from 5 to 69 nodes in the first meter of the wall were tested to survey the effect of node spacings on calculational results. The calculational errors are unacceptably large for the cases with few nodes and become more or less asymptotic for the finer node spacings. Cases with less than about 18 nodes in the first meter of the wall predict errors in excess of 1%.

Test cases were run for time step sizes ranging from 10 to 5000 seconds for both the 18 and 69 node structures. The errors in the integrated surface heat fluxes for both node structures remain within 1% for time step sizes below about 100 seconds. Most severe accident calculations use time step sizes of less than 60 seconds. The surface temperatures for runs up to about 120 seconds follow the analytical solution fairly closely (within about 0.5 K), however, small oscillations do occur and the amplitude of the oscillations increases with the size of the time step. The oscillations are somewhat smaller for the 18 node cases than for the 69 node cases indicating a relationship between the time step size and the size of the surface nodes. These oscillations appear to have little effect upon the integrated surface heat fluxes for the time step sizes of practical interest, but could become important in calculations with convective heat transfer correlations sensitive to the surface temperature.

The ability of MELCOR to predict the exact solution depends on the fineness of the node spacing and the time steps, and the precision of the computer. The inaccuracies in the standard test cases are stable and uniform throughout the calculations indicating the soundness of the MELCOR numerical models. The node spacing and time steps have been reduced to a fineness such that additional fineness does not increase the accuracy. The remaining inaccuracies then are

probably caused by computer round-off errors. In fact, the 35 node case results were slightly more accurate than the 69 node case implying that a use of more than 69 nodes will increase the round-off errors. A computer with more precision should calculate even better results.

While the exact analytical solution was predicted reasonably accurately with the case using 69 nodes and 10 second time steps (the CPU time is about 1500 seconds for these runs), realistic severe accident analysis calculations are more likely to use something like the 18 nodes and 30 second time steps for predicting the heat transfer into the containment walls (the CPU time is about 200 seconds for these runs). The integrated surface heat flux errors for the 69 and 18 node cases are 0.30 and 0.92%, respectively, and both are apparently free of the oscillations.

Cases 1 and 14 were rerun on MELCOR 1.6 with no significant differences from the results presented here.

## 6. References

1. J. P. Holman, Heat Transfer, 2nd Edition, McGraw-Hill Book Company, 1968.

MELCOR 1.5 Calculations  
for ABCOVE Aerosol Experiments AB5, AB6, and AB7

C. D. Leigh  
Sandia National Laboratories  
Albuquerque, New Mexico 87185  
United States of America

Abstract

The MELCOR code was used to simulate the ABCOVE Aerosol experiments AB5, AB6, and AB7. In these tests, a dry sodium aerosol was introduced into an 850 m<sup>3</sup> vessel and the aerosol behavior was monitored. Single and double component aerosols were used. Other codes have been used to simulate these tests including the CONTAIN[1] code at Sandia National Laboratories. Results from MELCOR were compared both to the experimental data and to the CONTAIN results. MELCOR results were nearly identical to the CONTAIN results. Code predictions for the suspended mass of aerosol track the experimental data to the end of the experiment to within a factor of two or three. Final predictions of the mass deposited by settling agree within an 11% error for all tests. In AB5, code predictions for the mass of material deposited by plating agree with the experimental data with a 12% error. However, in the other tests, the codes do not give accurate results for the amount of material deposited on the walls at the end of the test. These errors are probably related to the turbulence in the vessel which may cause inertial impaction. Impaction is not modeled in either of the codes.

1. Introduction

The Aerosol Behavior Code Validation and Evaluation (ABCOVE) program was a cooperative effort between the USDOE and the USNRC to validate aerosol behavior codes under the conditions found in an LMFBR containment during a severe accident. The expected aerosol suspended mass concentrations in an LMFBR accident exceed that expected of particulates in an LWR accident. Nevertheless, the ABCOVE experiments are also of interest for LWR modeling. The spherical cluster structure of the sodium oxide aerosols is similar to that expected of particulate aerosols in a steam environment. A series of validation experiments was conducted at the Containment Systems Test Facility (CSTF) at Hanford Engineering Development Laboratory (HEDL). Six codes were involved in a code comparison to these experiments including the CONTAIN[1] code run at Sandia National Laboratories. This test is a comparison of MELCOR results for the ABCOVE tests, AB5, AB6, and AB7 to both the experimental results and to the results from the CONTAIN code calculations. Both MELCOR and CONTAIN

CONTAIN incorporate MAEROS[2] in order to model aerosol behavior. However, the thermal hydraulic coupling is different in the two codes. The primary difference being that CONTAIN (at the time) used a user-specified thermal gradient when calculating the thermophoretic deposition, whereas MELCOR uses a thermal gradient calculated internally from the structure heat flux and the gas thermal conductivity. (CONTAIN has since been modified and follows the MELCOR approach). The input deck for these calculations is based on a CONTAIN input deck provided by K.K. Murata of Sandia National Laboratories (SNL). These calculations were most recently run on MELCOR 1.5.[3]

## 2. Test Descriptions

In all three tests, AB5, AB6 and AB7, the behavior of aerosols injected into a closed 850 m<sup>3</sup> vessel was examined. In Figure 1, a schematic diagram of the vessel is given. AB5 was a single component aerosol test while AB6 and AB7 were multicomponent aerosol tests. In the AB5 test, sodium oxide aerosols were generated from a sodium spray fire at a rate of 445 g/s for 885 seconds. In the AB6 test, two aerosol sources were provided to the vessel. One source, a simulated fission product aerosol, NaI, was generated by an ex-vessel vaporizer-condenser. The other source, NaOx, was generated by a sodium spray fire. The release rate of NaOx from the spray fire was approximately five hundred times that of the NaI, and the NaOx source was continued well past the NaI source cutoff. This overlap in the source rates was used in order to demonstrate the "washout" of the NaI by the continuing NaOx aerosol. The AB7 test was also a two component aerosol test; the NaI was generated by an ex-vessel vaporizer-condenser, and the sodium oxide was provided by a sodium pool fire. In the AB7 test, the quantity of NaOx released during the sodium pool fire was low, and all of the NaOx was reacted to sodium hydroxide, NaOH, by moisture in the vessel atmosphere. The NaI was released into the vessel atmosphere after the end of the sodium pool fire so that there was no overlap in the sources.

## 2. Computer Modeling of the ABCOVE Tests

The MELCOR calculations for AB5, AB6, and AB7 are based on the simulation that was originally performed with CONTAIN[3]. The aerosol sources were modeled by specifying lognormal source rates into the volume as indicated in Table 1.

For these three tests, the plating area and settling area used were about 750 m<sup>2</sup> and 88 m<sup>2</sup> respectively. For the CONTAIN calculations, a fitting procedure using the results of earlier experiments (AB1, AB2, and AB3) was used to obtain values for the agglomeration and dynamic shape factors[3]. The values obtained were 1.5 for the dynamic shape factor and 2.25 for the agglomeration shape factor. These values were used for the MELCOR calculations. A material density of 2500 kg/m<sup>3</sup> was assumed in AB5 and AB6, and 2130 kg/m<sup>3</sup> was assumed in AB7. The turbulent agglomeration coefficient was set at 1.0E-03 m<sup>2</sup>/s<sup>3</sup> for all three tests and the diffusional boundary layer thickness was set at 1.0E-5 m. A summary of these values is given in Table 2.

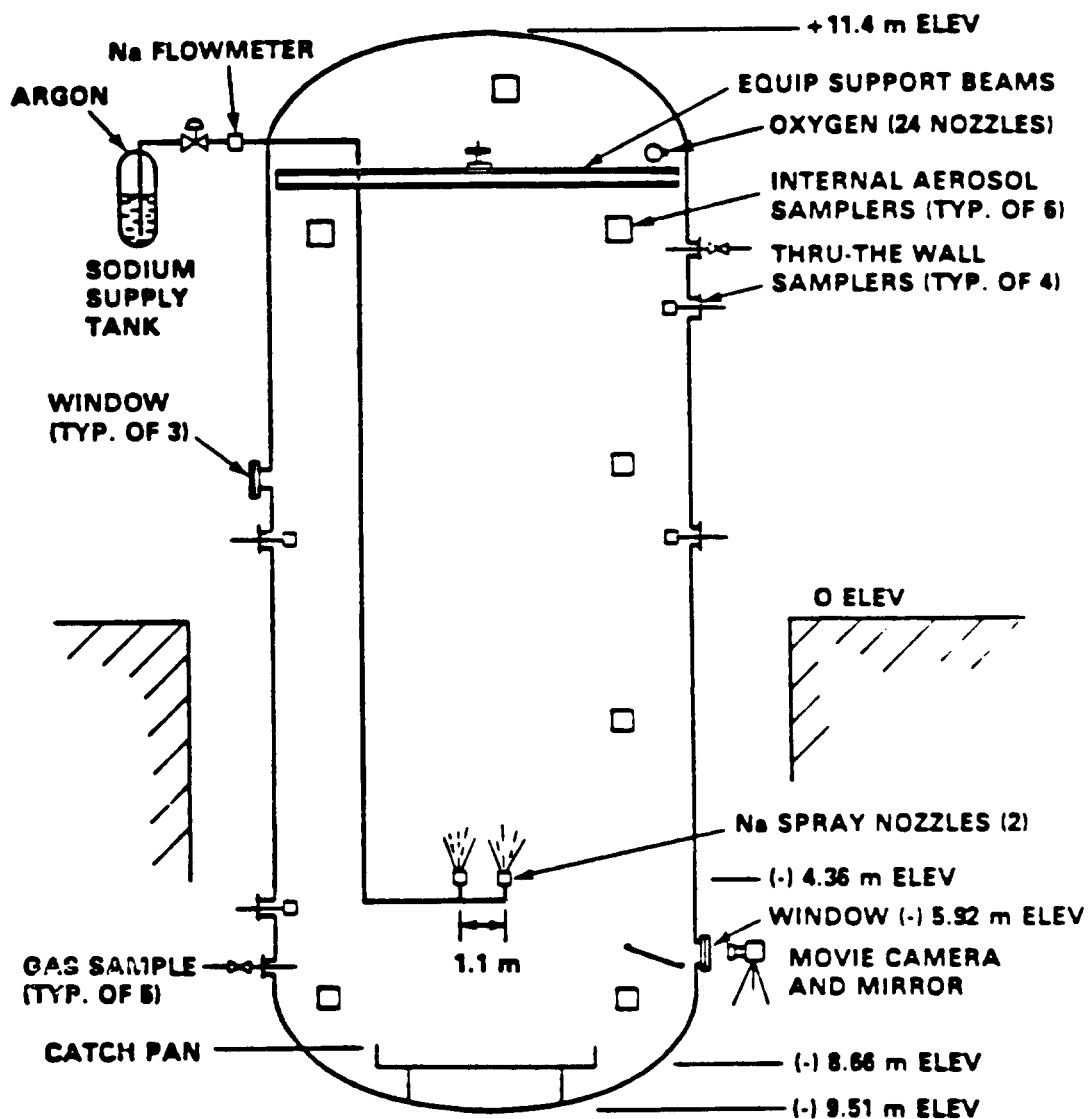


Figure 1. Schematic Diagram of the Aerosol Test Facility

Table 1. Aerosol Sources for Tests AB5, AB6, and AB7.

Aerosol	Source Rate (kg/s)	Time On (s)	Time Off (s)	Mass Median Diameter (m)	Standard Deviation
AB5-NaOx	4.45E-01	13.	885.	0.50E-06	1.50
AB6-NaOx	7.79E-02	620.	5400.	0.50E-06	2.00
AB6-NaI	1.40E-04	0.	300.	0.54E-06	1.55
AB7-NaOH	5.03E-03	0.	600.	0.50E-06	2.00
AB7-NaI	1.97E-04	600.	1800.	0.54E-06	1.55

Table 2. Parameter Values for MELCOR and CONTAIN Calculations for AB5, AB6, and AB7

Parameter	Test: AB5	AB6	AB7
Plating Area ( $m^2$ )	88.40	88.40	88.40
Settling Area ( $m^2$ )	749.7	750.5	750.5
Agglomeration Shape Factor	2.25	2.25	2.25
Dynamic Shape Factor	1.5	1.5	1.5
Material Density ( $kg/m^3$ )	2500.	2500.	2130.
Turb. Aggl. Coefficient ( $m^2/s^3$ )	.001	.001	.001
Diff. Boundary Layer Thickness (m)	1.E-5	1.E-5	1.E-5

One control volume and two heat structures (one representing vertical surfaces and one representing horizontal surfaces) were specified in the MELCOR simulation of these tests. In the experiments, the vessel temperature and pressure were monitored through time at approximately forty locations. For the calculations performed with the CONTAIN code, there was no attempt made to simulate the experimental temperature and pressure profiles. AB5 and AB7 were modeled with a constant temperature and pressure assumption, and AB6 was modeled with a series of step jumps in temperature.

To achieve a step temperature profile with MELCOR for AB6, heat was added incrementally to the vessel. The heat,  $Q$ , necessary to achieve a step jump,  $\Delta T$ , in the vessel temperature is:

$$Q(\Delta T) = c_v V p \Delta T \quad (1)$$

where  $c_v$  is the constant volume specific heat of the gas (assumed constant in this calculation),  $V$  is the vessel volume, and  $p$  is the density of the gas.

In CONTAIN (as in the stand-alone version of MAEROS), the thermal gradient used to calculate the thermophoretic deposition rate is an input quantity, whereas in MELCOR it is not. In order to obtain a constant thermal gradient at a surface in MELCOR, one must specify a constant heat flux boundary condition that will result in the appropriate thermal gradient according to the equation:

$$\nabla T k = - q \quad (2)$$

where  $\nabla T$  is the thermal gradient at the surface (K/m),  $k$  is the gas thermal conductivity (W/m K), and  $q$  is the heat flux at the surface (W/m<sup>2</sup>). The value of  $k$  used in the MELCOR radionuclide package is the thermal conductivity of air provided by the material properties package as a function of temperature. To maintain the energy content of the control volume and heat structure, an equal heat flux must be specified at the other side of the heat structure to transfer the energy back into the control volume.

### 3. Results

Figures 2 through 7 show the time dependent results of the MELCOR and CONTAIN calculations as well as available experimental data for experiments AB5, AB6, and AB7 respectively. Results are shown for the suspended aerosol mass, the mass deposited (settled) on the floor, and the mass deposited (plated) on the walls. End of experiment values for the deposited masses for MELCOR, CONTAIN, and the stand-alone version of MAEROS are compared to the experimental results in Table 3.

For AB5, CONTAIN and MELCOR are very close in their predictions of the suspended mass. Excellent agreement is apparent during the source and up to the time when the concentrations are reduced by a factor of  $10^{-2}$ . Agreement with experimental data to the end of the experiment where concentrations are

Table 3. Comparisons for Settled and Plated Masses

	MELCOR	CONTAIN	Hilliard[5]	MAEROS	MELCOR* % Error
AB5					
Settled Mass(kg)	370.5	370.5	382.0	370.1	3%
Plated Mass(kg)	16.1	17.0	18.3	17.4	12%
AB6					
Settled Mass(kg)	371.1	362.8	335.0	365.5	11%
Plated Mass(kg)	6.7	9.0	38.0	7.1	83%
AB7					
Settled Mass(kg)	3.2	3.3	3.3	3.3	3%
Plated Mass(kg)	.02	.02	.24	.02	90%

\* Calculated as  $100 \times (\text{MELCOR} - \text{Hilliard}) / \text{Hilliard}$

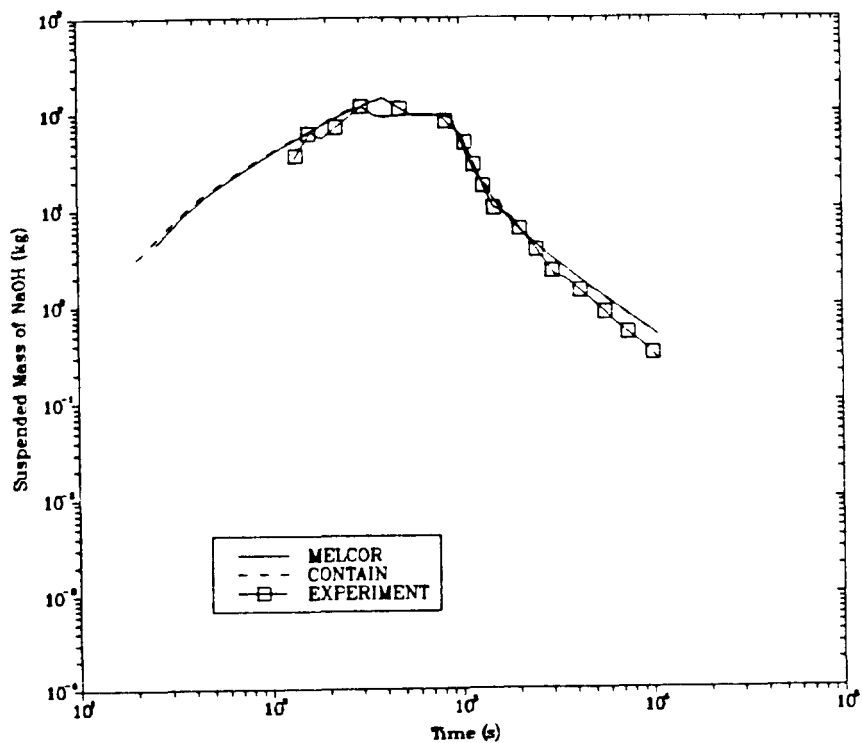


Figure 2 . Suspended Mass of Aerosol Predicted by CONTAIN and MELCOR for AB5



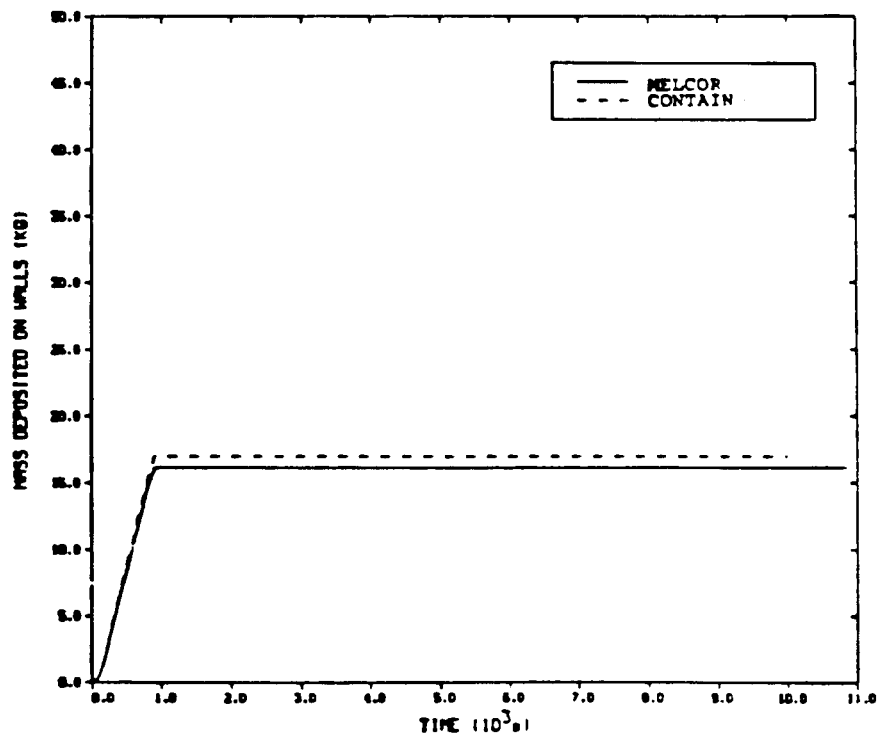
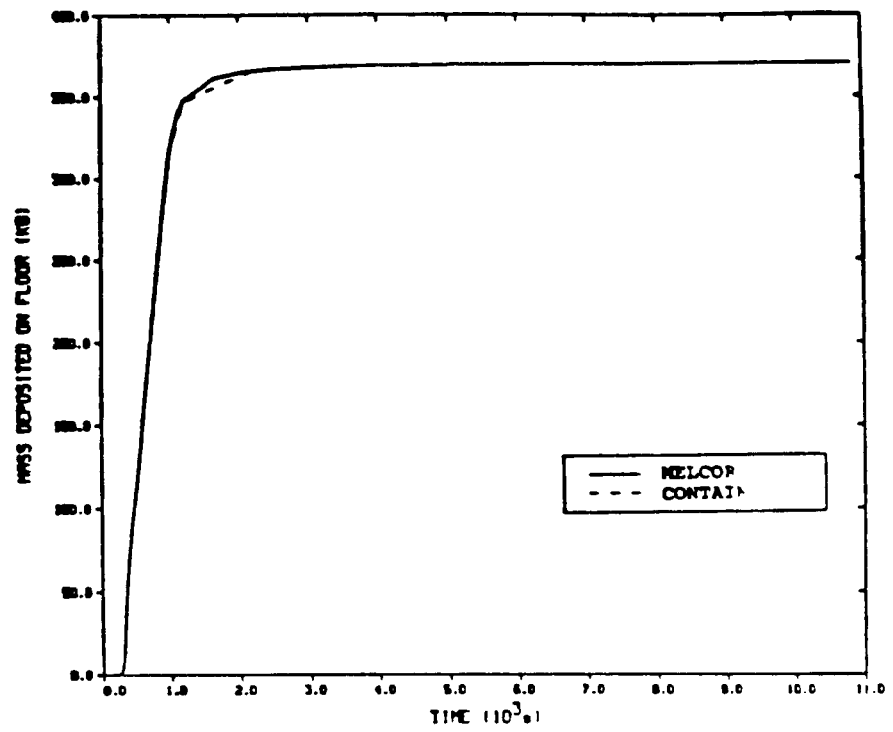


Figure 3. Deposited Mass Predicted by CONTAIN and MELCOR For AB5

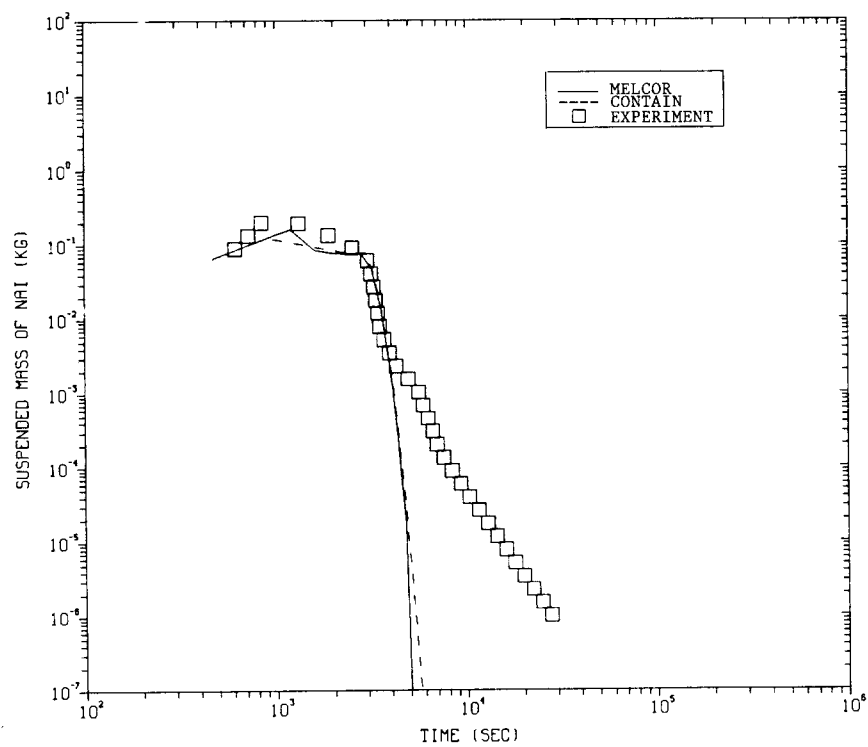
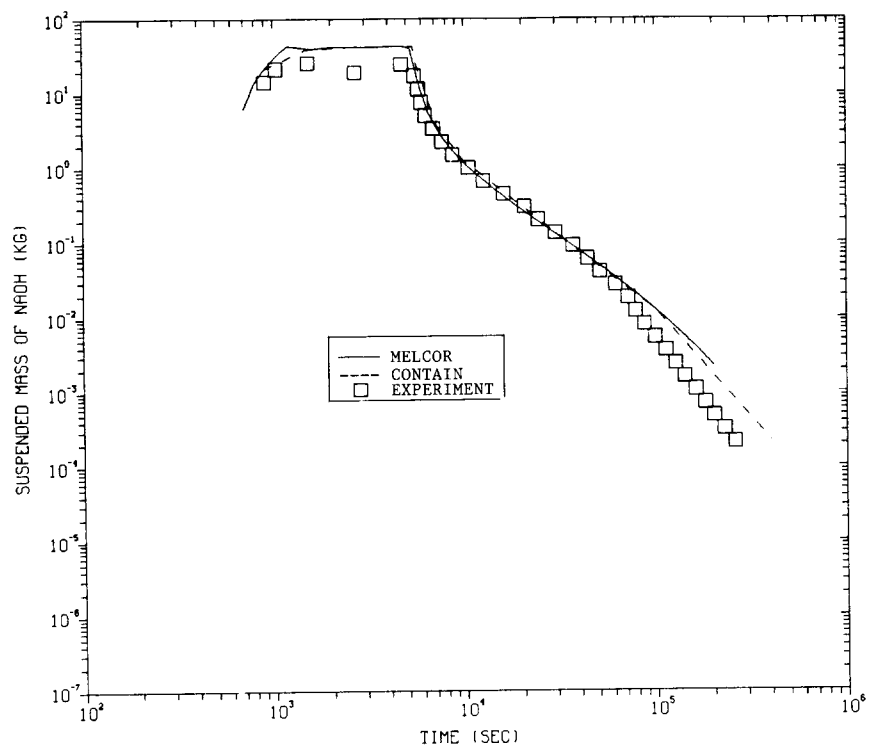


Figure 4. Suspended Aerosol Mass Predicted by CONTAIN and MELCOR for AB6

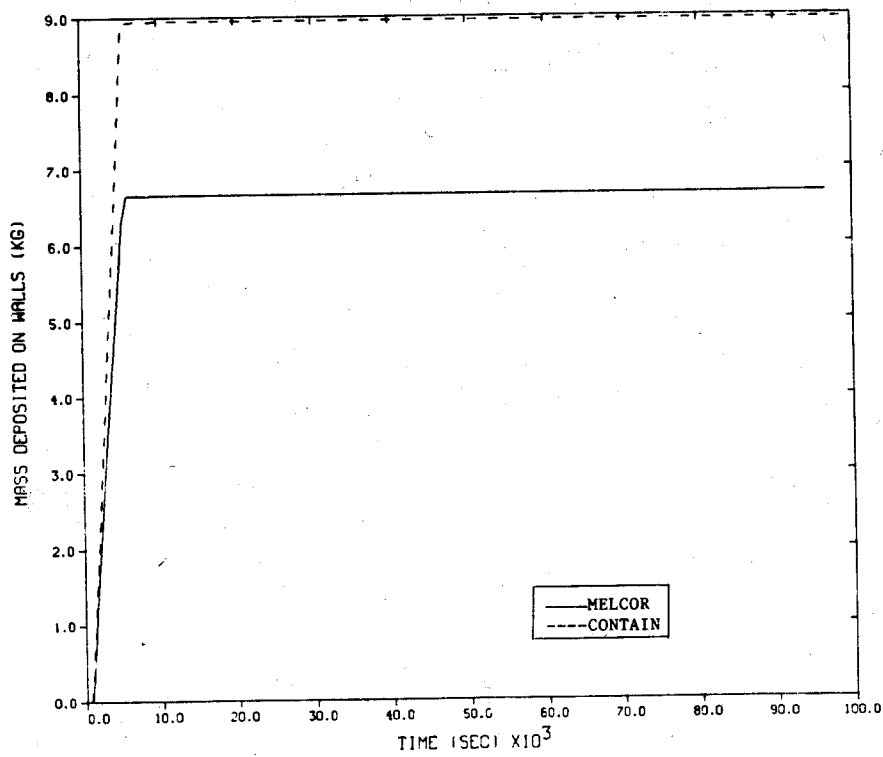
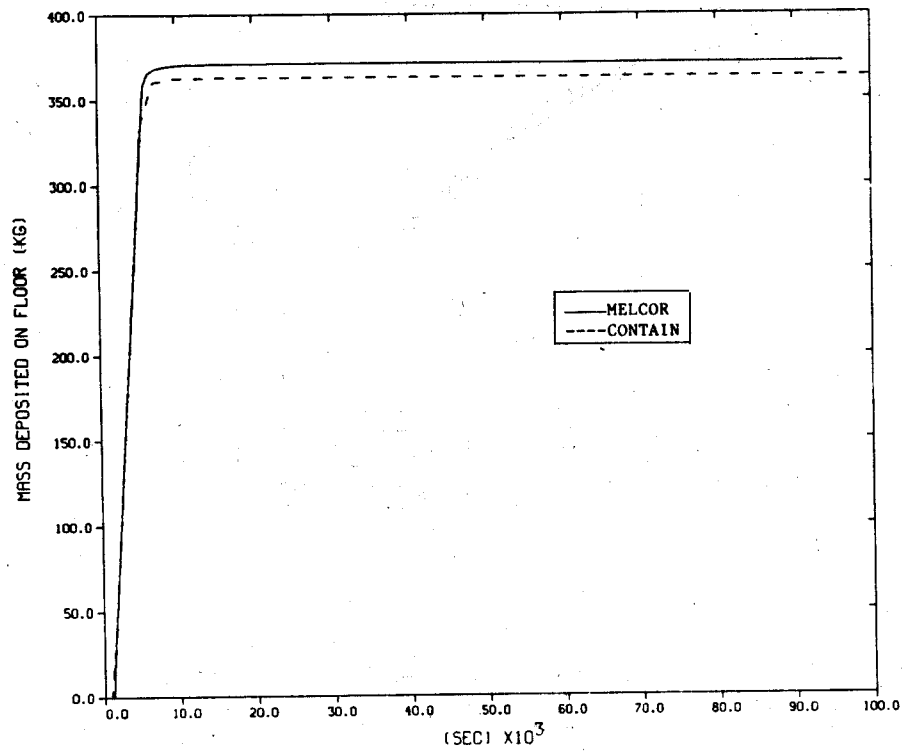


Figure 5. Deposited Aerosol Mass Predicted by CONTAIN and MELCOR for AB6

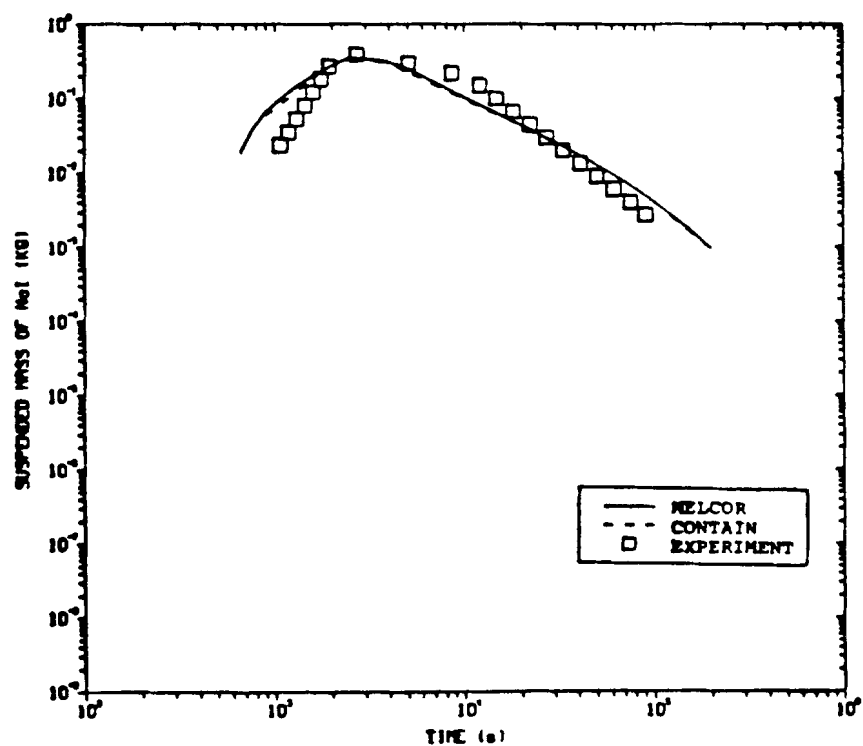
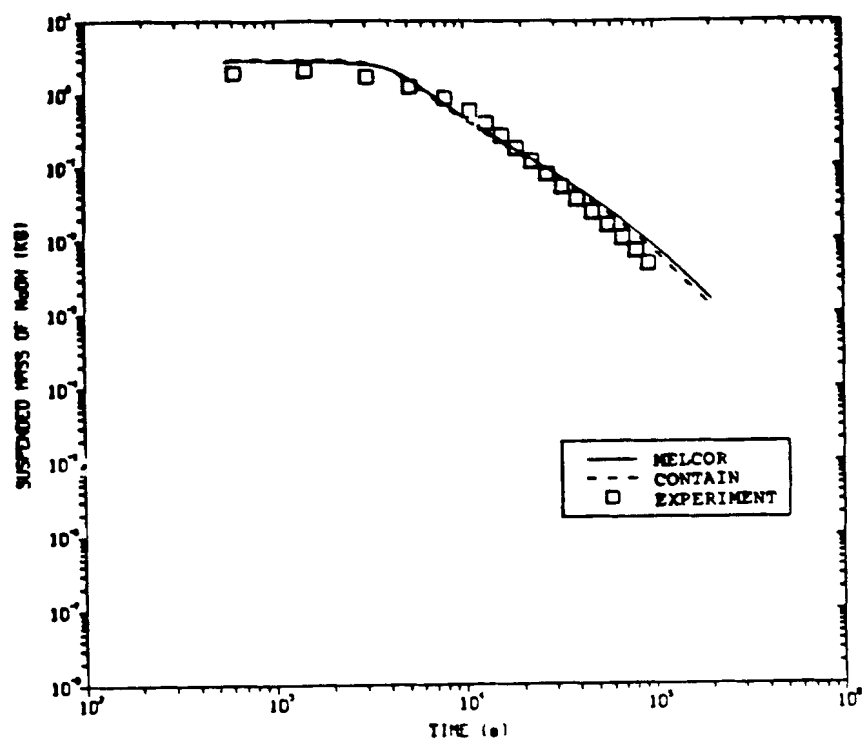


Figure 6. Suspended Aerosol Mass Predicted by CONTAIN and MELCOR for AB7

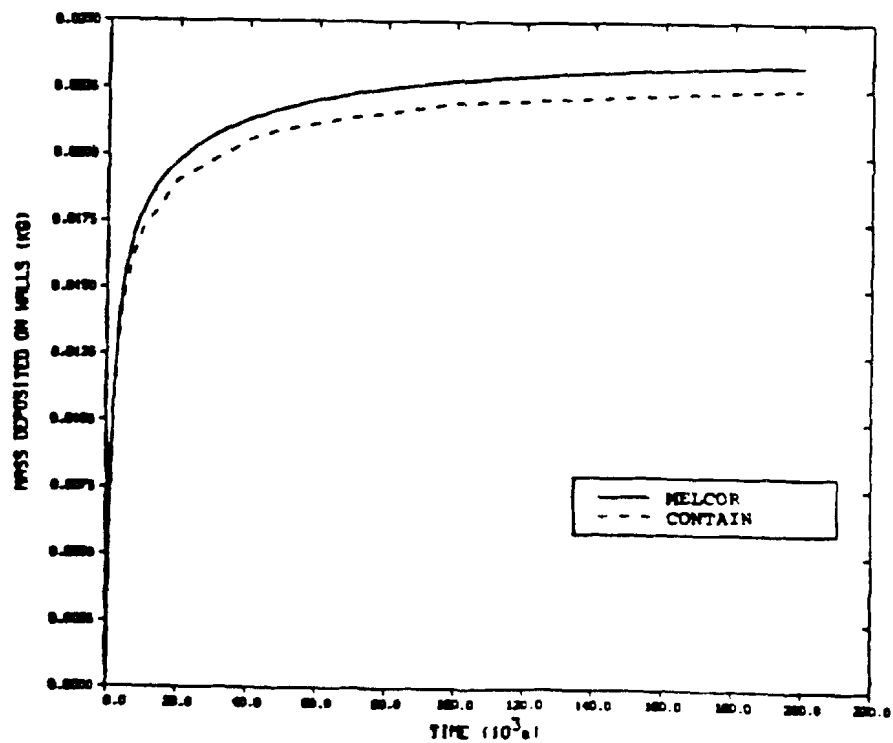
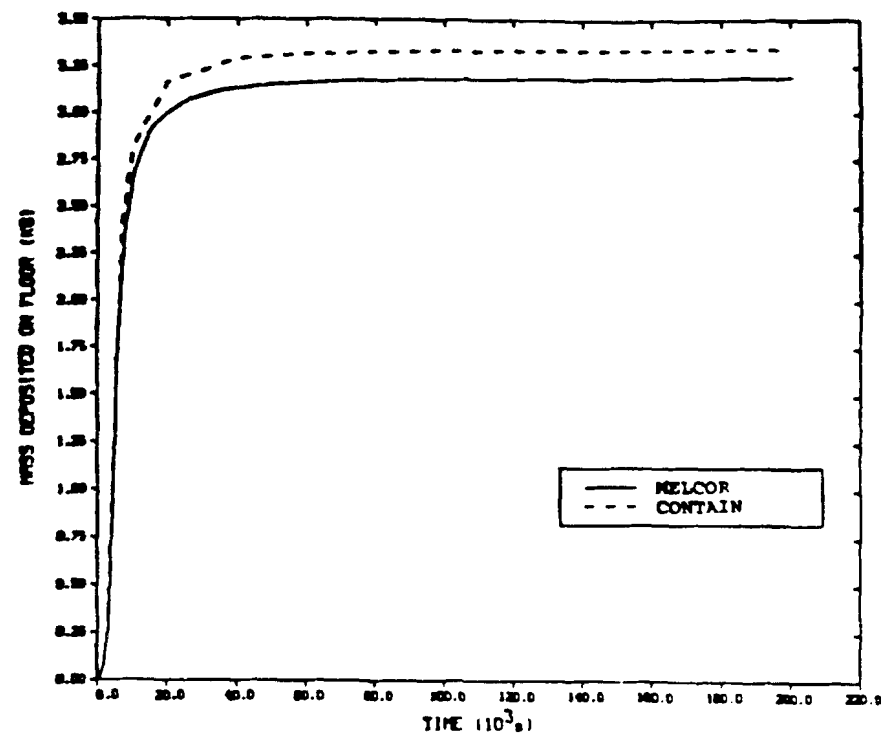


Figure 7. Deposited Aerosol Mass Predicted by CONTAIN and MELCOR for AB7

reduced by  $10^{-6}$  are within a factor of two to three. MELCOR and CONTAIN predictions of the settled mass also agree. Time dependent experimental results are not available for the settled mass. However, the total deposition on horizontal surfaces was measured at the end of the test and was 382.0 kg[5]. CONTAIN and MELCOR predict a settled mass of aerosol deposited on the floor of 370.5 kg. The percentage error in the MELCOR calculation for the settled mass in AB5 is 3%. The amount of material deposited on the walls in AB5 is 17.0 kg in the CONTAIN calculation and 16.1 kg in the MELCOR calculation. 18.3 kg of aerosol measured on vertical surfaces at the end of the experiment is reported by Hilliard et al.[5]. The MELCOR code predicts the mass deposited on the wall in AB5 with about a 12% error when compared to the experimental results and a 7% error when compared to the stand-alone MAEROS.

In AB6, CONTAIN and MELCOR are very close in their predictions of the NaOx suspended mass. Both codes slightly overpredict the NaOx suspended mass during the source and at later times when the suspended concentration has been significantly reduced. Code predictions are in excellent agreement with the experimental results between  $1.0E4$  and  $1.0E5$  seconds. The behavior of the suspended mass of NaI in AB6 differs significantly from the code predictions at late times. Both MELCOR and CONTAIN predict a rapid, continuous decay in the NaI concentration after the source has been cut off. The experimental results show that the rapid decay lasts only a short while before slowing down to a rate that is approximated by uniform coagglomeration[6]. Hilliard[6] suggests that phenomena not modeled by any of the codes may have caused this behavior. He suggests two possibilities: resuspension of previously deposited material or vaporization of the NaI (since the spray fire continues throughout the test) followed by condensation on the smaller NaOx particles (which causes a shift in the particle size distribution to smaller sizes that remain suspended longer). In addition, two mixing cells developed in the containment atmosphere during the test which are not modeled in any of the calculations. Once again, the two codes agree in their predictions of the settled and plated masses. Time dependent experimental results are not available for these quantities. However, Hilliard[6] reports a settled mass of 335.0 kg. MELCOR predicts a settled mass of 371.1 kg and CONTAIN predicts 362.8 kg. The MELCOR result has an 11% error. The experimental results indicate that 38.0 kg of aerosol were plated on vertical surfaces during the test. MELCOR predicts a plated mass of 6.7 kg and CONTAIN predicts 9.0 kg. The MELCOR value represents an 83% error when compared to experimental results and a 6% error when compared to the stand-alone MAEROS. None of the codes involved in the comparison were able to adequately predict the plated mass for this test. The testers conclude that the primary plating mechanism in this test was impaction, not thermophoresis, which is a phenomenon that none of the codes can predict.

For AB7, CONTAIN and MELCOR are very close in their predictions of the suspended aerosol masses and show good agreement with the experimental data. During the source and at later times when the concentrations have been significantly reduced, the codes slightly overpredict the suspended masses of both components. Both MELCOR and CONTAIN predict higher values (3.3 kg by CONTAIN and 3.2 by MELCOR) for the settled mass than Hilliard [5] who reports that a total of 3.1 kg is deposited on upward facing horizontal surfaces. The MELCOR prediction has a 3% error. Both MELCOR and CONTAIN predict a mass deposited on the wall of .02 kg. It is apparent that neither CONTAIN nor MELCOR adequately predicts deposition on the wall for this test since Hilliard [5] reports that .24 kg of aerosol is deposited on vertical surfaces in this

test. This is a 90% error, however, the MELCOR results do agree with stand-alone MAEROS predictions. None of the codes involved in the comparison was able to adequately predict the plated mass. The testers suggest that these errors may be caused by inertial impaction in the vessel.

#### 4. Code Limitations Identified

Currently in MELCOR, the suspended mass of an individual component is not available as an output variable although the MELCOR calculation is multicomponent. It is extremely important for LWR applications that the aerosol calculations be multicomponent[9], and AB6 and AB7 are ideal tests of the multicomponent nature of the MELCOR code. However, the comparison is very difficult because the suspended mass of each component is not available as an output variable. Since MELCOR does provide the suspended radioactive mass as an output variable, for AB6 and AB7, MELCOR was run first by specifying that all of the NaOx (component 1) was radioactive, and the radioactive mass (the mass of NaOx) was plotted. Then MELCOR was rerun specifying that all of the NaI was radioactive, and the radioactive mass (the mass of NaI) was plotted. This was a cumbersome process, and the need to output the suspended mass of individual components has been reported to the code developers.

While performing these calculations with the MELCOR code several defects were identified. First, instabilities in the heat structure package were identified and corrected. Second, the need for providing the diffusional boundary layer thickness as a user input was identified and the input parameter was added. Third, a defect in the logarithmic plotting option was identified and corrected. Finally, it was reported that the mass median diameter of the aerosol size distribution is a variable of interest in aerosol tests, and it should be made available as an output variable. This option has not yet been added.

#### 5. Summary and Conclusions

These MELCOR calculations showed good agreement with CONTAIN predictions for the ABCOVE aerosol tests AB5, AB6, and AB7. All quantities predicted by the two codes agreed very well although neither code adequately predicted the plated masses in AB6 and AB7.

In the future, it would be interesting to compare the time dependent behavior of the mass median diameter of the aerosol size distribution. However, this is not an output variable that is available in MELCOR at this time.

## 6. References

1. K.D. Bergeron et al., User's Manual for CONTAIN 1.0, NUREG/CR-4085, SAND84-1204, Sandia National Laboratories, May 1985.
2. F. Gelbard, MAEROS User's Manual, NUREG/CR-1391, SAND80-0822, Sandia National Laboratories, December 1982.
3. MELCOR 1.5 was released although not officially published.
4. K.K. Murata, et al., "CONTAIN: Recent Highlights in Code Testing and Validation, Proceedings from the International Meeting on Light Water Reactor Severe Accident Evaluation, Cambridge, Massachusetts, September 1983.
5. R.K. Hilliard, J.D. McCormack, and A.K. Postma, Results and Code Predictions for ABCOVE Aerosol Code Validation -- Test AB5, HEDL-TME 83-16, Hanford Engineering Laboratory, 1983.
6. R.K. Hilliard, J.D. McCormack, and L.D. Muhlestein, Results and Code Predictions for ABCOVE Aerosol Code Validation -- Test AB6 with Two Aerosol Species, HEDL-TME 84-19, Hanford Engineering Laboratory, December 1984.
7. R.K. Hilliard, J.D. McCormack, and L.D. Muhlestein, Results and Code Predictions for ABCOVE Aerosol Code Validation with Low Concentration NaOH and NaI Aerosol, HEDL-TME 85-1, Hanford Engineering Laboratory, October 1985.
9. R.J. Lipinski et al., Uncertainty in Radionuclide Release Under Specific LWR Accident Conditions: Volume II: TMLB' Analysis, SAND84-0410, Sandia National Laboratories, February 1986.



## Appendix A

### MELCOR Standard Test Problems from 1986

This appendix contains brief descriptions of the standard tests that have been developed in association with this report. One standard test has been developed from each paper. Appendix B contains copies of the input files for the tests, and Appendix C contains copies of the comparison plots. Requests for additional information should be directed to the editor of this report.

#### ST001: Adiabatic Expansion of Hydrogen, Two-Cell Flow

This test is Case 5 from the paper, "MELCOR 1.6 Calculations for Adiabatic Expansion of Hydrogen, Two-cell Flow". Two control volumes are pressurized with hydrogen. The pressure in control volume 1 is  $2.E5 \text{ Pa}$  and the pressure in control volume 2 is  $1.E5 \text{ Pa}$ . Both volumes are  $1000 \text{ m}^3$  and at  $300 \text{ K}$ . A  $50 \text{ m}^2$  flow path is opened between the volumes at time zero and they are allowed to equilibrate.

#### ST002: Radial Conduction in Annular Structures

This test is Case 4 from the paper, "MELCOR 1.0 Calculations for Radial Conduction in Annular Structures". An annular structure initially at  $600 \text{ K}$  is exposed to a  $550 \text{ K}$  environment on its outer surface and a  $600 \text{ K}$  environment on its inner surface. The structure is allowed to reach its steady state temperature distribution.

#### ST003: Cooling of a Structure in a Fluid

This test is taken from the paper, "MELCOR 1.0 Calculations for Cooling of Structures in a Fluid". Two uniform structures, a rectangular slab and a cylinder, are submersed in a fluid that is at  $500 \text{ K}$ . Both structures are initially at  $1000 \text{ K}$  and have constant thermal properties and constant surface heat transfer coefficients. The temperature of each solid as a function of time is noted.

#### ST004A and ST004B: Semi-Infinite Heat Structure Test

This test is Case 1 from the paper, "MELCOR 1.1 Calculations for a Semi-infinite Solid Heat Structure Test". This is a test of transient heat flow in a semi-infinite solid with convective boundary conditions. This case involves a  $10 \text{ m}$  thick concrete structure. The fluid temperature is  $450 \text{ K}$ , and the initial temperature of the structure is  $300 \text{ K}$ . For ST004A, there are 18 nodes in the first meter of the structure, and it is run with 30 second time steps. For ST004B, there are 69 nodes in the first meter of the structure, and it is run with 10 second time steps.

#### ST005: Saturated Liquid Depressurization Test

This test is taken from the paper, "MELCOR 1.6 Calculations for a Saturated Liquid Depressurization Test". A volume containing saturated water at high pressure is depressurized into a second larger volume. The two volumes are connected by a flow path and a heat structure.

#### ST006: Browns Ferry Reactor Building Burns

This test was taken from the paper, "MELCOR 1.0 and HECTR 1.5 Calculations for Browns Ferry Reactor Building Burns". It is a test of the reactor building response to hydrogen burns that occur when hydrogen is released to the building. This is an integrated test that involves three control volumes and six flow paths.

#### ST007: HDR Steam Blowdown Test

This test was taken from the paper, "MELCOR 1.6 Calculations for the HDR Containment Experiment V44". It is a test of the containment response to the depressurization of a reactor pressure vessel. This is an integrated test that involves five control volumes and nine flow paths.

#### ST008: ABCOVE Aerosol Experiment Test AB6

This is Case 2 from the paper, "MELCOR 1.5 Calculations for ABCOVE Aerosol Experiments AB5, AB6, and AB7". Two aerosol sources are introduced into an 850 m<sup>3</sup> volume. The two aerosols are NaI and NaOH. The NaI is introduced first with a small source rate. Following that, the NaOH is introduced with a large source rate. The NaOH source is continued well after the NaI source is discontinued. This is a dry aerosol problem.

#### ST009A and ST009B: Battelle-Frankfurt Gas Mixing Experiments

These are Case 2 and Case 19 from the paper, "MELCOR 1.0 Calculations for the Battelle-Frankfurt Mixing Tests". In both tests a hydrogen-nitrogen mixture is injected into a model containment. The containment in Case 2 is a sixteen compartment model; the containment in Case 19 is a twenty-eight volume model. Calculations for this test are normally run on the Cray.

## Appendix B

### Input Decks for MELCOR Standard Test Problems

In this appendix the input decks for the standard test problems are given. Three files are needed in order to run MELCOR. The first file is the input file for MELGEN. The second is the input file for MELCOR, and the third is the input file for MELPLT. All three decks for the standard test are given here. In addition, if there is experimental data or data generated by another computer code for the comparison, those files are given here. The MELGEN run produces two output files, MEGOUT.DAT and MEGDIA.DAT. These contain the MELGEN output and MELGEN diagnostics, respectively. The MELCOR run produces four files: MELOUT.DAT, MELDIA.DAT, MELRST.DAT, and MELPTF.DAT. These are the MELCOR output, the MELCOR diagnostics, the MELCOR restart file, and the plot data file respectively.

#### ST001: Adiabatic Expansion of Hydrogen

##### MELGEN Input

```
TITLE  'ADIABATIC FREE EXPANSION'
JOBID  'ST001'
CRTOUT
DTTIME 1.0
*
*      CONTROL VOLUME SETUP
*
CV00100 'VOLUME ONE' 1 1 1 *EQ THERMO, HORIZ FLOW, PRIMARY, HI PRESS CELL
CV00101 0 0                *POOL + FOG, ACTIVE
CV001A0 2                  *P, T, Q THERMO INPUT
CV001A1 PVOL 2.0E5 TPOL 300.0 TATM 300.0 PH2O 0.0
CV001A2 MFRC.1 0.0 MFRC.2 0.0 MFRC.3 0.0 MFRC.4 1.0
CV001B0 0.0 0.0 10. 1000. *Z-VOL TABLE
CV00200 'VOLUME TWO' 1 1 1 *EQ THERMO, HORIZ FLOW, PRIMARY, LO PRESS CELL
CV00201 0 0                *POOL + FOG, ACTIVE
CV002A0 2                  *P, T, Q THERMO INPUT
CV002A1 PVOL 1.0E5 TPOL 300.0 TATM 300.0 PH2O 0.0
CV002A2 MFRC.1 0.0 MFRC.2 0.0 MFRC.3 0.0 MFRC.4 1.0
CV002B0 0.0 0.0 10. 1000. *Z-VOL TABLE
*
*      FLOW PATH SETUP
*
FL00100 'FLOW PATH ONE' 1 2 5.0 5.0 *FROM, TO, Z-FROM, ZTO
FL00101 50.0 0.1 1.0 0.13 0.13      *AREA, LENGTH, FRAC OPEN, HEIGHTS
FL00102 4 0                          *TYPE, ACTIVE
FL00103 2.0 2.0                      *F-LOSS, R-LOSS
FL00104 0.0 0.0                      *A-VEL, P-VEL
```

```

FLO01S1 50. 0.1 0.13 5.E-5 0.0      *SEG AREA, L, D, ROUGH, LAM FL COEF
*
*          NON-CONDENSIBLE GAS
*
NCG000  H2      4

```

# ST001: Adiabatic Expansion of Hydrogen

## MELCOR Input

```

TITLE  'ADIABATIC FREE EXPANSION'
JOBID  'ST001'
RESTART 0
*      TSTART  DTMAX  DTMIN  DTEDIT  DTPLOT  DTREST
*TIME1  0.0      10.0    0.01    4.0    0.01    1000.0
TIME1   0.0      10.0    0.001   25.0    0.001    1000.0
TEND    .5 *100.
CPULIM  200.
CPULEFT 1.
COMTC   2
CRTOUT
DEBUG   0
DTTIME  0.1 * 1.0

```

# ST001: Adiabatic Expansion of Hydrogen

## MELPLT Input

```

FILE1 MELPTF.DAT
TITLE CASE ST001
XLABEL Donor Cell Mass (kg)
YLABEL Pressure (Pa)
*XLIMITS 270.0 430.0
*YLIMITS 100000. 500000.
LEGEND CELL 1
PLOT   CVH-P.1 CVH-MASS.1
LEGEND MELCOR
CPLOT  CVH-P.2 CVH-MASS.1
LEGEND ANALYTIC
DATA1 P1 CF01ANAL.DAT
LEGEND CELL 2
DATA1 P2 CF01ANAL.DAT
XLABEL Donor Cell Mass (kg)
YLABEL Temperature (K)
*XLIMITS 270.0 430.0
*YLIMITS 240. 360.
LEGEND CELL 1
PLOT   CVH-TVAP.1 CVH-MASS.1

```

LEGEND MELCOR  
 CPLOT CVH-TVAP.2 CVH-MASS.1  
 LEGEND ANALYTIC  
 DATA1 T1 CF01ANAL.DAT  
 LEGEND CELL 2  
 DATA1 T2 CF01ANAL.DAT  
 \*

# ST001: Adiabatic Expansion of Hydrogen

## Analytical Data

<>T1

0 0

TEMPERATURE

MASS

0.13165E+03	276.166
0.13464E+03	278.686
0.13763E+03	281.173
0.14063E+03	283.628
0.14362E+03	286.052
0.14662E+03	288.446
0.14961E+03	290.811
0.15260E+03	293.148
0.15560E+03	295.458
0.15859E+03	297.742
0.16158E+03	300.000
-12345	-12345

<>P1

0 0

PRESSURE

MASS

0.13165E+03	150000.0
0.13464E+03	154811.0
0.13763E+03	159665.5
0.14063E+03	164562.8
0.14362E+03	169502.4
0.14662E+03	174483.8
0.14961E+03	179506.4
0.15260E+03	184569.8
0.15560E+03	189673.6
0.15859E+03	194817.1
0.16158E+03	200000.0
-12345	-12345

<>T2

0 0

TEMPERATURE

MASS

0.13165E+03	328.336
0.13464E+03	326.637
0.13763E+03	324.739
0.14063E+03	322.628

0.14362E+03	320.285	
0.14662E+03	317.689	
0.14961E+03	314.819	
0.15260E+03	311.647	
0.15560E+03	308.143	
0.15859E+03	304.274	
0.16158E+03	300.000	
-12345	-12345	

◇P2

0	0
---	---

PRESSURE

MASS

0.13165E+03	150000.0	
0.13464E+03	145189.0	
0.13763E+03	140334.5	
0.14063E+03	135437.2	
0.14362E+03	130497.6	
0.14662E+03	125516.2	
0.14961E+03	120493.6	
0.15260E+03	115430.2	
0.15560E+03	110326.4	
0.15859E+03	105182.9	
0.16158E+03	100000.0	
-12345	-12345	

# ST002: Radial Conduction in Annular Structures

## MELGEN Input

TITLE ST002  
JOBID 'ST002'  
CRTOUT

\*

\* HEAT SLAB INPUT

\*

HS00001000 7 2 0 0  
HS00001001 'TEST SLAB'  
HS00001002 0. 1.  
HS00001100 -1 1 3.1856  
HS00001101 3.1886 2

\* NO. NODES, TYPE, SS INIT, TRANS ITER  
\*  
\* BOTTOM ALTITUDE, ORIENTATION  
\* NODALIZATION FLAGS, INSIDE RADIUS  
\* LOCATION, NODE NO.

HS00001102 3.1926 3  
HS00001103 3.2006 4  
HS00001104 3.2156 5  
HS00001105 3.2556 6  
HS00001106 3.3412 7  
HS00001201 STEEL 6  
HS00001300 0  
HS00001400 2001 -1  
HS00001600 2002 -1  
HS00001801 600. 7

\*

\* MATERIAL TYPE, MESH INTERVAL  
\* SOURCE TYPE, FLAG, SOURCE MULTIPLIER  
\* LHS BC TYPE, ASSOC CV  
\* RHS BC TYPE, ASSOC CV  
\* INITIAL TEMPERATURE, NODE NO.

```

*
* MATERIAL PROPERTY INPUT
*
MPMAT00100  STEEL
MPMAT00101  THC          3
MPMAT00102  RHO          4
MPMAT00103  CPS          5
*
* TABULAR FUNCTION INPUT
*
TF00100 'LHS SLAB TEMP' 1 1. 0. * NAME, NO. PAIRS, MUL CONST, ADD CONST
TF00102 0. 600.          * TIME, TEMPERATURE
TF00200 'RHS SLAB TEMP' 1 1. 0. * NAME, NO. PAIRS, MUL CONST, ADD CONST
TF00202 0. 550.          * TIME, TEMPERATURE
TF00300 'THC STEEL'      2 1. 0. * NAME, NO. PAIRS, MUL CONST, ADD CONST
TF00302 200. 43.24       * TEMPERATURE, CONDUCTIVITY
TF00303 5000. 43.24      *
TF00400 'RHO STEEL'      2 1. 0. * NAME, NO. PAIRS, MUL CONST, ADD CONST
TF00402 200. 7799.77     * TEMPERATURE, CONDUCTIVITY
TF00403 5000. 7799.77    *
TF00500 'CPS STEEL'      2 1. 0. * NAME, NO. PAIRS, MUL CONST, ADD CONST
TF00502 200. 475.72      * TEMPERATURE, CONDUCTIVITY
TF00503 5000. 475.72     *

```

#### ST002: Radial Conduction in Annular Structures

##### MELCOR Input

```

TITLE ST002
JOBID 'ST002'
CRTOUT
COMTC 2
DEBUG 0
RESTART 0
*
TSTART DTMAX DTMIN DTEDIT DTPLOT DTREST
TIME1 0. 30. .01 4. .01 1000.
TIME2 100. 30. .01 200. .01 1000.
TEND 2500.
CPULIM 200.
CPULEFT 1.

```

#### ST002: Radial Conduction in Annular Structures

##### MELPLT Input

```

TITLE HEAT SLAB TEST CASE ST002
XLABEL RADIUS (M)

```

YLABEL TEMPERATURE (K)  
 DATA-5 T-MELCOR-04  
 0 0  
 TEMPERATURE (K)  
 RADIUS (M)  
 3.1856 600.  
 3.1886 599.013  
 3.1926 597.698  
 3.2006 595.075  
 3.2156 590.172  
 3.2556 577.210  
 3.3412 550  
 -12345. -12345.  
 DATAB T-ANAL-04 HS06ANAL.DAT

# ST003: Cooling of a Structure in a Fluid

## MELGEN Input

TITLE 'MELCOR TEST ST003'  
 JOBID 'ST003'

\*

CRTOUT

\*

\* -----  
 \* CONTROL VOLUME AND NONCONDENSIBLE GAS INPUT  
 \* -----

\*

CV10000	'500 K RESERVOIR'	1	2	1
CV100A0	2			
CV100A1	PVOL	1.E05		
CV100A2	TATM	500.0		
CV100A3	TPOL	500.0		
CV100A4	MFRC.4	1.0		
CV100B1	-15.0	0.0		
CV100B2	15.0	1.0E20		

\*

NCG001 N2 4

\*

\* -----  
 \* HEAT STRUCTURE INPUT  
 \* -----

\*

HS10001000	11	1	-10
HS10001001	'SLAB'		
HS10001002	0.0	1.0	
HS10001100	-1	1	0.0
HS10001101	0.1	11	
HS10001200	-1		
HS10001201	'MATERIAL'	10	
HS10001300	0		



HS10001400	-4020	100	0.0	1.0
HS10001500	1.0	1.0	1.0	
HS10001600	-4020	100	0.0	1.0
HS10001700	1.0	1.0	1.0	
HS10001801	1000.0	11		
*				
HS10002000	11	2	-10	
HS10002001	'CYLINDER'			
HS10002002	0.0	1.0		
HS10002100	-1	1	0.0	
HS10002101	0.1	11		
HS10002200	-1			
HS10002201	'MATERIAL'		10	
HS10002300	0			
HS10002400	0			
HS10002600	-4020	100	0.0	1.0
HS10002700	6.2832E-1	1.0	1.0	
HS10002801	1000.0	11		
*				
* -----				
* MATERIAL PROPERTY INPUT				
* -----				
*				
MPMAT10000	'MATERIAL'			
MPMAT10001	'THC'	111		
MPMAT10002	'CPS'	112		
MPMAT10003	'RHO'	113		
*				
TF11100	'K-MATERIAL'	2	1.0	0.0
TF11110	0.0	50.0	10000.0	50.0
*				
TF11200	'CP-MATERIAL'	2	1.0	0.0
TF11210	0.0	1500.0	10000.0	1500.0
*				
TF11300	'RHO-MATERIAL'	2	1.0	0.0
TF11310	0.0	1.0	10000.0	1.0
*				
* -----				
* TABULAR FUNCTION INPUT FOR HEAT TRANSFER COEFFICIENT				
* -----				
*				
TF02000	'HTC'	2	1.0	
TF02010	0.0	50.0	10000.0	50.0
*				

# ST003: Cooling of a Structure in a Fluid

## MELCOR Input

TITLE 'MELCOR TEST ST003'

JOBID 'ST003'

\*

\*

```

CRTOUT
COMTC      3
*
RESTART    0
DTIME      0.0029
*
*          TIME      DTMAX      DTMIN      DTEDIT      DTPLOT      DTREST
TIME1      0.0       0.0029    0.001     1.0         0.1         10.0
*
TEND       10.0
CPULIM     1200.0
CPULEFT    60.0

```

ST003: Cooling of a Structure in a Fluid

MELPLT Input

```

*
* PLOT INPUT DATA FOR MELCOR TEST ST003
*
TITLE,SURFACE TEMPERATURE
XLIMITS,0.0 10.0
YLABEL,TEMPERATURE (K)
FILE1 MELPTF.DAT
LEGEND,MELCOR (RECTANGLE)
LISTS
PLOT HS-NODE-TEMPERATURE.1000111
LEGEND,MELCOR (CYLINDER)
LISTS
CPLOT1 HS-NODE-TEMPERATURE.1000211
LEGEND,ANALYTIC SOLUTION
LISTS
DATA2  temp  anal.dat

```

ST003: Cooling of a Structure in a Fluid

Analytical Data

```

<>temp
0 0
TEMPERATURE (K)
TIME (SEC)
1.00010E-01  9.67750E+02
2.00020E-01  9.37581E+02
3.00030E-01  9.09357E+02
4.00040E-01  8.82954E+02
5.00050E-01  8.58254E+02
6.00060E-01  8.35147E+02
7.00070E-01  8.13530E+02

```

8.00080E-01	7.93308E+02
9.00090E-01	7.74390E+02
1.00010E+00	7.56692E+02
1.10011E+00	7.40136E+02
1.20012E+00	7.24647E+02
1.30013E+00	7.10158E+02
1.40014E+00	6.96603E+02
1.50015E+00	6.83922E+02
1.60016E+00	6.72059E+02
1.70017E+00	6.60962E+02
1.80018E+00	6.50580E+02
1.90019E+00	6.40867E+02
2.00020E+00	6.31782E+02
2.10021E+00	6.23282E+02
2.20022E+00	6.15330E+02
2.30023E+00	6.07892E+02
2.40024E+00	6.00933E+02
2.50025E+00	5.94423E+02
2.60026E+00	5.88332E+02
2.70027E+00	5.82635E+02
2.80028E+00	5.77305E+02
2.90029E+00	5.72319E+02
3.00030E+00	5.67655E+02
3.10031E+00	5.63291E+02
3.20032E+00	5.59209E+02
3.30033E+00	5.55390E+02
3.40034E+00	5.51817E+02
3.50035E+00	5.48475E+02
3.60036E+00	5.45348E+02
3.70037E+00	5.42424E+02
3.80038E+00	5.39687E+02
3.90039E+00	5.37127E+02
4.00040E+00	5.34733E+02
4.10041E+00	5.32493E+02
4.20042E+00	5.30397E+02
4.30043E+00	5.28436E+02
4.40044E+00	5.26602E+02
4.50045E+00	5.24886E+02
4.60046E+00	5.23281E+02
4.70047E+00	5.21780E+02
4.80048E+00	5.20375E+02
5.00050E+00	5.17831E+02
5.10051E+00	5.16681E+02
5.20052E+00	5.15605E+02
5.30053E+00	5.14599E+02
5.40054E+00	5.13657E+02
5.50055E+00	5.12776E+02
5.60056E+00	5.11952E+02
5.70057E+00	5.11181E+02
5.80058E+00	5.10460E+02
5.90059E+00	5.09785E+02
6.00060E+00	5.09154E+02
6.10061E+00	5.08564E+02
6.20062E+00	5.08011E+02

6.30063E+00	5.07495E+02
6.40064E+00	5.07011E+02
6.50065E+00	5.06559E+02
6.60066E+00	5.06136E+02
6.70067E+00	5.05740E+02
6.80068E+00	5.05370E+02
7.00070E+00	5.04700E+02
7.10071E+00	5.04397E+02
7.20072E+00	5.04113E+02
7.30073E+00	5.03848E+02
7.40074E+00	5.03600E+02
7.50075E+00	5.03367E+02
7.60076E+00	5.03150E+02
7.70077E+00	5.02947E+02
7.80078E+00	5.02757E+02
7.90079E+00	5.02579E+02
8.00080E+00	5.02413E+02
8.10081E+00	5.02257E+02
8.20082E+00	5.02112E+02
8.30083E+00	5.01975E+02
8.40084E+00	5.01848E+02
8.50085E+00	5.01729E+02
8.60086E+00	5.01617E+02
8.70087E+00	5.01513E+02
8.80088E+00	5.01415E+02
9.00090E+00	5.01239E+02
9.10091E+00	5.01159E+02
9.20092E+00	5.01084E+02
9.30093E+00	5.01014E+02
9.40094E+00	5.00949E+02
9.50095E+00	5.00888E+02
9.70097E+00	5.00777E+02
9.80098E+00	5.00727E+02
9.90099E+00	5.00680E+02
1.00010E+01	5.00636E+02
-12345.	-12345.

#### ST004A: Semi-infinite Solid Heat Structure Test

---

Note: The input data for ST004B is not included here. The input data for ST004B can be obtained from the editor of this report.

---

#### MELGEN Input

```

*****
*****
***** This is a MELCOR test calculation for a semi-infinite
***** slab heat structure in an infinite medium at uniform
***** temperature at a uniform initial temperature.
*****
TITLE TEST:ST004A

```

CRTOUT

\*\*\*\*\*

\*\*\*\*\*

\*\*\*\*\* One noncondensable gas is modeled: N2

\*\*\*\*\*

\*\*\*\*\* GAS MATERIAL NUMBER

\*\*\*\*\*

NCG000 N2 4

\*\*\*\*\*

\*\*\*\*\*

\*\*\*\*\*

\*\*\*\*\* CV 100 is the Containment

\*\*\*\*\* CV 100 is control volume 1

\*\*\*\*\*

CV10000 TEST-CELL 1 2 3

CV100A0 2

CV100A1 PVOL 5.0E5 PH2O 0.0 TATM 450.0 TPOL 450.0

CV100A2 MFRC.1 0.0 MFRC.2 0.0 MFRC.3 0.0

CV100A3 MFRC.4 1.0

\*\*\*\*\*

\*\*\*\*\* ALTITUDE/VOLUME Table for Control Volume 100

\*\*\*\*\*

\*\*\*\*\* ALTITUDE VOLUME

\*\*\*\*\*

CV100B1 0.0 0.0

CV100B2 12.0 1.0E+10

\*\*\*\*\*

\*\*\*\*\*

\*\*\*\*\*

\*\*\*\*\* Heat structure data for

\*\*\*\*\* the infinite slab wall

\*\*\*\*\*

HS00001000 23 1 -1 20

HS00001001 WALL

HS00001002 1.0 1.0

HS00001100 -1 1 0.0

HS00001101 0.000500 2

HS00001102 0.001000 3

HS00001103 0.001585 4

HS00001104 0.002519 5

HS00001105 0.003981 6

HS00001106 0.006310 7

HS00001107 0.01000 8

HS00001108 0.01585 9

HS00001109 0.02519 10

HS00001110 0.03981 11

HS00001111 0.06310 12

HS00001112 0.1000 13

HS00001113 0.1585 14

HS00001114 0.2519 15

HS00001115 0.3981 16

HS00001116 0.6310 17

HS00001117 1.000 18

HS00001118 1.585 19

HS00001119	2.519	20		
HS00001120	3.981	21		
HS00001121	6.310	22		
HS00001122	10.000	23		
HS00001200	-1			
HS00001201	TEST-CONCRETE	22		
HS00001300	0			
HS00001400	4004	100	1.0	1.0
HS00001500	100.0	10.0	10.0	
HS00001600	0			
HS00001800	-1			
HS00001801	300.0	23		

\*\*\*\*\*

\*\*\*\*\*

\*\*\*\*\* Material 1 is test concrete \*\*\*\*\*

\*\*\*\*\*

MPMAT00100	TEST-CONCRETE			
MPMAT00101	RHO	1		
MPMAT00102	CPS	2		
MPMAT00103	THC	3		

\*\*\*\*\*

\*\*\*\*\* Density of test concrete \*\*\*\*\*

\*\*\*\*\*

TF00100	DENSITY	2	1.0	0.0
TF00111		0.00E+00	2300.0	
TF00112		1.00E+10	2300.0	

\*\*\*\*\*

\*\*\*\*\* Heat capacity of test concrete \*\*\*\*\*

\*\*\*\*\*

TF00200	SP.-HEAT	2	1.0	0.0
TF00211		0.00E+00	650.0	
TF00212		1.00E+10	650.0	

\*\*\*\*\*

\*\*\*\*\* Thermal conductivity of test concrete \*\*\*\*\*

\*\*\*\*\*

TF00300	THER-COND	2	1.0	0.0
TF00311		0.00E+00	1.6	
TF00312		1.00E+10	1.6	

\*\*\*\*\*

\*\*\*\*\*

\*\*\*\*\* Convection heat transfer coefficient \*\*\*\*\*

\*\*\*\*\*

TF00400	HTCOEF	2	1.0	0.0
TF00411		0.00E+00	10.0	
TF00412		1.00E+10	10.0	

\*\*\*\*\*

ST004: Semi-infinite Heat Structure Test

MELCOR Input

```
*****
*****
***** The MELCOR input file for heat structure test HS-SI-014
*****
*****
CPULEFT    20.0
CPULIM     15000.0
TEND       100000.0
RESTART    0
TIME1      0.0      30.0      1.0      5000.0      250.0      10000.0
TITLE      TEST:ST004A
*****
```

ST004: Semi-infinite Heat Structure Test

MELPLT Input

```
*
FILE1 MELPTF.DAT
*
TITLE,SEMI-INFINITE SLAB TEST : ST004A
YLABEL,TEMPERATURE (K)
LEGEND,MELCOR:X=0.0M
PLOT0 HS-NODE-TEMPERATURE.0000101
LEGEND,MELCOR:X=0.1M
CPLOT0 HS-NODE-TEMPERATURE.0000113
LEGEND,MELCOR:X=0.2519M
CPLOT0 HS-NODE-TEMPERATURE.0000115
LEGEND,MELCOR:X=0.3981M
CPLOT0 HS-NODE-TEMPERATURE.0000116
LEGEND,MELCOR:X=0.6310M
CPLOT0 HS-NODE-TEMPERATURE.0000117
LEGEND,MELCOR:X=1.0M
CPLOT0 HS-NODE-TEMPERATURE.0000118
LEGEND,ANALYTICAL:X=0.0M
DATA DATA-A
0 0
TEMPERATURE
TIME
      0.0      300.0000
      200.0     314.3039
      400.0     319.6037
      600.0     323.4492
      800.0     326.5515
     1000.0     329.1842
     1200.0     331.4869
```

1400.0	333.5422
1600.0	335.4036
1800.0	337.1081
2000.0	338.6824
2200.0	340.1466
2400.0	341.5164
2600.0	342.8039
2800.0	344.0193
3000.0	345.1705
3200.0	346.2644
3400.0	347.3067
3600.0	348.3023
3800.0	349.2553
4000.0	350.1694
4200.0	351.0476
4400.0	351.8928
4600.0	352.7074
4800.0	353.4937
5000.0	354.2534
5200.0	354.9885
5400.0	355.7003
5600.0	356.3905
5800.0	357.0602
6000.0	357.7107
6200.0	358.3429
6400.0	358.9580
6600.0	359.5567
6800.0	360.1400
7000.0	360.7085
7200.0	361.2631
7400.0	361.8043
7600.0	362.3328
7800.0	362.8491
8000.0	363.3539
8200.0	363.8475
8400.0	364.3304
8600.0	364.8031
8800.0	365.2660
9000.0	365.7195
9200.0	366.1639
9400.0	366.5996
9600.0	367.0269
9800.0	367.4461
10000.0	367.8574
10200.0	368.2613
10400.0	368.6578
10600.0	369.0474
10800.0	369.4301
11000.0	369.8062
11200.0	370.1760
11400.0	370.5396
11600.0	370.8973
11800.0	371.2491



---

Note: The data for this curve has been truncated here. Data is available out to 100,000 seconds. For a more complete data set contact the editor of this report.

---

100000.0 412.3937  
-12345 -12345

\*

LEGEND, ANALYTICAL: X=0.1M

DATA DATA-B

0 0

TEMPERATURE

TIME

0.0	300.0000
200.0	300.0000
400.0	300.0043
600.0	300.0497
800.0	300.1860
1000.0	300.4319
1200.0	300.7815
1400.0	301.2196
1600.0	301.7293
1800.0	302.2951
2000.0	302.9041
2200.0	303.5455
2400.0	304.2108
2600.0	304.8932
2800.0	305.5872
3000.0	306.2885
3200.0	306.9937
3400.0	307.7001
3600.0	308.4054
3800.0	309.1080
4000.0	309.8064
4200.0	310.4997
4400.0	311.1869
4600.0	311.8675
4800.0	312.5408
5000.0	313.2066
5200.0	313.8646
5400.0	314.5144
5600.0	315.1561
5800.0	315.7895
6000.0	316.4146
6200.0	317.0314
6400.0	317.6399
6600.0	318.2402
6800.0	318.8323
7000.0	319.4164
7200.0	319.9925
7400.0	320.5607
7600.0	321.1212

7800.0	321.6741
8000.0	322.2195
8200.0	322.7575
8400.0	323.2883

---

Note: The data for this curve has been truncated here. Data is available out to 100,000 seconds. For a more complete data set contact the editor of this report.

---

100000.0	389.7744
----------	----------

-12345 -12345

\*

LEGEND, ANALYTICAL: X=0.2519M

DATA DATA-C

0 0

TEMPERATURE

TIME

0.0	300.0000
200.0	300.0000
400.0	300.0000
600.0	300.0000
800.0	300.0000
1000.0	300.0000
1200.0	300.0000
1400.0	300.0000
1600.0	300.0002
1800.0	300.0006
2000.0	300.0015
2200.0	300.0034
2400.0	300.0067
2600.0	300.0119
2800.0	300.0196
3000.0	300.0303
3200.0	300.0447
3400.0	300.0630
3600.0	300.0859
3800.0	300.1137
4000.0	300.1467
4200.0	300.1851
4400.0	300.2291
4600.0	300.2789
4800.0	300.3345
5000.0	300.3960
5200.0	300.4634
5400.0	300.5367
5600.0	300.6158
5800.0	300.7006
6000.0	300.7910
6200.0	300.8869
6400.0	300.9881
6600.0	301.0946
6800.0	301.2061

7000.0	301.3225
7200.0	301.4436
7400.0	301.5693
7600.0	301.6994
7800.0	301.8337
8000.0	301.9721
8200.0	302.1143
8400.0	302.2603

---

Note: The data for this curve has been truncated here. Data is available out to 100,000 seconds. For a more complete data set contact the editor of this report.

---

100000.0 359.9601  
-12345 -12345  
\*  
LEGEND,ANALYTICAL:X=0.3981M  
DATA DATA-D  
0 0  
TEMPERATURE  
TIME

0.0	300.0000
200.0	300.0000
400.0	300.0000
600.0	300.0000
800.0	300.0000
1000.0	300.0000
1200.0	300.0000
1400.0	300.0000
1600.0	300.0000
1800.0	300.0000
2000.0	300.0000
2200.0	300.0000
2400.0	300.0000
2600.0	300.0000
2800.0	300.0000
3000.0	300.0000
3200.0	300.0000
3400.0	300.0000
3600.0	300.0001
3800.0	300.0002
4000.0	300.0003
4200.0	300.0005
4400.0	300.0007
4600.0	300.0011
4800.0	300.0016
5000.0	300.0023
5200.0	300.0033
5400.0	300.0045
5600.0	300.0060
5800.0	300.0078
6000.0	300.0101

6200.0	300.0128
6400.0	300.0160
6600.0	300.0198
6800.0	300.0242
7000.0	300.0293
7200.0	300.0351
7400.0	300.0416
7600.0	300.0490
7800.0	300.0572
8000.0	300.0663
8200.0	300.0763
8400.0	300.0874

---

Note: The data for this curve has been truncated here. Data is available out to 100,000 seconds. For a more complete data set please contact the editor of this report.

---

100000.0 337.7134  
-12345 -12345  
\*  
LEGEND, ANALYTICAL: X=0.6310M  
DATA DATA-E  
0 0  
TEMPERATURE  
TIME

0.0	300.0000
200.0	300.0000
400.0	300.0000
600.0	300.0000
2800.0	300.0000
3000.0	300.0000
3200.0	300.0000
3400.0	300.0000
3600.0	300.0000
3800.0	300.0000
4000.0	300.0000
4200.0	300.0000
4400.0	300.0000
4600.0	300.0000
4800.0	300.0000
5000.0	300.0000
5200.0	300.0000
5400.0	300.0000
5600.0	300.0000
5800.0	300.0000
6000.0	300.0000
6200.0	300.0000
6400.0	300.0000
6600.0	300.0000
6800.0	300.0000
7000.0	300.0000
7200.0	300.0000

7400.0	300.0000
7600.0	300.0000
7800.0	300.0000
8000.0	300.0000
8200.0	300.0000
8400.0	300.0001
8600.0	300.0001
8800.0	300.0001
9000.0	300.0001
9200.0	300.0002
9400.0	300.0002
9600.0	300.0003
9800.0	300.0003
10000.0	300.0004
10200.0	300.0005
10400.0	300.0006

---

Note: The data for this curve has been truncated here. Data is available out to 100,000 seconds. For a more complete data set contact the editor of this report.

---

100000.0 315.3271  
-12345 -12345  
\*  
LEGEND, ANALYTICAL: X=1.0M  
DATA DATA-F  
0 0  
TEMPERATURE  
TIME

0.0	300.0000
200.0	300.0000
400.0	300.0000
600.0	300.0000
800.0	300.0000
1000.0	300.0000
3200.0	300.0000
3400.0	300.0000
3600.0	300.0000
3800.0	300.0000
4000.0	300.0000
4200.0	300.0000
4400.0	300.0000
4600.0	300.0000
4800.0	300.0000
5000.0	300.0000
5200.0	300.0000
5400.0	300.0000
5600.0	300.0000
5800.0	300.0000
6000.0	300.0000
6200.0	300.0000
6400.0	300.0000

6600.0	300.0000
6800.0	300.0000
7000.0	300.0000
7200.0	300.0000
7400.0	300.0000
7600.0	300.0000
7800.0	300.0000
8000.0	300.0000
8200.0	300.0000
8400.0	300.0000
8600.0	300.0000
8800.0	300.0000
9000.0	300.0000
9200.0	300.0000
9400.0	300.0000
9600.0	300.0000

---

Note: The data for this curve has been truncated here. Data is available out to 100,000 seconds. For a more complete data set contact the editor of this report.

---

100000.0 302.3890  
-12345 -12345  
\*

# ST005: Saturated Liquid Depressurization Test

## MELGEN Input

```

*****
TITLE      ST005
CRTOUT
*****
*** CONTROL VOLUME HYDRODYNAMICS PACKAGE
*****
CV00100  CV1      2  2  1
CV00101  0        0
CV00102  0.0      0.0
CV001A0  2
CV001A1  PVOL    8.00E6  PH2O  8.00E6  TATM    568.23  TPOL    568.23
CV001A2  MFRC.1  1.0      MFRC.2   0.0    MFRC.3   0.0
***
***      ALTITUDE    VOLUME
CV001B1  0.0        0.0
CV001B2  10.0       100.0
***
SC00001  4407      1000.0    1  * FAST BUBBLE RISE VELOCITY
*****
CV00200  CV2      2  2  3
CV00201  0        0
CV00202  0.0      0.0

```

```

CV002A0      2
CV002A1      PVOL      1.0E4      PH2O      1.0E4      TATM      568.23      TPOL      568.23
CV002A2      MFRC.1    0.0          MFRC.2    0.0          MFRC.3    1.0
***
***          ALTITUDE      VOLUME
CV002B1      0.0          0.0
CV002B2      100.0        4000.0
***
*****
*** FLOW PATH PACKAGE INPUT
*****
FLO0100      FLOW1      1      2      9.9      10.1
FLO0101      0.02      0.2      1.0
FLO0102      3
FLO0103      1.0      1.0
FLO01S1      0.02      0.2      1.0
*****
***          HEAT STRUCTURE
*****
HS10001000      3      1      -1      20
HS10001001      HS1
HS10001002      1.0      1.0
HS10001003      500.0
HS10001100      -1      1      0.0
HS10001102      0.00001      2
HS10001103      0.00002      3
HS10001200      -1
HS10001201      DUMMY      2
HS10001300      0
HS10001400      4002      1      0.0      1.0
HS10001500      1.0      1.0      1.0
HS10001600      4002      2      0.0      1.0
HS10001700      1.0      1.0      1.0
HS10001800      -1
HS10001801      568.23      3
*****
TF00200      HTCDEF      4      1.0      0.0
TF002A1      0.0      1.0
TF002A2      50.0      1.0
TF002A3      60.0      600.0
TF002A4      1000.0      600.0
*****
MPMAT00100      DUMMY
MPMAT00101      RHO      3
MPMAT00102      CPS      4
MPMAT00103      THC      5
*****
TF00300      RHO      2      1.0      0.0
TF003A1      0.0      4000.0
TF003A2      1000.0      4000.0
*****
TF00400      CPS      2      1.0      0.0
TF004A1      0.0      10.0
TF004A2      1000.0      10.0

```

```
*****
TF00500      THC      2      1.0      0.0
TF005A1      0.0      50.0
TF005A2      1000.0    50.0
*****
```

ST005: Saturated Liquid Depressurization Test

MELCOR Input

```
*****
CPULEFT      20.0
CPULIM      15000.0
CRTOUT
TEND         3000.0
RESTART      0
DTIME        0.01
TIME1        0.0      0.01  0.005      1.0      0.01  1000.0
TIME2        1.0      0.1   0.05      5.0      0.1   1000.0
TIME3        10.0     1.0   0.1     500.0     2.0   1000.0
TIME4       1500.0     5.0   0.1    1000.0     5.0   1000.0
TITLE        ST005
*****
```

ST005: Saturated Liquid Depressurization Test

MELPLT Input

```
*
FILE1 MELPTF.DAT
*
TITLE ST005
*
YLABEL,PRESSURE (PA)
AYLABEL,PRESSURE (PSIA)
AYSCALE      0.00014504      0.0
LEGEND,CV1
PLOT CVH-P.001
LEGEND,CV2
CPLOT1 CVH-P.002
*
YLABEL,ATM TEMPERATURE (K)
AYLABEL,ATM TEMPERATURE (F)
AYSCALE      1.8      -459.67
LEGEND,CV1
PLOT CVH-TVAP.001
LEGEND,CV2
CPLOT1 CVH-TVAP.002
*
```



```

YLABEL,PRESSURE (PA)
LIST
LEGEND,CV1
PLOT    CVH-P.001
*
YLABEL,PRESSURE (PA)
LIST
LEGEND,CV2
PLOT    CVH-P.002
*
YLABEL,ATM. TEMPERATURE (K)
LIST
LEGEND,CV1
PLOT    CVH-TVAP.001
*
YLABEL,ATM. TEMPERATURE (K)
LIST
LEGEND,CV2
PLOT    CVH-TVAP.002
*
YLABEL,POOL TEMPERATURE (K)
LIST
LEGEND,CV1
PLOT    CVH-TLIQ.001
*
YLABEL,WATER MASS (KG)
LIST
LEGEND,CV1
PLOT    CVH-MASS.1.001
*
YLABEL,WATER MASS (KG)
LIST
LEGEND,CV2
PLOT    CVH-MASS.1.002
*
YLABEL,FOG MASS (KG)
LIST
LEGEND,CV1
PLOT    CVH-MASS.2.001
*
YLABEL,FOG MASS (KG)
LIST
LEGEND,CV2
PLOT    CVH-MASS.2.002
*
YLABEL,STEAM MASS (KG)
LIST
LEGEND,CV1
PLOT    CVH-MASS.3.001
*
YLABEL,STEAM MASS (KG)
LIST
LEGEND,CV2
PLOT    CVH-MASS.3.002

```

```

*
YLABEL,STEAM FLOW (KG)
LIST
LEGEND,CV1-CV2
PLOT FL-MFLOW.3.001
*

```

ST006: Browns Ferry Reactor Building Burns

MELGEN Input

```

TITLE ST006
JOBID 'ST006'
CRTOUT
TSTART 47739.5
*****
***** NCG INPUT
*****
NCG001 N2 4
NCG002 O2 5
NCG003 H2 6
NCG004 CO2 7
NCG005 CO 8
*****
***** CVH INPUT
*****
CV10000 REACTOR-BUILDING 2 2 2
CV100A0 2
CV100A1 PVOL 101461. PH2O 4800.
CV100A2 TATM 305.4 TPOL 305.4
CV100A3 MFRC.1 0. MFRC.3 1.
CV100A4 MFRC.4 .7671 MFRC.5 .2329
* ELEV VOL
CV100B1 -18.176 0.
CV100B2 26.172 49881.
*
* SOURCES
*
* TAB. FUNC 2 ==> USE RATE
*CV100C0 MASS.3 100 2
*CV100C1 TE 150 8
*CV100C2 MASS.4 110 2
*CV100C3 TE 150 8
*CV100C4 MASS.5 120 2
*CV100C5 TE 150 8
*CV100C6 MASS.6 130 2
*CV100C7 TE 150 8
*CV100C8 MASS.7 140 2
*CV100C9 TE 150 8
* CONTROL FUNC 3 ==> USE RATE
CV100C0 MASS.3 800 3

```

CV100C1	TE	850	9
CV100C2	MASS.4	810	3
CV100C3	TE	850	9
CV100C4	MASS.5	820	3
CV100C5	TE	850	9
CV100C6	MASS.6	830	3
CV100C7	TE	850	9
CV100C8	MASS.7	840	3
CV100C9	TE	850	9
*			
CF80000	H2O-MASS-SRC	TAB-FUN	1 1. 0.
CF80003	100		
CF80010	1. 0. TIME		
*	NAME	NUM PAIRS	MULT ADD
TF10000	H2O-MASS-SRC	108	1. 0.
*	X	Y	
TF10010	47402.00	0.0000000E+00	
TF10011	47711.00	0.0000000E+00	
TF10012	47749.00	54.79000	
TF10013	47752.00	44.11000	
TF10014	47812.00	43.34000	
TF10015	47872.00	35.83000	
TF10016	47932.00	28.56000	
TF10017	47992.00	23.28000	
TF10018	48052.00	19.23000	
TF10019	48112.00	16.03000	
TF10020	48172.00	13.49000	
TF10021	48232.00	11.48000	
TF10022	48292.00	9.920000	
TF10023	48352.00	8.730000	
TF10024	48412.00	10.07000	
TF10025	48472.00	12.75000	
TF10026	48532.00	11.38000	
TF10027	48592.00	11.88000	
TF10028	48652.00	13.59000	
TF10029	48712.00	11.79000	
TF10030	48772.00	13.98000	
TF10031	48832.00	16.22000	
TF10032	48892.00	13.89000	
TF10033	48952.00	16.21000	
TF10034	49012.00	15.25000	
TF10035	49072.00	15.49000	
TF10036	49132.00	15.97000	
TF10037	49192.00	16.98000	
TF10038	49252.00	14.82000	
TF10039	49312.00	16.32000	
TF10040	49372.00	19.13000	
TF10041	49432.00	16.59000	
TF10042	49492.00	17.79000	
TF10043	49552.00	20.03000	
TF10044	49612.00	17.05000	
TF10045	49672.00	15.36000	
TF10046	49732.00	16.74000	
TF10047	49792.00	19.55000	

TF10048	49852.00	16.94000
TF10049	49912.00	15.29000
TF10050	49972.00	17.53000
TF10051	50032.00	20.22000
TF10052	50092.00	17.49000
TF10053	50152.00	15.30000
TF10054	50212.00	16.67000
TF10055	50272.00	19.48000
TF10056	50332.00	16.87000
TF10057	50392.00	14.72000
TF10058	50452.00	16.19000
TF10059	50512.00	19.05000
TF10060	50572.00	16.52000
TF10061	50632.00	14.39000
TF10062	50692.00	15.91000
TF10063	50752.00	18.81000
TF10064	50812.00	16.31000
TF10065	50872.00	14.21000
TF10066	50932.00	15.64000
TF10067	50992.00	18.55000
TF10068	51052.00	16.02000
TF10069	51112.00	13.71000
TF10070	51172.00	15.53000
TF10071	51232.00	18.45000
TF10072	51292.00	16.01000
TF10073	51352.00	14.02000
TF10074	51412.00	15.44000
TF10075	51472.00	18.54000
TF10076	51532.00	16.06000
TF10077	51592.00	13.99000
TF10078	51652.00	15.41000
TF10079	51712.00	18.51000
TF10080	51772.00	16.03000
TF10081	51832.00	13.96000
TF10082	51892.00	15.29000
TF10083	51952.00	18.48000
TF10084	52012.00	16.02000
TF10085	52072.00	13.94000
TF10086	52132.00	15.32000
TF10087	52192.00	18.45000
TF10088	52252.00	16.03000
TF10089	52312.00	13.98000
TF10090	52372.00	15.57000
TF10091	52432.00	18.53000
TF10092	52492.00	10.65000
TF10093	52552.00	9.210000
TF10094	52612.00	8.390000
TF10095	52672.00	8.590000
TF10096	52732.00	10.22000
TF10097	52792.00	12.84000
TF10098	52852.00	10.23000
TF10099	52912.00	10.70000
TF100A0	52972.00	9.590000
TF100A1	53032.00	8.990000

TF100A2	53092.00	7.560000
TF100A3	53152.00	9.860000
TF100A4	53212.00	12.59000
TF100A5	53272.00	10.99000
TF100A6	53332.00	10.45000
TF100A7	53392.00	9.360000
TF100A8	53452.00	8.820000
TF100A9	53512.00	7.310000
TF100B0	53572.00	9.680000
TF100B1	53632.00	12.50000
TF100B2	53692.00	11.20000
TF100B3	53752.00	10.32000
TF100B4	53812.00	9.120000
TF100B5	53872.00	8.690000
TF100B6	53932.00	8.020000
TF100B7	53992.00	9.610000
*		
CF81000	N2-MASS-SRC	TAB-FUN 1 1. 0.
CF81003	110	
CF81010	1. 0. TIME	
*		
TF11000	N2-MASS-SRC	52 1. 0.
*	X	Y
TF11010	47402.00	0.0000000E+00
TF11011	47685.00	0.0000000E+00
TF11012	47711.00	1.760000
TF11013	47749.00	11.88000
TF11014	47752.00	11.23000
TF11015	47812.00	9.820000
TF11016	47872.00	9.800000
TF11017	47932.00	9.820000
TF11018	47992.00	9.500000
TF11019	48052.00	8.960000
TF11020	48112.00	8.340000
TF11021	48172.00	7.700000
TF11022	48232.00	7.050000
TF11023	48292.00	6.390000
TF11024	48352.00	5.740000
TF11025	48412.00	5.900000
TF11026	48472.00	5.710000
TF11027	48532.00	4.580000
TF11028	48592.00	3.870000
TF11029	48652.00	3.370000
TF11030	48712.00	2.700000
TF11031	48772.00	2.290000
TF11032	48832.00	2.010000
TF11033	48892.00	1.590000
TF11034	48952.00	1.300000
TF11035	49012.00	1.110000
TF11036	49072.00	0.8800000
TF11037	49132.00	0.7100000
TF11038	49192.00	0.5900000
TF11039	49252.00	0.4600000
TF11040	49312.00	0.3700000

TF11041	49372.00	0.3200000
TF11042	49432.00	0.2500000
TF11043	49492.00	0.2000000
TF11044	49552.00	0.1700000
TF11045	49612.00	0.1300000
TF11046	49672.00	0.1000000
TF11047	49732.00	7.9999998E-02
TF11048	49792.00	7.0000000E-02
TF11049	49852.00	5.0000001E-02
TF11050	49912.00	3.9999999E-02
TF11051	49972.00	2.9999999E-02
TF11052	50032.00	2.9999999E-02
TF11053	50092.00	2.0000000E-02
TF11054	50152.00	2.0000000E-02
TF11055	50212.00	9.9999998E-03
TF11056	50272.00	9.9999998E-03
TF11057	50332.00	9.9999998E-03
TF11058	50392.00	9.9999998E-03
TF11059	50452.00	9.9999998E-03
TF11060	50512.00	0.0000000E+00
TF11061	53992.00	0.0000000E+00
*		
CF82000	O2-MASS-SRC	TAB-FUN 1 1. 0.
CF82003	120	
CF82010	1. 0. TIME	
*		
TF12000	O2-MASS-SRC 35	1. 0.
* X Y		
TF12010	47402.00	0.0000000E+00
TF12011	47685.00	0.0000000E+00
TF12012	47711.00	7.0000000E-02
TF12013	47749.00	0.4900000
TF12014	47752.00	0.4700000
TF12015	47812.00	0.4100000
TF12016	47872.00	0.4100000
TF12017	47932.00	0.4100000
TF12018	47992.00	0.3900000
TF12019	48052.00	0.3700000
TF12020	48112.00	0.3500000
TF12021	48172.00	0.3200000
TF12022	48232.00	0.2900000
TF12023	48292.00	0.2600000
TF12024	48352.00	0.2400000
TF12025	48412.00	0.2400000
TF12026	48472.00	0.2400000
TF12027	48532.00	0.1900000
TF12028	48592.00	0.1600000
TF12029	48652.00	0.1400000
TF12030	48712.00	0.1100000
TF12031	48772.00	9.0000004E-02
TF12032	48832.00	7.9999998E-02
TF12033	48892.00	7.0000000E-02
TF12034	48952.00	5.0000001E-02
TF12035	49012.00	5.0000001E-02

TF12036	49072.00	3.9999999E-02
TF12037	49132.00	2.9999999E-02
TF12038	49192.00	2.0000000E-02
TF12039	49252.00	2.0000000E-02
TF12040	49312.00	2.0000000E-02
TF12041	49372.00	9.9999998E-03
TF12042	49612.00	9.9999998E-03
TF12043	49672.00	0.0000000E+00
TF12044	53992.00	0.0000000E+00
*		
CF83000	H2-MASS-SRC	TAB-FUN 1 1. 0.
CF83003	130	
CF83010	1. 0.	TIME
*		
TF13000	H2-MASS-SRC	46 1. 0.
* X Y		
TF13010	47402.00	0.0000000E+00
TF13011	47685.00	0.0000000E+00
TF13012	47711.00	0.2000000
TF13013	47749.00	1.370000
TF13014	47752.00	1.300000
TF13015	47812.00	1.150000
TF13016	47872.00	1.160000
TF13017	47932.00	1.180000
TF13018	47992.00	1.150000
TF13019	48052.00	1.090000
TF13020	48112.00	1.020000
TF13021	48172.00	0.9500000
TF13022	48232.00	0.8700000
TF13023	48292.00	0.8000000
TF13024	48352.00	0.7200000
TF13025	48412.00	0.7400000
TF13026	48472.00	0.7200000
TF13027	48532.00	0.5800000
TF13028	48592.00	0.4900000
TF13029	48652.00	0.4300000
TF13030	48712.00	0.3500000
TF13031	48772.00	0.3000000
TF13032	48832.00	0.2600000
TF13033	48892.00	0.2100000
TF13034	48952.00	0.1800000
TF13035	49012.00	0.1600000
TF13036	49072.00	0.1300000
TF13037	49132.00	0.1100000
TF13038	49192.00	9.0000004E-02
TF13039	49252.00	7.9999998E-02
TF13040	49312.00	7.0000000E-02
TF13041	49372.00	5.9999999E-02
TF13042	49432.00	5.0000001E-02
TF13043	49492.00	3.9999999E-02
TF13044	49612.00	3.9999999E-02
TF13045	49672.00	2.9999999E-02
TF13046	49912.00	2.9999999E-02
TF13047	49972.00	2.0000000E-02

TF13048	52372.00	2.0000000E-02
TF13049	52432.00	2.9999999E-02
TF13050	52492.00	2.0000000E-02
TF13051	53032.00	2.0000000E-02
TF13052	53092.00	2.9999999E-02
TF13053	53152.00	2.0000000E-02
TF13054	53212.00	2.9999999E-02
TF13055	53992.00	2.9999999E-02
*		
CF84000	CO2-MASS-SRC	TAB-FUN 1 1. 0.
CF84003	140	
CF84010	1. 0. TIME	
*		
TF14000	CO2-MASS-SRC	32 1. 0.
* X Y		
TF14010	47402.00	0.0000000E+00
TF14011	47685.00	0.0000000E+00
TF14012	47711.00	2.0000000E-02
TF14013	47749.00	0.1400000
TF14014	47752.00	0.1400000
TF14015	47812.00	0.1200000
TF14016	47872.00	0.1600000
TF14017	47932.00	0.1900000
TF14018	47992.00	0.2000000
TF14019	48052.00	0.2000000
TF14020	48112.00	0.1900000
TF14021	48172.00	0.1800000
TF14022	48232.00	0.1700000
TF14022	48292.00	0.1600000
TF14023	48352.00	0.1400000
TF14024	48412.00	0.1500000
TF14025	48472.00	0.1500000
TF14026	48532.00	0.1200000
TF14027	48592.00	0.1000000
TF14028	48652.00	9.0000004E-02
TF14029	48712.00	7.0000000E-02
TF14030	48772.00	5.9999999E-02
TF14031	48832.00	5.0000001E-02
TF14032	48892.00	3.9999999E-02
TF14033	48952.00	2.9999999E-02
TF14034	49012.00	2.9999999E-02
TF14035	49072.00	2.0000000E-02
TF14036	49132.00	2.0000000E-02
TF14037	49192.00	2.0000000E-02
TF14038	49252.00	9.9999998E-03
TF14039	49492.00	9.9999998E-03
TF14040	49552.00	0.0000000E+00
TF14041	53992.00	0.0000000E+00
*		
CF85000	TEMP-SRC	TAB-FUN 1 1. 0.
CF85003	150	
CF85010	1. 0. TIME	
*		
TF15000	TEMP-SOURCE	125 1. 0.



*	X	Y
TF15010	47402.00	428.9000
TF15011	47479.00	428.9000
TF15012	47485.00	428.8000
TF15013	47563.00	428.8000
TF15014	47569.00	428.7000
TF15015	47599.00	428.7000
TF15016	47605.00	429.1000
TF15017	47611.00	429.1000
TF15018	47617.00	428.8000
TF15019	47623.00	428.7000
TF15020	47653.00	428.7000
TF15021	47659.00	437.3000
TF15022	47660.00	437.5000
TF15023	47661.00	439.0000
TF15024	47663.00	439.7000
TF15025	47667.00	441.3000
TF15026	47673.00	442.2000
TF15027	47685.00	443.8000
TF15028	47711.00	444.6000
TF15029	47749.00	530.4000
TF15030	47752.00	533.1000
TF15031	47812.00	705.3000
TF15032	47872.00	833.0000
TF15033	47932.00	723.5000
TF15034	47992.00	698.2000
TF15035	48052.00	696.0000
TF15036	48112.00	697.0000
TF15037	48172.00	694.5000
TF15038	48232.00	672.7000
TF15039	48292.00	652.5000
TF15040	48352.00	649.8000
TF15041	48412.00	648.7000
TF15042	48472.00	622.5000
TF15043	48532.00	639.4000
TF15044	48592.00	636.9000
TF15045	48652.00	620.6000
TF15046	48712.00	628.5000
TF15047	48772.00	631.5000
TF15048	48832.00	609.7000
TF15049	48892.00	619.9000
TF15050	48952.00	625.7000
TF15051	49012.00	603.2000
TF15052	49072.00	614.1000
TF15053	49132.00	619.8000
TF15054	49192.00	603.7000
TF15055	49252.00	619.9000
TF15056	49312.00	622.4000
TF15057	49372.00	593.7000
TF15058	49432.00	614.0000
TF15059	49492.00	616.5000
TF15060	49552.00	595.5000
TF15061	49612.00	605.1000
TF15062	49672.00	611.3000

TF15063	49732.00	619.1000
TF15064	49792.00	590.3000
TF15065	49852.00	609.6000
TF15066	49912.00	612.9000
TF15067	49972.00	610.3000
TF15068	50032.00	591.2000
TF15069	50092.00	606.7000
TF15070	50152.00	610.2000
TF15071	50212.00	614.9000
TF15072	50272.00	588.1000
TF15073	50332.00	607.6000
TF15074	50392.00	611.2000
TF15075	50452.00	615.5000
TF15076	50512.00	586.8000
TF15077	50572.00	608.2000
TF15078	50632.00	611.8000
TF15079	50692.00	615.9000
TF15080	50752.00	586.1000
TF15081	50812.00	608.6000
TF15082	50872.00	612.2000
TF15083	50932.00	616.2000
TF15084	50992.00	594.9000
TF15085	51052.00	605.0000
TF15086	51112.00	610.2000
TF15087	51172.00	615.6000
TF15088	51232.00	595.4000
TF15089	51292.00	605.4000
TF15090	51352.00	610.3000
TF15091	51412.00	615.7000
TF15092	51472.00	595.7000
TF15093	51532.00	610.6000
TF15094	51592.00	611.8000
TF15095	51652.00	617.0000
TF15096	51712.00	595.7000
TF15097	51772.00	611.0000
TF15098	51832.00	612.4000
TF15099	51892.00	617.4000
TF150A0	51952.00	596.6000
TF150A1	52012.00	611.6000
TF150A2	52072.00	612.9000
TF150A3	52132.00	608.5000
TF150A4	52192.00	594.3000
TF150A5	52252.00	620.5000
TF150A6	52312.00	628.1000
TF150A7	52372.00	639.2000
TF150A8	52432.00	611.1000
TF150A9	52492.00	648.5000
TF150B0	52552.00	665.3000
TF150B1	52612.00	669.5000
TF150B2	52672.00	676.5000
TF150B3	52732.00	682.7000
TF150B4	52792.00	643.9000
TF150B5	52852.00	682.9000
TF150B6	52912.00	684.0000

TF150B7	52972.00	685.3000
TF150B8	53032.00	685.6000
TF150B9	53092.00	692.6000
TF150C0	53152.00	699.7000
TF150C1	53212.00	671.1000
TF150C2	53272.00	696.1000
TF150C3	53332.00	694.6000
TF150C4	53392.00	697.5000
TF150C5	53452.00	701.4000
TF150C6	53512.00	705.8000
TF150C7	53572.00	712.3000
TF150C8	53632.00	684.9000
TF150C9	53692.00	708.1000
TF150D0	53752.00	704.3000
TF150D1	53812.00	708.3000
TF150D2	53872.00	712.6000
TF150D3	53932.00	718.9000
TF150D4	53992.00	726.0000

\*

\*

CV20000	REFUELING-BAY	2	2	2
CV200A0	2			
CV200A1	PVOL 100967.	PH2O	3480.	
CV200A2	TATM 299.8	TPOL	299.8	
CV200A3	MFRC.1 0.	MFRC.3	1.	
CV200A4	MFRC.4 .7671	MFRC.5	.2329	

\* ELEV VOL

CV200B1	26.401	0.
---------	--------	----

CV200B2	41.869	74175.
---------	--------	--------

\*

CV30000	TURBINE-BUILDING	2	2	2
CV300A0	2			
CV300A1	PVOL 101130.	PH2O	3480.	
CV300A2	TATM 299.8	TPOL	299.8	
CV300A3	MFRC.1 0.	MFRC.3	1.	
CV300A4	MFRC.4 .7671	MFRC.5	.2329	

\* ELEV VOL

CV300B1	11.6943	0.
---------	---------	----

CV300B2	31.354	158303.
---------	--------	---------

\*

CV40000	ENVIRONMENT	2	2	2
CV400A0	2			
CV400A1	PVOL 101484.	PH2O	3480.	
CV400A2	TATM 299.8	TPOL	299.8	
CV400A3	MFRC.1 0.	MFRC.3	1.	
CV400A4	MFRC.4 .7671	MFRC.5	.2329	

\* ELEV VOL

CV400B1	-20.	0.
---------	------	----

CV400B2	80.	1.E10
---------	-----	-------

\*\*\*\*\*

\*\*\*\*\*

\*\*\*\*\* FLOW PATH INPUT

\*\*\*\*\*

*	NAME	FROM	TO	ZFROM	ZTO
FL11000	RB-REFUEL-BO	100	200	26.172	26.401
FL12000	RB-TURB-BO	100	300	-1.488	12.913
FL13000	RB-ENV-INF	100	400	11.923	11.923
FL14000	REFUEL-ENV-BO	200	400	35.202	35.202
FL15000	REFUEL-ENV-INF	200	400	33.64	33.64
FL16000	TURB-ENV-INF	300	400	16.342	16.342

\*

*	AREA	LENGTH	FLOPO	HGTF	HGTT0
FL11001	27.8	27.8	0.	.3	.3
FL12001	1.95	1.95	0.	.3	.3
FL13001	.07925	1.	1.	.1	.1
FL14001	297.3	297.3	0.	.3	.3
FL15001	.3991	.15	1.	.1	.1
FL16001	.8518	.15	1.	.1	.1

\*

*	TYPE	ACTIVE	IBUBF	IBUBTO
FL11002	0	0	0	0
FL12002	3	0	0	0
FL13002	3	0	0	0
FL14002	3	0	0	0
FL15002	3	0	0	0
FL16002	3	0	0	0

\*

*	FRICFO	FRICREV
FL11003	.5	.5
FL12003	.5	.5
FL13003	1.	1.
FL14003	.5	.5
FL15003	1.	1.
FL16003	1.	1.

\*

*	SAREA	SLEN	SHYD	SRGH	SLAM
FL110S1	27.8	.01	1.		
FL120S1	1.95	.01	1.		
FL130S1	.07925	.01	1.		
FL140S1	297.3	.01	1.		
FL150S1	.3991	.01	1.		
FL160S1	.8518	.01	1.		

\*

--- VALVES ---

*	TRIP NO.	CF-ON-FORWARD	CF-ON-REVERSE
FL110V1	110	111	111
FL120V1	120	121	121
FL140V1	140	141	141

\*

\* TABULAR AND CONTROL FUNCTIONS FOR VALVE INPUT

CF10900	110-DP	ADD	2	1.	0.
CF10910	1.	0.	CVH-P.100		
CF10911	-1.	0.	CVH-P.200		

\*

CF11000 110-TRIP T-O-F 1 1. 0.  
 CF11003 -1.E6 1551.3  
 CF11010 1. 0. CFVALU.109  
 \*  
 CF11100 110-FRAC HYST 1 1. 0.  
 CF11103 -410 -400  
 CF11110 1. 0. CFVALU.109  
 \*  
 TF40000 110-UNLOAD 1 1. 0.  
 TF40010 0. 1.  
 \*  
 \*TF41000 110-A-DP 5 1. 0.  
 \*TF41010 1551.3 0.1  
 \*TF41011 1637.5 0.2  
 \*TF41012 1723.7 0.85  
 \*TF41013 1809.9 0.92  
 \*TF41014 1896.0 1.  
 TF41000 110-A-DP 1 1. 0.  
 TF41010 1551.3 1.  
 \*  
 CF11900 120-DP ADD 2 1. 0.  
 CF11910 1. 0. CVH-P.100  
 CF11911 -1. 0. CVH-P.300  
 \*  
 CF12000 120-TRIP T-O-F 1 1. 0.  
 CF12003 -1.E6 1551.3  
 CF12010 1. 0. CFVALU.119  
 \*  
 CF12100 120-FRAC HYST 1 1. 0.  
 CF12103 -420 -400  
 CF12110 1. 0. CFVALU.119  
 \*  
 \*TF42000 120-A-DP 5 1. 0.  
 \*TF42010 1551.3 0.1  
 \*TF42011 1637.5 0.2  
 \*TF42012 1723.7 0.9  
 \*TF42013 1809.9 0.95  
 \*TF42014 1896.0 1.  
 TF42000 120-A-DP 1 1. 0.  
 TF42010 1551.3 1.  
 \*  
 CF13900 140-DP ADD 2 1. 0.  
 CF13910 1. 0. CVH-P.200  
 CF13911 -1. 0. CVH-P.400  
 \*  
 CF14000 140-TRIP T-O-F 1 1. 0.  
 CF14003 -1.E6 2154.6  
 CF14010 1. 0. CFVALU.139  
 \*  
 CF14100 140-FRAC HYST 1 1. 0.  
 CF14103 -440 -400  
 CF14110 1. 0. CFVALU.139  
 \*  
 \*TF44000 140-A-DP 5 1. 0.

```

*TF44010 2154.6 0.1
*TF44011 2274.3 0.2
*TF44012 2394.0 0.8
*TF44013 2513.7 0.9
*TF44014 2633.4 1.
TF44000 140-A-DP 1 1. 0.
TF44010 2154.6 1.
*
*****
*****
***** HEAT SLAB INPUT
*****
HS00001000 13 1 1 0 * NO. NODES, TYPE, SS INIT, TRANS ITER
HS00001000 13 1 0 0 * NO. NODES, TYPE, SS INIT, TRANS ITER
HS00001001 'EX WALL1' *
HS00001002 0. 1. * BOTTOM ALTITUDE, ORIENTATION
HS00001100 -1 1 0. * NODALIZATION FLAGS, INSIDE RADIUS
HS00001102 .001 2 * LOCATION, NODE NO.
HS00001103 .003 3
HS00001104 .007 4
HS00001105 .015 5
HS00001106 .023 6
HS00001107 .039 7
HS00001108 .071 8
HS00001109 .135 9
HS00001110 .263 10
HS00001111 .500 11
HS00001112 .750 12
HS00001113 1.07 13
HS00001201 CONCRETE 12 * MATERIAL TYPE, MESH INTERVAL
HS00001300 0 * SOURCE TYPE, FLAG, SOURCE MULTIPLIER
HS00001400 1 100 1. 1. * LHS BC TYPE, ASSOC CV, POOL HT FLAGS
HS00001500 374. 8.9 8.9 * LHS AREA, CHARAC LENGTH, AXIAL LENGTH
HS00001600 4200 400 1. 1. * RHS BC TYPE, ASSOC CV, POOL HT FLAGS
HS00001700 374. 8.9 8.9 * RHS AREA, CHARAC LENGTH, AXIAL LENGTH
HS00001801 300. 13 * INITIAL TEMPERATURE, NODE NO.
*
HS00002000 15 1 1 0 * NO. NODES, TYPE, SS INIT, TRANS ITER
HS00002000 15 1 0 0 * NO. NODES, TYPE, SS INIT, TRANS ITER
HS00002001 'CENTWALL' *
HS00002002 0. 1. * BOTTOM ALTITUDE, ORIENTATION
HS00002100 -1 1 0. * NODALIZATION FLAGS, INSIDE RADIUS
HS00002102 .001 2 *
HS00002103 .003 3
HS00002104 .007 4
HS00002105 .015 5
HS00002106 .023 6
HS00002107 .039 7
HS00002108 .071 8
HS00002109 .135 9
HS00002110 .263 10
HS00002111 .500 11
HS00002112 .750 12
HS00002113 1.00 13

```

HS00002114	1.50		14	
HS00002115	2.0		15	
HS00002201	CONCRETE		14	* MATERIAL TYPE, MESH INTERVAL
HS00002300	0			* SOURCE TYPE, FLAG, SOURCE MULTIPLIER
HS00002400	1	100	1.	1.* LHS BC TYPE, ASSOC CV, POOL HT FLAGS
HS00002500	644.	8.9	8.9	* LHS AREA, CHARAC LENGTH, AXIAL LENGTH
HS00002600	4200	400	1.	1.* RHS BC TYPE, ASSOC CV, POOL HT FLAGS
HS00002700	644.	8.9	8.9	* RHS AREA, CHARAC LENGTH, AXIAL LENGTH
HS00002801	300.	15		* INITIAL TEMPERATURE, NODE NO.
*				
HS00003000	11	1	1	0 * NO. NODES, TYPE, SS INIT, TRANS ITER
HS00003000	11	1	0	0 * NO. NODES, TYPE, SS INIT, TRANS ITER
HS00003001	'TORWALL'			*
HS00003002	0.	1.		* BOTTOM ALTITUDE, ORIENTATION
HS00003100	-1	1	0.	* NODALIZATION FLAGS, INSIDE RADIUS
HS00003102	.001		2	*
HS00003103	.003		3	
HS00003104	.007		4	
HS00003105	.015		5	
HS00003106	.023		6	
HS00003107	.039		7	
HS00003108	.071		8	
HS00003109	.135		9	
HS00003110	.263		10	
HS00003111	.500		11	
HS00003201	CONCRETE		10	* MATERIAL TYPE, MESH INTERVAL
HS00003300	0			* SOURCE TYPE, FLAG, SOURCE MULTIPLIER
HS00003400	1	100	1.	1.* LHS BC TYPE, ASSOC CV, POOL HT FLAGS
HS00003500	2516.	8.9	8.9	* LHS AREA, CHARAC LENGTH, AXIAL LENGTH
HS00003600	0			* RHS BC TYPE, ASSOC CV, POOL HT FLAGS
HS00003801	311.	11		* INITIAL TEMPERATURE, NODE NO.
*				
HS00004000	15	1	1	0 * NO. NODES, TYPE, SS INIT, TRANS ITER
HS00004000	15	1	0	0 * NO. NODES, TYPE, SS INIT, TRANS ITER
HS00004001	'FLOOR'			*
HS00004002	0.	0.		* BOTTOM ALTITUDE, ORIENTATION
HS00004100	00002	1	0.	* NODALIZATION FLAGS, INSIDE RADIUS
HS00004201	CONCRETE		14	* MATERIAL TYPE, MESH INTERVAL
HS00004300	0			* SOURCE TYPE, FLAG, SOURCE MULTIPLIER
HS00004400	1	100	1.	1.* LHS BC TYPE, ASSOC CV, POOL HT FLAGS
HS00004500	1172.	15.	15.	* LHS AREA, CHARAC LENGTH, AXIAL LENGTH
HS00004600	4200	400	1.	1.* RHS BC TYPE, ASSOC CV, POOL HT FLAGS
HS00004700	1172.	15.	15.	* RHS AREA, CHARAC LENGTH, AXIAL LENGTH
HS00004801	300.	15		* INITIAL TEMPERATURE, NODE NO.
*				
HS00005000	11	1	1	0 * NO. NODES, TYPE, SS INIT, TRANS ITER
HS00005000	11	1	0	0 * NO. NODES, TYPE, SS INIT, TRANS ITER
HS00005001	'PSPWALL'			*
HS00005002	0.	1.		* BOTTOM ALTITUDE, ORIENTATION
HS00005100	-1	1	0.	* NODALIZATION FLAGS, INSIDE RADIUS
HS00005102	.05		6	*
HS00005103	.1		7	
HS00005104	.5		11	
HS00005201	CONCRETE		10	* MATERIAL TYPE, MESH INTERVAL

HS00005300	0					* SOURCE TYPE, FLAG, SOURCE MULTIPLIER
HS00005400	1	100	1.	1.		* LHS BC TYPE, ASSOC CV, POOL HT FLAGS
HS00005500	3169.	9.4	9.4			* LHS AREA, CHARAC LENGTH, AXIAL LENGTH
HS00005600	0					* RHS BC TYPE, ASSOC CV, POOL HT FLAGS
HS00005801	396.	11				* INITIAL TEMPERATURE, NODE NO.
*						
HS00006000	13	1	1	0		* NO. NODES, TYPE, SS INIT, TRANS ITER
HS00006000	13	1	0	0		* NO. NODES, TYPE, SS INIT, TRANS ITER
HS00006001	'CEIL1'					*
HS00006002	26.1	0.				* BOTTOM ALTITUDE, ORIENTATION
HS00006100	-1	1	0.			* NODALIZATION FLAGS, INSIDE RADIUS
HS00006102	.001	2				*
HS00006103	.003	3				
HS00006104	.007	4				
HS00006105	.015	5				
HS00006106	.023	6				
HS00006107	.039	7				
HS00006108	.071	8				
HS00006109	.135	9				
HS00006110	.263	10				
HS00006111	.500	11				
HS00006112	.750	12				
HS00006113	1.15	13				
HS00006201	CONCRETE	12				* MATERIAL TYPE, MESH INTERVAL
HS00006300	0					* SOURCE TYPE, FLAG, SOURCE MULTIPLIER
HS00006400	1	100	1.	1.		* LHS BC TYPE, ASSOC CV, POOL HT FLAGS
HS00006500	1440.	11.	11.			* LHS AREA, CHARAC LENGTH, AXIAL LENGTH
HS00006600	0					* RHS BC TYPE, ASSOC CV, POOL HT FLAGS
HS00006801	311.	13				* INITIAL TEMPERATURE, NODE NO.
*						
HS00007000	13	1	1	0		* NO. NODES, TYPE, SS INIT, TRANS ITER
HS00007000	13	1	0	0		* NO. NODES, TYPE, SS INIT, TRANS ITER
HS00007001	'EXWALL2'					*
HS00007002	0.	1.				* BOTTOM ALTITUDE, ORIENTATION
HS00007100	-1	1	0.			* NODALIZATION FLAGS, INSIDE RADIUS
HS00007102	.001	2				*
HS00007103	.003	3				
HS00007104	.007	4				
HS00007105	.015	5				
HS00007106	.023	6				
HS00007107	.039	7				
HS00007108	.071	8				
HS00007109	.135	9				
HS00007110	.263	10				
HS00007111	.500	11				
HS00007112	.750	12				
HS00007113	0.90	13				
HS00007201	CONCRETE	12				* MATERIAL TYPE, MESH INTERVAL
HS00007300	0					* SOURCE TYPE, FLAG, SOURCE MULTIPLIER
HS00007400	1	100	1.	1.		* LHS BC TYPE, ASSOC CV, POOL HT FLAGS
HS00007500	4723.	7.5	7.5			* LHS AREA, CHARAC LENGTH, AXIAL LENGTH
HS00007600	4200	400	1.	1.		* RHS BC TYPE, ASSOC CV, POOL HT FLAGS
HS00007700	4723.	7.5	7.5			* RHS AREA, CHARAC LENGTH, AXIAL LENGTH
HS00007801	300.	13				* INITIAL TEMPERATURE, NODE NO.



\*

HS00008000 14 1 1 0  
 HS00008000 14 1 0 0  
 HS00008001 'PCWALL2'  
 HS00008002 0. 1.  
 HS00008100 -1 1 0.  
 HS00008102 .001 2  
 HS00008103 .003 3  
 HS00008104 .007 4  
 HS00008105 .015 5  
 HS00008106 .023 6  
 HS00008107 .039 7  
 HS00008108 .071 8  
 HS00008109 .135 9  
 HS00008110 .263 10  
 HS00008111 .500 11  
 HS00008112 .750 12  
 HS00008113 1.00 13  
 HS00008114 1.50 14  
 HS00008201 CONCRETE 13  
 HS00008300 0  
 HS00008400 1 100 1. 1.  
 HS00008500 586. 7.5 7.5  
 HS00008600 4200 400 1. 1.  
 HS00008700 586. 7.5 7.5  
 HS00008801 300. 14

\*

HS00009000 11 1 1 0  
 HS00009000 11 1 0 0  
 HS00009001 'INWALL2'  
 HS00009002 0. 1.  
 HS00009100 -1 1 0.  
 HS00009102 .001 2  
 HS00009103 .003 3  
 HS00009104 .007 4  
 HS00009105 .015 5  
 HS00009106 .023 6  
 HS00009107 .039 7  
 HS00009108 .071 8  
 HS00009109 .135 9  
 HS00009110 .263 10  
 HS00009111 .350 11  
 HS00009201 CONCRETE 10  
 HS00009300 0  
 HS00009400 1 100 1. 1.  
 HS00009500 2280. 7.5 7.5  
 HS00009600 0  
 HS00009801 300. 11

\*

HS00010000 12 1 1 0  
 HS00010000 12 1 0 0  
 HS00010001 'CEIL2'  
 HS00010002 0. 0.  
 HS00010100 -1 1 0.

\* NO. NODES, TYPE, SS INIT, TRANS ITER  
 \* NO. NODES, TYPE, SS INIT, TRANS ITER  
 \*  
 \* BOTTOM ALTITUDE, ORIENTATION  
 \* NODALIZATION FLAGS, INSIDE RADIUS  
 \*

\* MATERIAL TYPE, MESH INTERVAL  
 \* SOURCE TYPE, FLAG, SOURCE MULTIPLIER  
 \* LHS BC TYPE, ASSOC CV, POOL HT FLAGS  
 \* LHS AREA, CHARAC LENGTH, AXIAL LENGTH  
 \* RHS BC TYPE, ASSOC CV, POOL HT FLAGS  
 \* RHS AREA, CHARAC LENGTH, AXIAL LENGTH  
 \* INITIAL TEMPERATURE, NODE NO.

\* NO. NODES, TYPE, SS INIT, TRANS ITER  
 \* NO. NODES, TYPE, SS INIT, TRANS ITER  
 \*  
 \* BOTTOM ALTITUDE, ORIENTATION  
 \* NODALIZATION FLAGS, INSIDE RADIUS  
 \*

\* MATERIAL TYPE, MESH INTERVAL  
 \* SOURCE TYPE, FLAG, SOURCE MULTIPLIER  
 \* LHS BC TYPE, ASSOC CV, POOL HT FLAGS  
 \* LHS AREA, CHARAC LENGTH, AXIAL LENGTH  
 \* RHS BC TYPE, ASSOC CV, POOL HT FLAGS  
 \* INITIAL TEMPERATURE, NODE NO.

\* NO. NODES, TYPE, SS INIT, TRANS ITER  
 \* NO. NODES, TYPE, SS INIT, TRANS ITER  
 \*  
 \* BOTTOM ALTITUDE, ORIENTATION  
 \* NODALIZATION FLAGS, INSIDE RADIUS

HS00010102	.001	2		*
HS00010103	.003	3		
HS00010104	.007	4		
HS00010105	.015	5		
HS00010106	.023	6		
HS00010107	.039	7		
HS00010108	.071	8		
HS00010109	.135	9		
HS00010110	.263	10		
HS00010111	.500	11		
HS00010112	.600	12		
HS00010201	CONCRETE	11		* MATERIAL TYPE, MESH INTERVAL
HS00010300	0			* SOURCE TYPE, FLAG, SOURCE MULTIPLIER
HS00010400	1	100	1. 1.	* LHS BC TYPE, ASSOC CV, POOL HT FLAGS
HS00010500	4110.	11.	11.	* LHS AREA, CHARAC LENGTH, AXIAL LENGTH
HS00010600	0			* RHS BC TYPE, ASSOC CV, POOL HT FLAGS
HS00010801	300.	12		* INITIAL TEMPERATURE, NODE NO.
*				
HS00011000	2 1 1 0			* NO. NODES, TYPE, SS INIT, TRANS ITER
HS00011000	4 1 0 0			* NO. NODES, TYPE, SS INIT, TRANS ITER
HS00011001	'STEEL2'			*
HS00011002	0. 1.			* BOTTOM ALTITUDE, ORIENTATION
HS00011100	-1 1 0.			* NODALIZATION FLAGS, INSIDE RADIUS
HS00011102	.00635	4		*
HS00011201	'STAINLESS STEEL'	3		* MATERIAL TYPE, MESH INTERVAL
HS00011300	0			* SOURCE TYPE, FLAG, SOURCE MULTIPLIER
HS00011400	1	100	1. 1.	* LHS BC TYPE, ASSOC CV, POOL HT FLAGS
HS00011500	775.6	3.	3.	* LHS AREA, CHARAC LENGTH, AXIAL LENGTH
HS00011600	0			* RHS BC TYPE, ASSOC CV, POOL HT FLAGS
HS00011801	305.4	4		* INITIAL TEMPERATURE, NODE NO.
*				
HS00012000	15 1 1 0			* NO. NODES, TYPE, SS INIT, TRANS ITER
HS00012000	15 1 0 0			* NO. NODES, TYPE, SS INIT, TRANS ITER
HS00012001	'PCWALL3'			*
HS00012002	0. 1.			* BOTTOM ALTITUDE, ORIENTATION
HS00012100	-1 1 0.			* NODALIZATION FLAGS, INSIDE RADIUS
HS00012102	.001	2		*
HS00012103	.003	3		
HS00012104	.007	4		
HS00012105	.015	5		
HS00012106	.023	6		
HS00012107	.039	7		
HS00012108	.071	8		
HS00012109	.135	9		
HS00012110	.263	10		
HS00012111	.500	11		
HS00012112	.750	12		
HS00012113	1.0	13		
HS00012114	1.5	14		
HS00012115	1.7	15		
HS00012201	CONCRETE	14		* MATERIAL TYPE, MESH INTERVAL
HS00012300	0			* SOURCE TYPE, FLAG, SOURCE MULTIPLIER
HS00012400	1	100	1. 1.	* LHS BC TYPE, ASSOC CV, POOL HT FLAGS
HS00012500	291.	8.3	8.3	* LHS AREA, CHARAC LENGTH, AXIAL LENGTH

HS00012600	0					* RHS BC TYPE, ASSOC CV, POOL HT FLAGS
HS00012801	300.		1			* INITIAL TEMPERATURE, NODE NO.
HS00012802	300.1370		2			
HS00012803	300.4111		3			
HS00012804	300.9594		4			
HS00012805	302.0558		5			
HS00012806	303.1523		6			
HS00012807	305.3452		7			
HS00012808	309.7311		8			
HS00012809	318.5029		9			
HS00012810	336.0464	10				
HS00012811	368.5294	11				
HS00012812	402.7941	12				
HS00012813	437.0588	13				
HS00012814	505.5882	14				
HS00012815	533.	15				
*						
HS00013000	11 1 1 0					* NO. NODES, TYPE, SS INIT, TRANS ITER
HS00013000	11 1 0 0					* NO. NODES, TYPE, SS INIT, TRANS ITER
HS00013001	'INWALL3'					*
HS00013002	0. 1.					* BOTTOM ALTITUDE, ORIENTATION
HS00013100	-1 1 0.					* NODALIZATION FLAGS, INSIDE RADIUS
HS00013102	.001	2				*
HS00013103	.003	3				
HS00013104	.007	4				
HS00013105	.015	5				
HS00013106	.023	6				
HS00013107	.039	7				
HS00013108	.071	8				
HS00013109	.135	9				
HS00013110	.263	10				
HS00013111	.450	11				
HS00013201	CONCRETE	10				* MATERIAL TYPE, MESH INTERVAL
HS00013300	0					* SOURCE TYPE, FLAG, SOURCE MULTIPLIER
HS00013400	1 100 1. 1.					* LHS BC TYPE, ASSOC CV, POOL HT FLAGS
HS00013500	1868. 8.3 8.3					* LHS AREA, CHARAC LENGTH, AXIAL LENGTH
HS00013600	0					* RHS BC TYPE, ASSOC CV, POOL HT FLAGS
HS00013801	300. 11					* INITIAL TEMPERATURE, NODE NO.
*						
HS00014000	11 1 1 0					* NO. NODES, TYPE, SS INIT, TRANS ITER
HS00014000	11 1 0 0					* NO. NODES, TYPE, SS INIT, TRANS ITER
HS00014001	'CEIL3'					*
HS00014002	0. 0.					* BOTTOM ALTITUDE, ORIENTATION
HS00014100	-1 1 0.					* NODALIZATION FLAGS, INSIDE RADIUS
HS00014102	.001	2				*
HS00014103	.003	3				
HS00014104	.007	4				
HS00014105	.015	5				
HS00014106	.023	6				
HS00014107	.039	7				
HS00014108	.071	8				
HS00014109	.135	9				
HS00014110	.263	10				
HS00014111	.500	11				

HS00014201 CONCRETE	10	* MATERIAL TYPE, MESH INTERVAL
HS00014300 0		* SOURCE TYPE, FLAG, SOURCE MULTIPLIER
HS00014400 1 100 1. 1.		* LHS BC TYPE, ASSOC CV, POOL HT FLAGS
HS00014500 2610. 11. 11.		* LHS AREA, CHARAC LENGTH, AXIAL LENGTH
HS00014600 0		* RHS BC TYPE, ASSOC CV, POOL HT FLAGS
HS00014801 300. 11		* INITIAL TEMPERATURE, NODE NO.
*		
HS00015000 14 1 1 0		* NO. NODES, TYPE, SS INIT, TRANS ITER
HS00015000 14 1 0 0		* NO. NODES, TYPE, SS INIT, TRANS ITER
HS00015001 'PCWALL4'		*
HS00015002 0. 1.		* BOTTOM ALTITUDE, ORIENTATION
HS00015100 -1 1 0.		* NODALIZATION FLAGS, INSIDE RADIUS
HS00015102 .001 2		*
HS00015103 .003 3		
HS00015104 .007 4		
HS00015105 .015 5		
HS00015106 .023 6		
HS00015107 .039 7		
HS00015108 .071 8		
HS00015109 .135 9		
HS00015110 .263 10		
HS00015111 .500 11		
HS00015112 .750 12		
HS00015113 1.0 13		
HS00015114 1.5 14		
HS00015201 CONCRETE	13	* MATERIAL TYPE, MESH INTERVAL
HS00015300 0		* SOURCE TYPE, FLAG, SOURCE MULTIPLIER
HS00015400 1 100 1. 1.		* LHS BC TYPE, ASSOC CV, POOL HT FLAGS
HS00015500 127. 5.1 5.1		* LHS AREA, CHARAC LENGTH, AXIAL LENGTH
HS00015600 0		* RHS BC TYPE, ASSOC CV, POOL HT FLAGS
HS00015801 300. 1		* INITIAL TEMPERATURE, NODE NO.
HS00015802 300.1553 2		
HS00015803 300.466 3		
HS00015804 301.0873 4		
HS00015805 302.33 5		
HS00015806 303.5726 6		
HS00015807 306.058 7		
HS00015808 311.0286 8		
HS00015809 320.97 9		
HS00015810 340.8526 10		
HS00015811 377.6666 11		
HS00015812 416.5 12		
HS00015813 455.3333 13		
HS00015814 533. 14		
*		
HS00016000 15 1 1 0		* NO. NODES, TYPE, SS INIT, TRANS ITER
HS00016000 15 1 0 0		* NO. NODES, TYPE, SS INIT, TRANS ITER
HS00016001 'POOLWA4'		*
HS00016002 0. 1.		* BOTTOM ALTITUDE, ORIENTATION
HS00016100 -1 1 0.		* NODALIZATION FLAGS, INSIDE RADIUS
HS00016102 .001 2		*
HS00016103 .003 3		
HS00016104 .007 4		
HS00016105 .015 5		

HS00016106	.023		6								
HS00016107	.039		7								
HS00016108	.071		8								
HS00016109	.135		9								
HS00016110	.263		10								
HS00016111	.500		11								
HS00016112	.750		12								
HS00016113	1.0		13								
HS00016114	1.5		14								
HS00016115	1.8		15								
HS00016201	CONCRETE		14			*	MATERIAL TYPE, MESH INTERVAL				
HS00016300	0					*	SOURCE TYPE, FLAG, SOURCE MULTIPLIER				
HS00016400	1	100	1.	1.		*	LHS BC TYPE, ASSOC CV, POOL HT FLAGS				
HS00016500	234.	5.1	5.1			*	LHS AREA, CHARAC LENGTH, AXIAL LENGTH				
HS00016600	4200	400	1.	1.		*	RHS BC TYPE, ASSOC CV, POOL HT FLAGS				
HS00016700	234.	5.1	5.1			*	RHS AREA, CHARAC LENGTH, AXIAL LENGTH				
HS00016801	300.	15				*	INITIAL TEMPERATURE, NODE NO.				
*											
HS00017000	10	1	1	0		*	NO. NODES, TYPE, SS INIT, TRANS ITER				
HS00017000	10	1	0	0		*	NO. NODES, TYPE, SS INIT, TRANS ITER				
HS00017001	'INWALL4'					*					
HS00017002	0.	1.				*	BOTTOM ALTITUDE, ORIENTATION				
HS00017100	-1	1	0.			*	NODALIZATION FLAGS, INSIDE RADIUS				
HS00017102	.001		2			*					
HS00017103	.003		3								
HS00017104	.007		4								
HS00017105	.015		5								
HS00017106	.023		6								
HS00017107	.039		7								
HS00017108	.071		8								
HS00017109	.135		9								
HS00017110	.25		10								
HS00017201	CONCRETE		9			*	MATERIAL TYPE, MESH INTERVAL				
HS00017300	0					*	SOURCE TYPE, FLAG, SOURCE MULTIPLIER				
HS00017400	1	100	1.	1.		*	LHS BC TYPE, ASSOC CV, POOL HT FLAGS				
HS00017500	424.	5.1	5.1			*	LHS AREA, CHARAC LENGTH, AXIAL LENGTH				
HS00017600	0					*	RHS BC TYPE, ASSOC CV, POOL HT FLAGS				
HS00017801	300.	10				*	INITIAL TEMPERATURE, NODE NO.				
*											
HS00018000	10	1	1	0		*	NO. NODES, TYPE, SS INIT, TRANS ITER				
HS00018000	10	1	0	0		*	NO. NODES, TYPE, SS INIT, TRANS ITER				
HS00018001	'CEIL4'					*					
HS00018002	0.	0.				*	BOTTOM ALTITUDE, ORIENTATION				
HS00018100	-1	1	0.			*	NODALIZATION FLAGS, INSIDE RADIUS				
HS00018102	.001		2			*					
HS00018103	.003		3								
HS00018104	.007		4								
HS00018105	.015		5								
HS00018106	.023		6								
HS00018107	.039		7								
HS00018108	.071		8								
HS00018109	.135		9								
HS00018110	.15		10								
HS00018201	CONCRETE		9			*	MATERIAL TYPE, MESH INTERVAL				

HS00018300	0					* SOURCE TYPE, FLAG, SOURCE MULTIPLIER
HS00018400	1	100	1.	1.		* LHS BC TYPE, ASSOC CV, POOL HT FLAGS
HS00018500	2298.	11.	11.			* LHS AREA, CHARAC LENGTH, AXIAL LENGTH
HS00018600	0					* RHS BC TYPE, ASSOC CV, POOL HT FLAGS
HS00018801	300.	10				* INITIAL TEMPERATURE, NODE NO.
*						
HS00019000	15	1	1	0		* NO. NODES, TYPE, SS INIT, TRANS ITER
HS00019000	15	1	0	0		* NO. NODES, TYPE, SS INIT, TRANS ITER
HS00019001	'PCPOOL'					*
HS00019002	0.	1.				* BOTTOM ALTITUDE, ORIENTATION
HS00019100	-1	1	0.			* NODALIZATION FLAGS, INSIDE RADIUS
*						
HS00019102	.001		2			
HS00019103	.003		3			
HS00019104	.007		4			
HS00019105	.015		5			
HS00019106	.023		6			
HS00019107	.039		7			
HS00019108	.071		8			
HS00019109	.135		9			
HS00019110	.263		10			
HS00019111	.500		11			
HS00019112	.750		12			
HS00019113	1.0		13			
HS00019114	2.0		15			
HS00019201	CONCRETE		14			* MATERIAL TYPE, MESH INTERVAL
HS00019300	0					* SOURCE TYPE, FLAG, SOURCE MULTIPLIER
HS00019400	1	100	1.	1.		* LHS BC TYPE, ASSOC CV, POOL HT FLAGS
HS00019500	706.	7.2	7.2			* LHS AREA, CHARAC LENGTH, AXIAL LENGTH
HS00019600	4200	400	1.	1.		* RHS BC TYPE, ASSOC CV, POOL HT FLAGS
HS00019700	706.	7.2	7.2			* RHS AREA, CHARAC LENGTH, AXIAL LENGTH
HS00019801	300.	15				* INITIAL TEMPERATURE, NODE NO.
*						
HS00020000	23	1	1	0		* NO. NODES, TYPE, SS INIT, TRANS ITER
HS00020000	23	1	0	0		* NO. NODES, TYPE, SS INIT, TRANS ITER
HS00020001	'POSTS'					*
HS00020002	0.	1.				* BOTTOM ALTITUDE, ORIENTATION
HS00020100	-1	1	0.			* NODALIZATION FLAGS, INSIDE RADIUS
*						
HS00020102	.001		2			
HS00020103	.003		3			
HS00020104	.007		4			
HS00020105	.015		5			
HS00020106	.023		6			
HS00020107	.039		7			
HS00020108	.071		8			
HS00020109	.135		9			
HS00020110	.262		10			
HS00020111	.400		11			
HS00020112	.600		13			
HS00020113	.738		14			
HS00020114	.865		15			
HS00020115	.929		16			
HS00020116	.961		17			
HS00020117	.977		18			
HS00020118	.985		19			

```

* MATERIAL TYPE, MESH INTERVAL
* SOURCE TYPE, FLAG, SOURCE MULTIPLIER
* LHS BC TYPE, ASSOC CV, POOL HT FLAGS
* LHS AREA, CHARAC LENGTH, AXIAL LENGTH
* RHS BC TYPE, ASSOC CV, POOL HT FLAGS
* RHS AREA, CHARAC LENGTH, AXIAL LENGTH
* INITIAL TEMPERATURE, NODE NO.

* NO. NODES, TYPE, SS INIT, TRANS ITER
* NO. NODES, TYPE, SS INIT, TRANS ITER
*
* BOTTOM ALTITUDE, ORIENTATION
* NODALIZATION FLAGS, INSIDE RADIUS
*

* MATERIAL TYPE, MESH INTERVAL
* SOURCE TYPE, FLAG, SOURCE MULTIPLIER
* LHS BC TYPE, ASSOC CV, POOL HT FLAGS
* LHS AREA, CHARAC LENGTH, AXIAL LENGTH
* RHS BC TYPE, ASSOC CV, POOL HT FLAGS
* INITIAL TEMPERATURE, NODE NO.

* NO. NODES, TYPE, SS INIT, TRANS ITER
* NO. NODES, TYPE, SS INIT, TRANS ITER
*
* BOTTOM ALTITUDE, ORIENTATION
* NODALIZATION FLAGS, INSIDE RADIUS
*

* MATERIAL TYPE, MESH INTERVAL
* SOURCE TYPE, FLAG, SOURCE MULTIPLIER
* LHS BC TYPE, ASSOC CV, POOL HT FLAGS

```

HS00023500	4756.	16.	16.		* LHS AREA, CHARAC LENGTH, AXIAL LENGTH
HS00023600	0				* RHS BC TYPE, ASSOC CV, POOL HT FLAGS
HS00023801	300.	9			* INITIAL TEMPERATURE, NODE NO.
*					
HS00024000	10	1	1	0	* NO. NODES, TYPE, SS INIT, TRANS ITER
HS00024000	10	1	0	0	* NO. NODES, TYPE, SS INIT, TRANS ITER
HS00024001	'FLOOR'				*
HS00024002	33.	0.			* BOTTOM ALTITUDE, ORIENTATION
HS00024100	-1	1	0.		* NODALIZATION FLAGS, INSIDE RADIUS
HS00024102	.001			2	*
HS00024103	.003			3	
HS00024104	.007			4	
HS00024105	.015			5	
HS00024106	.023			6	
HS00024107	.039			7	
HS00024108	.071			8	
HS00024109	.135			9	
HS00024110	.230			10	
HS00024201	CONCRETE		9		* MATERIAL TYPE, MESH INTERVAL
HS00024300	0				* SOURCE TYPE, FLAG, SOURCE MULTIPLIER
HS00024400	1	200	1.	1.	* LHS BC TYPE, ASSOC CV, POOL HT FLAGS
HS00024500	4184.	16.	16.		* LHS AREA, CHARAC LENGTH, AXIAL LENGTH
HS00024600	0				* RHS BC TYPE, ASSOC CV, POOL HT FLAGS
HS00024801	300.	10			* INITIAL TEMPERATURE, NODE NO.
*					
HS00025000	4	1	0	0	* NO. NODES, TYPE, SS INIT, TRANS ITER
HS00025001	'STEEL'				*
HS00025002	33.	1.			* BOTTOM ALTITUDE, ORIENTATION
HS00025100	-1	1	0.		* NODALIZATION FLAGS, INSIDE RADIUS
HS00025102	.00635	4			*
HS00025201	'STAINLESS STEEL'		3		* MATERIAL TYPE, MESH INTERVAL
HS00025300	0				* SOURCE TYPE, FLAG, SOURCE MULTIPLIER
HS00025400	1	200	1.	1.	* LHS BC TYPE, ASSOC CV, POOL HT FLAGS
HS00025500	712.	3.	3.		* LHS AREA, CHARAC LENGTH, AXIAL LENGTH
HS00025600	0				* RHS BC TYPE, ASSOC CV, POOL HT FLAGS
HS00025801	299.8	4			* INITIAL TEMPERATURE, NODE NO.
*					
HS00026000	6	1	1	0	* NO. NODES, TYPE, SS INIT, TRANS ITER
HS00026000	6	1	0	0	* NO. NODES, TYPE, SS INIT, TRANS ITER
HS00026001	'EXTWALL'				*
HS00026002	12.	1.			* BOTTOM ALTITUDE, ORIENTATION
HS00026100	-1	1	0.		* NODALIZATION FLAGS, INSIDE RADIUS
HS00026102	.001			6	*
HS00026201	'STAINLESS STEEL'		5		* MATERIAL TYPE, MESH INTERVAL
HS00026300	0				* SOURCE TYPE, FLAG, SOURCE MULTIPLIER
HS00026400	1	300	1.	1.	* LHS BC TYPE, ASSOC CV, POOL HT FLAGS
HS00026500	76248.	65.	16.		* LHS AREA, CHARAC LENGTH, AXIAL LENGTH
HS00026600	0				* RHS BC TYPE, ASSOC CV, POOL HT FLAGS
HS00026801	300.	6			* INITIAL TEMPERATURE, NODE NO.
*					
HS00027000	9	1	0	0	* NO. NODES, TYPE, SS INIT, TRANS ITER
HS00027001	'CEILING'				*
HS00027002	12.	0.			* BOTTOM ALTITUDE, ORIENTATION
HS00027100	-1	1	0.		* NODALIZATION FLAGS, INSIDE RADIUS



HS00027102	.7	8	*
HS00027103	.76	9	
HS00027201	'STAINLESS STEEL'	8	* MATERIAL TYPE, MESH INTERVAL
HS00027300	0		* SOURCE TYPE, FLAG, SOURCE MULTIPLIER
HS00027400	1	300 1. 1.	* LHS BC TYPE, ASSOC CV, POOL HT FLAGS
HS00027500	8279.	16. 16.	* LHS AREA, CHARAC LENGTH, AXIAL LENGTH
HS00027600	0		* RHS BC TYPE, ASSOC CV, POOL HT FLAGS
HS00027801	300.	9	* INITIAL TEMPERATURE, NODE NO.
*			
HS00028000	6 1 1 0		* NO. NODES, TYPE, SS INIT, TRANS ITER
HS00028000	6 1 0 0		* NO. NODES, TYPE, SS INIT, TRANS ITER
HS00028001	'FLOOR'		*
HS00028002	12. 0.		* BOTTOM ALTITUDE, ORIENTATION
HS00028100	-1 1 0.		* NODALIZATION FLAGS, INSIDE RADIUS
HS00028102	.2	5	*
HS00028103	.23	6	
HS00028201	CONCRETE	5	* MATERIAL TYPE, MESH INTERVAL
HS00028300	0		* SOURCE TYPE, FLAG, SOURCE MULTIPLIER
HS00028400	1	300 1. 1.	* LHS BC TYPE, ASSOC CV, POOL HT FLAGS
HS00028500	8279.	16. 16.	* LHS AREA, CHARAC LENGTH, AXIAL LENGTH
HS00028600	0		* RHS BC TYPE, ASSOC CV, POOL HT FLAGS
HS00028801	300.	6	* INITIAL TEMPERATURE, NODE NO.
*			
HS00029000	4 1 1 0		* NO. NODES, TYPE, SS INIT, TRANS ITER
HS00029000	4 1 0 0		* NO. NODES, TYPE, SS INIT, TRANS ITER
HS00029001	'STEEL'		*
HS00029002	12. 1.		* BOTTOM ALTITUDE, ORIENTATION
HS00029100	-1 1 0.		* NODALIZATION FLAGS, INSIDE RADIUS
HS00029102	.00635	4	*
HS00029201	'STAINLESS STEEL'	3	* MATERIAL TYPE, MESH INTERVAL
HS00029300	0		* SOURCE TYPE, FLAG, SOURCE MULTIPLIER
HS00029400	1	300 1. 1.	* LHS BC TYPE, ASSOC CV, POOL HT FLAGS
HS00029500	712.	3. 3.	* LHS AREA, CHARAC LENGTH, AXIAL LENGTH
HS00029600	0		* RHS BC TYPE, ASSOC CV, POOL HT FLAGS
HS00029801	299.8	4	* INITIAL TEMPERATURE, NODE NO.
*			
*****			
***** MATERIAL PROPERTY INPUT			
*****			
MPMAT00100	CONCRETE		
MPMAT00101	THC	310	
MPMAT00102	RHO	320	
MPMAT00103	CPS	330	
*****			
***** TABULAR FUNCTION INPUT FOR HEAT SLABA			
*****			
TF20000	'RHS HT COEF'	1 1. 0.	* NAME, NO. PAIRS, MUL CONST, ADD CONST
TF20010	0. 6.08		* TIME, HEAT TRANSFER COEFFICIENT
*			
TF31000	'THC CONC'	2 1. 0.	* NAME, NO. PAIRS, MUL CONST, ADD CONST
TF31010	200. 1.454		* TEMPERATURE, CONDUCTIVITY
TF31011	5000. 1.454		*
*			

```

TF32000 'RHO CONC'      2 1. 0. * NAME, NO. PAIRS, MUL CONST, ADD CONST
TF32010 200. 2520.      * TEMPERATURE, CONDUCTIVITY
TF32011 5000. 2520.     *
*
TF33000 'CPS CONC'      2 1. 0. * NAME, NO. PAIRS, MUL CONST, ADD CONST
TF33010 200. 994.8      * TEMPERATURE, CONDUCTIVITY
TF33011 5000. 994.8     *
*****
*****
***** BURN MODEL INPUT
*****
BUR000 0
*
*      XH2IGN  XCOIGN  XH2IGY  XCOIGY  XO2IG  XMSCIG
*BUR001
*      CVNUM  IGNTR   CDIM    TFRAC
BUR101 100    1      36.8    .25
BUR102 200    1      42.     .5
BUR103 300    1      54.1    .5
*****
*****
***** CONTROL FUNCTIONS FOR MAXIMUM P, MAXIMUM T'S, AND PLOT EDITS
*****
CF70000 MAX-T-100 MAX 2 1. 0.
CF70001 0.
CF70010 1. 0. CFVALU.700
CF70011 1. 0. CVH-TVAP.100
*
CF71000 MAX-P-100 MAX 2 1. 0.
CF71001 0.
CF71010 1. 0. CFVALU.710
CF71011 1. 0. CVH-P.100
*
CF70100 MAX-T-200 MAX 2 1. 0.
CF70101 0.
CF70110 1. 0. CFVALU.701
CF70111 1. 0. CVH-TVAP.200
*
CF70200 MAX-T-300 MAX 2 1. 0.
CF70201 0.
CF70210 1. 0. CFVALU.702
CF70211 1. 0. CVH-TVAP.300
*
CF63000 PLOT-TRIP L-OR 2 1. 0.
CF63001 .FALSE.
CF63010 1. 0. CFVALU.612
CF63011 1. 0. CFVALU.622
*
CF61000 DP-PLOT ADD 2 1. 0.
CF61001 0.
CF61010 1. 0. CVH-P.100
CF61011 -1. 0. CFVALU.643
*

```

```

CF61100  ABSDP  ABS  1  1. 0.
CF61110  1. 0.  CFVALU.610
*
CF61200  PLOT-TRIP-DP  L-GE  2 1. 0.
CF61210  1. 0.  CFVALU.611
CF61211  0. 500. TIME
*
CF64300  PLAST  L-A-IFTE  3  1. 0.
CF64301  0.
CF64310  1. 0.  CFVALU.630
CF64311  1. 0.  CVH-P.100
CF64312  1. 0.  CFVALU.643
*
CF62000  DT-PLOT  ADD  2  1. 0.
CF62001  0.
CF62010  1. 0.  CVH-TVAP.100
CF62011 -1. 0.  CFVALU.653
*
CF62100  ABSDT  ABS  1  1. 0.
CF62110  1. 0.  CFVALU.620
*
CF62200  PLOT-TRIP-DT  L-GE  2  1. 0.
CF62210  1. 0.  CFVALU.621
CF62211  0. 10.  TIME
*
CF65300  TLAST  L-A-IFTE  3  1. 0.
CF65301  0.
CF65310  1. 0.  CFVALU.630
CF65311  1. 0.  CVH-TVAP.100
CF65312  1. 0.  CFVALU.653
***
***  SENSITIVITY COEFFICIENTS
***
SC00001  2200  10.  1
SC00002  2200   0.  2

```

ST006: Browns Ferry Reactor Building Burns

MELCOR Input

```

TITLE ST006
JOBID 'ST006'
CRTOUT
COMTC  2
DEBUG  0
RESTART 0
DTTIME .05
PLOTCF 630
*      TSTART DTMAX DTMIN DTEDIT DTPLOT DTREST
TIME1  0.    1.    .001  400.   50.   300.
TIME2 47850. 10.    .001  400.   50.   300.

```

TEND 48939.5  
CPULIM 500.  
CPULEFT 1.  
.

ST006: Browns Ferry Reactor Building Burns

MELPLT Input

TITLE BROWNS FERRY SEC. CONT. - ST006  
FILE1 MELPTF.DAT  
PLOT CVH-P.100  
PLOT CVH-P.200  
PLOT CVH-P.300  
\*PLOT CVH-PPART.3.100  
\*CPLOT0 CVH-PPART.5.100  
\*CPLOT1 CVH-PPART.6.100  
\*PLOT CVH-PPART.3.200  
\*CPLOT0 CVH-PPART.5.200  
\*CPLOT1 CVH-PPART.6.200  
\*PLOT CVH-PPART.3.300  
\*CPLOT0 CVH-PPART.5.300  
\*CPLOT1 CVH-PPART.6.300  
PLOT CVH-TVAP.100  
CPLOT0 CVH-TVAP.200  
CPLOT1 CVH-TVAP.300  
\*PLOT FL-MFLOW.110  
\*PLOT FL-MFLOW.120  
\*PLOT FL-MFLOW.130  
\*PLOT FL-MFLOW.140  
\*PLOT FL-MFLOW.150  
\*PLOT FL-MFLOW.160  
\*PLOT FL-VELVAP.110  
\*PLOT FL-VELVAP.120  
\*PLOT FL-VELVAP.130  
\*PLOT FL-VELVAP.140  
\*PLOT FL-VELVAP.150  
\*PLOT FL-VELVAP.160  
\*PLOT CVH-VELVAPCV.100  
\*PLOT CVH-VELVAPCV.200  
\*PLOT CVH-VELVAPCV.300  
PLOT HS-FILM-THICKNESS-L.00011  
PLOT HS-HEAT-FLUX-ATMS-L.00011  
PLOT HS-NODE-TEMPERATURE.0001101  
PLOT HS-FILM-THICKNESS-L.00005  
PLOT HS-HEAT-FLUX-ATMS-L.00005  
PLOT HS-NODE-TEMPERATURE.0000501  
\*PLOT HS-FILM-THICKNESS-L.00007  
\*PLOT HS-HEAT-FLUX-ATMS-L.00007  
\*PLOT HS-NODE-TEMPERATURE.0000701  
\*PLOT HS-FILM-THICKNESS-L.00008  
\*PLOT HS-HEAT-FLUX-ATMS-L.00008  
\*PLOT HS-NODE-TEMPERATURE.0000801

```

*PLOT  HS-HEAT-FLUX-ATMS-L.00022
*PLOT  HS-HEAT-FLUX-ATMS-L.00023
*PLOT  HS-HEAT-FLUX-ATMS-L.00024
PLOT  DT
PLOT  BUR-XH20.100
CPLOT0 BUR-XH2.100
CPLOT1 BUR-XO2.100
PLOT  BUR-XH20.200
CPLOT0 BUR-XH2.200
CPLOT1 BUR-XO2.200
PLOT  BUR-XH20.300
CPLOT0 BUR-XH2.300
CPLOT1 BUR-XO2.300
*YLABEL,SOURCE TEMPERATURE (K)
*PLOT CFVALU.850
*YLABEL,STEAM INJECTION RATE (KG/S)
*PLOT CFVALU.800
*YLABEL,H2 INJECTION RATE (KG/S)
*PLOT CFVALU.830
YLABEL,MAXIMUM TEMPERATURE (K)
LEGEND,CV100
PLOT CFVALU.700
LEGEND,CV200
CPLOT0 CFVALU.701
LEGEND,CV300
CPLOT1 CFVALU.702
YLABEL,MAXIMUM PRESSURE (PA)
LEGEND,MAXIMUM P - CV100
PLOT CFVALU.710
YLABEL,CPU TIME ((S)
LEGEND,TOTAL TIME
PLOT CPU
LEGEND,HEAT SLAB
CPLOT5 HS-CPUC
LEGEND,CV HYDRO
CPLOT6 CVH-CPUT

```

ST007: HDR Steam Blowdown Test

MELGEN Input

```

*****
*****
*****      This is a MELCOR test calculation for the HDR containment
*****      experiment V44.
*****
TITLE      ST007
CRTOUT
*****
*****      NONCONDENSIBLE GASES DATA
*****
*****

```

```

*****      Noncondensable gases are O2 AND N2
*****
NCG000      O2      4
NCG001      N2      5
*****
*****
*****      CONTROL VOLUME DATA
*****
*****
*****      Control Volume 1 ---- Blowdown Cell, Room 1603
*****
CV00100      BLOWDOWN  2    2    2
CV00101      0        0
CV00102      0.0      0.0
CV001A0      2
CV001A1      PVOL      1.0E5    PH2O      3494.0    TATM      300.0    TPOL      300.0
CV001A2      MFRC.1    0.0      MFRC.2    0.0      MFRC.3    1.0
CV001A3      MFRC.4    0.2319    MFRC.5    0.7681
*****
*****      Altitude      Volume
CV001B1      18.8        0.0
CV001B2      26.3        280.0
*****
*****
*****      EXTERNAL VAPOR SOURCE
*****
CV001C1      MASS.2      1      2
CV001C2      AE          2      2
*****
*****
*****      Control Volume 2 ---- Inner Ring Around RPV, Room 1701 U
*****
CV00200      INNER-RING  2    2    2
CV00201      0        0
CV00202      0.0      0.0
CV002A0      2
CV002A1      PVOL      1.0E5    PH2O      3494.0    TATM      300.0    TPOL      300.0
CV002A2      MFRC.1    0.0      MFRC.2    0.0      MFRC.3    1.0
CV002A3      MFRC.4    0.2319    MFRC.5    0.7681
*****
*****      Altitude      Volume
CV002B1      24.0        0.0
CV002B2      34.4        44.0
*****
*****
*****      Control Volume 3 ---- Outer Ring Around RPV and Steam Downcomer
*****      Rooms 1701 O, 1704
*****
CV00300      OUTER-RING  2    2    2
CV00301      0        0
CV00302      0.0      0.0
CV003A0      2

```

```

CV003A1  PVOL    1.0E5  PH2O    3494.0  TATM    300.0  TPOL    300.0
CV003A2  MFRC.1  0.0    MFRC.2  0.0    MFRC.3  1.0
CV003A3  MFRC.4  0.2319 MFRC.5  0.7681
*****
*****  Altitude    Volume
CV003B1    27.6      0.0
CV003B2    35.9     912.0
*****
*****
*****
*****  Control Volume 4 ---- Lower Rooms, 1201 through 1514
*****
CV00400  LOWER-ROOMS  2    2    2
CV00401    0         0
CV00402    0.0      0.0
CV004A0    2
CV004A1  PVOL    1.0E5  PH2O    3494.0  TATM    300.0  TPOL    300.0
CV004A2  MFRC.1  0.0    MFRC.2  0.0    MFRC.3  1.0
CV004A3  MFRC.4  0.2319 MFRC.5  0.7681
*****
*****  Altitude    Volume
CV004B1     4.0      0.0
CV004B2    18.0     3003.0
*****
*****
*****
*****  Control Volume 5 ---- Upper Rooms, 1602 through 11004
*****
CV00500  UPPER-ROOMS  2    2    2
CV00501    0         0
CV00502    0.0      0.0
CV005A0    2
CV005A1  PVOL    1.0E5  PH2O    3494.0  TATM    300.0  TPOL    300.0
CV005A2  MFRC.1  0.0    MFRC.2  0.0    MFRC.3  1.0
CV005A3  MFRC.4  0.2319 MFRC.5  0.7681
*****
*****  Altitude    Volume
CV005B1    35.4      0.0
CV005B2    63.5     7102.0
*****
*****
*****  FLOW PATH DATA
*****
*****  Volume 1 to Volume 2
*****
FL00100  V1-V2    1      2      24.0    25.0
FL00101    3.196    2.0    1.0    2.017    2.017
FL00102    3        0      0      0
FL00103    1.028    1.028  1.028  1.028
FL00104    0.0      0.0
FL001S1    3.196    1.0    2.017  1.0E-6  16.0
*****

```

```

*****      Volume 1 to Volume 3
*****
FL00200      V1-V3      1          3          26.0      27.7
FL00201      2.593      3.0        1.0        0.909      0.909
FL00202      0          0          0          0
FL00203      0.866      0.866      0.866      0.866
FL00204      0.0        0.0
FL002S1      2.593      1.0        1.817      1.0E-6      16.0
*****
*****      Volume 1 to Volume 4
*****
FL00300      V1-V4      1          4          18.9      17.0
FL00301      0.283      3.0        1.0        0.3002      0.3002
FL00302      0          0          0          0
FL00303      1.636      1.636      1.636      1.636
FL00304      0.0        0.0
FL003S1      0.283      1.0        0.6003      1.0E-6      16.0
*****
*****      Volume 1 to Volume 5
*****
FL00400      V1-V5      1          5          26.0      35.5
FL00401      2.128      11.0       1.0        0.823      0.823
FL00402      0          0          0          0
FL00403      1.116      1.116      1.116      1.116
FL00404      0.0        0.0
FL004S1      2.128      1.0        1.646      1.0E-6      16.0
*****
*****      Volume 2 to Volume 3
*****
FL00500      V2-V3      2          3          28.0      29.0
FL00501      1.700      2.0        1.0        1.471      1.471
FL00502      3          0          0          0
FL00503      1.020      1.020      1.020      1.020
FL00504      0.0        0.0
FL005S1      1.700      1.0        1.471      1.0E-6      16.0
*****
*****      Volume 2 to Volume 5
*****
FL00600      V2-V5      2          5          34.0      35.5
FL00601      1.374      3.0        1.0        0.662      0.622
FL00602      0          0          0          0
FL00603      1.389      1.389      1.389      1.389
FL00604      0.0        0.0
FL006S1      1.374      1.0        1.323      1.0E-6      16.0
*****
*****      Volume 3 to Volume 4
*****
FL00700      V3-V4      3          4          27.7      17.0
FL00701      1.500      12.0       1.0        0.691      0.691
FL00702      0          0          0          0
FL00703      1.389      1.389      1.389      1.389
FL00704      0.0        0.0
FL007S1      1.500      1.0        1.382      1.0E-6      16.0
*****

```



```

*****      Volume 3 to Volume 5
*****
FL00800      V3-V5      3      5      35.0      35.5
FL00801      15.014      12.0      1.0      2.186      2.186
FL00802      0      0      0      0
FL00803      0.782      0.782      0.782      0.782
FL00804      0.0      0.0
FL008S1      15.014      1.0      4.372      1.0E-6      16.0
*****
*****      Volume 4 to Volume 5
*****
FL00900      V4-V5      4      5      17.0      35.5
FL00901      14.049      20.0      1.0      2.115      2.115
FL00902      0      0      0      0
FL00903      0.803      0.803      0.803      0.803
FL00904      0.0      0.0
FL009S1      14.049      1.0      4.229      1.0E-6      16.0
*****
*****
*****      HEAT STRUCTURES
*****
*****      VOLUME 1
*****
*****      Structure 1
*****
HS00001000      4      1      -1      20
HS00001001      V1-S01
HS00001002      18.9      1.0
HS00001003      2.0
HS00001100      -1      1      0.0
HS00001102      0.0001      2
HS00001103      0.0002519      3
HS00001104      0.0006755      4
HS00001200      -1
HS00001201      STEEL      3
HS00001300      0
HS00001400      1      1      1.0      1.0
HS00001500      196.8      3.0      7.3
HS00001600      0
HS00001800      -1
HS00001801      293.0      4
*****
*****      Structure 2
*****
HS00002000      5      1      -1      20
HS00002001      V1-S02
HS00002002      18.9      1.0
HS00002003      2.0
HS00002100      -1      1      0.0
HS00002102      0.0001      2
HS00002103      0.0002519      3
HS00002104      0.001      4
HS00002105      0.003059      5
HS00002200      -1

```

HS00002201	STEEL	4		
HS00002300	0			
HS00002400	1	1	1.0	1.0
HS00002500	287.0	3.0	7.3	
HS00002600	0			
HS00002800	-1			
HS00002801	293.0	5		
*****				
*****	Structure 3			
*****				
HS00003000	6	1	-1	20
HS00003001	V1-S003			
HS00003002	18.9	1.0		
HS00003003	2.0			
HS00003100	-1	1	0.0	
HS00003102	0.0001	2		
HS00003103	0.0002519	3		
HS00003104	0.001	4		
HS00003105	0.002519	5		
HS00003106	0.01109	6		
HS00003200	-1			
HS00003201	STEEL	5		
HS00003300	0			
HS00003400	1	1	1.0	1.0
HS00003500	144.2	3.0	7.3	
HS00003600	0			
HS00003800	-1			
HS00003801	293.0	6		
*****				
*****	Structure 4			
*****				
HS00004000	6	1	-1	20
HS00004001	V1-S04			
HS00004002	18.9	1.0		
HS00004003	2.0			
HS00004100	-1	1	0.0	
HS00004102	0.0001	2		
HS00004103	0.0002519	3		
HS00004104	0.001	4		
HS00004105	0.002519	5		
HS00004106	0.010145	6		
HS00004200	-1			
HS00004201	STEEL	5		
HS00004300	0			
HS00004400	1	1	1.0	1.0
HS00004500	1.5	3.0	1.0	
HS00004600	0			
HS00004800	-1			
HS00004801	293.0	6		
*****				
*****	Structure 5			
*****				
HS00005000	16	1	-1	20
HS00005001	V1-S05			

HS00005002	18.9	1.0		
HS00005100	-1	1	0.0	
HS00005102	0.0005	2		
HS00005103	0.001	3		
HS00005104	0.001585	4		
HS00005105	0.002519	5		
HS00005106	0.003981	6		
HS00005107	0.006310	7		
HS00005108	0.01	8		
HS00005109	0.01585	9		
HS00005110	0.02519	10		
HS00005111	0.03981	11		
HS00005112	0.06310	12		
HS00005113	0.1	13		
HS00005114	0.1585	14		
HS00005115	0.2519	15		
HS00005116	0.3048	16		
HS00005200	-1			
HS00005201	CONCRETE	15		
HS00005300	0			
HS00005400	1	1	1.0	1.0
HS00005500	240.0	3.0	7.3	
HS00005600	0			
HS00005800	-1			
HS00005801	293.0	16		
*****				
*****	Structure 6			
*****				
HS00006000	16	1	-1	20
HS00006001	V1-S06			
HS00006002	26.3	0.0		
HS00006100	-1	1	0.0	
HS00006102	0.0005	2		
HS00006103	0.001	3		
HS00006104	0.001585	4		
HS00006105	0.002519	5		
HS00006106	0.003981	6		
HS00006107	0.006310	7		
HS00006108	0.01	8		
HS00006109	0.01585	9		
HS00006110	0.02519	10		
HS00006111	0.03981	11		
HS00006112	0.06310	12		
HS00006113	0.1	13		
HS00006114	0.1585	14		
HS00006115	0.2519	15		
HS00006116	0.3048	16		
HS00006200	-1			
HS00006201	CONCRETE	15		
HS00006300	0			
HS00006400	1	1	1.0	1.0
HS00006500	45.2	3.0	6.7	
HS00006600	0			
HS00006800	-1			

HS00006801	293.0	16		
*****				
*****	Structure 7			
*****				
HS00007000	16	1	-1	20
HS00007001	V1-S07			
HS00007002	18.8	0.0		
HS00007100	-1	1	0.0	
HS00007102	0.0005	2		
HS00007103	0.001	3		
HS00007104	0.001585	4		
HS00007105	0.002519	5		
HS00007106	0.003981	6		
HS00007107	0.006310	7		
HS00007108	0.01	8		
HS00007109	0.01585	9		
HS00007110	0.02519	10		
HS00007111	0.03981	11		
HS00007112	0.06310	12		
HS00007113	0.1	13		
HS00007114	0.1585	14		
HS00007115	0.2519	15		
HS00007116	0.3048	16		
HS00007200	-1			
HS00007201	CONCRETE	15		
HS00007300	0			
HS00007400	1	1	0.0	0.0
HS00007500	45.2	3.0	6.7	
HS00007600	0			
HS00007800	-1			
HS00007801	293.0	16		
*****				
*****	Structure 8			
*****				
HS00008000	4	1	-1	20
HS00008001	V2-S08			
HS00008002	24.1	1.0		
HS00008003	2.0			
HS00008100	-1	1	0.0	
HS00008102	0.0001	2		
HS00008103	0.0002519	3		
HS00008104	0.0007305	4		
HS00008200	-1			
HS00008201	STEEL	3		
HS00008300	0			
HS00008400	1	2	1.0	1.0
HS00008500	92.95	5.0	10.2	
HS00008600	0			
HS00008800	-1			
HS00008801	330.0	4		
*****				
*****	Structure 9			
*****				
HS00009000	5	1	-1	20

HS00009001	V2-S09				
HS00009002	24.1	1.0			
HS00009003	2.0				
HS00009100	-1	1	0.0		
HS00009102	0.0001	2			
HS00009103	0.0002519	3			
HS00009104	0.001	4			
HS00009105	0.003373	5			
HS00009200	-1				
HS00009201	STEEL	4			
HS00009300	0				
HS00009400	1	2	1.0	1.0	
HS00009500	63.8	5.0	10.2		
HS00009600	0				
HS00009800	-1				
HS00009801	330.0	5			
*****					
*****	Structure 10				
*****					
HS00010000	6	1	-1	20	
HS00010001	V2-S10				
HS00010002	24.1	1.0			
HS00010003	2.0				
HS00010100	-1	1	0.0		
HS00010102	0.0001	2			
HS00010103	0.0002519	3			
HS00010104	0.001	4			
HS00010105	0.002519	5			
HS00010106	0.01039	6			
HS00010200	-1				
HS00010201	STEEL	5			
HS00010300	0				
HS00010400	1	2	1.0	1.0	
HS00010500	20.9	5.0	10.2		
HS00010600	0				
HS00010800	-1				
HS00010801	330.0	6			
*****					
*****	Structure 11				
*****					
HS00011000	8	1	-1	20	
HS00011001	V2-S11				
HS00011002	24.1	1.0			
HS00011003	2.0				
HS00011100	-1	1	0.0		
HS00011102	0.0001	2			
HS00011103	0.0002519	3			
HS00011104	0.001	4			
HS00011105	0.002519	5			
HS00011106	0.01	6			
HS00011107	0.02519	7			
HS00011108	0.0598	8			
HS00011200	-1				
HS00011201	STEEL	7			

HS00011300	0			
HS00011400	1	2	1.0	1.0
HS00011500	28.32	5.0	10.2	
HS00011600	0			
HS00011800	-1			
HS00011801	330.0	8		
*****				
*****	Structure 12			
*****				
HS00012000	22	1	-1	20
HS00012001	V2-S12			
HS00012002	24.1	1.0		
HS00012100	-1	1	0.0	
HS00012102	0.0001	2		
HS00012103	0.0002519	3		
HS00012104	0.001	4		
HS00012105	0.002519	5		
HS00012106	0.01	6		
HS00012107	0.0254	7		
HS00012108	0.0259	8		
HS00012109	0.0264	9		
HS00012110	0.026985	10		
HS00012111	0.027919	11		
HS00012112	0.029381	12		
HS00012113	0.03171	13		
HS00012114	0.0354	14		
HS00012115	0.04125	15		
HS00012116	0.05059	16		
HS00012117	0.06521	17		
HS00012118	0.0885	18		
HS00012119	0.1254	19		
HS00012120	0.1839	20		
HS00012121	0.2773	21		
HS00012122	0.3302	22		
HS00012200	-1			
HS00012201	STEEL	6		
HS00012202	CONCRETE	21		
HS00012300	0			
HS00012400	1	2	1.0	1.0
HS00012500	46.12	5.0	10.2	
HS00012600	0			
HS00012800	-1			
HS00012801	293.0	22		
*****				
*****	Structure 13			
*****				
HS00013000	16	1	-1	20
HS00013001	V2-S13			
HS00013002	24.1	1.0		
HS00013100	-1	1	0.0	
HS00013102	0.0005	2		
HS00013103	0.001	3		
HS00013104	0.001585	4		
HS00013105	0.002519	5		

HS00013106	0.003981	6		
HS00013107	0.006310	7		
HS00013108	0.01	8		
HS00013109	0.01585	9		
HS00013110	0.02519	10		
HS00013111	0.03981	11		
HS00013112	0.06310	12		
HS00013113	0.1	13		
HS00013114	0.1585	14		
HS00013115	0.2519	15		
HS00013116	0.3048	16		
HS00013200	-1			
HS00013201	CONCRETE	15		
HS00013300	0			
HS00013400	1	2	1.0	1.0
HS00013500	28.7	5.0	10.2	
HS00013600	0			
HS00013800	-1			
HS00013801	293.0	16		
*****				
*****	Structure 14			
*****				
HS00014000	16	1	-1	20
HS00014001	V2-S14			
HS00014002	34.4	0.0		
HS00014100	-1	1		0.0
HS00014102	0.0005	2		
HS00014103	0.001	3		
HS00014104	0.001585	4		
HS00014105	0.002519	5		
HS00014106	0.003981	6		
HS00014107	0.006310	7		
HS00014108	0.01	8		
HS00014109	0.01585	9		
HS00014110	0.02519	10		
HS00014111	0.03981	11		
HS00014112	0.06310	12		
HS00014113	0.1	13		
HS00014114	0.1585	14		
HS00014115	0.2519	15		
HS00014116	0.3048	16		
HS00014200	-1			
HS00014201	CONCRETE	15		
HS00014300	0			
HS00014400	1	2	1.0	1.0
HS00014500	35.94	5.0	6.0	
HS00014600	0			
HS00014800	-1			
HS00014801	293.0	16		
*****				
*****	Structure 15			
*****				
HS00015000	16	1	-1	20
HS00015001	V2-S15			

HS00015002	24.0	0.0		
HS00015100	-1	1	0.0	
HS00015102	0.0005	2		
HS00015103	0.001	3		
HS00015104	0.001585	4		
HS00015105	0.002519	5		
HS00015106	0.003981	6		
HS00015107	0.006310	7		
HS00015108	0.01	8		
HS00015109	0.01585	9		
HS00015110	0.02519	10		
HS00015111	0.03981	11		
HS00015112	0.06310	12		
HS00015113	0.1	13		
HS00015114	0.1585	14		
HS00015115	0.2519	15		
HS00015116	0.3048	16		
HS00015200	-1			
HS00015201	CONCRETE	15		
HS00015300	0			
HS00015400	1	2	0.0	0.0
HS00015500	35.9	5.0	6.0	
HS00015600	0			
HS00015800	-1			
HS00015801	293.0	16		
*****				
*****	Structure 16			
*****				
HS00016000	4	1	-1	20
HS00016001	V3-S16			
HS00016002	27.7	1.0		
HS00016003	2.0			
HS00016100	-1	1	0.0	
HS00016102	0.0001	2		
HS00016103	0.0002519	3		
HS00016104	0.0005845	4		
HS00016200	-1			
HS00016201	STEEL	3		
HS00016300	0			
HS00016400	1	3	1.0	1.0
HS00016500	1028.0	3.0	8.1	
HS00016600	0			
HS00016800	-1			
HS00016801	293.0	4		
*****				
*****	Structure 17			
*****				
HS00017000	5	1	-1	20
HS00017001	V3-S17			
HS00017002	27.7	1.0		
HS00017003	2.0			
HS00017100	-1	1	0.0	
HS00017102	0.0001	2		
HS00017103	0.0002519	3		



HS00017104	0.001	4		
HS00017105	0.002886	5		
HS00017200	-1			
HS00017201	STEEL	4		
HS00017300	0			
HS00017400	1	3	1.0	1.0
HS00017500	87.52	3.0	8.1	
HS00017600	0			
HS00017800	-1			
HS00017801	293.0	5		
*****				
*****	Structure 18			
*****				
HS00018000	6	1	-1	20
HS00018001	V3-S18			
HS00018002	27.7	1.0		
HS00018003	2.0			
HS00018100	-1	1		0.0
HS00018102	0.0001	2		
HS00018103	0.0002519	3		
HS00018104	0.001	4		
HS00018105	0.002519	5		
HS00018106	0.00999	6		
HS00018200	-1			
HS00018201	STEEL	5		
HS00018300	0			
HS00018400	1	3	1.0	1.0
HS00018500	28.43	3.0	8.1	
HS00018600	0			
HS00018800	-1			
HS00018801	293.0	6		
*****				
*****	Structure 19			
*****				
HS00019000	7	1	-1	20
HS00019001	V3-S19			
HS00019002	27.7	1.0		
HS00019003	2.0			
HS00019100	-1	1		0.0
HS00019102	0.0001	2		
HS00019103	0.0002519	3		
HS00019104	0.001	4		
HS00019105	0.002519	5		
HS00019106	0.01	6		
HS00019107	0.024885	7		
HS00019200	-1			
HS00019201	STEEL	6		
HS00019300	0			
HS00019400	1	3	1.0	1.0
HS00019500	12.37	3.0	8.1	
HS00019600	0			
HS00019800	-1			
HS00019801	293.0	7		
*****				

```

*****      Structure 20
*****
HS00020000      16      1      -1      20
HS00020001      V3-S20
HS00020002      27.7      1.0
HS00020100      -1      1      0.0
HS00020102      0.0005      2
HS00020103      0.001      3
HS00020104      0.001585      4
HS00020105      0.002519      5
HS00020106      0.003981      6
HS00020107      0.006310      7
HS00020108      0.01      8
HS00020109      0.01585      9
HS00020110      0.02519      10
HS00020111      0.03981      11
HS00020112      0.06310      12
HS00020113      0.1      13
HS00020114      0.1585      14
HS00020115      0.2519      15
HS00020116      0.3048      16
HS00020200      -1
HS00020201      CONCRETE      15
HS00020300      0
HS00020400      1      3      1.0      1.0
HS00020500      730.5      3.0      8.1
HS00020600      0
HS00020800      -1
HS00020801      293.0      16
*****
*****      Structure 21
*****
HS00021000      8      1      -1      20
HS00021001      V3-S21
HS00021002      27.7      1.0
HS00021100      -1      1      0.0
HS00021102      0.0001      2
HS00021103      0.0002519      3
HS00021104      0.001      4
HS00021105      0.002519      5
HS00021106      0.01      6
HS00021107      0.02519      7
HS00021108      0.06      8
HS00021200      -1
HS00021201      STEEL      7
HS00021300      0
HS00021400      1      3      1.0      1.0
HS00021500      6.2      3.0      4.0
HS00021600      0
HS00021800      -1
HS00021801      293.0      8
*****
*****      Structure 22
*****

```

HS00022000	22	1	-1	20
HS00022001	V3-S22			
HS00022002	27.7	1.0		
HS00022100	-1	1	0.0	
HS00022102	0.0001	2		
HS00022103	0.0002519	3		
HS00022104	0.001	4		
HS00022105	0.002519	5		
HS00022106	0.01	6		
HS00022107	0.0254	7		
HS00022108	0.0259	8		
HS00022109	0.0264	9		
HS00022110	0.026985	10		
HS00022111	0.027919	11		
HS00022112	0.029381	12		
HS00022113	0.03171	13		
HS00022114	0.0354	14		
HS00022115	0.04125	15		
HS00022116	0.05059	16		
HS00022117	0.06521	17		
HS00022118	0.0885	18		
HS00022119	0.1254	19		
HS00022120	0.1839	20		
HS00022121	0.2773	21		
HS00022122	0.3302	22		
HS00022200	-1			
HS00022201	STEEL	6		
HS00022202	CONCRETE	21		
HS00022300	0			
HS00022400	1	3	1.0	1.0
HS00022500	30.17	3.0	8.1	
HS00022600	0			
HS00022800	-1			
HS00022801	293.0	22		
*****				
*****	Structure 23			
*****				
HS00023000	16	1	-1	20
HS00023001	V3-S23			
HS00023002	35.9	0.0		
HS00023100	-1	1	0.0	
HS00023102	0.0005	2		
HS00023103	0.001	3		
HS00023104	0.001585	4		
HS00023105	0.002519	5		
HS00023106	0.003981	6		
HS00023107	0.006310	7		
HS00023108	0.01	8		
HS00023109	0.01585	9		
HS00023110	0.02519	10		
HS00023111	0.03981	11		
HS00023112	0.06310	12		
HS00023113	0.1	13		
HS00023114	0.1585	14		

HS00023115	0.2519	15		
HS00023116	0.3048	16		
HS00023200	-1			
HS00023201	CONCRETE	15		
HS00023300	0			
HS00023400	1	3	1.0	1.0
HS00023500	106.3	3.0	10.0	
HS00023600	0			
HS00023800	-1			
HS00023801	293.0	16		
*****				
*****	Structure 24			
*****				
HS00024000	16	1	-1	20
HS00024001	V3-S24			
HS00024002	27.6	0.0		
HS00024100	-1	1	0.0	
HS00024102	0.0005	2		
HS00024103	0.001	3		
HS00024104	0.001585	4		
HS00024105	0.002519	5		
HS00024106	0.003981	6		
HS00024107	0.006310	7		
HS00024108	0.01	8		
HS00024109	0.01585	9		
HS00024110	0.02519	10		
HS00024111	0.03981	11		
HS00024112	0.06310	12		
HS00024113	0.1	13		
HS00024114	0.1585	14		
HS00024115	0.2519	15		
HS00024116	0.3048	16		
HS00024200	-1			
HS00024201	CONCRETE	15		
HS00024300	0			
HS00024400	1	3	0.0	0.0
HS00024500	106.3	3.0	10.0	
HS00024600	0			
HS00024800	-1			
HS00024801	293.0	16		
*****				
*****	Structure 25			
*****				
HS00025000	4	1	-1	20
HS00025001	V4-S25			
HS00025002	4.1	1.0		
HS00025003	2.0			
HS00025100	-1	1	0.0	
HS00025102	0.0001	2		
HS00025103	0.0002519	3		
HS00025104	0.0004791	4		
HS00025200	-1			
HS00025201	STEEL	3		
HS00025300	0			

HS00025400	1	4	1.0	1.0
HS00025500	3253.0	5.0	8.1	
HS00025600	0			
HS00025800	-1			
HS00025801	293.0	4		
*****				
*****	Structure 26			
*****				
HS00026000	5	1	-1	20
HS00026001	V4-S26			
HS00026002	4.1	1.0		
HS00026003	2.0			
HS00026100	-1	1		0.0
HS00026102	0.0001	2		
HS00026103	0.0002519	3		
HS00026104	0.001	4		
HS00026105	0.003138	5		
HS00026200	-1			
HS00026201	STEEL	4		
HS00026300	0			
HS00026400	1	4	1.0	1.0
HS00026500	1967.0	5.0	8.1	
HS00026600	0			
HS00026800	-1			
HS00026801	293.0	5		

\*\*\*\*\*

\*\*\*\*\* Structure 27

\*\*\*\*\*

HS00027000	6	1	-1	20
HS00027001	V4-S27			
HS00027002	4.1	1.0		
HS00027003	2.0			
HS00027100	-1	1		0.0
HS00027102	0.0001	2		
HS00027103	0.0002519	3		
HS00027104	0.001	4		
HS00027105	0.002519	5		
HS00027106	0.011145	6		
HS00027200	-1			
HS00027201	STEEL	5		
HS00027300	0			
HS00027400	1	4	1.0	1.0
HS00027500	40.62	5.0	8.1	
HS00027600	0			
HS00027800	-1			
HS00027801	293.0	6		

\*\*\*\*\*

\*\*\*\*\* Structure 28

\*\*\*\*\*

HS00028000	6	1	-1	20
HS00028001	V4-S28			
HS00028002	4.1	1.0		
HS00028003	2.0			
HS00028100	-1	1		0.0

HS00028102	0.0001	2			
HS00028103	0.0002519	3			
HS00028104	0.001	4			
HS00028105	0.002519	5			
HS00028106	0.01814	6			
HS00028200	-1				
HS00028201	STEEL	5			
HS00028300	0				
HS00028400	1	4		1.0	1.0
HS00028500	11.32	5.0		6.0	
HS00028600	0				
HS00028800	-1				
HS00028801	293.0	6			
*****					
***** Structure 29					
*****					
HS00029000	16	1	-1	20	
HS00029001	V4-S29				
HS00029002	4.1	1.0			
HS00029100	-1	1		0.0	
HS00029102	0.0005	2			
HS00029103	0.001	3			
HS00029104	0.001585	4			
HS00029105	0.002519	5			
HS00029106	0.003981	6			
HS00029107	0.006310	7			
HS00029108	0.01	8			
HS00029109	0.01585	9			
HS00029110	0.02519	10			
HS00029111	0.03981	11			
HS00029112	0.06310	12			
HS00029113	0.1	13			
HS00029114	0.1585	14			
HS00029115	0.2519	15			
HS00029116	0.3048	16			
HS00029200	-1				
HS00029201	CONCRETE	15			
HS00029300	0				
HS00029400	1	4		1.0	1.0
HS00029500	3370.4	5.0		8.1	
HS00029600	0				
HS00029800	-1				
HS00029801	293.0	16			
*****					
***** Structure 30					
*****					
HS00030000	7	1	-1	20	
HS00030001	V4-S30				
HS00030002	4.1	1.0			
HS00030100	-1	1		0.0	
HS00030102	0.0001	2			
HS00030103	0.0002519	3			
HS00030104	0.001	4			
HS00030105	0.002519	5			

HS00030106	0.01	6			
HS00030107	0.030	7			
HS00030200	-1				
HS00030201	STEEL	6			
HS00030300	0				
HS00030400	1	4	1.0	1.0	
HS00030500	199.6	5.0	8.1		
HS00030600	0				
HS00030800	-1				
HS00030801	293.0	7			
*****					
*****	Structure 31				
*****					
HS00031000	16	1	-1	20	
HS00031001	V4-S31				
HS00031002	18.0	0.0			
HS00031100	-1	1		0.0	
HS00031102	0.0005	2			
HS00031103	0.001	3			
HS00031104	0.001585	4			
HS00031105	0.002519	5			
HS00031106	0.003981	6			
HS00031107	0.006310	7			
HS00031108	0.01	8			
HS00031109	0.01585	9			
HS00031110	0.02519	10			
HS00031111	0.03981	11			
HS00031112	0.06310	12			
HS00031113	0.1	13			
HS00031114	0.1585	14			
HS00031115	0.2519	15			
HS00031116	0.3048	16			
HS00031200	-1				
HS00031201	CONCRETE	15			
HS00031300	0				
HS00031400	1	4	1.0	1.0	
HS00031500	624.8	5.0	25.0		
HS00031600	0				
HS00031800	-1				
HS00031801	293.0	16			
*****					
*****	Structure 32				
*****					
HS00032000	16	1	-1	20	
HS00032001	V4-S32				
HS00032002	4.0	0.0			
HS00032100	-1	1		0.0	
HS00032102	0.0005	2			
HS00032103	0.001	3			
HS00032104	0.001585	4			
HS00032105	0.002519	5			
HS00032106	0.003981	6			
HS00032107	0.006310	7			
HS00032108	0.01	8			

HS00032109	0.01585	9			
HS00032110	0.02519	10			
HS00032111	0.03981	11			
HS00032112	0.06310	12			
HS00032113	0.1	13			
HS00032114	0.1585	14			
HS00032115	0.2519	15			
HS00032116	0.3048	16			
HS00032200	-1				
HS00032201	CONCRETE	15			
HS00032300	0				
HS00032400	1	4		0.0	0.0
HS00032500	624.8	5.0		25.0	
HS00032600	0				
HS00032800	-1				
HS00032801	293.0	16			

\*\*\*\*\*

\*\*\*\*\* Structure 33

\*\*\*\*\*

HS00033000	4	1	-1	20	
HS00033001	V5-S33				
HS00033002	35.5	1.0			
HS00033003	2.0				
HS00033100	-1	1		0.0	
HS00033102	0.0001	2			
HS00033103	0.0002519	3			
HS00033104	0.0004954	4			
HS00033200	-1				
HS00033201	STEEL	3			
HS00033300	0				
HS00033400	1	5		1.0	1.0
HS00033500	3197.0	10.0		28.0	
HS00033600	0				
HS00033800	-1				
HS00033801	293.0	4			

\*\*\*\*\*

\*\*\*\*\* Structure 34

\*\*\*\*\*

HS00034000	5	1	-1	20	
HS00034001	V5-S34				
HS00034002	35.5	1.0			
HS00034003	2.0				
HS00034100	-1	1		0.0	
HS00034102	0.0001	2			
HS00034103	0.0002519	3			
HS00034104	0.001	4			
HS00034105	0.0029615	5			
HS00034200	-1				
HS00034201	STEEL	4			
HS00034300	0				
HS00034400	1	5		1.0	1.0
HS00034500	3667.0	10.0		28.0	
HS00034600	0				
HS00034800	-1				



HS00034801	293.0	5			
*****					
*****	Structure 35				
*****					
HS00035000	6	1	-1	20	
HS00035001	V5-S35				
HS00035002	35.5	1.0			
HS00035003	2.0				
HS00035100	-1	1		0.0	
HS00035102	0.0001	2			
HS00035103	0.0002519	3			
HS00035104	0.001	4			
HS00035105	0.002519	5			
HS00035106	0.00701	6			
HS00035200	-1				
HS00035201	STEEL	5			
HS00035300	0				
HS00035400	1	5		1.0	1.0
HS00035500	404.6	10.0		28.0	
HS00035600	0				
HS00035800	-1				
HS00035801	293.0	6			
*****					
*****	Structure 36				
*****					
HS00036000	7	1	-1	20	
HS00036001	V5-S36				
HS00036002	35.5	1.0			
HS00036003	2.0				
HS00036100	-1	1		0.0	
HS00036102	0.0001	2			
HS00036103	0.0002519	3			
HS00036104	0.001	4			
HS00036105	0.002519	5			
HS00036106	0.01	6			
HS00036107	0.02598	7			
HS00036200	-1				
HS00036201	STEEL	6			
HS00036300	0				
HS00036400	1	5		1.0	1.0
HS00036500	190.3	10.0		28.0	
HS00036600	0				
HS00036800	-1				
HS00036801	293.0	7			
*****					
*****	Structure 37				
*****					
HS00037000	16	1	-1	20	
HS00037001	V5-S37				
HS00037002	35.5	1.0			
HS00037100	-1	1		0.0	
HS00037102	0.0005	2			
HS00037103	0.001	3			
HS00037104	0.001585	4			

HS00037105	0.002519	5			
HS00037106	0.003981	6			
HS00037107	0.006310	7			
HS00037108	0.01	8			
HS00037109	0.01585	9			
HS00037110	0.02519	10			
HS00037111	0.03981	11			
HS00037112	0.06310	12			
HS00037113	0.1	13			
HS00037114	0.1585	14			
HS00037115	0.2519	15			
HS00037116	0.3048	16			
HS00037200	-1				
HS00037201	CONCRETE	15			
HS00037300	0				
HS00037400	1	5		1.0	1.0
HS00037500	1896.5	10.0		28.0	
HS00037600	0				
HS00037800	-1				
HS00037801	293.0	16			
*****					
*****	Structure 38				
*****					
HS00038000	7	1	-1	20	
HS00038001	V5-S38				
HS00038002	35.5	1.0			
HS00038100	-1	1		0.0	
HS00038102	0.0001	2			
HS00038103	0.0002519	3			
HS00038104	0.001	4			
HS00038105	0.002519	5			
HS00038106	0.01	6			
HS00038107	0.027	7			
HS00038200	-1				
HS00038201	STEEL	6			
HS00038300	0				
HS00038400	1	5		1.0	1.0
HS00038500	1605.25	10.0		28.0	
HS00038600	0				
HS00038800	-1				
HS00038801	293.0	7			
*****					
*****	Structure 39				
*****					
HS00039000	22	1	-1	20	
HS00039001	V5-S39				
HS00039002	35.5	1.0			
HS00039100	-1	1		0.0	
HS00039102	0.0001	2			
HS00039103	0.0002519	3			
HS00039104	0.001	4			
HS00039105	0.002519	5			
HS00039106	0.01	6			
HS00039107	0.0254	7			

HS00039108	0.0259	8		
HS00039109	0.0264	9		
HS00039110	0.026985	10		
HS00039111	0.027919	11		
HS00039112	0.029381	12		
HS00039113	0.03171	13		
HS00039114	0.0354	14		
HS00039115	0.04125	15		
HS00039116	0.05059	16		
HS00039117	0.06521	17		
HS00039118	0.0885	18		
HS00039119	0.1254	19		
HS00039120	0.1839	20		
HS00039121	0.2773	21		
HS00039122	0.3302	22		
HS00039200	-1			
HS00039201	STEEL	6		
HS00039202	CONCRETE	21		
HS00039300	0			
HS00039400	1	5	1.0	1.0
HS00039500	599.86	10.0	28.0	
HS00039600	0			
HS00039800	-1			
HS00039801	293.0	22		
*****				
*****	Structure 40			
*****				
HS00040000	16	1	-1	20
HS00040001	V5-S40			
HS00040002	63.5	0.0		
HS00040100	-1	1	0.0	
HS00040102	0.0005	2		
HS00040103	0.001	3		
HS00040104	0.001585	4		
HS00040105	0.002519	5		
HS00040106	0.003981	6		
HS00040107	0.006310	7		
HS00040108	0.01	8		
HS00040109	0.01585	9		
HS00040110	0.02519	10		
HS00040111	0.03981	11		
HS00040112	0.06310	12		
HS00040113	0.1	13		
HS00040114	0.1585	14		
HS00040115	0.2519	15		
HS00040116	0.3048	16		
HS00040200	-1			
HS00040201	CONCRETE	15		
HS00040300	0			
HS00040400	1	5	1.0	1.0
HS00040500	595.9	10.0	24.0	
HS00040600	0			
HS00040800	-1			
HS00040801	293.0	16		

```

*****
*****      Structure 41
*****
HS00041000      16      1      -1      20
HS00041001      V5-S41
HS00041002      35.4      0.0
HS00041100      -1      1      0.0
HS00041102      0.0005      2
HS00041103      0.001      3
HS00041104      0.001585      4
HS00041105      0.002519      5
HS00041106      0.003981      6
HS00041107      0.006310      7
HS00041108      0.01      8
HS00041109      0.01585      9
HS00041110      0.02519      10
HS00041111      0.03981      11
HS00041112      0.06310      12
HS00041113      0.1      13
HS00041114      0.1585      14
HS00041115      0.2519      15
HS00041116      0.3048      16
HS00041200      -1
HS00041201      CONCRETE      15
HS00041300      0
HS00041400      1      5      0.0      0.0
HS00041500      595.9      10.0      24.0
HS00041600      0
HS00041800      -1
HS00041801      293.0      16
*****
*****
*****      MATERIAL PROPERTIES
*****
*****
*****      Steel
*****
MPMAT00100      STEEL
MPMAT00101      RHO      3
MPMAT00102      CPS      4
MPMAT00103      THC      5
*****
*****      Concrete
*****
MPMAT00200      CONCRETE
MPMAT00201      RHO      6
MPMAT00202      CPS      7
MPMAT00203      THC      8
*****
*****
*****      TABULAR INPUT
*****
*****      H2O External Source
*****
*****      H2O Mass Addition Rate (kg/s)

```

```

*****
TF00100    MASS          90      1.0    0.0
TF001A0      0.0          0.0
TF001A1      0.02        1391.0
TF001A2      0.04        1245.0
TF001A3      0.06        1307.0
TF001A4      0.08        1422.0
TF001A5      0.10        1405.0
TF001A6      0.12        1362.0
TF001A7      0.14        1283.0
TF001A8      0.16        1277.0
TF001A9      0.18        1315.0
TF001B0      0.20        1335.0
TF001B1      0.22        1248.0
TF001B2      0.24        1230.0
TF001B3      0.26        1230.0
TF001B4      0.28        1268.0
TF001B5      0.30        1306.0
TF001B6      0.40        1497.0
TF001B7      0.50        1688.0
TF001B8      0.60        1879.0
TF001B9      0.70        2038.0
TF001C0      0.80        2152.0
TF001C1      0.90        2227.0
TF001C2      1.0         2282.1
TF001C3      1.1         2324.0
TF001C4      1.2         2352.0
TF001C5      1.3         2375.0
TF001C6      1.4         2388.0
TF001C7      1.5         2401.2
TF001C8      1.6         2406.0
TF001C9      1.7         2469.0
TF001D0      1.8         2404.0
TF001D1      1.9         2400.0
TF001D2      2.0         2395.2
TF001D3      2.5         2344.4
TF001D4      3.0         2283.1
TF001D5      3.5         2216.1
TF001D6      4.0         2148.6
TF001D7      4.5         2081.8
TF001D8      5.0         2016.5
TF001D9      5.5         1950.7
TF001E0      6.0         1883.3
TF001E1      6.5         1817.3
TF001E2      7.0         1750.8
TF001E3      7.5         1684.2
TF001E4      8.0         1622.7
TF001E5      8.5         1511.9
TF001E6      9.0         1460.0
TF001E7      9.5         1413.4
TF001E8     10.0         1365.0
TF001E9     11.0         1262.9
TF001F0     12.0         1159.0
TF001F1     13.0         1055.7

```

TF001F2	14.0	957.62
TF001F3	15.0	864.28
TF001F4	16.0	774.33
TF001F5	17.0	691.92
TF001F6	18.0	617.09
TF001F7	19.0	547.40
TF001F8	20.0	479.19
TF001F9	21.0	416.62
TF001G0	22.0	363.80
TF001G1	23.0	319.37
TF001G2	24.0	287.92
TF001G3	25.0	259.30
TF001G4	26.0	236.02
TF001G5	27.0	215.81
TF001G6	28.0	196.81
TF001G7	29.0	179.10
TF001G8	30.0	166.96
TF001G9	31.0	157.05
TF001H0	32.0	147.75
TF001H1	33.0	138.84
TF001H2	34.0	130.49
TF001H3	35.0	118.43
TF001H4	36.0	103.46
TF001H5	37.0	91.452
TF001H6	38.0	82.058
TF001H7	39.0	74.413
TF001H8	40.0	67.821
TF001H9	41.0	62.054
TF001I0	42.0	57.036
TF001I1	43.0	52.618
TF001I2	44.0	48.630
TF001I3	45.0	45.052
TF001I4	46.0	41.756
TF001I5	47.0	38.707
TF001I6	48.0	35.865
TF001I7	50.0	30.733
TF001I8	70.0	0.0
TF001I9	10000.0	0.0

\*\*\*\*\*

\*\*\*\*\*

\*\*\*\*\*

\*\*\*\*\* H2O Energy Addition Rate (j/s)

\*\*\*\*\*

TF00200	ENERGY	90	1.0	0.0
TF002A0	0.00	0.000E0		
TF002A1	0.02	3.765E9		
TF002A2	0.04	3.370E9		
TF002A3	0.06	3.538E9		
TF002A4	0.08	3.849E9		
TF002A5	0.10	3.803E9		
TF002A6	0.12	3.687E9		
TF002A7	0.14	3.473E9		
TF002A8	0.16	3.457E9		
TF002A9	0.18	3.560E9		

TF002B0	0.20	3.614E9
TF002B1	0.22	3.378E9
TF002B2	0.24	3.330E9
TF002B3	0.26	3.330E9
TF002B4	0.28	3.346E9
TF002B5	0.30	3.358E9
TF002B6	0.4	3.341E9
TF002B7	0.5	3.197E9
TF002B8	0.6	2.922E9
TF002B9	0.7	3.094E9
TF002C0	0.8	3.219E9
TF002C1	0.9	3.300E9
TF002C2	1.0	3.360E9
TF002C3	1.1	3.405E9
TF002C4	1.2	3.436E9
TF002C5	1.3	3.460E9
TF002C6	1.4	3.472E9
TF002C7	1.5	3.486E9
TF002C8	1.6	3.489E9
TF002C9	1.7	3.578E9
TF002D0	1.8	3.481E9
TF002D1	1.9	3.473E9
TF002D2	2.0	3.465E9
TF002D3	2.5	3.392E9
TF002D4	3.0	3.308E9
TF002D5	3.5	3.218E9
TF002D6	4.0	3.128E9
TF002D7	4.5	3.041E9
TF002D8	5.0	2.958E9
TF002D9	5.5	2.874E9
TF002E0	6.0	2.787E9
TF002E1	6.5	2.705E9
TF002E2	7.0	2.622E9
TF002E3	7.5	2.537E9
TF002E4	8.0	2.462E9
TF002E5	8.5	2.345E9
TF002E6	9.0	2.270E9
TF002E7	9.5	2.204E9
TF002E8	10.0	2.136E9
TF002E9	11.0	2.001E9
TF002F0	12.0	1.864E9
TF002F1	13.0	1.728E9
TF002F2	14.0	1.598E9
TF002F3	15.0	1.472E9
TF002F4	16.0	1.350E9
TF002F5	17.0	1.235E9
TF002F6	18.0	1.130E9
TF002F7	19.0	1.031E9
TF002F8	20.0	9.344E8
TF002F9	21.0	8.450E8
TF002G0	22.0	7.677E8
TF002G1	23.0	7.024E8
TF002G2	24.0	6.526E8
TF002G3	25.0	6.067E8

TF002G4	26.0	5.675E8
TF002G5	27.0	5.316E8
TF002G6	28.0	4.973E8
TF002G7	29.0	4.651E8
TF002G8	30.0	4.393E8
TF002G9	31.0	4.160E8
TF002H0	32.0	3.939E8
TF002H1	33.0	3.725E8
TF002H2	34.0	3.524E8
TF002H3	35.0	3.208E8
TF002H4	36.0	2.804E8
TF002H5	37.0	2.479E8
TF002H6	38.0	2.224E8
TF002H7	39.0	2.016E8
TF002H8	40.0	1.837E8
TF002H9	41.0	1.681E8
TF002I0	42.0	1.545E8
TF002I1	43.0	1.426E8
TF002I2	44.0	1.318E8
TF002I3	45.0	1.222E8
TF002I4	46.0	1.133E8
TF002I5	47.0	1.050E8
TF002I6	48.0	9.735E7
TF002I7	50.0	8.348E7
TF002I8	70.0	0.000E0
TF002I9	10000.0	0.000E0

\*\*\*\*\*

\*\*\*\*\*

\*\*\*\*\* Density of Steel

\*\*\*\*\*

TF00300	RHO-STEEL	2	1.0	0.0
TF00311	200.0	7850.0		
TF00312	5000.0	7850.0		

\*\*\*\*\*

\*\*\*\*\*

\*\*\*\*\* Specific Heat of Steel

\*\*\*\*\*

TF00400	CPS-STEEL	2	1.0	0.0
TF00411	200.0	500.0		
TF00412	5000.0	500.0		

\*\*\*\*\*

\*\*\*\*\*

\*\*\*\*\* Thermal Conductivity of Steel

\*\*\*\*\*

TF00500	THC-STEEL	2	1.0	0.0
TF00511	200.0	47.0		
TF00512	5000.0	47.0		

\*\*\*\*\*

\*\*\*\*\*

\*\*\*\*\* Density of Concrete

\*\*\*\*\*

TF00600	RHO-CONCRETE	2	1.0	0.0
TF00611	200.0	2320.0		
TF00612	5000.0	2320.0		



```

*****
*****
*****      Specific Heat of Concrete
*****
TF00700      CPS-CONCRETE      2      1.0      0.0
TF00711      200.0      650.0
TF00712      5000.0      650.0
*****
*****
*****      Thermal Conductivity of Concrete
*****
TF00800      THC-CONCRETE      2      1.0      0.0
TF00811      200.0      1.6
TF00812      5000.0      1.6
*****
*****

```

ST007: HDR Steam Blowdown Test

MELCOR Input

```

*****
*****
*****      This is a MELCOR test calculation for the HDR containment
*****      experiment V44.
*****
*****
*****
CPULEFT      20.0
CPULIM      20000.0
TEND      3600.0
RESTART      0
DTTIME      0.01
TIME1      0.0      0.01      0.001      0.5      0.1      50.0
TIME2      1.0      0.1      0.01      5.0      1.0      50.0
TIME3      20.0      1.0      0.1      50.0      2.0      50.0
TIME4      100.0      1.0      0.1      500.0      20.0      500.0
TITLE      ST007
*****

```

ST007: HDR Steam Blowdown Test

MELPLT Input

```

*
FILE1 MELPTF.DAT
*
TITLE, .

```

```

YLABEL, Temperature (K)
AYLABEL, Temperature (F)
AYSCALE 1.8 -459.67
XLABEL, Time (Sec)
FONTS2
XLIMITS 0.0 1500.0
TEXTSIZE 1.2
TEXTPOSITION 0.29 0.109
TEXT Figure 10: Containment Dome Temperature
POSLEGEND 0.20 0.35
LEGEND, MELCOR
PLOT CVH-TVAP.5
*
LEGEND, CT404 (40M)
DATA2 CT404
0 0
TEMPERATURE
TIME
    0.00 300.75
    2.96 304.58
    5.88 313.17
    7.42 326.05
    9.43 338.17
   11.43 351.51
   15.13 361.93
   18.67 367.15
   23.75 372.67
   29.61 371.90
   34.69 372.82
   38.24 371.59
   42.86 371.13
   48.56 369.75
   53.03 369.75
   59.03 368.99
   65.66 370.21
   69.51 368.68
   72.59 368.22
   81.22 367.61
   85.22 367.30
   90.31 369.60
   98.47 369.45
  100.48 367.91
  108.64 367.76
  111.42 368.83
  117.42 367.76
  123.89 367.76
  130.21 368.07
  136.06 368.07
  144.08 366.84
  151.47 366.84
  159.17 366.53
  166.72 365.15
  174.27 365.15
  182.28 364.69

```

190.45	364.54
279.83	358.90
376.89	355.83
460.08	353.83
612.61	350.60
765.13	347.22
959.24	345.53
1264.28	342.30
1541.60	339.85
1860.50	337.85
2234.87	334.62
2678.57	332.32
2969.75	330.32
3288.65	329.55
3468.91	329.09

-12345 -12345

\*

LEGEND,CT410 (34M)

DATA0 CT410

0 0

TEMPERATURE

TIME

0.00	299.47
3.86	302.99
5.86	309.26
8.33	320.12
12.64	338.94
14.18	348.73
16.80	354.70
19.57	356.69
23.72	358.53
28.03	361.59
32.65	361.59
38.81	362.35
44.97	361.74
51.74	361.89
58.52	362.66
66.37	362.51
77.30	360.98
87.00	360.82
95.47	359.60
109.48	359.14
118.40	360.52
128.57	359.45
139.50	359.75
148.43	360.36
157.82	360.21
168.75	359.75
176.29	359.75
186.76	359.14
193.38	358.83
239.66	353.96
309.04	352.58
364.54	349.97

489.42	348.13
558.80	346.14
669.80	344.61
766.93	343.07
877.93	341.08
1058.30	339.09
1224.81	337.55
1377.44	336.17
1516.19	334.79
1654.94	333.72
1835.32	332.95
1974.07	331.73
2140.57	330.96
2320.95	329.73
2598.46	328.81
2875.96	328.05
3056.34	327.28
3208.97	326.51
3375.47	326.05
3486.47	325.90

-12345 -12345

\*

LEGEND, CONTAIN

DATA1 CONTAIN

0 0

TEMPERATURE

TIME

2.26	358.29
6.77	372.53
9.03	380.23
15.80	386.77
15.80	390.27
20.31	392.14
38.36	390.97
49.65	388.40
58.67	384.90
72.21	381.40
97.04	379.06
126.38	375.80
155.71	372.53
178.28	370.43
194.08	367.39
234.70	364.82
273.06	362.02
313.68	359.92
365.59	357.35
419.75	355.25
491.96	353.38
564.18	351.05
645.42	348.95
719.89	347.31
801.13	345.45
873.34	344.04
925.25	342.88

1001.97	341.01
1083.22	340.08
1168.97	339.61
1243.44	338.44
1329.20	337.97
1414.95	337.51
1457.83	336.81
1500.71	336.34
-12345	-12345

\*

FILE1 MELPTF.DAT

\*

TITLE, .

YLABEL, Temperature (K)

AYLABEL, Temperature (F)

AYSCALE 1.8 -459.67

XLABEL, Time (Sec)

FONTS2

XLIMITS 0.0 1500.0

TEXTSIZE 1.2

TEXTPOSITION 0.29 0.109

TEXT Figure 10: Containment Dome Temperature

POSLEGEND 0.20 0.35

LEGEND, MELCOR

PLOT CVH-TVAP.5

\*

LEGEND, CT404 (40M)

DATA2 CT404

0 0

TEMPERATURE

TIME

0.00	300.75
2.96	304.58
5.88	313.17
7.42	326.05
9.43	338.17
11.43	351.51
15.13	361.93
18.67	367.15
23.75	372.67
29.61	371.90
34.69	372.82
38.24	371.59
42.86	371.13
48.56	369.75
53.03	369.75
59.03	368.99
65.66	370.21
69.51	368.68
72.59	368.22
81.22	367.61
85.22	367.30
90.31	369.60

98.47	369.45
100.48	367.91
108.64	367.76
111.42	368.83
117.42	367.76
123.89	367.76
130.21	368.07
136.06	368.07
144.08	366.84
151.47	366.84
159.17	366.53
166.72	365.15
174.27	365.15
182.28	364.69
190.45	364.54
279.83	358.90
376.89	355.83
460.08	353.83
612.61	350.60
765.13	347.22
959.24	345.53
1264.28	342.30
1541.60	339.85
1860.50	337.85
2234.87	334.62
2678.57	332.32
2969.75	330.32
3288.65	329.55
3468.91	329.09

-12345 -12345

\*

LEGEND, CT410 (34M)

DATA0 CT410

0 0

TEMPERATURE

TIME

0.00	299.47
3.86	302.99
5.86	309.26
8.33	320.12
12.64	338.94
14.18	348.73
16.80	354.70
19.57	356.69
23.72	358.53
28.03	361.59
32.65	361.59
38.81	362.35
44.97	361.74
51.74	361.89
58.52	362.66
66.37	362.51
77.30	360.98
87.00	360.82

95.47	359.60
109.48	359.14
118.40	360.52
128.57	359.45
139.50	359.75
148.43	360.36
157.82	360.21
168.75	359.75
176.29	359.75
186.76	359.14
193.38	358.83
239.66	353.96
309.04	352.58
364.54	349.97
489.42	348.13
558.80	346.14
669.80	344.61
766.93	343.07
877.93	341.08
1058.30	339.09
1224.81	337.55
1377.44	336.17
1516.19	334.79
1654.94	333.72
1835.32	332.95
1974.07	331.73
2140.57	330.96
2320.95	329.73
2598.46	328.81
2875.96	328.05
3056.34	327.28
3208.97	326.51
3375.47	326.05
3486.47	325.90

-12345 -12345

\*

LEGEND, CONTAIN

DATA1 CONTAIN

0 0

TEMPERATURE

TIME

2.26	358.29
6.77	372.53
9.03	380.23
15.80	386.77
15.80	390.27
20.31	392.14
38.36	390.97
49.65	388.40
58.67	384.90
72.21	381.40
97.04	379.06
126.38	375.80
155.71	372.53
178.28	370.43

194.08	367.39
234.70	364.82
273.06	362.02
313.68	359.92
365.59	357.35
419.75	355.25
491.96	353.38
564.18	351.05
645.42	348.95
719.89	347.31
801.13	345.45
873.34	344.04
925.25	342.88
1001.97	341.01
1083.22	340.08
1168.97	339.61
1243.44	338.44
1329.20	337.97
1414.95	337.51
1457.83	336.81
1500.71	336.34
-12345	-12345

\*

ST008: ABCOVE Aerosol Experiments Test AB6

MELGEN Input

TITLE 'ST008'

\*

```

**** CONTROL VOLUME INPUT:  THERE ARE THREE CONTROL VOLUMES  ****
**** THE FIRST IS THE EXPERIMENTAL VESSEL, THE OTHER TWO      ****
**** ARE INFINITE VOLUMES THAT BORDER THE VESSEL              ****
CV00100  EXPVOL  1  2  2  * EQUIL THERM, VERTICAL FLOW, CONTAINMENT
CV001A0   2
CV001A1  PVOL  1.14E05  PH2O  0.0
CV001A2  TATM  304.
CV001A3  TPOL  304.
CV001A4  MFRC.1 0.0  MFRC.2 0.0  MFRC.3 0.0
CV001A5  MFRC.4 0.77 MFRC.5 0.23
CV001B1  0.0  0.0
CV001B2  20.3  850.  * HEIGHT, VOLUME
CV001C1  AE  2  0
TF00200  HTFLUX  13  1.0  0.0
TF00210  0.0 0.0  595.0 0.0  600.0 3.893E7  605.00 3.893E7
TF00211  1795.0 3.893E7  1800.0 7.458E7  1805.0 7.458E7
TF00212  3550.0 7.458E7  3555.0 9.853E7  3560.0 9.853E7
TF00213  5400.0 9.853E7  5405.0 4.31E6  1.0E5 4.31E6
*CV001C2  AE  4  0
*TF00400  HTFLUX  5  1.0  0.0
*TF00410  0.0 0.0  600.0 0.0  1795.0 3.410E8  3555.0 8.397E8
*TF00411  5400.0 1.364E9

```



```

*
CV00200  ATMW  1  2  2  * EQUIL THERM, VERTICAL FLOW, CONTAINMENT
CV002A0    2
CV002A1  PVOL  1.01E05  PH2O  0.0
CV002A2  TATM  298.00
CV002A3  TPOL  298.00
CV002A4  MFRC.1 0.0  MFRC.2 0.0  MFRC.3 0.0
CV002A5  MFRC.4 0.79 MFRC.5 0.21
CV002B1    0.0  0.0
CV002B2  10020.3  850.E20  * HEIGHT, VOLUME
*
CV00300  ATMF  1  2  2  * EQUIL THERM, VERTICAL FLOW, CONTAINMENT
CV003A0    2
CV003A1  PVOL  1.01E05  PH2O  0.0
CV003A2  TATM  304.0
CV003A3  TPOL  304.0
CV003A4  MFRC.1 0.0  MFRC.2 0.0  MFRC.3 0.0
CV003A5  MFRC.4 0.79 MFRC.5 0.21
CV003B1    0.0  0.0
CV003B2  10020.3  850.E20  * HEIGHT, VOLUME
* NON-CONDENSIBLE GAS INPUT
NCG000    N2    4
NCG001    O2    5
*
**** HEAT STRUCTURE INPUT:  THERE ARE TWO  ****
**** HEAT STRUCTURES.  ONE IS THE FLOOR  ****
**** THE OTHER REPRESENTS THE WALLS OF  ****
**** THE VESSEL  ****
HS00002000 2  1  -10
HS00002001 'WALLS'
HS00002002 0.0  1.0
HS00002100 -1  2  5.88
HS00002101 .02  1
HS00002200 -1
HS00002201 'STAINLESS STEEL' 1
HS00002300 0
HS00002400 3001  1  0.0 1.0
TF00100    FLUXL  5  1.0 0.0
TF00110    0.0 0.0  599.9 0.0  600.0 -2.901E2  5400.0 -2.901E2  5400.1 0.0
HS00002500 750.6  20.3 20.3
HS00002600 3011  1  0.0 1.0
TF01100    FLUXR  5  1.0 0.0
TF01110    0.0 0.0  599.9 0.0  600.0 2.901E2  5400.0 2.901E2  5400.1 0.0
HS00002700 750.6  20.3 20.3
HS00002801 298.0 2
*
HS00003000 3  1  -10
HS00003001 'FLOOR'
HS00003002 0.0  0.0
HS00003100 -1  2  0.0
HS00003101 .01  2
HS00003200 -1
HS00003201 'STAINLESS STEEL' 2
HS00003300 0

```

```

HS00003400 3003 1 0.0 1.0
TF00300 FLUX2 2 1.0 0.0
TF00310 0.0 0.0 5.E3 0.0
HS00003500 88.4 7.30 7.30
HS00003600 1 3 0.0 1.0
HS00003700 88.4 7.30 7.30
HS00003801 304.0 3
* RADIONUCLIDE PACKAGE INPUT
RN1000 0 * ACTIVATE RN1 PACKAGE
RN1001 20 1 7 7 1 2 0 * NSEC, NCOMP, NCLAS, NCLSW, NCLSBX, NA,
NV
RN1100 0.1E-6 500.E-6 2500. * AEROSOL SECTIONAL PARAMETERS
RNPT000 1.0E5 1.60E5 298. 428. * P-T CONDITIONS FOR AEROSOL COEFFICIENTS
* CV / PHASE / CLASS / RAD. FRAC. / MASS. SOURCE RATE / TF / SEC. DISTR.
RNAS000 1 2 6 0.0 0.0779 5 2 * AEROSOL SOURCE (CLASS 2)
RNAS001 0.5E-6 2. * GMD, GSD
TF00500 ASOURCE 5 1.0 0.0 * TF FOR AEROSOL SOURCE
TF00510 0.0 0.0 619.95 0.0 620.0 1.0 5400.0 1.0 5401.0 0.0
RNAS002 1 2 6 1.0 1.4E-4 6 2 * AEROSOL SOURCE (CLASS 4)
RNAS003 0.544E-6 1.55 * GMD, GSD
TF00600 ASOURCE 3 1.0 0.0 * TF FOR AEROSOL SOURCE
TF00610 0.0 1.0 3000.0 1.0 3001.0 0.0
* CHI GAMMA FSLIP STICK TURBDS TKGOP FTHERM DELDIF
RNMS000 1.5 2.25 1.37 1.0 0.001 0.05 1.0 1.0E-5
RNSD000 1 2 2 -1 2 3 -1 3 * DEP SURFACES FOR RADIONUCLIDES
*
RNAG000 1 6 0.10E-6 * INITIAL AEROSOL MASSES (CLASS 2)
RNAG001 .2E-12 .34E-11 .21E-10 .45E-10 .36E-10 .11E-6 .12E-11
RNAG002 .46E-13 .65E-15 .33E-17 .56E-20 .32E-23 .62E-27 .40E-31
RNAG003 .86E-36 .60E-41 .14E-46 .11E-52 .28E-59 .24E-66
RNACOE 1
*
DCHDECPOW TF-007
DCHCLSNORM YES
DCHDEFCLS0 1 2 3 4 5 6 7
TF00700 DECAY 2 1.0 0.0
TF00710 0.0 0.0 100.E5 0.0
.

```

ST008: ABCOVE Aerosol Experiments Test AB6

MELCOR Input

```

TITLE 'ST008'
RESTART 0
DTTIME 10.
* TSTART DTMAX DTMIN DTEDIT DTPLOT DTREST
TIME1 0.0 10. 0.01 10000. 10. 5.0E04
TIME2 10. 10. 0.01 10000. 10. 5.0E04
TIME3 30. 10. 0.01 10000. 10. 5.0E04
TIME4 60. 10. 0.01 10000. 40. 5.0E04
TIME5 300. 10. 0.01 10000. 50. 5.0E04

```

TIME6 600. 10. 0.01 10000. 100. 5.0E04  
 TIME7 1200. 10. 0.01 12000. 400. 5.0E04  
 TIME8 4800. 1000. 0.01 12000. 400. 5.0E04  
 TEND 2.0E5  
 CPULIM 2500.  
 CPULEFT 10.  
 CRTOUT  
 .

ST008: ABCOVE Aerosol Experiments Test AB6

MELPLT Input

FILE1 MELPTF1.DAT  
 TITLE ST006  
 \*\*\*\* PLOT SUSPENDED MASS OF NAOH \*\*\*\*  
 YLABEL SUSPENDED MASS OF NAOH (KG)  
 XLABEL TIME (SEC)  
 XLIMITS 600. 1.E6  
 YLIMITS 1.E-6 1.E2  
 LISTS  
 LOGX  
 LOGY  
 PLOT RN1-ARMG.1  
 DATA1 COMP1 CONTAB6.DAT  
 DATAJ AB6-NAOH AB61.DAT  
 FILE2 MELPTF2.DAT  
 \*\*\*\* PLOT SUSPENDED MASS OF NAI \*\*\*\*  
 YLABEL SUSPENDED MASS OF NAI (KG)  
 XLABEL TIME (SEC)  
 XLIMITS 600. 1.E6  
 YLIMITS 1.E-6 1.E2  
 LISTS  
 LOGX  
 LOGY  
 PLOT RN1-ARMG.1  
 DATA1 COMP2 CONTAB6.DAT  
 DATAJ AB6-NAI AB62.DAT  
 \*\*\*\* PLOT TOTAL DEPOSITED MASS \*\*\*\*  
 YLABEL TOTAL DEPOSITED MASS (KG)  
 XLABEL TIME (SEC)  
 LISTS  
 PLOT RN1-TMDTT  
 DATA1 DEPMASS CONTAB6.DAT  
 \*\*\*\* PLOT MASS DEPOSITED ON THE WALLS \*\*\*\*  
 YLABEL MASS DEPOSITED ON WALLS (KG)  
 XLABEL TIME (SEC)  
 LISTS  
 PLOT RN1-MDTT-2-1  
 DATA1 WALLM CONTAB6.DAT  
 \*\*\*\* PLOT MASS DEPOSITED ON THE FLOOR \*\*\*\*  
 YLABEL MASS DEPOSITED ON FLOOR (KG)

XLABEL (SEC)  
 LISTS  
 PLOT RN1-MDTT-3-1  
 DATA1 FLOORM CONTAB6.DAT

ST008: ABCOVE Aerosol Experiments Test AB6

NaOH Data

◇AB6-NAOH

0 0

YLABEL SUSPENDED MASS DEPOSITED OF NAOH (KG)

XLABEL TIME (SEC)

0.8899E+03	0.1362E+02
0.1012E+04	0.2116E+02
0.1319E+04	0.2860E+02
0.2412E+04	0.1929E+02
0.3541E+04	0.1929E+02
0.4833E+04	0.2547E+02
0.5394E+04	0.2067E+02
0.5698E+04	0.1300E+02
0.5910E+04	0.8769E+01
0.6130E+04	0.5645E+01
0.6656E+04	0.3896E+01
0.7361E+04	0.2627E+01
0.8290E+04	0.1652E+01
0.9864E+04	0.1194E+01
0.1184E+05	0.7513E+00
0.1530E+05	0.4837E+00
0.1941E+05	0.3578E+00
0.2267E+05	0.2358E+00
0.2722E+05	0.1627E+00
0.3517E+05	0.1047E+00
0.4071E+05	0.7572E-01
0.4800E+05	0.4989E-01
0.5607E+05	0.3212E-01
0.6984E+05	0.2322E-01
0.7378E+05	0.1530E-01
0.8234E+05	0.1056E-01
0.9105E+05	0.6955E-02
0.1044E+06	0.4912E-02
0.1187E+06	0.3090E-02
0.1337E+06	0.2036E-02
0.1492E+06	0.1341E-02
0.1696E+06	0.9696E-03
0.1875E+06	0.6242E-03
0.2093E+06	0.4209E-03
0.2379E+06	0.2838E-03
0.2729E+06	0.1827E-03
-12345.00000	-12345.00000

ST008: ABCOVE Aerosol Experiments Test AB6

NaI Data

◇AB6-NAI

0 0

YLABEL SUSPENDED MASS OF NAI (KG)

XLABEL TIME (SEC)

600.00	8.3810E-02
900.00	2.3375E-01
1500.00	1.8275E-01
2400.00	9.7750E-02
3000.00	7.2250E-02
3250.00	3.0600E-02
3555.00	6.8000E-03
4160.00	2.5500E-03
4760.00	1.7000E-03
5400.00	1.2750E-03
5600.00	1.0200E-03
7200.00	1.6150E-04
10000.00	4.4200E-05
30000.00	7.6500E-07
-12345.00000	-12345.00000

ST009A: Battelle-Frankfurt Gas Mixing Experiments

---

Note: The input data for ST009B is not included here. Input data for ST009B can be obtained from the editor of this report.

---

MELGEN Input

TITLE 'BATELLE-FRANKFURT TEST 2 (TOTAL VOLUME 70.62 stere)'

\*

DTTIME 0.5

RESTARTF 'MELRST2'

\*

NCG001 N2 4

NCG002 O2 5

NCG003 H2 6

\*

\* SOURCE IN VOLUME 15

\*

CV015C0 MASS.4 1 2

CV015C1 TE 2 8

CV015C2 MASS.6 3 2

CV015C3 TE 2 8

\*

TF00100 'N2SOURCE' 3 1.1775 0. \* RHO AT TOTAL P,290.15 K

TF00101 0 0

TF00110 0.,1.1E-04 1.361E4,1.1E-04 1.362E4,0. \* TABLE VALUES ARE VOL/S

```

*
TF00200  SOURCETEMP      2      1.  0.
TF00201  0  0
TF00210  0.,290.15 1.362E4,290.15
*
TF00300  'H2SOURCE'  3      8.47316E-02  0.  * RHO AT TOTAL P,290.15 K
TF00301  0  0
TF00310  0.,2.2E-04  1.361E4,2.2E-04  1.362E4,0.  * TABLE VALUES ARE VOL/S
* VOLUME DATA
*
CV00100  TOPCENTER  1  0  2
* DEFAULT CV SWITCHES
* NO INITIAL VELOCITIES, DEFAULT FLOW AREA
CV00101  1  0
CV001A0  2 * P,Ts, AND MASS FRACTIONS ARE SPECIFIED
*
* NO LIQUID WATER OR FOG IN INITIAL CONDITIONS
CV001A4  MFRC.1  0.  MFRC.2  0. MFRC.3  1.
*
* DRY AIR IS APPROXIMATED AS
* FREE OXYGEN MOLE FRACTION = 0.21,
* FREE NITROGEN MOLE FRACTION = 0.79
*
CV001A5  MFRC.4  0.76708  MFRC.5  0.23292
*
*
* ALTITUDE-VOLUME PAIRS
CV001B0  5.085  0.  6.010  0.2313
*
CV00200  TOPMIDDLE  1  0  2
*
CV00201  1  0
CV002A0  2 * P,Ts, AND MASS FRACTIONS ARE SPECIFIED
*
CV002A5  MFRC.1  0.
CV002A6  MFRC.2  0.
CV002A7  MFRC.3  1.
*
CV002A8  MFRC.4  0.76708  * N2
CV002A9  MFRC.5  0.23292  * O2
*
*
* ALTITUDE-VOLUME PAIRS
CV002B0  5.085  0.  6.010  0.6938
*
CV00300  TOPOUTER  1  0  2
*
CV00301  1  0
CV003A0  2 * P,Ts, AND MASS FRACTIONS ARE SPECIFIED
*
CV003A5  MFRC.1  0.
CV003A6  MFRC.2  0.
CV003A7  MFRC.3  1.
*

```

```

CV003A8 MFRC.4 0.76708 * N2
CV003A9 MFRC.5 0.23292 * O2
*
*
* ALTITUDE-VOLUME PAIRS
CV003B0 5.085 0. 6.010 14.1814
*
CV00400 LEV6CENTER 1 0 2
*
CV00401 1 0
CV004A0 2 * P,Ts, AND MASS FRACTIONS ARE SPECIFIED
*
CV004A5 MFRC.1 0.
CV004A6 MFRC.2 0.
CV004A7 MFRC.3 1.
*
CV004A8 MFRC.4 0.76708 * N2
CV004A9 MFRC.5 0.23292 * O2
*
*
* ALTITUDE-VOLUME PAIRS
CV004B0 4.160 0. 5.085 0.2313
*
CV00500 LEV6MIDDLE 1 0 2
*
CV00501 1 0
CV005A0 2 * P,Ts, AND MASS FRACTIONS ARE SPECIFIED
*
CV005A5 MFRC.1 0.
CV005A6 MFRC.2 0.
CV005A7 MFRC.3 1.
*
CV005A8 MFRC.4 0.76708 * N2
CV005A9 MFRC.5 0.23292 * O2

* ALTITUDE-VOLUME PAIRS
CV005B0 4.160 0. 5.085 0.6938
*
CV00600 LEV6OUTER 1 0 2
*
CV00601 1 0
CV006A0 2 * P,Ts, AND MASS FRACTIONS ARE SPECIFIED
*
CV006A5 MFRC.1 0.
CV006A6 MFRC.2 0.
CV006A7 MFRC.3 1.
*
CV006A8 MFRC.4 0.76708 * N2
CV006A9 MFRC.5 0.23292 * O2
*
*
* ALTITUDE-VOLUME PAIRS
CV006B0 4.160 0. 5.085 14.1814
*

```

```

CV00700  LEV5CENTER  1  0  2
*
CV00701    1  0
CV007A0  2 * P,Ts, AND MASS FRACTIONS ARE SPECIFIED
*
CV007A5  MFRC.1  0.
CV007A6   MFRC.2  0.
CV007A7   MFRC.3  1.
*
CV007A8  MFRC.4  0.76708 *  N2
CV007A9  MFRC.5  0.23292 *  O2
*
*
*      ALTITUDE-VOLUME PAIRS
CV007B0  3.255  0.  4.160  0.905
*
CV00800  LEV5OUTER  1  0  2
*
CV00801    1  0
CV008A0  2 * P,Ts, AND MASS FRACTIONS ARE SPECIFIED
*
CV008A5  MFRC.1  0.
CV008A6   MFRC.2  0.
CV008A7   MFRC.3  1.
*
CV008A8  MFRC.4  0.76708 *  N2
CV008A9  MFRC.5  0.23292 *  O2
*
*
*      ALTITUDE-VOLUME PAIRS
CV008B0  3.255  0.  4.160  8.8256
*
CV00900  LEV4CENTER  1  0  2
*
CV00901    1  0
CV009A0  2 * P,Ts, AND MASS FRACTIONS ARE SPECIFIED
*
CV009A5  MFRC.1  0.
CV009A6   MFRC.2  0.
CV009A7   MFRC.3  1.
*
CV009A8  MFRC.4  0.76708 *  N2
CV009A9  MFRC.5  0.23292 *  O2
*
*
*      ALTITUDE-VOLUME PAIRS
CV009B0  2.350  0.  3.255  0.905
*
CV01000  LEV4OUTER  1  0  2
*
CV01001    1  0
CV010A0  2 * P,Ts, AND MASS FRACTIONS ARE SPECIFIED
*
CV010A5  MFRC.1  0.

```



CV010A6 MFRC.2 0.  
 CV010A7 MFRC.3 1.  
 \*  
 CV010A8 MFRC.4 0.76708 \* N2  
 CV010A9 MFRC.5 0.23292 \* O2  
 \*  
 \*  
 \* ALTITUDE-VOLUME PAIRS  
 CV010B0 2.350 0. 3.255 8.8256  
 \*  
 CV01100 LEV3CENTER 1 0 2  
 \*  
 CV01101 1 0  
 CV011A0 2 \* P,Ts, AND MASS FRACTIONS ARE SPECIFIED  
 \*  
 CV011A5 MFRC.1 0.  
 CV011A6 MFRC.2 0.  
 CV011A7 MFRC.3 1.  
 \*  
 CV011A8 MFRC.4 0.76708 \* N2  
 CV011A9 MFRC.5 0.23292 \* O2  
 \*  
 \*  
 \* ALTITUDE-VOLUME PAIRS  
 CV011B0 1.850 0. 2.350 0.5  
 \*  
 CV01200 LEV3OUTER 1 0 2  
 \*  
 CV01201 1 0  
 CV012A0 2 \* P,Ts, AND MASS FRACTIONS ARE SPECIFIED  
 \*  
 CV012A5 MFRC.1 0.  
 CV012A6 MFRC.2 0.  
 CV012A7 MFRC.3 1.  
 \*  
 CV012A8 MFRC.4 0.76708 \* N2  
 CV012A9 MFRC.5 0.23292 \* O2  
 \*  
 \*  
 \* ALTITUDE-VOLUME PAIRS  
 CV012B0 1.850 0. 2.350 3.7765  
 \*  
 CV01300 LEV2CENTER 1 0 2  
 \*  
 CV01301 1 0  
 CV013A0 2 \* P,Ts, AND MASS FRACTIONS ARE SPECIFIED  
 \*  
 CV013A5 MFRC.1 0.  
 CV013A6 MFRC.2 0.  
 CV013A7 MFRC.3 1.  
 \*  
 CV013A8 MFRC.4 0.76708 \* N2  
 CV013A9 MFRC.5 0.23292 \* O2  
 \*

```

*
*      ALTITUDE-VOLUME PAIRS
CV013B0  0.925  0.  1.850  .925
*
CV01400  LEV2OUTER  1  0  2
*
CV01401  1  0
CV014A0  2 * P,Ts, AND MASS FRACTIONS ARE SPECIFIED
*
CV014A5  MFRC.1  0.
CV014A6  MFRC.2  0.
CV014A7  MFRC.3  1.
*
CV014A8  MFRC.4  0.76708  *  N2
CV014A9  MFRC.5  0.23292  *  O2
*
*
*      ALTITUDE-VOLUME PAIRS
CV014B0  0.925  0.  1.850  9.0207
*
CV01500  BOTCENTER  1  0  2  *  H2-N2 SOURCE IS IN THIS VOLUME
*
CV01501  1  0
CV015A0  2 * P,Ts, AND MASS FRACTIONS ARE SPECIFIED
*
CV015A5  MFRC.1  0.
CV015A6  MFRC.2  0.
CV015A7  MFRC.3  1.
*
CV015A8  MFRC.4  0.76708  *  N2
CV015A9  MFRC.5  0.23292  *  O2
*
*
*      ALTITUDE-VOLUME PAIRS
CV015B0  0.3  0.  0.925  0.625
*
CV01600  BOTOUTER  1  0  2
*
CV01601  1  0
CV016A0  2 * P,Ts, AND MASS FRACTIONS ARE SPECIFIED
*
CV016A5  MFRC.1  0.
CV016A6  MFRC.2  0.
CV016A7  MFRC.3  1.
*
CV016A8  MFRC.4  0.76708  *  N2
CV016A9  MFRC.5  0.23292  *  O2
*
*      ALTITUDE-VOLUME PAIRS
CV016B0  0.3  0.  0.925  6.0951
*
CV001A1  TATM  -290.15  TPOL  290.15
CV001A2  PVOL  1.013359E+05  PH2O  1.933487E+03
*

```

CV002A1	TATM	-290.15	TPOL	290.15	
CV002A2	PVOL	1.013359E+05	PH20		1.933487E+03
*					
CV003A1	TATM	-290.15	TPOL	290.15	
CV003A2	PVOL	1.013359E+05	PH20		1.933487E+03
*					
CV004A1	TATM	-290.15	TPOL	290.15	
CV004A2	PVOL	1.013468E+05	PH20		1.933487E+03
*					
CV005A1	TATM	-290.15	TPOL	290.15	
CV005A2	PVOL	1.013468E+05	PH20		1.933487E+03
*					
CV006A1	TATM	-290.15	TPOL	290.15	
CV006A2	PVOL	1.013468E+05	PH20		1.933487E+03
*					
CV007A1	TATM	-290.15	TPOL	290.15	
CV007A2	PVOL	1.013575E+05	PH20		1.933487E+03
*					
CV008A1	TATM	-290.15	TPOL	290.15	
CV008A2	PVOL	1.013575E+05	PH20		1.933487E+03
*					
CV009A1	TATM	-290.15	TPOL	290.15	
CV009A2	PVOL	1.013682E+05	PH20		1.933487E+03
*					
CV010A1	TATM	-290.15	TPOL	290.15	
CV010A2	PVOL	1.013682E+05	PH20		1.933487E+03
*					
CV011A1	TATM	-290.15	TPOL	290.15	
CV011A2	PVOL	1.013741E+05	PH20		1.933487E+03
*					
CV012A1	TATM	-290.15	TPOL	290.15	
CV012A2	PVOL	1.013741E+05	PH20		1.933487E+03
*					
CV013A1	TATM	-290.15	TPOL	290.15	
CV013A2	PVOL	1.013850E+05	PH20		1.933487E+03
*					
CV014A1	TATM	-290.15	TPOL	290.15	
CV014A2	PVOL	1.013850E+05	PH20		1.933487E+03
*					
CV015A1	TATM	-290.15	TPOL	290.15	
CV015A2	PVOL	1.013924E+05	PH20		1.933487E+03
*					
CV016A1	TATM	-290.15	TPOL	290.15	
CV016A2	PVOL	1.013924E+05	PH20		1.933487E+03
*					
* CONTROL FUNCTIONS					
*					
CF00100	'MOLESIN1'	ADD	6	1.	0.
CF00110	5.55062E-2	0.	CVH-MASS.1.1	*	LIQUID H2O
CF00111	5.55062E-2	0.	CVH-MASS.2.1	*	FOG H2O
CF00112	5.55062E-2	0.	CVH-MASS.3.1	*	VAPOR H2O
CF00113	3.56939E-2	0.	CVH-MASS.4.1	*	N2
CF00114	3.12500E-2	0.	CVH-MASS.5.1	*	O2
CF00115	0.496032	0.	CVH-MASS.6.1	*	H2

CF00300	'MOLESIN2'	ADD	6	1.	0.	
CF00310	5.55062E-2	0.	CVH-MASS.1.2	*	LIQUID H2O	
CF00311	5.55062E-2	0.	CVH-MASS.2.2	*	FOG H2O	
CF00312	5.55062E-2	0.	CVH-MASS.3.2	*	VAPOR H2O	
CF00313	3.56939E-2	0.	CVH-MASS.4.2	*	N2	
CF00314	3.12500E-2	0.	CVH-MASS.5.2	*	O2	
CF00315	0.496032	0.	CVH-MASS.6.2	*	H2	
CF00500	'MOLESIN3'	ADD	6	1.	0.	
CF00510	5.55062E-2	0.	CVH-MASS.1.3	*	LIQUID H2O	
CF00511	5.55062E-2	0.	CVH-MASS.2.3	*	FOG H2O	
CF00512	5.55062E-2	0.	CVH-MASS.3.3	*	VAPOR H2O	
CF00513	3.56939E-2	0.	CVH-MASS.4.3	*	N2	
CF00514	3.12500E-2	0.	CVH-MASS.5.3	*	O2	
CF00515	0.496032	0.	CVH-MASS.6.3	*	H2	
CF00700	'MOLESIN4'	ADD	6	1.	0.	
CF00710	5.55062E-2	0.	CVH-MASS.1.4	*	LIQUID H2O	
CF00711	5.55062E-2	0.	CVH-MASS.2.4	*	FOG H2O	
CF00712	5.55062E-2	0.	CVH-MASS.3.4	*	VAPOR H2O	
CF00713	3.56939E-2	0.	CVH-MASS.4.4	*	N2	
CF00714	3.12500E-2	0.	CVH-MASS.5.4	*	O2	
CF00715	0.496032	0.	CVH-MASS.6.4	*	H2	
CF00900	'MOLESIN5'	ADD	6	1.	0.	
CF00910	5.55062E-2	0.	CVH-MASS.1.5	*	LIQUID H2O	
CF00911	5.55062E-2	0.	CVH-MASS.2.5	*	FOG H2O	
CF00912	5.55062E-2	0.	CVH-MASS.3.5	*	VAPOR H2O	
CF00913	3.56939E-2	0.	CVH-MASS.4.5	*	N2	
CF00914	3.12500E-2	0.	CVH-MASS.5.5	*	O2	
CF00915	0.496032	0.	CVH-MASS.6.5	*	H2	
CF01100	'MOLESIN6'	ADD	6	1.	0.	
CF01110	5.55062E-2	0.	CVH-MASS.1.6	*	LIQUID H2O	
CF01111	5.55062E-2	0.	CVH-MASS.2.6	*	FOG H2O	
CF01112	5.55062E-2	0.	CVH-MASS.3.6	*	VAPOR H2O	
CF01113	3.56939E-2	0.	CVH-MASS.4.6	*	N2	
CF01114	3.12500E-2	0.	CVH-MASS.5.6	*	O2	
CF01115	0.496032	0.	CVH-MASS.6.6	*	H2	
CF01300	'MOLESIN7'	ADD	6	1.	0.	
CF01310	5.55062E-2	0.	CVH-MASS.1.7	*	LIQUID H2O	
CF01311	5.55062E-2	0.	CVH-MASS.2.7	*	FOG H2O	
CF01312	5.55062E-2	0.	CVH-MASS.3.7	*	VAPOR H2O	
CF01313	3.56939E-2	0.	CVH-MASS.4.7	*	N2	
CF01314	3.12500E-2	0.	CVH-MASS.5.7	*	O2	
CF01315	0.496032	0.	CVH-MASS.6.7	*	H2	
CF01500	'MOLESIN8'	ADD	6	1.	0.	
CF01510	5.55062E-2	0.	CVH-MASS.1.8	*	LIQUID H2O	
CF01511	5.55062E-2	0.	CVH-MASS.2.8	*	FOG H2O	
CF01512	5.55062E-2	0.	CVH-MASS.3.8	*	VAPOR H2O	
CF01513	3.56939E-2	0.	CVH-MASS.4.8	*	N2	
CF01514	3.12500E-2	0.	CVH-MASS.5.8	*	O2	
CF01515	0.496032	0.	CVH-MASS.6.8	*	H2	
CF01700	'MOLESIN9'	ADD	6	1.	0.	
CF01710	5.55062E-2	0.	CVH-MASS.1.9	*	LIQUID H2O	
CF01711	5.55062E-2	0.	CVH-MASS.2.9	*	FOG H2O	
CF01712	5.55062E-2	0.	CVH-MASS.3.9	*	VAPOR H2O	
CF01713	3.56939E-2	0.	CVH-MASS.4.9	*	N2	

CF01714	3.12500E-2	0.	CVH-MASS.5.9	* O2
CF01715	0.496032	0.	CVH-MASS.6.9	* H2
CF01900	'MOLESIN10'	ADD	6 1. 0.	
CF01910	5.55062E-2	0.	CVH-MASS.1.10	* LIQUID H2O
CF01911	5.55062E-2	0.	CVH-MASS.2.10	* FOG H2O
CF01912	5.55062E-2	0.	CVH-MASS.3.10	* VAPOR H2O
CF01913	3.56939E-2	0.	CVH-MASS.4.10	* N2
CF01914	3.12500E-2	0.	CVH-MASS.5.10	* O2
CF01915	0.496032	0.	CVH-MASS.6.10	* H2
CF02100	'MOLESIN11'	ADD	6 1. 0.	
CF02110	5.55062E-2	0.	CVH-MASS.1.11	* LIQUID H2O
CF02111	5.55062E-2	0.	CVH-MASS.2.11	* FOG H2O
CF02112	5.55062E-2	0.	CVH-MASS.3.11	* VAPOR H2O
CF02113	3.56939E-2	0.	CVH-MASS.4.11	* N2
CF02114	3.12500E-2	0.	CVH-MASS.5.11	* O2
CF02115	0.496032	0.	CVH-MASS.6.11	* H2
CF02300	'MOLESIN12'	ADD	6 1. 0.	
CF02310	5.55062E-2	0.	CVH-MASS.1.12	* LIQUID H2O
CF02311	5.55062E-2	0.	CVH-MASS.2.12	* FOG H2O
CF02312	5.55062E-2	0.	CVH-MASS.3.12	* VAPOR H2O
CF02313	3.56939E-2	0.	CVH-MASS.4.12	* N2
CF02314	3.12500E-2	0.	CVH-MASS.5.12	* O2
CF02315	0.496032	0.	CVH-MASS.6.12	* H2
CF02500	'MOLESIN13'	ADD	6 1. 0.	
CF02510	5.55062E-2	0.	CVH-MASS.1.13	* LIQUID H2O
CF02511	5.55062E-2	0.	CVH-MASS.2.13	* FOG H2O
CF02512	5.55062E-2	0.	CVH-MASS.3.13	* VAPOR H2O
CF02513	3.56939E-2	0.	CVH-MASS.4.13	* N2
CF02514	3.12500E-2	0.	CVH-MASS.5.13	* O2
CF02515	0.496032	0.	CVH-MASS.6.13	* H2
CF02700	'MOLESIN14'	ADD	6 1. 0.	
CF02710	5.55062E-2	0.	CVH-MASS.1.14	* LIQUID H2O
CF02711	5.55062E-2	0.	CVH-MASS.2.14	* FOG H2O
CF02712	5.55062E-2	0.	CVH-MASS.3.14	* VAPOR H2O
CF02713	3.56939E-2	0.	CVH-MASS.4.14	* N2
CF02714	3.12500E-2	0.	CVH-MASS.5.14	* O2
CF02715	0.496032	0.	CVH-MASS.6.14	* H2
CF02900	'MOLESIN15'	ADD	6 1. 0.	
CF02910	5.55062E-2	0.	CVH-MASS.1.15	* LIQUID H2O
CF02911	5.55062E-2	0.	CVH-MASS.2.15	* FOG H2O
CF02912	5.55062E-2	0.	CVH-MASS.3.15	* VAPOR H2O
CF02913	3.56939E-2	0.	CVH-MASS.4.15	* N2
CF02914	3.12500E-2	0.	CVH-MASS.5.15	* O2
CF02915	0.496032	0.	CVH-MASS.6.15	* H2
CF03100	'MOLESIN16'	ADD	6 1. 0.	
CF03110	5.55062E-2	0.	CVH-MASS.1.16	* LIQUID H2O
CF03111	5.55062E-2	0.	CVH-MASS.2.16	* FOG H2O
CF03112	5.55062E-2	0.	CVH-MASS.3.16	* VAPOR H2O
CF03113	3.56939E-2	0.	CVH-MASS.4.16	* N2
CF03114	3.12500E-2	0.	CVH-MASS.5.16	* O2
CF03115	0.496032	0.	CVH-MASS.6.16	* H2
*				
CF00200	'MOLFH2IN1'	DIVIDE	2 1. 0.	
CF00210	1.. 0.	CFVALU.1		

CF00211 0.496032 0. CVH-MASS.6.1  
 CF00400 'MOLFH2IN2' DIVIDE 2 1. 0.  
 CF00410 1. 0. CFVALU.3  
 CF00411 0.496032 0. CVH-MASS.6.2  
 CF00600 'MOLFH2IN3' DIVIDE 2 1. 0.  
 CF00610 1. 0. CFVALU.5  
 CF00611 0.496032 0. CVH-MASS.6.3  
 CF00800 'MOLFH2IN4' DIVIDE 2 1. 0.  
 CF00810 1. 0. CFVALU.7  
 CF00811 0.496032 0. CVH-MASS.6.4  
 CF01000 'MOLFH2IN5' DIVIDE 2 1. 0.  
 CF01010 1. 0. CFVALU.9  
 CF01011 0.496032 0. CVH-MASS.6.5  
 CF01200 'MOLFH2IN6' DIVIDE 2 1. 0.  
 CF01210 1. 0. CFVALU.11  
 CF01211 0.496032 0. CVH-MASS.6.6  
 CF01400 'MOLFH2IN7' DIVIDE 2 1. 0.  
 CF01410 1. 0. CFVALU.13  
 CF01411 0.496032 0. CVH-MASS.6.7  
 CF01600 'MOLFH2IN8' DIVIDE 2 1. 0.  
 CF01610 1. 0. CFVALU.15  
 CF01611 0.496032 0. CVH-MASS.6.8  
 CF01800 'MOLFH2IN9' DIVIDE 2 1. 0.  
 CF01810 1. 0. CFVALU.17  
 CF01811 0.496032 0. CVH-MASS.6.9  
 CF02000 'MOLFH2IN10' DIVIDE 2 1. 0.  
 CF02010 1. 0. CFVALU.19  
 CF02011 0.496032 0. CVH-MASS.6.10  
 CF02200 'MOLFH2IN11' DIVIDE 2 1. 0.  
 CF02210 1. 0. CFVALU.21  
 CF02211 0.496032 0. CVH-MASS.6.11  
 CF02400 'MOLFH2IN12' DIVIDE 2 1. 0.  
 CF02410 1. 0. CFVALU.23  
 CF02411 0.496032 0. CVH-MASS.6.12  
 CF02600 'MOLFH2IN13' DIVIDE 2 1. 0.  
 CF02610 1. 0. CFVALU.25  
 CF02611 0.496032 0. CVH-MASS.6.13  
 CF02800 'MOLFH2IN14' DIVIDE 2 1. 0.  
 CF02810 1. 0. CFVALU.27  
 CF02811 0.496032 0. CVH-MASS.6.14  
 CF03000 'MOLFH2IN15' DIVIDE 2 1. 0.  
 CF03010 1. 0. CFVALU.29  
 CF03011 0.496032 0. CVH-MASS.6.15  
 CF03200 'MOLFH2IN16' DIVIDE 2 1. 0.  
 CF03210 1. 0. CFVALU.31  
 CF03211 0.496032 0. CVH-MASS.6.16  
 \*  
 CF50000 'MASSH2' ADD 16 1.00 0.  
 CF50010 1.00 0. CVH-MASS.6.1  
 CF50011 1.00 0. CVH-MASS.6.2  
 CF50012 1.00 0. CVH-MASS.6.3  
 CF50013 1.00 0. CVH-MASS.6.4  
 CF50014 1.00 0. CVH-MASS.6.5  
 CF50015 1.00 0. CVH-MASS.6.6

CF50016	1.00	0.	CVH-MASS.6.7
CF50017	1.00	0.	CVH-MASS.6.8
CF50018	1.00	0.	CVH-MASS.6.9
CF50019	1.00	0.	CVH-MASS.6.10
CF50020	1.00	0.	CVH-MASS.6.11
CF50021	1.00	0.	CVH-MASS.6.12
CF50022	1.00	0.	CVH-MASS.6.13
CF50023	1.00	0.	CVH-MASS.6.14
CF50024	1.00	0.	CVH-MASS.6.15
CF50025	1.00	0.	CVH-MASS.6.16
*			
* HORIZONTAL FLOWPATHS			
*			
FL00100	L7INNER	1 2	5.5475 5.5475
FL00101		1.6396 .2821	1. .925 .925
FL00102		3 0 0 0	
FL00103		1. 1. 1. 1.	
FL001S1		1.6396 .2821	.925
*			
FL00200	L7MIDDLE	2 3	5.5475 5.5475
FL00201		3.2791 .99895	1. .925 .925
FL00202		3 0 0 0	
FL00203		1. 1. 1. 1.	
FL002S1		3.2791 .99895	.925
*			
FL00600	L6INNER	4 5	4.6225 4.6225
FL00601		1.6396 .2821	1. .925 .925
FL00602		3 0 0 0	
FL00603		1. 1. 1. 1.	
FL006S1		1.6396 .2821	.925
*			
FL00700	L6MIDDLE	5 6	4.6225 4.6225
FL00701		3.2791 .99895	1. .925 .925
FL00702		3 0 0 0	
FL00703		1. 1. 1. 1.	
FL007S1		3.2791 .99895	.925
*			
FL01000	L5INNER	7 8	3.7075 3.7075
FL01001		3.2082 .925	1. .905 .905
FL01002		3 0 0 0	
FL01003		1. 1. 1. 1.	
FL010S1		3.2082 .925	.905
*			
FL01300	L4INNER	9 10	2.8025 2.8025
FL01301		3.2082 .925	1. .905 .905
FL01302		3 0 0 0	
FL01303		1. 1. 1. 1.	
FL013S1		3.2082 .925	.905
*			
FL01600	L3INNER	11 12	2.1 2.1
FL01601		1.7725 0.825	1. .5 .5
FL01602		3 0 0 0	
FL01603		1. 1. 1. 1.	
FL016S1		1.7725 0.825	.5

```

*
FL01900 L2INNER 13 14 1.3875 1.3875
FL01901 3.2791 0.925 1. .925 .925
FL01902 3 0 0 0
FL01903 1. 1. 1. 1.
FL019S1 3.2791 0.925 .925
*
FL02200 L1INNER 15 16 0.6125 0.6125
FL02201 2.2156 0.925 1. .625 .625
FL02202 3 0 0 0
FL02203 1. 1. 1. 1.
FL022S1 2.2156 0.925 .625
*
* "VERTICAL" FLOW PATHS
*
FL00300 L7INNERV 1 4 5.085 5.085
FL00301 0.25 0.925 1. 0.05 0.05
FL00302 0 0 0 0
FL00303 1. 1. 1. 1.
FL003S1 0.25 0.925 0.2821
*
FL00800 L6INNERV 4 7 4.160 4.160
FL00801 0.25 0.905 1. 0.05 0.05
FL00802 0 0 0 0
FL00803 1. 1. 1. 1.
FL008S1 0.25 0.905 0.2821
*
FL00400 L7MIDDLEV 2 5 5.085 5.085
FL00401 0.75 0.925 1. 0.05 0.05
FL00402 0 0 0 0
FL00403 1. 1. 1. 1.
FL004S1 0.75 0.925 0.2821
*
FL00900 L6MIDDLEV 5 7 4.160 4.160
FL00901 0.75 0.905 1. 0.05 0.05
FL00902 0 0 0 0
FL00903 1. 1. 1. 1.
FL009S1 0.75 0.905 0.2821
*
FL00500 L7OUTERV 3 6 5.085 5.085
FL00501 15.3312 0.925 1. 0.05 0.05
FL00502 0 0 0 0
FL00503 1. 1. 1. 1.
FL005S1 15.3312 0.925 1.7158
*
FL01100 L5INNERV 7 9 3.255 3.255
FL01101 1. 0.905 1. 0.05 0.05
FL01102 0 0 0 0
FL01103 1. 1. 1. 1.
FL011S1 1. 0.905 0.5642
*
FL01200 L5OUTERV 8 10 3.255 3.255
FL01201 9.7521 0.905 1. 0.05 0.05
FL01202 0 0 0 0

```



FL01203 1. 1. 1. 1.  
 FL012S1 9.7521 0.905 1.2858  
 \*  
 FL01400 L4INNERV 9 11 2.350 2.350  
 FL01401 1. 0.5 1. 0.05 0.05  
 FL01402 0 0 0 0  
 FL01403 1. 1. 1. 1.  
 FL014S1 1. 0.5 0.5642  
 \*  
 FL01500 L4OUTERV 10 12 2.350 2.350  
 FL01501 7.5529 0.5 1. 0.05 0.05  
 FL01502 0 0 0 0  
 FL01503 1. 1. 1. 1.  
 FL015S1 7.5529 0.5 1.0858  
 \*  
 FL01700 L3INNERV 11 13 1.850 1.850  
 FL01701 1. 0.925 1. 0.05 0.05  
 FL01702 0 0 0 0  
 FL01703 1. 1. 1. 1.  
 FL017S1 1. 0.925 0.5642  
 \*  
 FL01800 L3OUTERV 12 14 1.850 1.850  
 FL01801 7.5529 0.925 1. 0.05 0.05  
 FL01802 0 0 0 0  
 FL01803 1. 1. 1. 1.  
 FL018S1 7.5529 0.925 1.2858  
 \*  
 FL02000 L2INNERV 13 15 0.925 0.925  
 FL02001 1. 0.925 1. 0.05 0.05  
 FL02002 0 0 0 0  
 FL02003 1. 1. 1. 1.  
 FL020S1 1. 0.925 0.5642  
 \*  
 FL02100 L2OUTERV 14 16 0.925 0.925  
 FL02101 9.7521 0.925 1. 0.05 0.05  
 FL02102 0 0 0 0  
 FL02103 1. 1. 1. 1.  
 FL021S1 9.7521 0.925 1.2858  
 \*  
 MPMAT00100 'CONCRETE'  
 MPMAT00101 CPS 101  
 MPMAT00102 THC 102  
 MPMAT00103 RHO 103  
 \*  
 TF10100 CONCP 2 879. 0.  
 TF10101 0 0  
 TF10110 0. 1. 1000. 1.  
 \*  
 TF10200 CONTHC 2 1.385 0.  
 TF10201 0 0  
 TF10210 0. 1. 1000. 1.  
 \*  
 TF10300 CONRHO 2 2.2E3 0.  
 TF10301 0 0

```

TF10310 0. 1. 1000. 1.
*
HS00001000 2 1 -1 3
HS00001001 'TOPINNER'
HS00001002 6.010 0.
HS00001100 -1 1 0.
HS00001102 0.25 2
HS00001201 'CONCRETE' 1
HS00001300 0
HS00001400 1 1 1. 1.
HS00001500 0.25 0.2821 0.2821
HS00001600 0
HS00001801 290.15 1
HS00001802 290.15 2
*
HS00002000 2 1 -1 3
HS00002001 'TOPMIDDLE'
HS00002002 6.010 0.
HS00002100 1 1 0.
HS00002200 1
HS00002300 0
HS00002400 1 2 1. 1.
HS00002500 .75 .2821 .2821
HS00002600 0
HS00002800 1
*
HS00003000 2 1 -1 3
HS00003001 'TOPOUTER'
HS00003002 6.010 0.
HS00003100 1 1 0.
HS00003200 1
HS00003300 0
HS00003400 1 2 1. 1.
HS00003500 28.582 1.716 1.716
HS00003600 0
HS00003800 1
*
HS00006000 2 2 -1 3
HS00006001 'L6OUTER'
HS00006002 4.160 1.
HS00006100 -1 1 2.28
HS00006102 2.53 2
HS00006200 1
HS00006300 0
HS00006400 1 6 1. 1.
HS00006500 13.251 0.925 0.925
HS00006600 0
HS00006800 1
*
HS00008000 2 2 -1 3
HS00008001 'L5OUTER'
HS00008002 3.255 1.
HS00008100 -1 1 1.85
HS00008102 2.10 2

```

HS00008200	1
HS00008300	0
HS00008400	1 8 1. 1.
HS00008500	10.52 0.905 0.905
HS00008600	0
HS00008800	1
*	
HS00010000	2 2 -1 3
HS00010001	'L4OUTER'
HS00010002	2.350 1.
HS00010100	-1 1 1.85
HS00010102	2.10 2
HS00010200	1
HS00010300	0
HS00010400	1 10 1. 1.
HS00010500	10.52 0.905 0.905
HS00010600	0
HS00010800	1
*	
HS00012000	2 2 -1 3
HS00012001	'L3OUTER'
HS00012002	1.850 1.
HS00012100	-1 1 1.65
HS00012102	1.9 2
HS00012200	1
HS00012300	0
HS00012400	1 12 1. 1.
HS00012500	5.184 0.5 0.5
HS00012600	0
HS00012800	1
*	
HS00014000	2 2 -1 3
HS00014001	'L2OUTER'
HS00014002	0.925 1.
HS00014100	-1 1 1.85
HS00014102	2.10 2
HS00014200	1
HS00014300	0
HS00014400	1 14 1. 1.
HS00014500	10.752 0.925 0.925
HS00014600	0
HS00014800	1
*	
HS00015000	2 1 -1 3
HS00015001	'BOTINNER'
HS00015002	.05 0.
HS00015100	-1 1 0.
HS00015102	.25 2
HS00015200	1
HS00015300	0
HS00015400	0
HS00015600	1 15 1. 1.
HS00015700	1. .5642 .5642
HS00015800	1

```

*
HS00016000  2  1  -1  3
HS00016001  'BOTOUTER'
HS00016002  .05  0.
HS00016100  -1  1  0.
HS00016102  0.25  2
HS00016200  1
HS00016300  0
HS00016400  0
HS00016600  1  16  1.  1.
HS00016700  20.504  1.286  1.286
HS00016800  1
.

```

#### MELCOR Input

```

TITLE 'BATELLE-FRANKFURT TEST 2 (TOTAL VOLUME 70.62 stere)'
COMTC 65
CPULEFT 5.
OUTPUTF 'MELOUT2'
PLOTf 'MELPTF2'
RESTART 0
RESTARTF 'MELRST2'
TEND 20000.
TIME1 0. 20. 0.01 1400. 70. 30000.
.

```

#### MELPLT Input

```

*
title,battelle-frankfurt test 2, cell 1
file1 melptf2
*
xlabel t
ime (s)
ylabel h
ydrogen ^c
oncentration
ylimits 0. 0.05
legend d
ata
yscale 0.01
data-1 b-f2c1 BAFRE
legend melcor
cplot cfvalu.2
legend hectr
xscale 79.546
yscale 4.0984e-4
data4 b-f2clh BAFRH
yscale 0.01
legend raloc
data6 b-f2clr BAFRRAL
*

```

```

title,battelle-frankfurt test 2, cell 3
xlabel t
ime (s)
ylabel h
ydrogen ^c
oncentration
ylimits 0. 0.05
legend d
ata
yscale 0.01
data-1 b-f2c3 BAFRE
legend melcor
cplot cfvalu.6
*
title,battelle-frankfurt test 2, cell 13
*
xlabel t
ime (s)
ylabel h
ydrogen ^c
oncentration
ylimits 0. 0.05
legend d
ata
yscale 0.01
data-1 b-f2c13 BAFRE
legend melcor
cplot cfvalu.26
legend raloc
yscale 0.01
data6 b-f2c13r BAFRRAL
*
title battelle-frankfurt test 2
ylabel t
imestep (s)
legend m
aximum \d
t is 20 s
plot dt
*
xlabel t
ime (s)
ylabel c
alc-^cpu t
ime ^r
atio
legend nolegend
plot warp
*
xlabel t
ime (s)
ylabel cpu t
ime (s)
legend nolegend

```

```

plot cpu
*
ylabel t
imstep (s)
xlabel t
ime (s)
legend nolegend
plot dt
*
ylabel cpu t
ime (s)
xlabel t
ime (s)
legend nolegend
plot cpu
*
ylabel c
alc-^cpu t
ime ^r
atio
xlabel t
ime (s)
legend nolegend
plot warp
*
ylabel m
ass ^f
low ^r
ate (kg/s)
xlabel t
ime (s)
legend 13 to 15
plot4 fl-mflow.20
legend 15 to 16
cplotb fl-mflow.22
legend 14 to 16
cplotc fl-mflow.21
legend 13 to 14
cplotd fl-mflow.19
*
ylabel m
ass ^f
low ^r
ate (kg/s)
xlabel t
ime (s)
legend 2 to 3
plot4 fl-mflow.2
legend 3 to 6
cplotb fl-mflow.5
legend 2 to 5
cplotc fl-mflow.4
legend 5 to 6
cplotd fl-mflow.7

```

```

*
title,battelle-frankfurt test 19
*
file2 melptf19
*
ylabel t
imstep (s)
xlabel t
ime (s)
legend nolegend
plot dt
*
ylabel cpu t
ime (s)
xlabel t
ime (s)
legend nolegend
plot cpu
*
ylabel c
alc-^cpu t
ime ^r
atio
xlabel t
ime (s)
legend nolegend
plot warp
*
ylabel m
ass ^f
low ^r
ate (kg/s)
xlabel t
ime (s)
legend 13 to 15
plot4 fl-mflow.20
legend 15 to 16
cplotb fl-mflow.22
legend 14 to 16
cplotc fl-mflow.21
legend 13 to 14
cplotd fl-mflow.19
*
ylabel m
ass ^f
low ^r
ate (kg/s)
xlabel t
ime (s)
legend 2 to 3
plot4 fl-mflow.2
legend 3 to 6
cplotb fl-mflow.5
legend 2 to 5

```

```

cplotc fl-mflow.4
legend 5 to 6
cplotd fl-mflow.7
*
title,battelle-frankfurt test 19 cell 13
*
ylabel h
ydrogen ^c
oncentration
xlabel t
ime (s)
legend d
ata
yscale 0.01
data-1 b-fl9c13 BAFRE
legend melcor
cplot cfvalu.26
legend hectr
xscale 41.48
yscale 4.0984e-4
data4 b-fl9c13h BAFRH
legend raloc
yscale 0.01
data6 b-fl9c13r BAFRRAL
*
title,battelle-frankfurt test 19 cell 4
*
ylabel h
ydrogen ^c
oncentration
xlabel t
ime (s)
legend d
ata
yscale 0.01
data-1 b-fl9c4 BAFRE
legend melcor
cplot cfvalu.8
legend hectr
xscale 41.48
yscale 4.0984e-4
data4 b-fl9c4h BAFRH
*
title,battelle-frankfurt test 19 cell 17
*
ylabel h
ydrogen ^c
oncentration
xlabel t
ime (s)
legend d
ata
yscale 0.01
data-1 b-fl9c17 BAFRE

```



```

legend melcor
cplot cfvalu.34
legend hectr
xscale 41.48
yscale 4.0984e-4
data4 b-f19c17h BAFRH
legend raloc
yscale 0.01
data6 b-f19c13r BAFRRAL
*
title,battelle-frankfurt test 19 cell 22
*
ylabel h
ydrogen ^c
oncentration
xlabel t
ime (s)
legend d
ata
yscale 0.01
data-1 b-f19c22 BAFRE
legend melcor
cplot cfvalu.44
legend nolegend
cplot cfvalu.54
legend nolegend
cplot cfvalu.56
legend hectr
xscale 41.48
yscale 4.0984e-4
data4 b-f19c22h BAFRH
legend raloc
yscale 0.01
data6 b-f19c22r BAFRRAL
legend nolegend
yscale 0.01
data6 b-f19c23r BAFRRAL
*
```

#### Experimental Data

```

<>B-F2C1
0 1
H2CON1
TIME
FROM CHANNY'S [HECTR.BF.DATA]B2Z1D.88
    0.00      0.00
    78.08     0.00
    156.16    .01
    234.24    .01
    335.75    .06
    374.79    .08
    413.83    .11
```

452.87	.14
530.95	.16
554.38	.14
609.04	.11
671.50	.12
671.50	.15
671.50	.20
726.16	.20
827.66	.19
929.17	.19
991.63	.20
1046.29	.22
1124.37	.26
1202.45	.27
1288.34	.31
1343.00	.34
1460.12	.37
1522.59	.38
1561.63	.38
1624.09	.39
1717.79	.40
1764.64	.42
1819.30	.47
1858.34	.50
1936.42	.49
1998.88	.55
2061.35	.54
2076.97	.57
2139.43	.61
2178.47	.57
2217.51	.59
2295.59	.63
2319.02	.66
2397.10	.62
2436.14	.62
2498.61	.62
2514.22	.65
2553.26	.68
2631.34	.70
2654.77	.73
2732.85	.75
2795.32	.75
2873.40	.77
2928.05	.80
2974.90	.82
3029.56	.83
3107.64	.85
3146.68	.89
3209.15	.91
3349.69	.93
3388.73	.97
3427.77	.99
3505.86	1.01
3583.94	1.05

3662.02	1.09
3724.48	1.06
3724.48	1.12
3802.57	1.14
3865.03	1.16
3966.54	1.15
4005.58	1.17
4083.66	1.22
4122.70	1.24
4177.36	1.29
4200.78	1.31
4278.86	1.29
4278.86	1.34
4341.33	1.35
4419.41	1.39
4435.03	1.41
4481.87	1.45
4536.53	1.47
4599.00	1.49
4614.61	1.45
4653.65	1.40
4692.69	1.47
4739.54	1.51
4872.28	1.53
4895.71	1.57
4934.75	1.60
4973.79	1.63
5051.87	1.62
5090.91	1.60
5114.33	1.63

---

Note: This data file has been truncated here. For a more complete data set contact the editor of this report.

---

#### HECTR Data

<>B-F2C1H

0 3

H2CON1

TIME

FOR NOW, DATA FROM hectr REPORT GRAPH FOR TEST 2, CELL 1

DATA ARE IN MM: 176 MM 14 KS; 122 MM 0.05

XSCALE = 79.546, YSCALE = 4.0984E-4

0. 0.

3. 0.

5. 3.

10. 6.5

20. 13.

40. 25.

60. 38.

80. 50.

```

100.  63.
120.  74.
140.  87.5
160.  99.
171.8 105.
172.8 103.
173.5 104.
175.9 104.
-12345 -12345
◇B-F6C1H
  0    3
  H2CON1
  TIME
FOR NOW, DATA FROM hectr REPORT GRAPH FOR TEST 6, CELL 1
      DATA ARE IN MM: 176 MM   14 KS; 122 MM   0.05
      XSCALE = 79.546, YSCALE = 4.0984E-4
0.    0.
25.    0.
30.    .8
40.    1.5
45.    2.
50.     3.
55.     4.
60.     5.3
65.     6.8
70.     7.8
75.     9.
80.    10.7
85.    13.3
90.    17.2
92.8   20.
95.    23.
101.   31.
102.8  35.
105.   35.
108.   60.
111.   75.
112.   78.
113.   80.
115.   82.5
116.   84.
117.   84.9
119.   86.
121.   86.9
124.   87.
128.   86.5
135.   85.
140.   84.5
150.   82.9
155.   82.4
160.   82.
161.5  81.5
165.   77.5
167.   75.

```

```

        170.    72.5
        172.    71.
        175.    69.4
-12345 -12345
<B-F6C12H
0 3
h2con12
time
this may be hectr output digitized for test 6, cell 12
from channy's file bf6z12.dat
maybe heat structures
    0.000    0.0000
    47.039    0.0000
    78.039    0.0000
   101.539    0.0000
   119.039    0.0001
   138.039    0.0005
   175.539    0.0015
   204.539    0.0023
   238.039    0.0033
   278.039    0.0044
   312.039    0.0052
   364.039    0.0062
   423.539    0.0071
   480.539    0.0082
   537.039    0.0093
   587.039    0.0104
   640.539    0.0116
   697.539    0.0127
   735.039    0.0131
   754.539    0.0131
   771.039    0.0131
   786.539    0.0130
   801.039    0.0128
   815.539    0.0124
   833.539    0.0116
   847.539    0.0110
   860.539    0.0105

```

---

Note: This data file has been truncated here. For a more complete data set contact the editor of this report.

---

#### RALOC Data

```

<B-F2C1R
0 1
H2CON1
TIME
FROM CHANNY'S R2Z1.DAT (RALOC) ALL ORDINATE VALUES ARE per centum
+1.49864E+01, +1.67673E-02
+8.99183E+01, +1.67673E-02
+1.34877E+02, +4.35949E-02

```

```

+1.94823E+02, +8.38364E-02
+1.94823E+02, +1.17371E-01
+3.74659E+02, +2.01207E-01
+6.14441E+02, +2.91751E-01
+8.39237E+02, +3.82294E-01
+1.22888E+03, +5.26492E-01
+1.49864E+03, +6.10329E-01
+1.96322E+03, +7.74648E-01
+2.71253E+03, +1.04628E+00
+3.47684E+03, +1.31791E+00
+4.27112E+03, +1.58954E+00
+5.06540E+03, +1.88464E+00
+6.39918E+03, +2.33065E+00
+7.46322E+03, +2.68276E+00
+8.52725E+03, +3.04829E+00
+9.69619E+03, +3.43058E+00
+1.05954E+04, +3.72569E+00
+1.15845E+04, +4.04427E+00
+1.24537E+04, +4.32931E+00
+1.32180E+04, +4.58082E+00
+1.35627E+04, +4.69484E+00
+1.36376E+04, +4.64453E+00
+1.37875E+04, +4.65795E+00
+1.50463E+04, +4.65795E+00
+1.69046E+04, +4.65795E+00
+1.92875E+04, +4.65795E+00
+2.01417E+04, +4.65795E+00
-12345 -12345
<B-F2C13R
0 1
H2CON13
TIME
FROM CHANNY'S R2Z13.DAT (RALOC)
+9.05971E+01, +1.01215E-02
+1.35896E+02, +8.43455E-02
+1.35896E+02, +1.51822E-01
+2.26493E+02, +2.02429E-01
+4.52986E+02, +3.07018E-01
+6.79478E+02, +4.31849E-01
+1.01167E+03, +5.97166E-01
+1.31366E+03, +7.08502E-01
+1.63075E+03, +8.29959E-01
+2.20453E+03, +1.02227E+00
+2.67262E+03, +1.21458E+00
+3.15580E+03, +1.39676E+00
+3.69938E+03, +1.58907E+00
+4.21277E+03, +1.75439E+00
+4.69595E+03, +1.93995E+00
+5.36033E+03, +2.16599E+00
+6.20590E+03, +2.44939E+00
+6.85518E+03, +2.67207E+00
+7.53466E+03, +2.91498E+00
+8.28964E+03, +3.17476E+00
+9.25601E+03, +3.49528E+00

```

```

+1.00714E+04, +3.75169E+00
+1.11434E+04, +4.11606E+00
+1.17927E+04, +4.31849E+00
+1.26836E+04, +4.61538E+00
+1.35443E+04, +4.87854E+00
+1.36651E+04, +4.69973E+00
+1.40426E+04, +4.67949E+00
+1.48579E+04, +4.66599E+00
+1.59602E+04, +4.65587E+00
+1.75003E+04, +4.64912E+00
+1.86328E+04, +4.65587E+00
+2.01126E+04, +4.65587E+00
-12345 -12345
◇B-F6C1R
0 1
H2CON1
TIME
FROM CHANNY'S R6Z1.DAT (RALOC)
+6.80735E+01, +1.63044E-03
+4.76515E+02, +4.89130E-03
+8.91763E+02, +1.30435E-02
+1.20490E+03, +1.95652E-02
+1.27978E+03, +1.95652E-02
+1.47720E+03, +2.93478E-02
+1.74268E+03, +3.26087E-02
+2.00817E+03, +4.07609E-02
+2.14432E+03, +5.54348E-02
+2.30769E+03, +7.33696E-02
+2.48468E+03, +7.98913E-02
+2.57999E+03, +1.01087E-01
+2.74336E+03, +1.05978E-01
+2.96801E+03, +1.10870E-01
+3.07012E+03, +1.33696E-01
+3.17223E+03, +1.27174E-01
+3.27434E+03, +1.77717E-01
+3.32199E+03, +2.34783E-01
+3.38325E+03, +2.72283E-01
+3.47175E+03, +2.60870E-01
+3.47856E+03, +3.35870E-01
+3.60109E+03, +3.04891E-01
+3.69639E+03, +2.60870E-01
+3.75766E+03, +2.60870E-01
+3.79170E+03, +2.70652E-01
+3.79850E+03, +3.47283E-01
+3.83254E+03, +4.48370E-01

```

---

Note: This data file has been truncated here. For a more complete data set contact the editor of this report.

---





## Appendix C

### Comparison Plots for MELCOR Standard Test Problems

Included in this appendix are the key plots for comparison for the MELCOR Standard Test Problems. As mentioned in the preface, all of the results in this appendix were produced with the latest available version of the code, MELCOR 1.6.0.

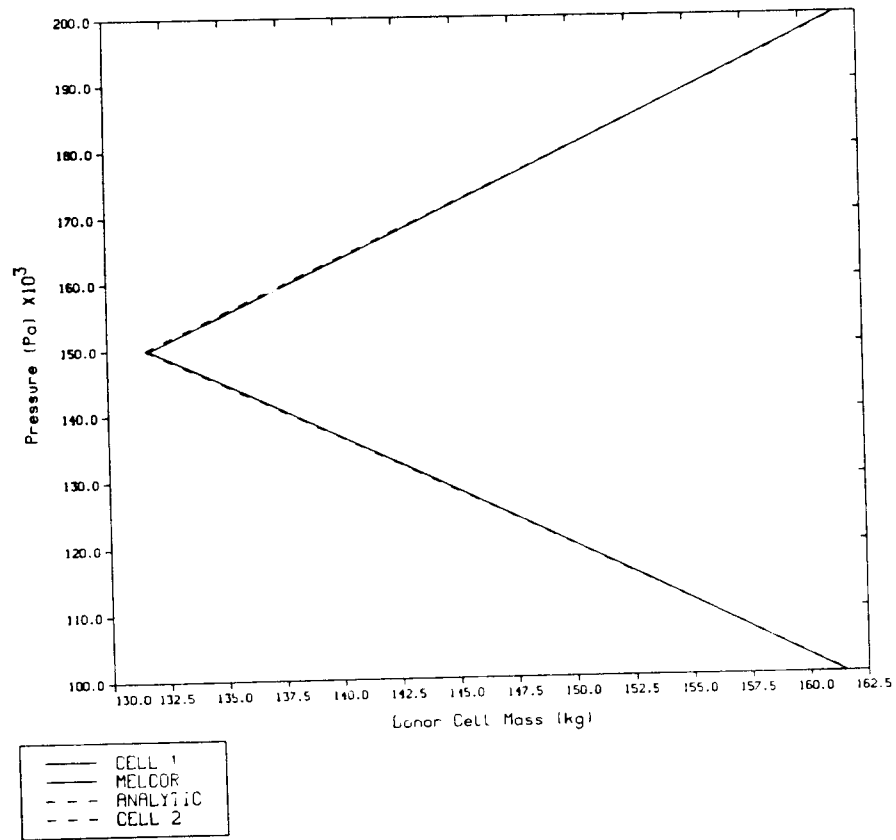


Figure C.1 Pressure versus time for both cells for ST001

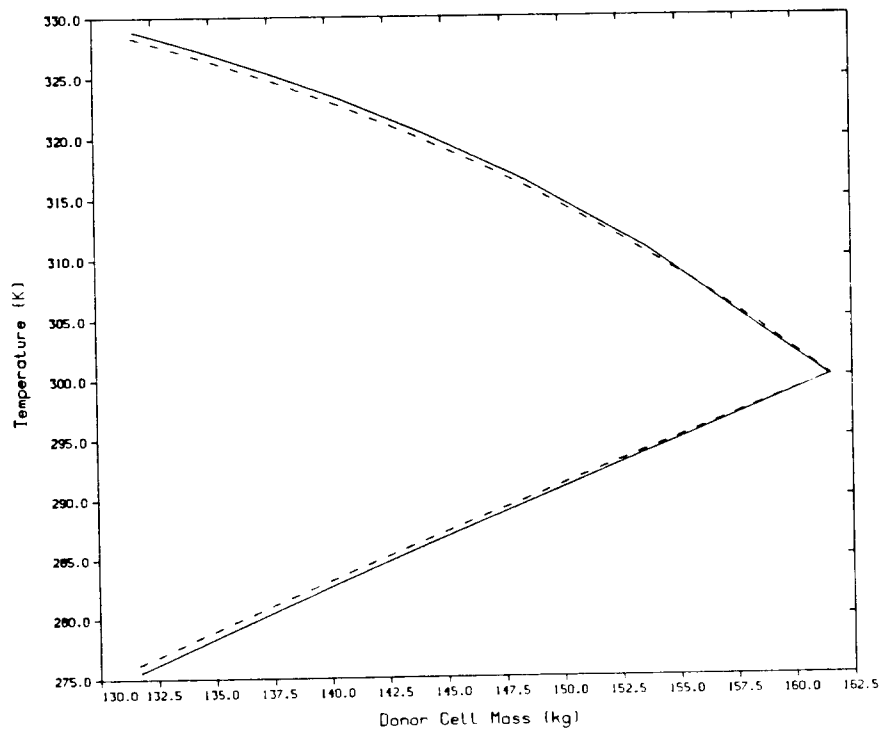


Figure C.2 Temperature versus time for both cells for ST001

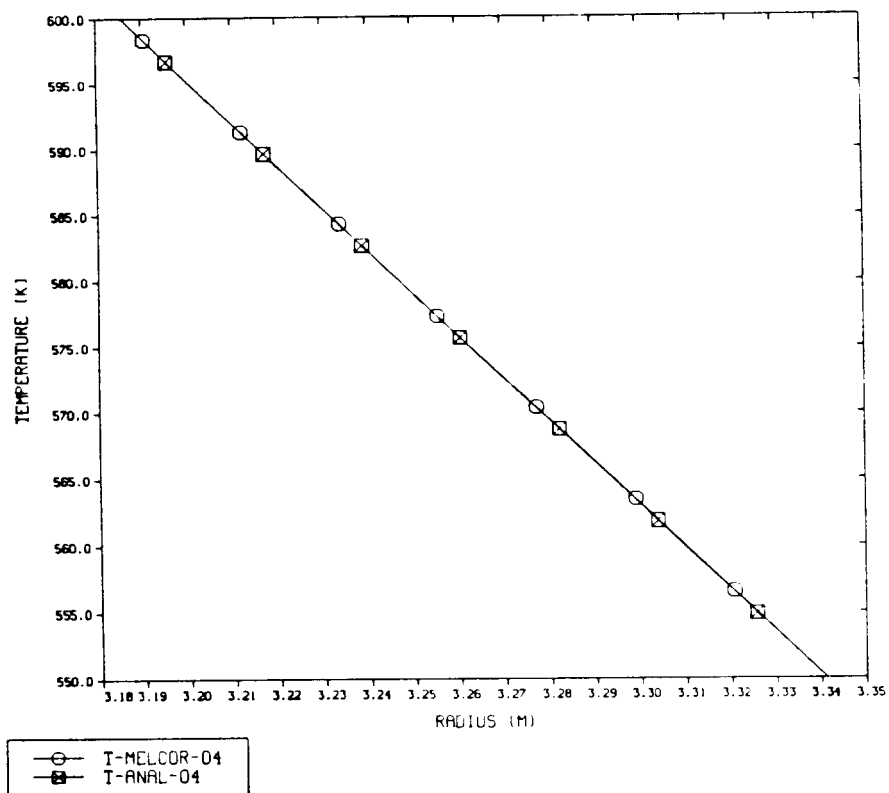


Figure C.3. Temperature versus Radius for ST002

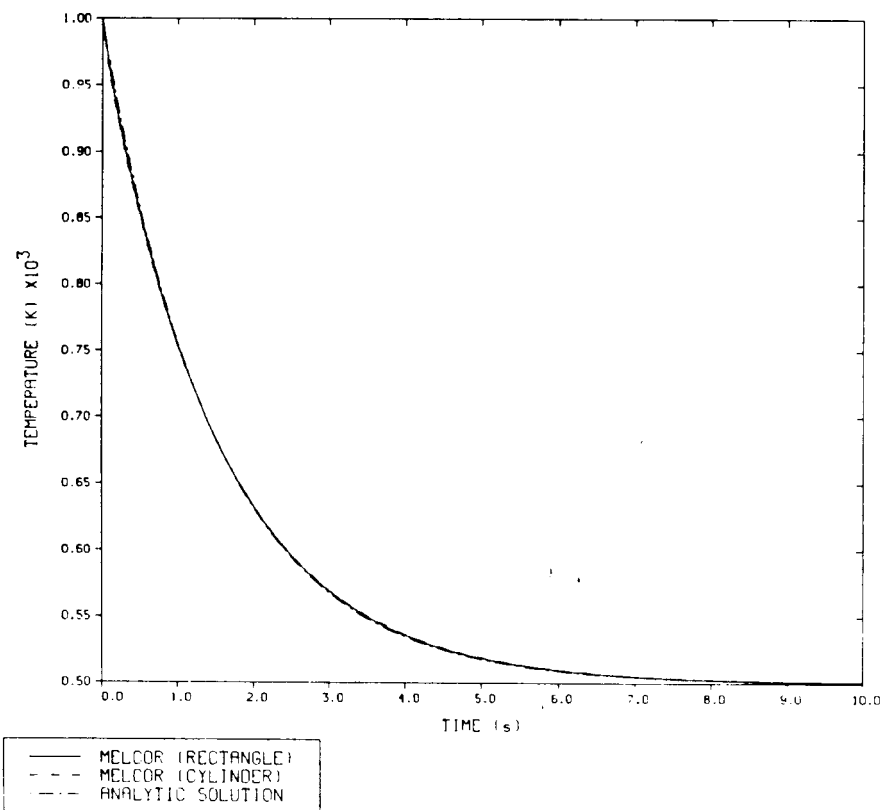


Figure C.4. Temperature versus Time for ST003

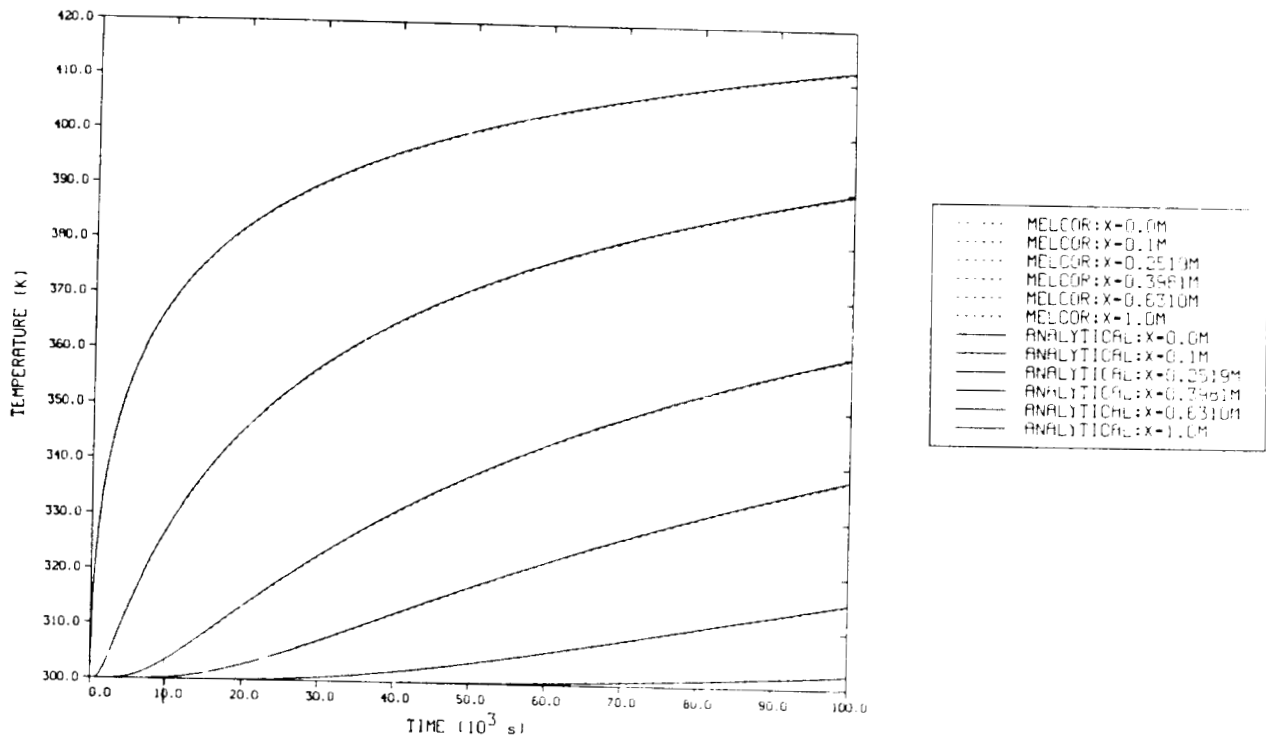
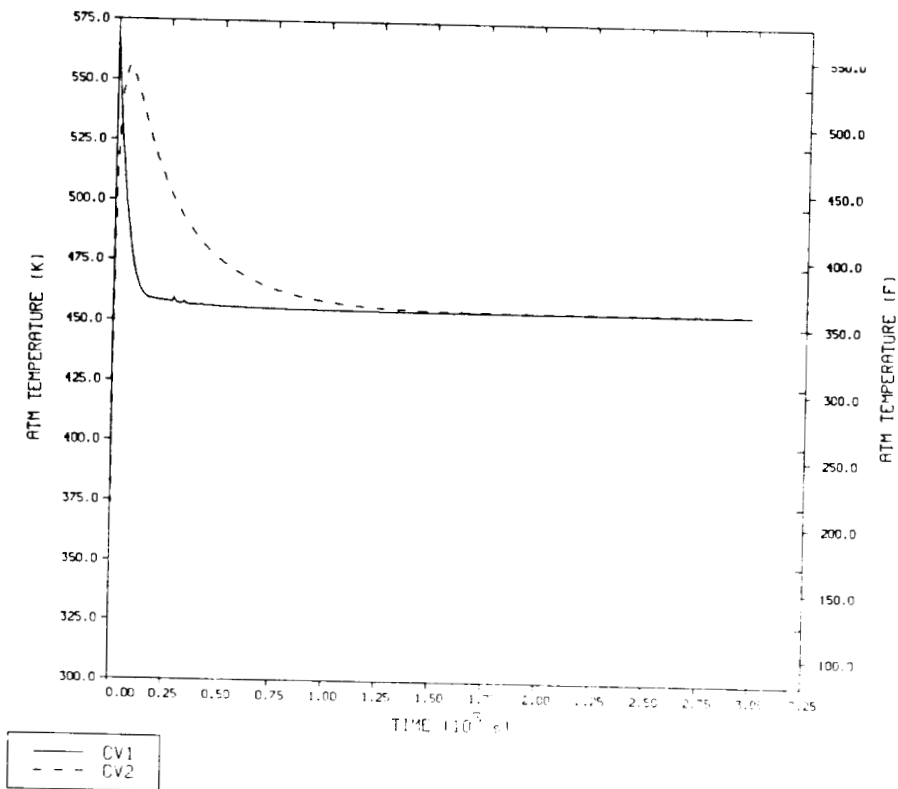
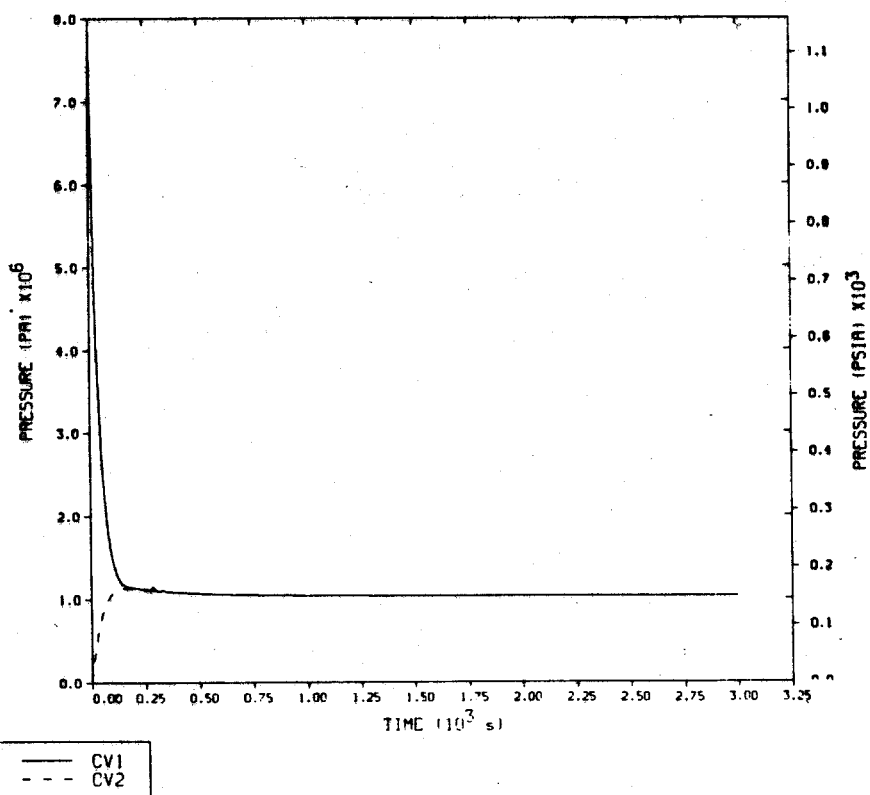


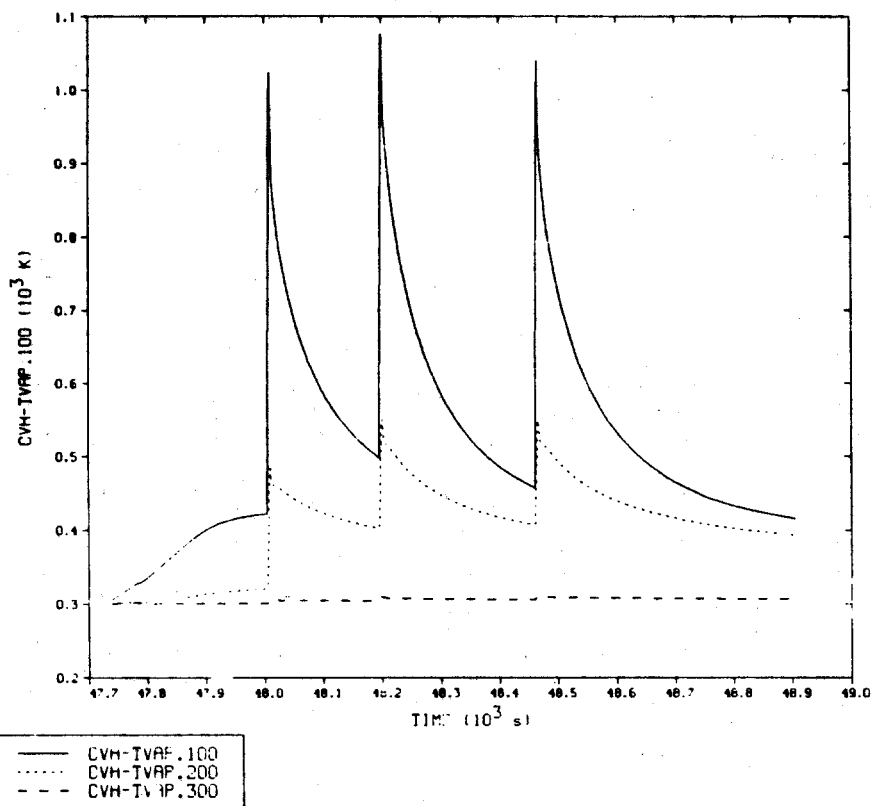
Figure C.5. Temperature versus Time within the structure for ST004A



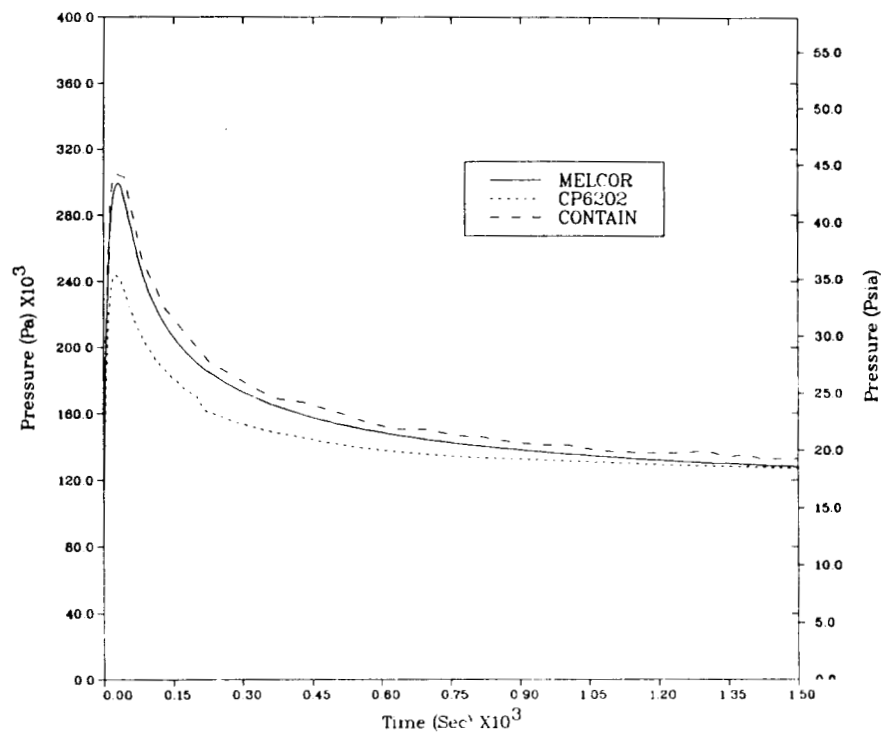
C.6. Temperature of Both Cells as a Function of Time for ST005



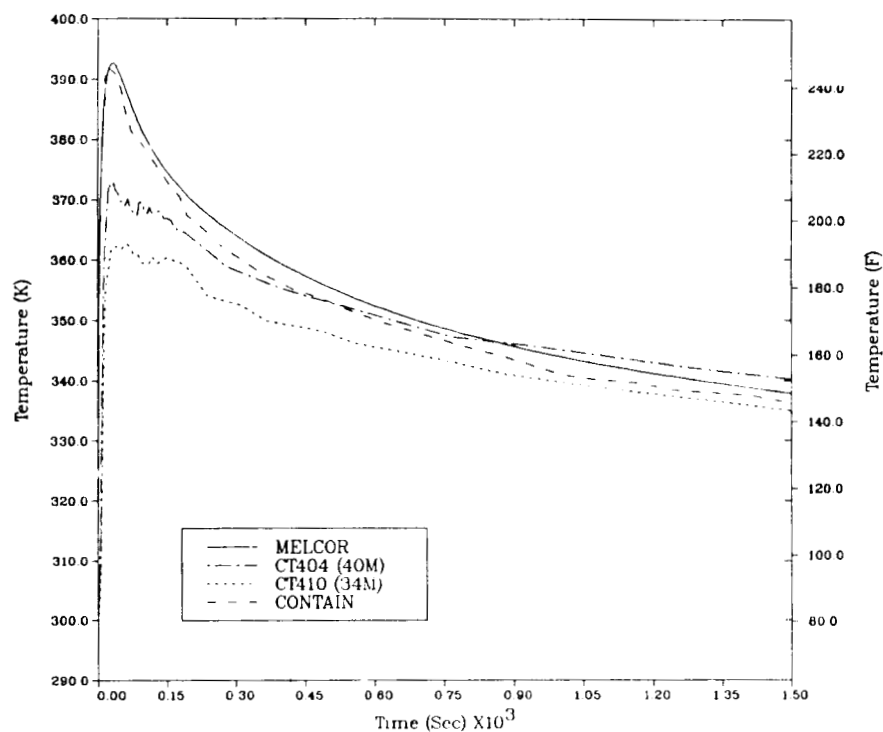
C.7. Pressure in Both Cells as a Function of Time for ST005



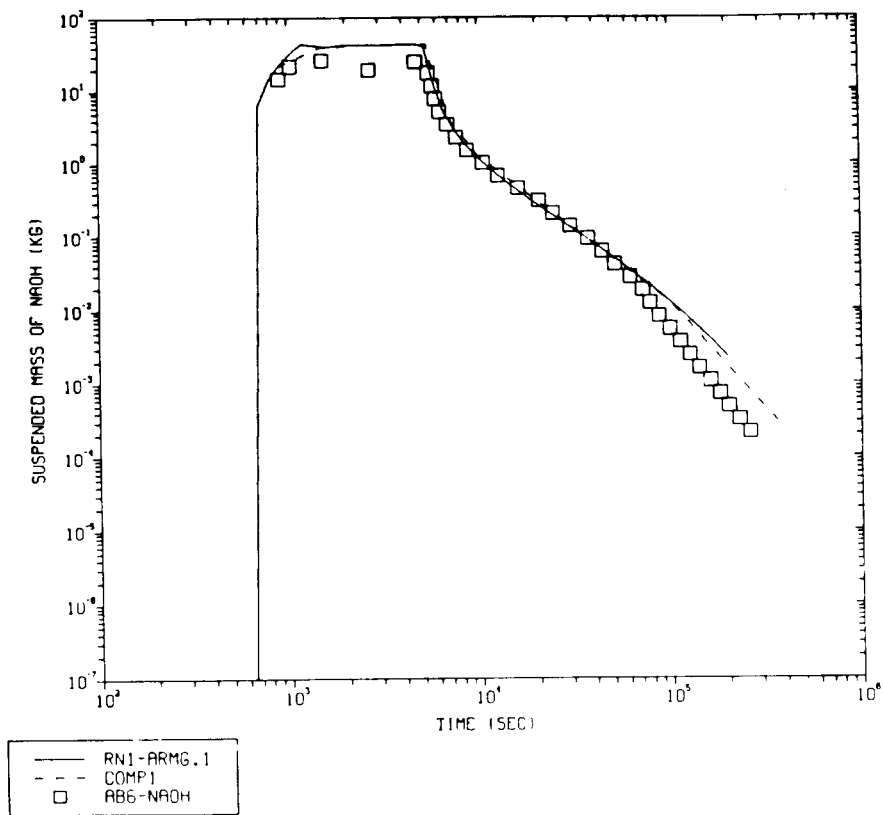
C.8. Temperature versus Time for Control Volume 1 for ST006



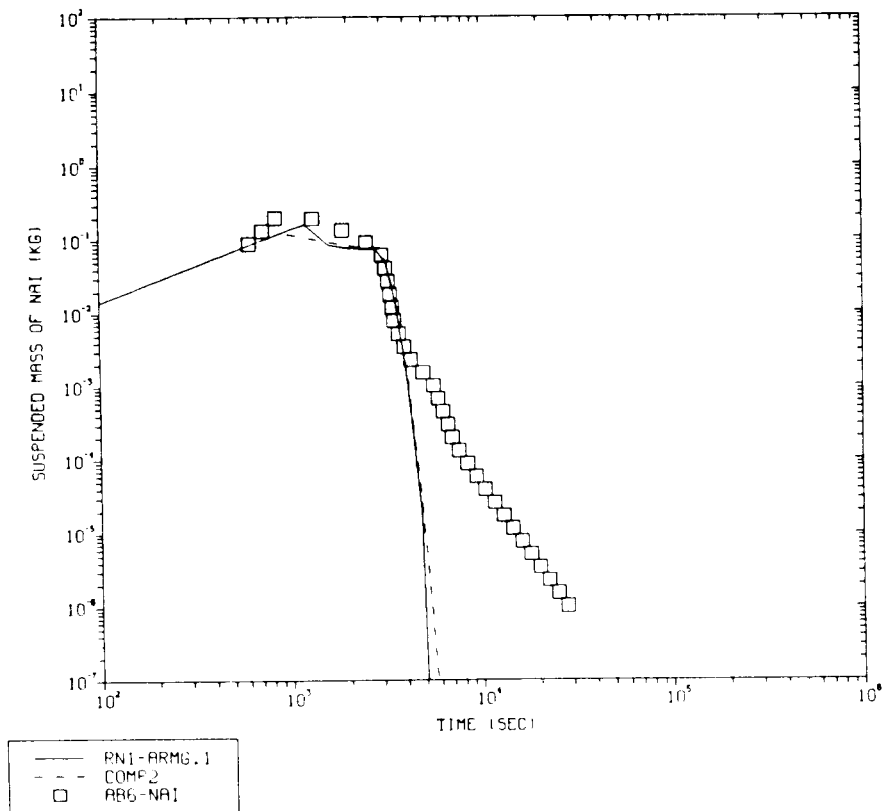
C.9. Containment Dome Pressure for ST007



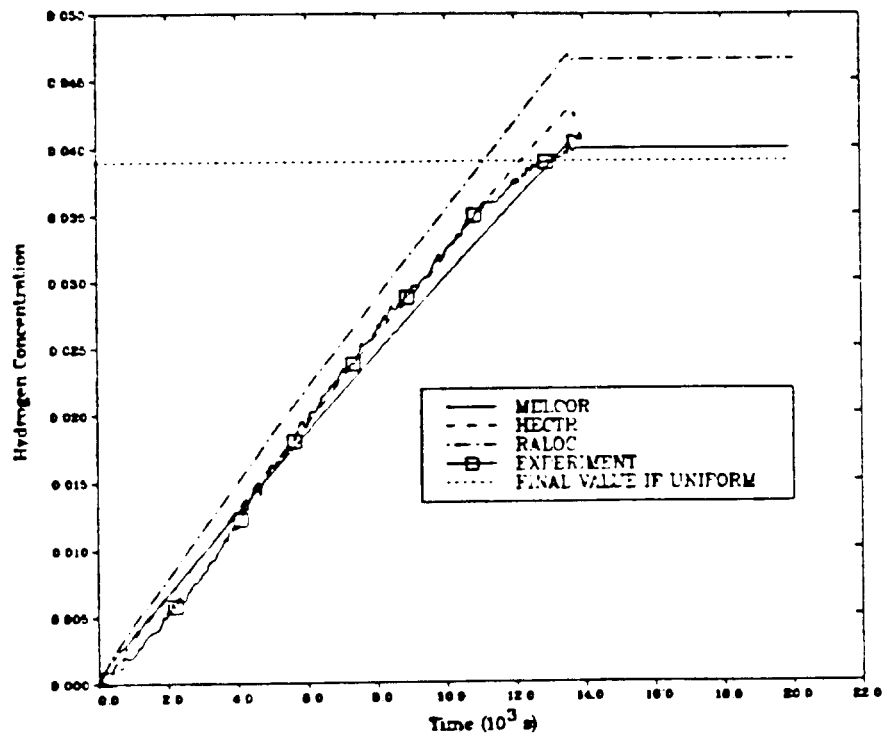
C.10. Containment Dome Temperature for ST007



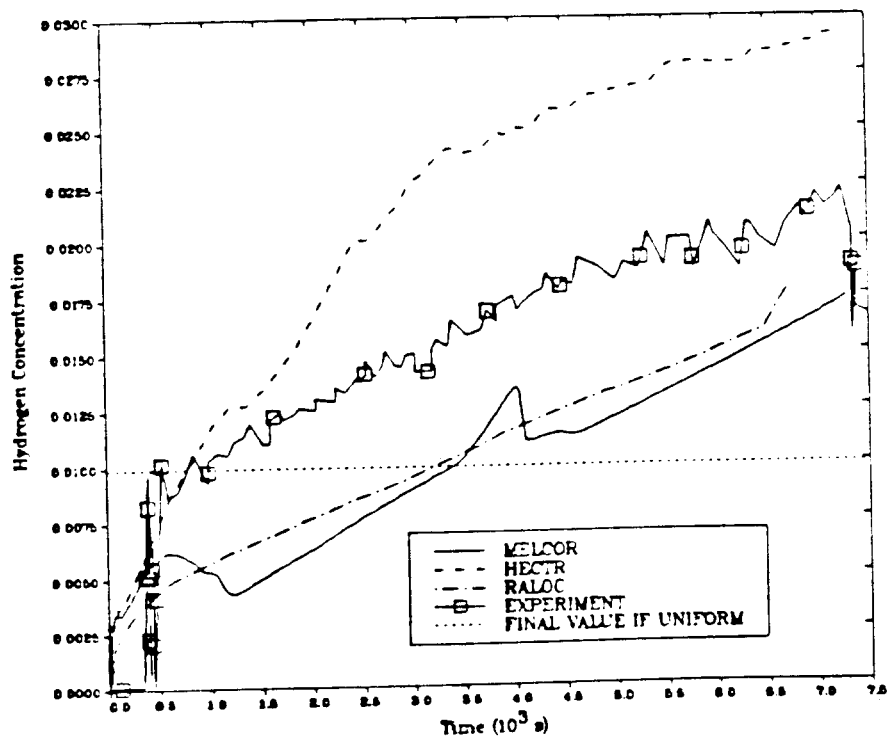
C.11. Suspended Mass of NaOH as a Function of Time for ST008



C.12. Suspended Mass of NaI as a Function of Time for ST008

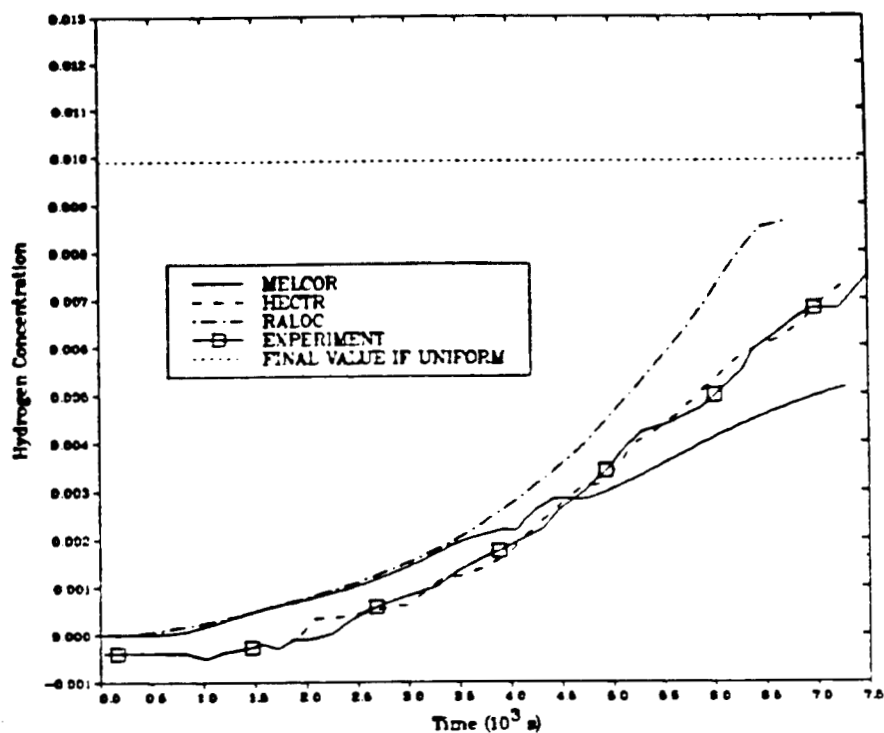


C.13. Hydrogen Concentration for Cell 1 for Battelle-Frankfurt Test 2 (ST009)

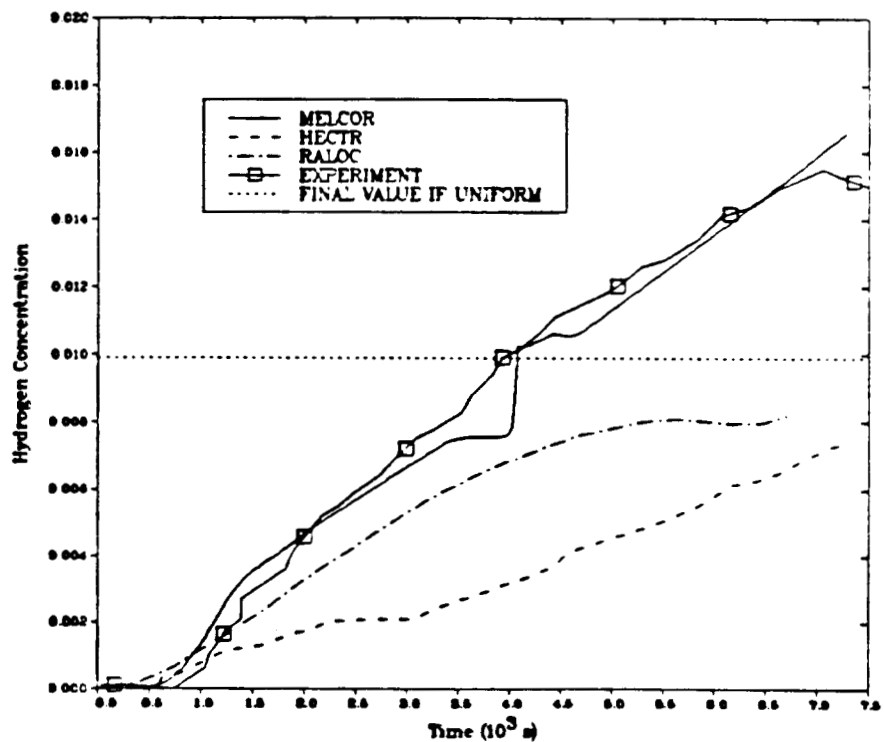


C.14. Hydrogen Concentration for Cell 13 for Battelle-Frankfurt Test 19 (ST009)





C.15. Hydrogen Concentration for Cell 23 for Battelle-Frankfurt Test 19(ST009)



C.16. Hydrogen Concentration for Cell 27 for Battelle-Frankfurt Test 19(ST009)



Distribution:

U.S. Government Printing Office  
Receiving Branch (Attn: NRC Stock)  
8610 Cherry Lane  
Laurel, MD 20707  
250 copies for R3

R. S. Denning  
Battelle Columbus Laboratories  
505 King Avenue  
Columbus, OH 43201

K. R. Perkins  
Brookhaven National Laboratories  
Building 130  
Upton, NY 11973

M. S. Barents  
EES(UK)  
Granford ouse  
16 Carfax  
Horsham  
West Sussex RH12UP  
England

B. R. Sehgal  
Electric Power Research Inst.  
3412 Hillview Ave.  
Palo Alto, CA 94304

J. A. Blackburn  
Office of Nuclear Facility Safety  
State of Illinois  
Dept. of Nuclear Safety  
1035 Outer Park Drive  
Springfield, IL 62704

R. J. Dallman  
INEL  
P.O. Box 1625  
Idaho Falls, ID 83401

K. C. Wagner  
INEL  
P.O. Box 1625  
Idaho Falls, ID 83401

R. J. Barrett  
Nuclear Regulatory Commission  
Washington, DC 20555

M. A. Cunningham  
U. S. Nuclear Regulatory Commission  
5650 Nicholson Lane  
Rockville, MD 20852

R. O. Meyer  
U. S. Nuclear Regulatory Commission  
Washington, DC 20555

J. Mitchell  
U. S. Nuclear Regulatory Commission  
Washington, DC 20555

S. R. Greene  
Oak Ridge National Laboratories  
Building 9104-1, MS 1  
Station 59, 9201-3  
Y-12 Plant  
Bear Creek Road  
Oak Ridge, TN 37831

S. A. Hodge  
Oak Ridge National Laboratories  
Building 9104-1, MS1  
Station 59, 9201-3  
Y-12 Plant  
Bear Creek Road  
Oak Ridge, TN 37830

T. S. Kress  
Oak Ridge National Laboratories  
Building 91-4-1, MS1  
Station 59, 9201-3  
Y-12 Plant  
Bear Creek Road  
Oak Ridge, TN 37830

A. Torri  
Pickard, Lowe & Garrick  
1421 Hymettus Ave.  
La Conita, CA 92024

F. A. Koontz  
Tennessee Valley Authority  
400 W. Summit Hill Dr.  
Knoxville, TN 37922

S. R. Kinnersly  
Atomic Energy Establishment  
Winfrith  
Dorchester  
Dorset DT28DH  
England

R. Young  
UKAEA, SRD  
Wigshaw Lane  
Culcheth  
Warrington WA3 4NE  
England

M. L. Corradini  
University of Wisconsin  
Dept. of Nuclear Engineering  
Engineering Research Bldg.  
1500 Johnson Drive  
Madison, WI 53706

G. A. Moses  
University of Wisconsin  
Dept. of Nuclear Engineering  
Engineering Research Bldg.  
1500 Johnson Drive  
Madison, WI 53706

1531	J. M. McGlaun
6400	D. J. McCloskey
6410	N. R. Ortiz
6412	A. L. Camp
6414	A. S. Benjamin
6415	F. E. Haskin
6415	D. I. Chanin
6415	S. E. Dingman
6415	J. D. Johnson
6415	C. D. Leigh
6415	L. T. Ritchie
6415	C. J. Shaffer
6415	J. L. Sprung
6418	L. D. Buxton
6418	R. K. Byers
6418	R. K. Cole
6418	L. N. Kmetyk
6418	J. L. Orman
6418	R. M. Summers
6418	S. W. Webb
6422	D. A. Powers
6419	K. D. Bergeron
6419	K. K. Murata
6419	D. C. Williams
6440	D. A. Dahlgren
3141	S. A. Landenberger (5)
3151	W. L. Garner
8024	P. W. Dean



NRC FORM 335 (2-84) NRCM 1102, 3201, 3202 SEE INSTRUCTIONS ON THE REVERSE		U.S. NUCLEAR REGULATORY COMMISSION <b>BIBLIOGRAPHIC DATA SHEET</b>		1. REPORT NUMBER (Assigned by TIDC, add Vol. No., if any) NUREG/CR-4830	
2. TITLE AND SUBTITLE MELCOR Validation and Verification 1986 Papers				3. LEAVE BLANK	
5. AUTHOR(S) C. D. Leigh, Editor				4. DATE REPORT COMPLETED MONTH: January YEAR: 1987	
				6. DATE REPORT ISSUED MONTH: March YEAR: 1987	
7. PERFORMING ORGANIZATION NAME AND MAILING ADDRESS (Include Zip Code) Safety and Environmental Studies Division 6415 Sandia National Laboratories Albuquerque, NM 87185				8. PROJECT/TASK/WORK UNIT NUMBER	
				9. FIN OR GRANT NUMBER A1339	
10. SPONSORING ORGANIZATION NAME AND MAILING ADDRESS (Include Zip Code) U. S. Nuclear Regulatory commission Washington, DC 20555				11a. TYPE OF REPORT b. PERIOD COVERED (Inclusive dates)	
12. SUPPLEMENTARY NOTES					
13. ABSTRACT (200 words or less) <p>MELCOR validation and verification results from 1986 are presented. Results of comparisons to analytic solutions and experiments are included. The major areas tested in these comparisons are the control volume hydrodynamics and thermodynamics, the heat transfer and the aerosol behavior in MELCOR. A set of nine standard tests is included.</p>					
14. DOCUMENT ANALYSIS - a. KEYWORDS/DESCRIPTORS b. IDENTIFIERS/OPEN-ENDED TERMS				15. AVAILABILITY STATEMENT Unlimited	
				16. SECURITY CLASSIFICATION (This page) Unclassified (This report) Unclassified	
				17. NUMBER OF PAGES	
				18. PRICE	